



USC Michelson Center for Convergent Bioscience
2024 Annual Report

Contents

Executive Summary	2
Fundraising & Financials	5
Meet Our Faculty	7
Institutes & Centers	13
Core Facilities	19
Scientific & Social Impact	27
Manuscripts & Publications	41
Featured Article	59
Highlighted Publications	61
Faculty At a Glance	64
Addendum: Journal Articles	101



Executive Summary

Since 2017 the Michelson Center for Convergent Bioscience has supported collaborations both on a national and global scale, harnessing the combined knowledge of varied research communities, enhancing exploration and expediting advancements. It fosters innovative breakthroughs by dismantling traditional disciplinary barriers, encouraging the emergence of groundbreaking discoveries.

Thanks to a generous donation of \$50 million from retired orthopedic spinal surgeon Dr. Gary Michelson and his wife, Alya Michelson, the \$185 million, 190,000-square-foot building establishes the necessary infrastructure for research aimed at developing life-saving therapeutics and devices. This dynamic infrastructure effectively embodies Dr. Michelson's vision for a research landscape characterized by increased openness, convergence, and the sharing of information.

The 2024 Michelson Center for Convergent Bioscience Annual Report outlines the center's initiatives and showcases the research undertaken by Michelson faculty from January to December 2023. This report details the scientific and social impact, milestones, and accolades attained by faculty members, as well as the shared

research facilities, institutes, and centers housed at Michelson Hall. Additionally, it provides financial information regarding research labs and core facilities.

Michelson faculty — USC researchers whose laboratory is located at Michelson Hall and/or who are directors of Michelson centers, institutes, and/or core facilities — continue to grow in number, currently 37 from the original 20 named faculty, and who have appointments with the USC Viterbi School of Engineering, the Keck School of Medicine at USC and/or the USC Dana and David Dornsife College of Letters, Arts and Sciences. Michelson Hall also houses five centers/institutes and five research core facilities, detailed later in this report.

The new arrival to the Michelson Center in 2023 is Dr. Ye Tian. Dr. Tian is a Research Assistant Professor at the Viterbi School Ming Hsieh Department of Electrical and Computer Engineering. His research utilizes a 0.55 Tesla Magnetic Resonance Imaging (MRI) scanner to improve dynamic imaging capabilities, with a focus on cardiovascular and fetal imaging, and novel acquisition and reconstruction methods. He received his Ph.D. at the University of Utah in 2019 and completed his postdoc training at the University of Southern California, receiving a Postdoctoral Scholarship from the American Heart Association (AHA). He was also selected as a Junior Fellow of the International

Society of Magnetic Resonance in Medicine (ISMRM).

Michelson faculty have submitted 1,192 grant proposals to federal, state and local government funding agencies and foundations since the center's inauguration six years ago, being awarded \$250M within this time period. In 2023 alone, 32 grants proposals were submitted with 28 awarded, totaling \$15.6M in funds received as grants, subcontracts or cooperative agreements. Additionally, over 195 manuscripts were published/submitted to peer-reviewed journals (detailed in the Manuscripts & Publications section of this report). As well, in 2023, Michelson Hall core facilities invoiced over \$885,000 in charges to USC users, not including income derived from charges made to non-USC researchers in industry and academia.

Recognition of the impactful nature of the groundbreaking research conducted by Michelson faculty comes in the form of numerous national and international awards:

- Dr. Steve Kay: awarded USC's 2023 Associates Award for Creativity in Research and Scholarship. The USC Associates Award is the highest honor the university bestows on its members for their distinguished achievements.
- Dr. Carl Kesselman: awarded the 2023 IEEE Internet Award from the Institute of Electrical and Electronics Engineers (IEEE), the largest global technical professional organization for the advancement of technology. The award salutation reads "For contributions to the design, deployment, and application of practical Internet-scale global computing platforms." Dr. Kesselman is also an IEEE Fellow.
- Dr. Shrikanth Narayanan: awarded the 2023 International Speech Communication Association (ISCA) Medal for Scientific Achievement, the most prestigious award offered by the ISCA in the field of human speech communication research at the global level.
- Dr. Eun Ji Chung: named 2023 BMES Grade of Fellow Class by the Biomedical Engineering Society Fellow. The Chung Laboratory and Co-PI Meena Madhur were also presented with the American Heart Association Collaborative Sciences Award for their research on novel T cell targeted nanomedicine approaches for hypertension.
- Dr. Isabella Suzuki: awarded the 2023 Agilent Fellowship, a prestigious two-year postdoctoral fellowship offered through USC's Agilent Center of Excellence in Biomolecular Characterization. Her research is focused on developing new and alternative therapeutic strategies for atherosclerosis.
- Drs. Vsevolod Katritch and Vadim Cherezov: named Web of Science (Clarivate) Highly Cited Researcher. Dr. Katritch was named in two categories: "Pharmacology & Toxicology" and "Biology & Biochemistry;" Dr. Cherezov was named in the "Biology & Biochemistry" category. The honor recognizes researchers who have demonstrated significant and broad influence reflected in their publication of multiple highly cited papers over the last decade. Of the world's population of scientists and social scientists, Highly Cited Researchers™ are 1 in 1,000.
- Dr. Yasser Khan: awarded the 2023 Google Research Scholar Award. The prestigious award will fund research to support a race-aware oximeter project to optimize racial bias correction in oximetry with Google's skin tone framework.
- Dr. Remo Rohs: named AAAS Fellow. The prestigious American Association for the Advancement of Science honor recognizes excellence in research, technology, industry and government, teaching, and communicating and interpreting science to the public.

We also congratulate the Michelson faculty promoted in 2023. Dr. Vadim Cherezov was appointed Ester Dornsife Chair in Biological Sciences and Professor of Chemistry. Dr.

Vsevolod Katritch was promoted to Full Professor, Quantitative and Computational Biology and Chemistry, Dornsife College. Both faculty are associated with the Bridge Institute, located at Michelson Hall. Congratulations also to Dr. Stacey Finley on her promotion to Professor of Biomedical Engineering and Quantitative and Computational Biology, Viterbi School of Engineering.

Research conducted by Michelson faculty also aligns with the goals of the Michelson Philanthropies' Found Animals Foundation. In 2023, the USC Office of Research & Innovation (OORI) created the *Alternative Methods to Animal Research Award (AMAR) Special Solicitation*, aiming to support research to develop alternative methods of testing and to replace and reduce the use of animals in research. Dr. Eun Ji Chung was one of two awardees funded through the program for her proposal *Screening combination therapy for ADPKD nanomedicine*. Autosomal dominant polycystic kidney disease (ADPKD) is the most common genetic kidney disease, but the one drug available is not efficacious, causes adverse effects, and does not target the kidney. Dr. Chung's research will identify drug combinations based on DNA methyltransferase inhibitors and ADPKD drugs that show drug synergy using human ADPKD mimetic systems in vitro toward future clinical trials.

Research Highlights

The featured article for this year's report is [*Computational approaches streamlining drug discovery*](#), by Drs. Anastasiia V. Sadybekov and Vsevolod Katritch, was published in the journal *Nature*. The article reviews "recent advances in ligand discovery technologies, their potential for reshaping the whole process of drug discovery and development, as well as the challenges they encounter;" it has been accessed over 59K times and is in the 99th percentile (ranked 1,900th) of the 398,874 tracked articles of a similar age in all journals and the 87th percentile (ranked 133th) of the 1,088 tracked articles of a similar age in *Nature*. Dr. Katritch authored/co-authored five articles published *Nature* journals in 2023.

We also highlight the two additional articles: [*Detecting disruption of HER2 membrane protein organization in cell membranes with nanoscale precision*](#), by Drs. Yasaman Moradi, Jerry S. H. Lee, and Andrea M. Armani, published in *ACS Sensors*. Dr. Armani has developed light-emitting molecules capable of detecting subtle changes in HER2 organization and clustering within cells, providing researchers with a clearer picture of HER2 behavior, allowing the evaluation of thousands of cells at once, compared to the single-cell limitations of previous methods.

The second featured article, [*Agent-based modeling of tumor-immune interactions reveals determinants of final tumor states*](#), by Drs. Manal Ahmidoucha, Neel Tangellab and Stacey D. Finley, was published in *Molecular Imaging and Biology*. The authors investigate the interactions between tumor and immune cells in the tumor microenvironment and have developed a model to "predict how cell-specific properties influence tumor progression." The research suggests a "significant role of computational models in unraveling the intricate dynamics of tumor-immune interactions and their potential for guiding the development of tailored immunotherapeutic strategies."

We celebrate the scientific breakthroughs and social impact of Michelson faculty, passionate innovators and tireless pioneers in the fight for a healthier future, dedicated to pushing boundaries and paving new frontiers in medicine. The research supported by the Michelson Center is fueled by Dr. Michelson's vision to develop new life-saving devices and therapeutics, to reach "undreamed-of advances in the biological sciences in the near future" and ultimately "make life less unfair."

The Michelson Center for Convergent Bioscience is a testament to Dr. Michelson's visionary leadership, building a brighter tomorrow through the power of scientific excellence.

Silvia da Costa, Ph.D.

Director, Research Initiatives and Infrastructure

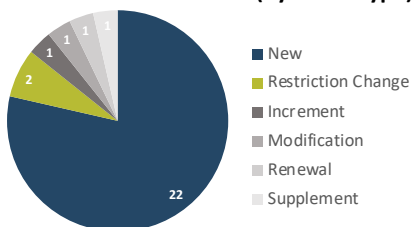
Fundraising & Financials

Data reflect a reporting period from January 1 to December 9, 2023 of grants submitted by/awarded to Michelson faculty.

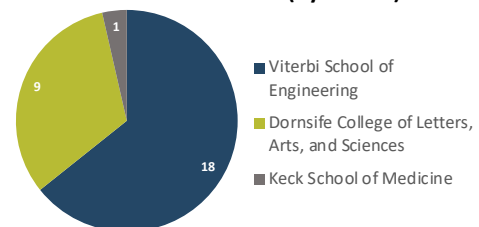
Proposals Awarded

	Grant proposals awarded as PI	
	# of proposals	Total obligated
Carl Kesselman	2	\$1,183,304.00
Cristina Zavaleta	1	\$693,108.00
Demetri Christodoulides	1	\$136,458.00
Ellis Meng	1	\$5,000.00
Eun Ji Chung	3	\$897,320.00
James Boedicker	1	\$200,000.00
Jayakanth Ravichandran	2	\$283,580.00
Justin Haldar	1	\$836,443.00
Khalil Iskarous	1	\$599,998.00
Krishna Nayak	1	\$525,550.00
Laura Shin	1	\$400,638.00
Mahta Moghaddam	1	\$190,000.00
Maryam Shanechi	1	\$113,475.00
Mercedeh Khajavikhan	1	\$60,000.00
Moh El-Naggar	1	\$185,250.00
Morteza Dehghani	1	\$999,393.00
Peter Kuhn	4	\$4,186,534.00
Shrikanth Narayanan	3	\$3,686,585.00
Steven Finkel	1	\$448,800.00
Total	28	\$15,631,436.00

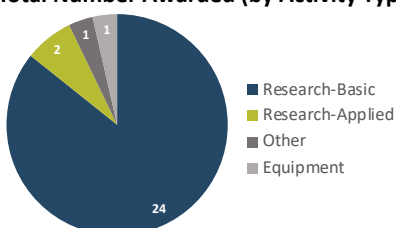
Total Number Awarded (by Grant Type)



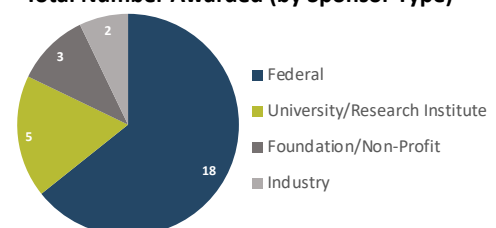
Total Number Awarded (by School)



Total Number Awarded (by Activity Type)



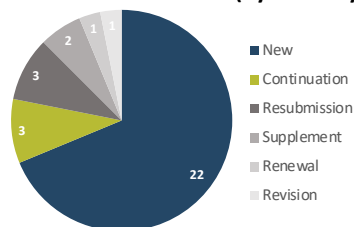
Total Number Awarded (by Sponsor Type)



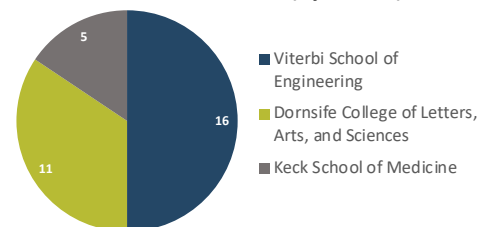
Proposals Submitted

	Grant proposals submitted as PI	
	# of proposals	Total requested
Carl Kesselman	2	\$3,204,308.00
Charles McKenna	1	\$444,000.00
Dong Song	1	\$1,455,085.00
Ellis Meng	1	\$3,253,949.00
Jennifer Treweek	1	\$168,244.00
Jeremy Mason	1	\$149,947.00
Kate White	2	\$822,163.00
Krishna Nayak	1	\$596,750.00
Maryam Shanechi	3	\$7,423,486.00
Morteza Dehghani	1	\$999,613.00
Niema Pahlevan	1	\$182,920.00
Peter Kuhn	4	\$5,683,021.00
Shrikanth Narayanan	3	\$760,655.00
Steve Kay	3	\$8,600,000.00
Vadim Cherezov	2	\$4,964,625.00
Vsevolod Katritch	1	\$8,602.00
William Mack	1	\$2,823,040.00
Yasser Khan	3	\$1,260,000.00
Total	32	\$42,800,408.00

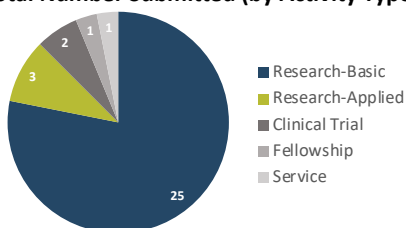
Total Number Submitted (by Grant Type)



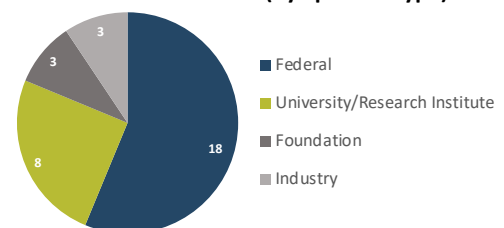
Total Number Submitted (by School)



Total Number Submitted (by Activity Type)



Total Number Submitted (by Sponsor Type)



Meet Our Faculty

Faculty and research teams are forging new frontiers in biomedical research, leading to life-saving therapies.

MICHELSON FACULTY



Andrea Armani, Ph.D.
USC Viterbi School of Engineering

Ray Irani Chair in Chemical Engineering and Materials Science and Professor of Chemical Engineering and Materials Science, Biomedical Engineering, Electrical Engineering-Electrophysics, and Chemistry



James Boedicker, Ph.D.
USC Dornsife College of Letters, Arts, and Sciences

Associate Professor of Physics and Astronomy and Biological Sciences



Dani Byrd, Ph.D.
USC Dornsife College of Letters, Arts, and Sciences

Professor of Linguistics



Vadim Cherezov, Ph.D.
USC Dornsife College of Letters, Arts, and Sciences

Professor of Chemistry, Physics & Astronomy



Eun Ji Chung, Ph.D.
USC Viterbi School of Engineering

The Dr. Karl Jacob Jr. and Karl Jacob III Early Career Chair and Assistant Professor of Biomedical Engineering, Chemical Engineering and Materials Science, Surgery, and Medicine



Moh El-Naggar, Ph.D.
USC Dornsife College of Letters, Arts, and Sciences

Dean's Professor of Physics and Astronomy, and Professor of Physics, Biological Sciences, and Chemistry

Diverse in age, ethnicity and expertise, and drawn from across a broad spectrum of research fields, ranging from computational sciences and applied mathematics to nanoengineering and biology, Michelson faculty create new collaborative interfaces and technological innovation spanning the entire science, engineering and medical enterprise.



Stacey Finley, Ph.D.
USC Viterbi School of Engineering

Gordon S. Marshall Early Career Chair
and Associate Professor of Biomedical
Engineering and Biological Sciences



Valery Fokin, Ph.D.
USC Dornsife College of
Letters, Arts, and Sciences

Professor of Chemistry



Peter Foster, Ph.D.
USC Dornsife College of
Letters, Arts, and Sciences

Assistant Professor of Physics and Astronomy



Scott E. Fraser, Ph.D.
Provost's Office

Provost Professor of Biological Sciences,
Biomedical Engineering, Physiology
and Biophysics, Stem Cell Biology and
Regenerative Medicine, Pediatrics, Radiology
and Ophthalmology Elizabeth Garrett
Chair in Convergent Bioscience; Director of
Science Initiatives



Cornelius Gati, Ph.D.
USC Dornsife College of
Letters, Arts, and Sciences

Assistant Professor of Biology



Justin Haldar, Ph.D.
USC Viterbi School of Engineering

Associate Professor of Electrical and
Computer Engineering and Biomedical
Engineering



James Hicks, Ph.D.

USC Dornsife College of
Letters, Arts, and Sciences

Research Professor, Biological Sciences



Khalil Iskarous, Ph.D.

USC Dornsife College of
Letters, Arts, and Sciences

Associate Professor of Linguistics



Rehan Kapadia, Ph.D.

USC Viterbi School of Engineering

Associate Professor of Electrical and
Computer Engineering



Vsevolod Katritch, Ph.D.

USC Dornsife College of
Letters, Arts, and Sciences

Assistant Professor of Biological Sciences
and Chemistry



Steve Kay, Ph.D., D.Sc.

Keck School of Medicine of USC

Director of Convergent Bioscience and
Provost Professor of Neurology, Biomedical
Engineering and Biological Sciences



Carl F. Kesselman, Ph.D.

USC Viterbi School of Engineering

William H. Keck Professor of Engineering
and Professor of Industrial and Systems
Engineering, Computer Science, Population
and Public Health Sciences, and Biomedical
Sciences



**Mercedeh Khajavikhan,
Ph.D.**

USC Viterbi School of Engineering

Professor of Electrical and Computer
Engineering



Yasser Khan, Ph.D.

USC Viterbi School of Engineering

Assistant Professor of Electrical and
Computer Engineering



Peter Kuhn, Ph.D.

USC Dornsife College of
Letters, Arts, and Sciences

Dean's Professor of Biological Sciences;
Professor of Medicine, Biomedical
Engineering, Aerospace & Mechanical
Engineering, and Urology



Gianluca Lazzi, Ph.D.
Keck School of Medicine of USC

Provost Professor of Ophthalmology, Electrical Engineering, Clinical Entrepreneurship and Biomedical Engineering; Fred H. Cole Professorship in Engineering; Director, Institute for Technology and Medical Systems; Director for Bioengineering Mentorship



Jeremy Mason, Ph.D.
Keck School of Medicine of USC

Assistant Professor of Research, Department of Urology



Charles E. McKenna, Ph.D.

USC Dornsife College of Letters, Arts, and Sciences

Professor of Chemistry & Pharmacology and Pharmaceutical Sciences



Ellis Meng, Ph.D.

USC Viterbi School of Engineering

Shelly and Ofer Nemirovsky Chair of Convergent Biosciences, Professor of Biomedical Engineering and Electrical and Computer Engineering and Vice Dean of Technology Innovation and Entrepreneurship



Shrikanth Narayanan, Ph.D.

USC Viterbi School of Engineering

University Professor and Niki & C. L. Max Nikias Chair in Engineering; Professor of Electrical and Computer Engineering, Computer Science, Linguistics, Psychology, Neuroscience, Otolaryngology-Head and Neck Surgery, and Pediatrics; Research Director, Information Science Institute; Director, Ming Hsieh Institute



Krishna S. Nayak, Ph.D.

USC Viterbi School of Engineering

Professor of Electrical and Computer Engineering, Biomedical Engineering, and Radiology; Director, Dynamic Imaging Science Center; Director, Signal and Image Processing Institute; Director, Magnetic Resonance Engineering Laboratory



Niema Pahlevan, Ph.D.

USC Viterbi School of Engineering

Assistant Professor of Aerospace and Mechanical Engineering



Jayakanth Ravichandran, Ph.D.

USC Viterbi School of Engineering

Associate Professor of Chemical Engineering and Materials Science



Richard W. Roberts, Ph.D.

USC Dornsife College of Letters, Arts, and Sciences

Professor and Chair, Mork Family Department of Chemical Engineering and Materials Science and Professor of Chemistry, Chemical Engineering, and Biomedical Engineering

**Remo Rohs, Ph.D.**USC Dornsife College of
Letters, Arts, and SciencesProfessor of Biological Sciences, Chemistry,
Physics & Astronomy, and Computer Science**Maryam Shanechi, Ph.D.**

USC Viterbi School of Engineering

Associate Professor of Electrical and
Computer Engineering**Terry Takahashi, Ph.D.**USC Dornsife College of
Letters, Arts, and Sciences

Assistant Professor (Research) of Chemistry

**Ye Tian, Ph.D.**

USC Viterbi School of Engineering.

Research Assistant Professor of Electrical
and Computer Engineering**Jennifer Treweek, Ph.D.**

USC Viterbi School of Engineering

Assistant Professor of Biomedical
Engineering**Kate White, Ph.D.**USC Dornsife College of
Letters, Arts, and SciencesGabilan Assistant Professor of Chemistry;
Director, Pancreatic Beta Cell Consortium
(PBCC)**Cristina Zavaleta, Ph.D.**

USC Viterbi School of Engineering

Assistant Professor of Biomedical Engineering

“We try to go into areas that nobody else wants to go. We try to lead with the principles that Dr. Michelson made all his devices and discoveries with: Be innovative, don’t be afraid to disrupt things, and be creative.”

Alya Michelson

Institutes & Centers

More than just buildings and equipment, research centers and institutes are vibrant networks, sustained with the energy of intellectual exchange and driven by a shared ambition to make the world a better place.

Michelson Hall serves as a nexus for interdisciplinary research excellence, housing five centers and institutes and providing the infrastructure and staff to support a diverse network of scientists, engineers and scholars from the USC Dornsife College of Letters, Arts and Sciences, USC Viterbi School of Engineering and Keck School of Medicine at USC.

Fostering both national and international partnerships, centers leverage the collective expertise of diverse research communities, enriching inquiry and accelerating innovation. Centers and institutes provide strategic direction and foster creative breakthroughs by dismantling disciplinary silos and nurturing the emergence of paradigm-shifting discoveries. This robust infrastructure actively embodies Dr. Gary Michelson's vision of a "more open, convergent, and information-sharing approach" to research.

By removing disciplinary walls and promoting collaborative knowledge exchange, Michelson Hall empowers researchers to strive to meet Dr. Michelson's objective to "work smarter," not just harder, propelling scientific progress into a paradigm of collective intelligence and impactful discovery. Importantly, Michelson Hall centers and institutes prioritize the highest ethical standards and social responsibility in the conduct of science, upholding the core principles of research integrity, ensuring discoveries not only illuminate fundamental knowledge but also address pressing societal challenges to achieve real-world impact.

Michelson Center Events

Co-sponsored by the Center for New Technologies in Drug Discovery and Development (CNT3D), the USC Michelson Center for Convergent Bioscience, the MESH Academy and the Bridge Institute, the CNT3D hosted its first [*Drug Discovery Innovation Workshop*](#) aiming to catalyze USC drug discovery and to spark drug research across the university. The workshop, held on February 22, 2023, brought together over 170 scientists from USC and the SoCal biotech community to discuss new ways to expand and accelerate drug discovery efforts and develop new drug discovery technologies.

Awards

CNT3D was awarded \$300,000 by Dornsife College for a Phase II study for Dornsife faculty-led initiatives. The award will support CNT3D growth, and facilitate research and educational activities, including new courses, seminars and yearly Drug Discovery Innovation Workshop.



The Bridge Institute

Institute Directors:

Dr. Scott Fraser, Director, Provost Professor of Biological Sciences and Biomedical Engineering, Elizabeth Garrett Chair of Convergent Biosciences

Dr. Kate White, Associate Director, Gabilan Assistant Professor of Chemistry, Director of the Pancreatic Beta Cell Consortium

Angela (Angie) Walker, Assistant Director, Bridge Institute

The Bridge Institute aims to create a paradigm shift in academic exploration, disrupting the conventional research landscape by fostering transdisciplinary convergence for radical progress in improving the human condition. Building upon the Michelson Center for Convergent Bioscience Initiative, it represents a nexus of intellectual capital, uniting renowned faculty from the USC Dornsife College of Letters, Arts and Sciences, the USC Viterbi School of Engineering, and the Keck School of Medicine of USC, as well as animators and cinematographers in the USC School of Cinematic Arts and the USC Institute for Creative Technologies, and technology transfer experts in the USC Stevens Center for Innovation.

It functions as a platform to untether the power of humanities and social sciences to inform scientific inquiry and ethical considerations; to bridge the gap between theoretical frameworks and practical solutions, translating scientific breakthroughs into tangible impact and to facilitate medical advancements through synergistic collaborations with engineers and artists. It reimagines healthcare delivery and patient experience and, importantly, it injects artistic vision and narrative power into scientific communication, fostering public engagement and amplifying the impact of research. In doing so, it accelerates the translation of discoveries from bench to bedside and beyond, ensuring societal benefit from intellectual pursuits.

This convergence of expertise creates a potent launchpad for groundbreaking projects that defy disciplinary boundaries. From biomimetic robotics to AI-powered medical diagnostics, the Bridge Institute fosters interdisciplinary collaborations that push the frontiers of knowledge and address pressing global challenges.



Center for Discovery Informatics (CDI)

Center Director:

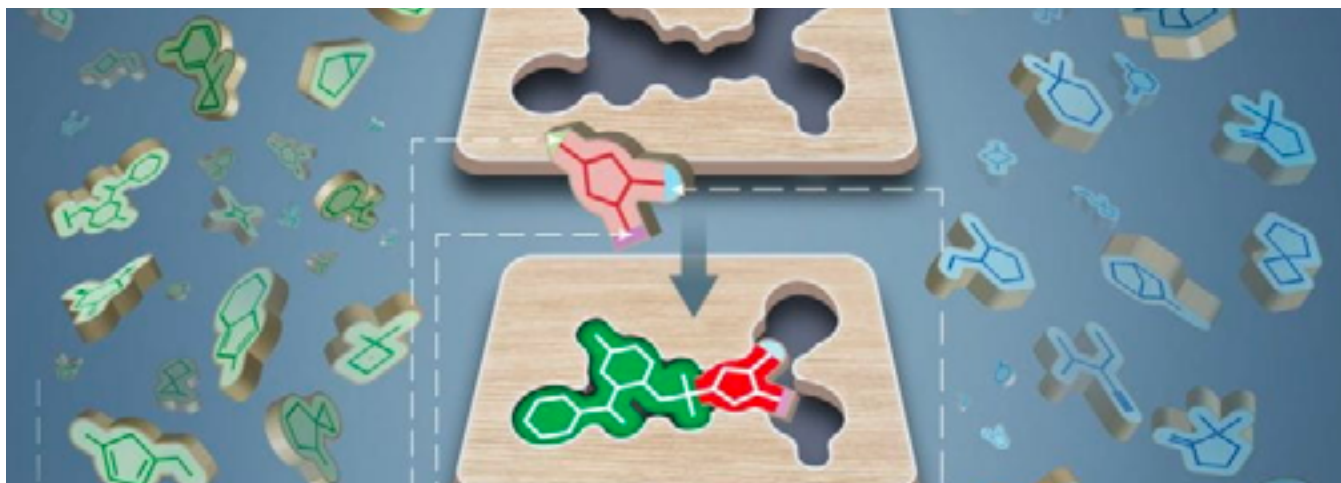
Dr. Carl Kesselman, William H. Keck Professor of Engineering, Professor, Epstein Department of Industrial and Systems Engineering, Fellow, Information Sciences Institute, Viterbi School of Engineering

Convergent bioscience research thrives in the fertile ground of interdisciplinarity, where diverse data streams from microscopy, mass spectrometry, flow cytometry, sequencing, and other modalities interweave into a rich tapestry of knowledge. At CDI, discovery informatics plays an integral and critical role to address the challenges associated with data management by providing the fundamental abstractions, methods, and infrastructure to enable transformative discovery in complex biological systems.

CDI bridges the gap between data and breakthroughs in bioscience. By providing user-friendly tools and high-performance computing, and based on a data-driven foundation, it equips researchers to navigate complex data and uncover hidden insights, fueling new discoveries and personalized healthcare solutions.

CDI supports collaborating scientists to address the significant and challenging issue of how to better capture, organize and share data as part of the discovery process, and to understand how intertwining technology, with the daily practice of science, can create opportunities to develop and integrate advanced analysis, data mining, visualization and interaction methods.

The center's innovative research program pioneers new approaches to data management and analysis, pushing the boundaries of what's possible in complex biological systems. By combining expertise in computer science and informatics, the center fosters a collaborative environment, transforming how knowledge is created, explored, and translated into tangible benefits for humankind.



Center for New Technologies in Drug Discovery and Development (CNT3D)

Center Directors:

Dr. Vsevolod "Seva" Katritch, Professor of Quantitative and Computational Biology and Chemistry
Dr. Charles McKenna, Professor of Chemistry and Pharmacology & Pharmaceutical Sciences

The Center for New Technologies in Drug Discovery and Development (CNT3D) was established as a research center at Dornsife College and joined Michelson Hall in 2022. The center harnesses the power of cutting-edge technologies like AI, machine learning, computational chemistry, and structural biology to drug discovery and development, making it affordable and accessible for researchers. Its goal is to serve the USC and broader SoCal biomedical community by facilitating cost-effective and well-curated entry points into drug discovery at the molecular level.

One of the key platforms of the center includes V-SYNTHES, a giga-scale structure-based virtual screening technology for hit and lead discovery. V-SYNTHES employs a modular approach to perform fast structure-based screening of combinatorial chemical spaces of billions or even trillions of compounds to predict those with high therapeutic potential. Selected make-on-demand compounds from such chemical spaces, e.g. the REAL Space, can then be easily synthesized and tested, streamlining the discovery process.

CNT3D supports USC researchers and scientists, paving the way for seamless preclinical and clinical development, accelerating the journey from the lab to the bedside. The aim is more than just drug discovery — it's a path towards a healthier future, one groundbreaking molecule at a time.



Convergent Science Institute in Cancer (CSI-Cancer)

Institute Directors:

Dr. Peter Kuhn, Director, Dean's Professor of Biological Sciences and Professor of Medicine, Biomedical Engineering, and Aerospace & Mechanical Engineering and Urology

Dr. James Hicks, Deputy Director, Research Professor of Biological Sciences

Dr. Jeremy Mason, Director of Data Science, Assistant Professor of Research, Urology

Dr. Liya Xu, Director of Applied Genomics, Assistant Professor of Research, Ophthalmology, CHLA
Allison Welsh, Director of Finance

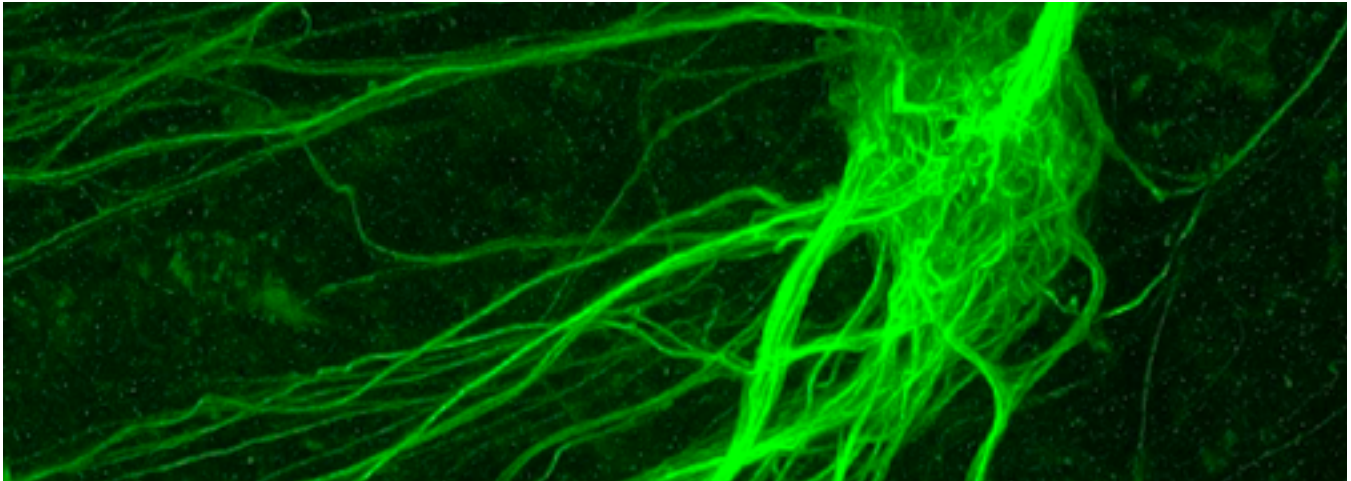
Elvia Nunez, Director of Research Administration

USC Michelson Center's Convergent Science Institute in cancer (CSI-Cancer) seeks to bridge the gap between clinical observations and mechanistic insights to unify patient, model system, and high-content single-cell data. This approach translates clinical observations into a mechanistic understanding of cancer dynamics, from cellular interactions to population-level trends. Spatiotemporal analysis of disease progression forms the research core, encompassing both lab experiments and human population studies. This deep understanding fuels the development of precision therapies that disrupt the progressions of the disease, leading to transformative breakthroughs in cancer treatment.

The center fosters a robust interdisciplinary network across USC (Viterbi, Dornsife, Keck, Norris Cancer Center, Roski Eye Institute, and Stevens Center for Innovation) and beyond (federal/state agencies, private/corporate partners, hospitals and research facilities). This network fuels collaboration on evolving physical sciences concepts with potential to address specific cancer challenges, aligning with both CSI-Cancer's framework and broader scientific community priorities.

The center is grounded on three complementary aims: characterizing the quantitative dynamics of cancer progression from localized to disseminated stages, delineating the evolving complexity and phenotypic diversity of a cancer through its life cycle, and delineating the temporal dynamics of disease in good-prognosis and poor-prognosis patient populations.

Educational outreach is also an important component of the center's activities. In partnership with Neighborhood Academic Initiative (NAI), a number of CURE students from the REACH program led a five-session workshop at USC for 110 local high school students. The Cancer Undergraduate Research Experience (CURE) program is the undergraduate program of USC Michelson CSI-Cancer.



Translational Imaging Center (TIC)

Center Directors:

Dr. Scott Fraser, Director, Director of Science Initiatives, Provost Professor of Biological Sciences and Biomedical Engineering, Elizabeth Garrett Chair of Convergent Biosciences

Dr. Francesco Cutrale, Assistant Director, Assistant Professor (Research) Viterbi

Dr. Thai V Truong, Assistant Director, Assistant Professor (Research) Dornsife

Dr. Le A Trinh, Assistant Director, Associate Professor (Research) Dornsife

The Translational Imaging Center (TIC) serves dual, complementary roles as a research center and user facility and is led by Dr. Scott Fraser, who also serves as director of the Michelson Center's Bridge Institute. The Center fuels breakthrough discoveries by developing transformative imaging technologies that push the boundaries of resolution, speed, and depth, empowering scientists to explore the unseen landscape of biological complexity addressing the world's most pressing biological challenges. It is home to a vibrant community of renowned scientists from diverse fields - biology, physics, engineering, chemistry, and mathematics. This collaborative spirit is further enriched by scientific partnerships, both within USC and across the globe.

The center empowers the research community with a state-of-the-art arsenal of microscopy tools, encompassing cutting-edge commercial multiphoton and confocal laser scanning systems, advanced optical coherence tomography, and high-resolution MRI microscopy. Beyond commercial offerings, the center boasts custom-built Light Sheet systems, further pushing the boundaries of imaging capabilities.

TIC's research scope spans embryonic development, genetics, and neuroscience, united by a shared mission: utilizing cutting-edge imaging to visualize living processes within organisms. This approach bridges basic science and medicine, propelling discoveries that translate into innovative biomedical devices and treatments for diverse diseases, from eye conditions to cancer.

Core Facilities

Dedicated researchers driven by a shared passion for scientific discovery.

A collaborative spirit meets cutting-edge technology at Michelson Hall's shared cores. They provide investigators from diverse disciplines access to sophisticated facilities, tools, world-class technical expertise, specialized consultation services and state-of-the-art instrumentation. In addition to providing equipment, Michelson Hall fosters the synergy that breaks down research walls, fuels interdisciplinary breakthroughs, tackling challenges and forging discoveries that resonate within USC, nationally and internationally.

Core facilities provide fee-for-service to researchers. They consolidate resources, providing equitable access to niche and emerging areas of research and increasing access to instrumentation and services that could otherwise be prohibitively expensive. The five cores housed at Michelson Hall offer a broad range of technical expertise, specialized consultation services and state-of-the-art instrumentation to researchers, including robotics, imaging, biomolecular characterization, development of new peptides and antibody-like proteins, among many others.

In 2023, Michelson Hall core facilities invoiced over \$885,000 in charges to USC users, not including income derived from charges made to non-USC researchers in industry and academia.

Catalyzing Innovation Through Academia-Industry Collaboration

Michelson Center cores facilitate transformative partnerships between academia and industry, fostering instrument development capacity within academic settings. These collaborations result in viable products with wide scientific and commercial reach, propelling groundbreaking research and

solutions to complex problems, ultimately driving economic growth.

Michelson Center's Dynamic Imaging Science Center core facility is an example of an academia/industry partnership between USC's Viterbi School of Engineering and Siemens "healthineers." The Agilent Center of Excellence (COE) in Biomolecular Characterization core facility, housed at Michelson Hall since the core's opening in 2018, is another example of such a collaboration and serves as the cornerstone of a larger partnership between USC and Agilent to accelerate fundamental discoveries in life sciences research.

The Agilent COE also supports the Agilent Fellows program. Each year, one Agilent Fellow is selected for a non-renewable two-year postdoctoral fellowship. Dr. Isabella Suzuki was named the 2023 Agilent Fellow. She joined USC in February 2023 and is currently a postdoctoral scholar in Dr. Eun Ji Chung's Laboratory. Her research is focused on developing new and alternative therapeutic strategies for atherosclerosis, a disease characterized by the rupture of plaques, which is highly associated with mitochondrial dysfunction. The main goal of Isabella's project is to evaluate the benefits of nanoparticle-mediated delivery of a specific microRNA (miR-145) on mitochondria function as an alternative therapy for atherosclerosis.

USC Support of Core Facilities

In 2023, the USC Office of Research & Innovation (OORI) invested \$2.15 million in a game-changing program that empowers researchers with access to top-of-the-line equipment. This initiative equips core facilities with cutting-edge instruments, not only expanding access for researchers but also

nurturing the development of groundbreaking new equipment. The award program fosters collaborations between researchers and industry partners to create instruments with wider applicability and the potential to unlock entirely new research avenues. It also supports the training of future leaders, allowing graduate and undergraduate students to gain invaluable hands-on experience with industry-standard equipment, preparing them for successful careers in research.

In June 2023, Dr. Jayakanth Ravichandran, Philip and Cayley MacDonald Endowed Early Career Chair and Associate Professor of Chemical Engineering and Materials Science and Electrical and Computer Engineering was awarded \$450,000 from the OORI Instrumentation Award for the proposal *Novel instrumentation of advanced materials: from nanoscale manipulation to characterization* for the purchase of a Scanning Electron Microscope (SEM)/ Focused Ion Beam (FIB) to be housed at Michelson's Center of Excellence in Nano Imaging core. This is the second consecutive year Dr. Ravichandran was awarded through the Instrumentation Award program. In 2022 he was awarded \$650,000 for the proposal *Chemical analysis from atomic to bulk length scales* for the purchase of a Kratos AXIS Supra+ : XPS surface analysis instrument.

The OORI Instrumentation Award aims to establish and bolster USC's research infrastructure by supporting the purchase of shared instrumentation and further preparing faculty to submit large-scale instrumentation grants to external sponsors. The program also facilitates the acquisition of new instrumentation by encouraging and supporting the submission of instrumentation grant proposals to federal agencies, such as the National Institutes of Health S10 program and the National Science Foundation Major Research Instrumentation (MRI) program, as well as to other federal and state agencies and private foundations.

A portrait of Dr. Isabella Suzuki, a woman with long dark hair, wearing a white button-down shirt and a gold heart necklace. She is smiling and looking towards the camera. In the background, there is laboratory equipment, including a stack of blue boxes labeled 'HPLC Columns'.

© 2023 Agilent Fellow — Dr. Isabella Suzuki



Agilent Center of Excellence in Biomolecular Characterization

Located at Michelson since 2018.

Core Directors:

Dr. Valery Fokin, Professor of Chemistry

Dr. Richard Roberts, Professor of Chemistry

The Agilent Center of Excellence in Biomolecular Characterization was established as a partnership between USC and Agilent technologies with the goal to converge researchers across science and engineering to work together on multidisciplinary approaches for the development of new drugs, diagnostics, and medical devices. The center features first-in-class research instruments ranging from advanced mass spectrometry, chromatography, robotic high-throughput reaction screening, genomics, and optical characterization.



John O'Brien Nanofabrication Laboratory

Located at Michelson since 2021. Opened for operations in 2022.

Core Directors:

Dr. Rehan Kapadia, Director, Associate Professor of Electrical and Computer Engineering
Dr. Shiva Bhaskaran, Associate Director, Nanofabrication Laboratory

The vision behind the design of the John O'Brien Nanofabrication Laboratory is to move beyond conventional silicon processing. The breadth of instrumentation enables the core to support diverse research activities, from fundamental quantum transport studies to nano/bioconvergent research. Enabling interdisciplinary research with next generation nanomaterials is a strong focus of the facility. This emphasis is unique among nanofabrication facilities and enables researchers to translate novel materials into transformational devices for a wide range of applications.

In September 2023, the Defense Department awarded nearly \$27M for a USC-led Microelectronics Commons project. The university will lead a coalition of research and industry organizations with the power to accelerate the development and manufacturing of microelectronics in the United States.

"This is a really big deal," Dr. Rehan Kapadia stated. "We're trying to figure out a way to build the connective tissue between what we would call academic-scale labs — like what we have here at USC's John O'Brien Nanofabrication Laboratory and what Caltech and UCSB have — and the high-volume manufacturing fabrication making millions of devices."

In a conservative environment, innovation is frequently slowed down; it is therefore necessary to establish an open innovation ecosystem that relies on the complementary strengths of different actors. Here, the user often plays a central role and liaises expertise from cores with tech providers. Leading institutes have realized that innovation has become a novel and extra mandate for their cores on top of the daily service activities. Not to innovate is no longer an option if you want to stay in the game.

EMBO reports, Science and Society (2019) 20: e48017



Dynamic Imaging Science Center

Located at Michelson since 2021. Opened for operations in 2022.

DISC Management and Oversight Board:

Dr. Dani Byrd, Professor of Linguistics

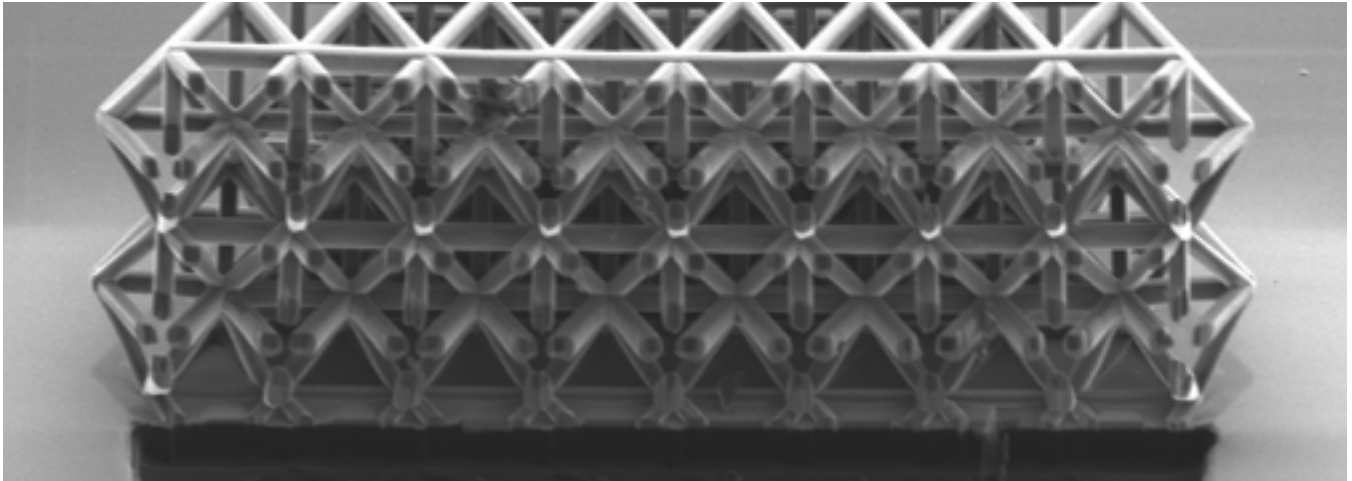
Dr. Justin Haldar, Associate Professor of Electrical Engineering

Dr. Khalil Iskarous, Associate Professor of Linguistics

Dr. Shrikanth Narayanan, Professor and Niki and Max Nikias Chair in Engineering

Dr. Krishna Nayak, Professor, Viterbi ECE Systems

The mission of the Dynamic Imaging Science Center (DISC) is to better understand the science of human movement in health and disease through the development and use of non-invasive imaging. The center is supported by the National Science Foundation, the Viterbi School of Engineering, and Siemens "healthineers." It is home to an ultra-rare low field MRI machine, one of only three of its kind in the world, which is being used in research at Viterbi to develop "forever implants" to better understand when implants are failing, and to help manufacturers optimize new devices and doctors avoid unnecessary surgeries.



Center of Excellence in Nano Imaging

Located at Michelson since 2021.

Core Directors:

Dr. Jayakanth Ravichandran, Associate Professor of Chemical Engineering and Materials Science
Dr. James Boedicker, Associate Professor of Physics and Astronomy and Biological Sciences

The Center of Excellence in Nano Imaging (CNI) provides state-of-the-art imaging and characterization capabilities to the university and research communities. Its mission is to promote and advance the science and application of research tools for imaging, visualization, and analysis of nano- through meso-scale features and structures, both man-made and natural, including biological structures.



Center for Peptide and Protein Engineering

Located at Michelson since 2018.

Core Directors:

Dr. Richard Roberts, Professor of Chemistry, Chemical Engineering and Materials Science and Biomedical Engineering

Dr. Terry Takahashi, Assistant Research Professor of Chemistry

Peptides and proteins are the cornerstones of existing technology in biological recognition, diagnostics and human therapies. The Center for Protein and Peptide Engineering (CPPE) is advancing the field of protein and peptide engineering, similar to the gains seen when the assembly line was introduced, by providing high-throughput generation of new reagents that recognize proteins and biological molecules.

Scientific & Social Impact

Current scientific challenges cut across the traditional boundaries of disciplines and the lifecycle of innovation — from research, to knowledge development, to its clinical application. Public understanding and engagement with science, and citizen participation — including through the popularization of science — are essential to equip citizens to make informed personal and professional choices. The scientific and social impact of the groundbreaking research being conducted at the Michelson Center is presented here — research that addresses societal needs and global health challenges.

Faculty

Andrea Armani

Events

Speaker: *Organic small molecule based photonic devices*. [Welch Foundation & Robert B. Trull Lectureship in Engineering](#), at the McKetta Department of Chemical Engineering, University of Texas at Austin, March 4, 2023.

In the News

Cancer illuminated: A new light on HER2 detection: Dr. Armani and her Ph.D. student, Yasaman Moradi, have unveiled a light-emitting molecule capable of detecting subtle changes in HER2 organization and clustering within cells. This protein, found on the cell surface, plays a crucial role in both breast cancer diagnosis and treatment. Dr. Armani's groundbreaking technology seamlessly integrates with existing imaging methods, including the high-throughput

platforms used in pharmaceutical research. This compatibility allows scientists to analyze entire cell plates simultaneously, significantly increasing efficiency. As Dr. Armani explained, "We can now evaluate thousands of cells at once, compared to the single-cell limitations of previous methods." This translates to faster results at a fraction of the cost. This innovative technique holds immense promise for the future of cancer research and treatment. By providing researchers with a clearer picture of HER2 behavior and its response to therapeutic interventions, Dr. Armani's work paves the way for the development of more targeted and effective cancer therapies. Reported in [USC Viterbi News](#), November 14, 2023.

Lab on a chip: Nanomedicine takes the stage— the podcast interview with Dr. Armani explored the current state of lab on chip

New Fluorescent Probe Illuminates Breast Cancer

Vadim Cherezov Appointed Chair

technology, developments in nanomedicine, commercialization and its potential to reshape the future of medicine. Dr. Armani shed light on the latest advancements and breakthroughs in this rapidly evolving field, highlighting its potential to revolutionize diagnostics and healthcare delivery, providing insights into the cutting-edge research and applications of nanomedicine, from targeted drug delivery to personalized medicine. Reported in [PhotonicsMedia](#), October 24, 2023.

James Boedicker

Events

Speaker: The collective motion and merging of macroscopic bacterial aggregates.
[American Physical Society](#) March meeting, Las Vegas, NV, March 10, 2023.

Dani Byrd

Training the Next Generation

Hosted: Open House tour and seminar of the USC Dynamic Imaging Science Center for incoming PhD students for the USC Dornsife Linguistics Department, March 2023.

Vadim Cherezov

Honors & Awards

Appointed: Ester Dornsife Chair in Biological Sciences and Professor of Chemistry.
Reported in [USC Dornsife News](#), October 23, 2023.

In the News

Shining a light on cancer: Targeting the Artemis: DNA-PKcs complex: Dr. Go Watanabe and his team at the Michelson Center have made a groundbreaking discovery in the fight against cancer. They have successfully visualized and characterized the basal state of the Artemis:DNA-PKcs complex, a protein pairing crucial for DNA repair in cancer cells. This pioneering work has revealed previously unknown binding

sites for Artemis on DNA-PKcs, opening a new avenue for the development of targeted cancer therapies. By blocking the formation of the Artemis:DNA-PKcs complex, scientists could potentially disrupt the DNA repair mechanisms that cancer cells rely on for survival and proliferation. This would effectively halt their growth and spread, offering a promising new approach to cancer treatment. The significance of Dr. Watanabe's research lies in its potential to pave the way for the development of more effective and personalized cancer therapies. By targeting specific binding sites on the Artemis:DNA-PKcs complex, scientists can design drugs that are highly selective and have minimal side effects compared to traditional treatment options. Reported in [Research Outreach](#), February 10, 2023.

Eun Ji Chung

Honors & Awards

Awarded: *2023 BMES Grade of Fellow Class.* Dr. Chung received the meritorious honor of being named Biomedical Engineering Society Fellow. The honor recognized her pioneering drug delivery strategies for new diseases and indications as well as her mentoring and supporting the diversity of the next generation of biomedical engineers. Reported in [Biomedical Engineering Society](#), August 31, 2023.

Awarded: *The American Heart Association Collaborative Sciences Award* was presented to the [Chung Laboratory and Co-PI Meena Madhur](#), on their research on *Novel T cell targeted nanomedicine approaches for hypertension*. (July, 2023).

Postdoc award: Supervised a postdoctoral researcher in the USC Alfred E. Mann Department of Biomedical Engineering, Dr. Isabella Suzuki, who was awarded the 2023 Agilent Fellowship, a prestigious two-year postdoctoral fellowship offered through USC's Agilent Center of Excellence in Biomolecular

Targeting the Artemis: DNA-PKcs Complex

Eun Ji Chung Named 2023 BMES Fellow



Characterization. The Center is the result of a partnership between Agilent Technologies and the USC Michelson Center for Convergent Bioscience. Reported [USC News](#), February 23, 2023.

Funding

Awarded: *Novel approaches for advancing musculoskeletal regeneration*. DoD PRMRP IIRA (PI: Evseenko, Role: Co-I). January, 2024.

Awarded: *Screening combination therapy for ADPKD nanomedicine*. USC Research and Innovation Alternative Methods to Animal Research Award (as PI). January 2024.

Awarded: *Engineering urinary extracellular vesicles for ADPKD Therapy*. NIH NIDDK. Innovative Science Accelerator Program (PI), November, 2023.

Awarded: *mRNA Delivery for polycystic kidney disease*. Department of Defense (DoD) Congressionally Directed Medical Research Program (CDMRP) Discovery Award (as PI). October, 2023.

Awarded: *Screening combination therapy for ADPKD nanomedicine*. Alternative Methods to Animal Research Award (PI) grant, USC Research and Innovation awards program. September, 2023.

Awarded: *Resource development core*, 1U54DK137516-01 grant (PI and Director). NIH, National Institute of Diabetes and Digestive and Kidney Diseases. Northwestern University O'Brien Kidney National Resource Center. September, 2023.

Awarded: *Investigation of urinary extracellular vesicles as novel and safe therapeutics for autosomal recessive polycystic kidney disease*, 1R21HD113263-01 grant (PI). NIH, Eunice Kennedy Shriver National Institute of Child Health and Human Development. September, 2023.

Awarded: *T cell targeted nanomedicine for immune modulation in cardiovascular disease*. American Heart Association, Collaborative Sciences Award (MPI: Madhur and Chung). August 2023.

Awarded: *Safety investigation of citric acid-based materials on marine life*. National Oceanic and Atmospheric Administration Sea Grant to support early-stage project for evaluating the effects of biodegradable materials on marine life. The Sea Grant's mission is to enhance the practical use and conservation of coastal, marine and Great Lakes resources in order to create a sustainable economy and environment. May 2023.

Events

Moderator: [Renal Mechanisms](#), American Heart Association - Hypertension Conference, Boston, MA, September 9, 2023.

Speaker: *Nanomedicine for genetic and chronic diseases*. [Moving Targets Symposium, Advances in Drug Delivery Systems](#). American Association of Pharmaceutical Scientists, USC School of Pharmacy, Los Angeles, CA, August 17, 2023.

Speaker: *Designing nanomedicine for polycystic kidney disease*. Biochemistry and Molecular Biology/PKG Joint Seminar, [Mayo Clinic](#), May 23rd, 2023.

Speaker: *Designing nanoparticles for the kidney*. [W. M. Keck Science Department](#), April 14, 2023.

Speaker: *Combining metformin and drug-loaded kidney-targeting micelles for PKD*. World Congress of Nephrology ([WCN](#)), March 29-April 2, 2023.

Speaker: *Combining metformin and drug-loaded kidney-targeting micelles for polycystic kidney disease*. [Biomedical Engineering Seminar Series](#), Department of Biomedical Engineering, an interdisciplinary program of Translational Biomedical Research

Isabella Suzuki Awarded 2023 Agilent Fellowship

Moh El-Naggar at Symposium

with the Institute of Engineering-Driven Medicine, Stony Brook University, March 22, 2023.

Hosted: [Andy Tay](#) as seminar speaker from National University of Singapore, March 8, 2023.

Speaker: *Nanomedicine for genetic kidney diseases*. Engineering for Mental Health. University of Southern California, January 27, 2023.

Moh El-Naggar

Events

Speaker: *Symposium on noncommutative algebras*, in honor of Dr. Susan Montgomery and her contributions to mathematics and women in science and engineering, and to celebrate her birthday. In Susan's honor, the leadership award was changed to the "M. Susan Montgomery Leadership Award for PhD Students and Postdoctoral Scholars." Women in Science and Engineering ([WISE USC](#)), April 14, 2023.

In the News

Converting bacterial activity to batteries + new electronics. USC Dr. Moh El-Naggar, Dean's Professor of Physics and Astronomy and Professor of Physics and Astronomy and Chemistry and Divisional Dean for the Physical Sciences and Mathematics, explains the possibility of garbage powering our devices, by turning waste into electricity. Reported in [USC Dornsife Twitter](#), July 6, 2023.

Stacey Finley

Events

Speaker: *Modeling the effects of cell-cell interactions in the tumor microenvironment*, H. Lee Moffitt Cancer Center, Cancer Biology and Evolution, Florida, September 2023.

Speaker: [Mathematical oncology: Revealing quantitative insights into the tumor microenvironment](#), Ohio State University

Center for Engineering Cancer Research Summit, Columbus, OH, September 13, 2023.

Speaker: *Exploring the tumor-immune ecosystem using computational modeling*. [USC San Diego Jacobs School of Engineering](#), May 19, 2023.

Co-Chair: [12th Annual Southern California Systems Biology](#) (SoCal SysBio) meeting at USC. USC Michelson Building for Convergent Bioscience. April 29, 2023.

In the News

Co-Chair: *2023 Biomedical Engineering Society Annual Meeting*. USC Viterbi research and thought leadership were highlighted in 25 research and panel sessions at the leading event for biomedical engineering research and innovation. Reported in [USC Viterbi News](#), October 26, 2023.

Valery Fokin

Events

Hosted: *Agilent Sustainability Program Introduction Seminar* (by Agilent at USC). July 17, 2023.

Training the Next Generation

Participant: [USC 2023 Industry Days](#). The event provided physical and life science undergraduate and graduate students at Dornsife College the opportunity to meet with industry representatives and hear about career opportunities. April 3-4, 2023.

Peter Foster

Events

Speaker: *From cytoskeletal assemblies to living machines*. [Soft Matter Colloquium](#). Cal State Long Beach, October 30, 2023.

Attendee: [The soft and sustainable building blocks of living and active systems](#). Gordon Research Conference, August 13-18, 2023.



Garbage Powering Our Devices

Stacey Finley Co-Chairs 2023 BMES

© Straughan Photography

Training the Next Generation

Co-organizer: Physical Biology bootcamp at Catalina Island for 1st and 2nd year USC graduate students. Oct, 2023. The Foster Lab is an interdisciplinary research group focused on the Physics of Living systems.

Scott Fraser

Events

Speaker: *First Look SoCal Innovation Showcase*. [Commercializing breakthroughs at top Southern California research institutions](#).

Sponsored by the Alliance for Southern California Innovation, the Alliance seeks to develop and connect SoCal's diverse nodes of innovation excellence while attracting new capital to the region. June 14, 2023.

In the News

Scott Fraser: explorer through invention. An interview with physicist, engineer and developmental biologist Scott Fraser. Reported in [USC Today](#), September 18, 2023.

Telling left from right: Cilia as cellular force sensors during embryogenesis. A new study reveals that cilia function as sensors for mechanical force exerted by flow to shape the left-right body plan of the developing embryo. Reported in [Science Daily](#), January 5, 2023.

Cornelius Gati

In the News

Unlocking secrets of immune system proteins: A potential path to new treatments. Dr. Gati's recent publication "Molecular basis of anaphylatoxin binding, activation, and signaling bias at complement receptors" outlines how detailed imaging reveals intricate workings of key receptors, offering fresh insights into combating disease. Reported in [USC Dornsife News](#), October 17, 2023.

Justin Haldar

Funding

Awarded: *Multicomponent modeling of high-dimensional multiparametric MRI data*. National Institute of Biomedical Imaging and Bioengineering (NIBIB) grant (as PI) R56 EB034349. August, 2023.

Events

Speaker: *On reference-based image quality assessment in medical image reconstruction: potential pitfalls and possible solutions*.

C.C. Chan, J. Wang, T. Nadeem, J.P. Halder. Pacific Grove, October, 2023.

[Asilomar Conference on Signals, Systems and Computers](#).

Speaker: *Constrained magnetic resonance imaging and the blessings of dimensionality*.

[Max Planck Institute for Human Cognitive and Brain Sciences](#). September 13, 2023.

Speaker: *The problem of hidden noise in MR image reconstruction*. J. Wang, D. An, J. P. Haldar. Toronto, June, 2023. International Society for Magnetic Resonance in Medicine Annual Meeting.

Speaker: *Spherical Echo-Planar Time-resolved Imaging (SEPT) for 3D highly-accelerated, distortion-free, time-resolved whole-brain T2* mapping*. N. Wang, Y. W. E. Brackenier, C. Liao, S. S. Iyer, X. Cao, J. Haldar, K. Setsompop. Toronto, June, 2023. [International Society for Magnetic Resonance in Medicine Annual Meeting](#).

Khalil Iskarous

Funding

Awarded: *CompCog: Deep causal inference grounds the perception of cognitive objects in speech*. NSF Perception, Action, and Cognition Program (PAC) Award: Iskarous (as PI), Byrd, and Narayanan. Grant (2240349). 2023.

Events

Speaker: *Cepstral Phonetics*, USC Linguistics Department [event](#), March 6, 2023.

Physical Biology Bootcamp at Catalina Island

Scott Fraser in USA Today

Vsevolod Katritch

Honors & Awards

Promoted: Congratulations to Bridge faculty member Dr. Katritch, promoted to Full Professor, Quantitative and Computational Biology and Chemistry. Reported in [USC Dornsife News](#), December 1, 2023.

Named: *Web of Science (Clarivate) Highly Cited Researcher*, in two categories: "Pharmacology & Toxicology" and "Biology & Biochemistry."

Funding

Awarded: *Targeting the allosteric sodium site with novel probes for delta opioid receptor*. National Institutes of Health/NIDA, R01DA057790 (role: MPI), July, 2023.

Awarded: Phase II (\$300K) funding for the *Center for New Technologies in Drug Discovery and Development (CNT3D)* Dornsife faculty led initiatives.

In the News

Using artificial intelligence to speed up discovery of new drugs. Dr. Katritch, Center for New Technologies in Drug Discovery and Development (CNT3D) at the USC Michelson Center, was interviewed on the use of AI and drug discovery. He explained how computational methods will streamline drug discovery by predicting which drug molecules are most likely to bind with the target receptor. The structure-based and AI-based approaches complement each other and can save time and money while yielding better results than traditional trial-and-error methods. Reported in [Neuroscience News](#), April 30, 2023.

Steve Kay

Honors & Awards

Awarded: *2023 Associates Award for Creativity in Research and Scholarship*. The USC [Associates Award](#) is the highest honor the

university bestows on its members for their distinguished achievements.

Funding

Awarded: *Discovery of small molecule ligands that directly bind Bmal1 and inhibit Bmal1 CLOCK interactions*. USC Norris Comprehensive Cancer Center, Center for Cancer Drug Development ([NCCC CCDD](#)).

Events

Speaker: *Drugging the circadian clock for novel cancer therapeutics*. University of Cape Town, Cape Town, South Africa, July 2023.

In the News

The Discovery and Translational Hub: Steve Kay, USC Provost Professor and Director of the USC Michelson Center for Convergent Bioscience worked with Dr. Tom Buchanan, University Professor of Medicine and Vice Dean for Research to spearhead a proposed building aimed at improving community health. The seven-story 202,000-square-foot building proposed for the USC Health Sciences Campus, seeks to unite interdisciplinary research teams to fast-track discoveries and address the health concerns of adjacent communities. The project was up for consideration for preliminary approval at the city Planning Commission meeting on October 12th, before being considered by the City Council on a date to be determined. Reported in [USC News](#), September 12, 2023.

Unplugging to Recharge. A conversation with Dr. Steve Kay and insights on "Maximizing a good night's sleep with customized products." Reported in [LinkedIn](#), April 23, 2023.

Submitted: [Ivy Foundation](#), USC Ming Hsieh Institute for Research on Engineering Medicine for Cancer ([MHIRA](#)), and NIH Research Evaluation and Commercialization Hubs ([REACH](#)).

Awarded: *Targeting circadian clock proteins for novel therapeutics to treat acute myeloid leukemia (AML)*. [2023 Ming Hsieh Institute Research Award](#) with co-PI Dr. Vsevolod

Vsevolod Katritch Named Highly Cited Researcher

Discovery and Translational Hub





“The most important thing is to never stop questioning.”

Albert Einstein

Katritch, co-PI). The [Ming Hsieh Institute Research Award \(MHIRA\)](#) promotes the integration of engineering, scientific, and medical research that advances novel thinking and the interdisciplinary and collaborative research needed to speed discovery and be translated into human health improvements. July, 2023.

Submitted: Letter of Intent, Department of Defense IDEA Award. The IDEA Award supports innovative basic research that may introduce a new paradigm, challenge existing paradigms, look at existing problems from new perspectives, or exhibit other highly creative qualities.

Training the Next Generation

Hosted: *Convergent-STEM (c-STEM)*. [c-STEM](#) is a student and postdoc-run organization for advancing convergent research within and beyond Molecular and Computational Biology (MCB). The goal is to provide a training, social events, and a resource platform for researchers to gain knowledge and skills for interdisciplinary research. c-STEM Events presented the following topics at MCB between January-March 2023: Scientific Communication (Feb 8); Long Read Sequencing (Feb 21); Mechanistic Modeling (Mar 8); Fluorescent Microscopy (Mar 21) and From Patients to the Laboratory: Technologies for Cancer Biomarker Discovery (March 10).

Hosted: *Convergent-STEM (c-STEM) Coffee Hour*. c-STEM is a student and postdoc-run organization for advancing convergent research within and beyond MCB. The goal is to provide training and host social events, to provide a resource platform for researchers to gain knowledge and skills for interdisciplinary research. July 24, 2023.

Carl Kesselman

Honors & Awards

Awarded. Dr. Carl Kesselman was recognized with the *2023 IEEE Internet Award* from the Institute of Electrical and Electronics

Engineers (IEEE), the largest global technical professional organization for the advancement of technology. The award salutation reads "For contributions to the design, deployment, and application of practical Internet-scale global computing platforms." Kesselman, who was also recently named an IEEE Fellow, will receive the award with his long-time collaborator Ian T. Foster. Carl Kesselman is the William H. Keck Chair of Engineering in the USC Viterbi School of Engineering and is a Professor in the Daniel J. Epstein Department of Industrial and Systems Engineering. He also holds joint appointments as Professor in Computer Science at the USC Viterbi School of Engineering, the Department of Population and Public Health Sciences at the Keck School of Medicine and at the Herman Ostrow School of Dentistry. He is the director of the Informatics Systems Research Division at the USC Viterbi Information Sciences Institute (ISI) and an ISI Fellow, the institute's highest honor.

Funding

Awarded: *CranioRate: An imaging-based, deep-phenotyping analysis toolset, repository, and online clinician interface for craniosynostosis*, developed as part of a pilot study (R21EBO26061) that objectively quantifies cranial dysmorphology, or deep phenotypes, in patients with metopic craniosynostosis (MC). December, 2023.

Awarded: *Hybrid- and multi-cloud storage strategies for cost-effective deployment of data resources*. 5U01DE028729-04 National Institute of Dental and Craniofacial Research, September, 2023.

Events

Speaker: *You learned what? Artificial Intelligence Research for Health*, the USC Information Science AI Research for Health seminar, featured AI and health researchers presenting their research on AI and Data Science with an impact on human health. The goal was to foster new collaborations among researchers in these fields. May 22, 2023.

Convergent-STEM (c-STEM)

Carl Kesselman Presented AI Seminar



In the News

USC Computer scientists are tackling dental health and birth defects. Dr. Kesselman leads the team of researchers and staff at ISI who run FaceBase's coordinating center (i.e., the Hub). FaceBase is a research resource that provides open access to genetic, molecular and imaging data to the dental, oral and craniofacial (DOC) research community. FaceBase provides a platform to manage the data, integrate it into meaningful information, and create a comprehensive picture that is useful and accessible to researchers. Reported in [USC Viterbi News](#), May 1, 2023.

Yasser Khan

Honors & Awards

Awarded: *2023 Google Research Scholar Award*, this prestigious award offered by [Google](#), will fund research to support a race-aware oximeter project to optimize racial bias correction in oximetry with Google's skin tone framework.

Events

Speaker: [Distinguished BMEN GSA Seminar series](#),. Dr. Khan spoke on the complex and multi-faceted obstacles facing mental health care, such as social stigma, high cost, and limited or no access to local care. His lab has designed a wearable that continuously measures physiological parameters linked to chronic stress and other mental health and wellness conditions, namely, heart rate variability, skin conductance, sweat rate, and the stress hormone, cortisol. Additive manufacturing and flexible hybrid electronics were used to make the device scalable and low-cost. April 25, 2023.

Peter Kuhn

Funding

Awarded: *A multiomic analysis of HER2/ERBB2 in African American men with prostate cancer.* NIH / RFA-MD-23-001, *Convergent Science Cancer Consortium*, Department of

Defense, Role: PI. Role: Aim 2 Subaward PI (Kuhn), December, 2023.

Awarded: *Convergent Science Cancer Consortium.* [Peer Reviewed Cancer Research Program](#). Department of Defense, 2023.

Awarded: *INTERCEPT: Data science-driven liquid biopsy in early breast cancer detection.* 2023 Ming Hsieh Institute Research Award, with co-PI Dr. Jeremy Mason. July, 2023.

Awarded: *Digital tools enabling remote clinical trials.* USC Research and Innovation Small Business Innovation Research award for the project to develop technologies and services for fully remote interventional clinical trials, in collaboration with pharmaceutical companies. The award aims to establish and bolster USC's ongoing technology transfer and commercialization efforts. July, 2023.

Awarded: *Multi-modal liquid biopsy early assessment of breast cancer, pancreatic cancer, and multiple myeloma.* NIH / RFA-CA-23-018 (1U01CA285013-01) for the project to advance biologically informed liquid biopsy (LBx) technology to fill gaps in current clinical practice of early cancer assessment. September, 2023.

Awarded: *Fluid biopsy in breast cancer patients to characterize cell free and cellular constituents.* Breast Cancer Research Foundation grant for the project, with Co-PI Dr. James Hicks, to extend their published research on identification of pre-symptomatic breast cancer using additional cases in their archives and newly acquired samples from normal blood donors to further test the robustness of their results. 2023.

Awarded: *Next generation T cell therapies for mutant KRAS solid tumors with the goal of patient-derived T cell receptor (TCRs) targeting mutant KRAS (mKRAS)* grant, with the NIH/University of Pennsylvania for the project addressing an unmet need for solid tumors. 2023.

Awarded: USC [COMPASS: Creating Opportunities through Mentorship and Partnership Across Stem Cell Science](#), CIRM, Role: PI. To provide undergraduates from underrepresented backgrounds with an interest in studying stem cell biology and regenerative medicine opportunities to be mentored and perform research in a lab. Multi-school collaboration (Dornsife, KSOM, Viterbi). 2023.

Submitted: Department of Defense subcontract with Johns Hopkins University for *Control of therapeutic resistance through the p53-independent Rb/p21 axis in prostate cancer* with co-PI Dr. James Hicks, to identify shifts in copy number analysis at a single cell level sufficient so as to discern relatedness of cancer cells within the same clade of a treated tumor sample. 2023.

Submitted: Department of Defense subcontract with Cedars-Sinai for *The role of large oncosomes in prostate cancer metastasis*, for continued research on IMC panel development and to perform single-cell proteomics on 20 of the most promising cells using the Fluidigm Hyperion imaging mass cytometry (IMC). 2023.

Events

Chairperson and Speaker: *Early detection and interception of cancer*, [American Association for Cancer Research Annual Meeting \(AACR\)](#), April 17, 2023.

Keynote Speaker: *An Unforgettable Night*, Los Angeles, [Women's Cancer Research Fund - WCRF-BCRF](#). March 15, 2023. Gave keynote address together with Dr. James Hicks. The event raised over \$2M to benefit WCRF.

Speaker: *MultiOmics, single cell science, liquid biopsy and mathematics for survival predictions*. The Comprehensive Cancer Center Seminar Series and Department of Hematology and Hematopoietic Cell Transplantation, City of Hope, Duarte, CA, February 6, 2023.

Panelist: *Challenges in providing global access to precision health*. [22nd Precision Medicine World Conference \(PMWC\) 2023 Silicon Valley](#), January 25-27, 2023.

In the News

[The Convergent Science Virtual Cancer Center \(CSVCC\) Video](#). The Department of Defense CDMRP Peer Reviewed Cancer Research Program aims to be a leader in convergent science in cancer research. Led by Dr. Dan Theodorescu at Cedars-Sinai and Dr. Peter Kuhn at CSI-Cancer: USC Michelson Center Convergent Science Institute in Cancer, the program began with eight early-career investigators and has recently expanded to 15 in its second year. Reported in the USC Michelson Center Convergent Science Institute in Cancer, August 24, 2023.

Convergent Science Virtual Cancer Center (CSVCC) workshop held at the Michelson Center: *The cancer solution we need: uniting experts from science, engineering and the humanities*. Scientists from USC Dornsife and Cedars-Sinai rallied scholars around the country and in diverse fields to find better ways of beating cancer. Reported in [USC Dornsife News](#), February 23, 2023.

New liquid biopsy technique may help personalize breast cancer diagnosis and prognosis. Researchers have developed a next-generation liquid biopsy technology that can be used to analyze patient's blood samples and precisely distinguish those with breast cancer from those without. Analysis reveals key factors that can distinguish patients with early-stage versus late-stage breast cancer versus age-matched donors without breast cancer. Reported in [BCRF](#), February 15, 2023.

Training the Next Generation

Spring 2023 Undergraduate Research Fellowships: Christina Chang, Srikar Kolluru, Theresa Luo, Amelia Marvit, Anya Shah, Divya Suresh and Brandon Ye.

Kuhns and James Hicks at WCRF-BCRF

Peter Kuhn in DoD CSVCC Video



Dornsife SOAR research fellowship: Emmett Liljegren, Andrew Udov, Monica Rodriguez, Lily Bai, and Amy Huang.

Gianluca Lazzi

Events

Speaker: *Neuroimplants for neurodegenerative conditions of the eye and the brain: predictive multiscale computational modeling, system design, and experimental testing*. Computer, Electrical and Mathematical Sciences and Engineering Seminar ([CEMSE](#)), March 16, 2023.

Jeremy Mason

Funding

Submitted: *HORNET Center for Autonomic Nerve Recording and Stimulation Systems (CARSS) Supplement*. The Polymer Implantable Electrode (PIE) Foundry Technology Resource.

Events

Program Participant: Scientist-Survivor Program (SSP) at [American Association for Cancer Research \(AACR\)](#). [SSP](#) provides connections between scientists, patient advocates and cancer survivors with seminars and discussions.

Training the Next Generation

Mentor: Dr. Mason served as a mentor in the Bridge Undergraduate Science (BUGS) summer research symposium on August 4-5, 2023.

Charles McKenna

In the News

Hear, Hear! The power of music that affects our brain. USC Dornsife's Dr. Charles McKenna believes he and scientists at Harvard Medical School's Massachusetts Eye and Ear Institute may have discovered a drug to repair inner ear cells that are damaged not only from aging, but from prolonged exposure to noise. This drug can potentially treat damaged areas without being washed away by the

ear's natural fluid — a crucial breakthrough. Reported in [Technology.org](#), March 27, 2023.

Ellis Meng

Events

Speaker: *Microwave characterization of parylene c dielectric and barrier properties*. Transducers 2023, June 25-29, 2023.

Speaker: *A shared resource for building polymer-based microelectrode arrays as neural interfaces*. 11th International IEEE EMBS Conference on Neural Engineering, [IEEE NER 2023](#), April 25-27, 2023.

Speaker: *Polymer-based microfabricated implants for neural applications*. [Washington State University Lecture Series](#), March 28, 2023.

Attended: NIH Stimulating peripheral activity to relieve conditions ([SPARC](#)) HORNET Grantee Meeting, February 27-28, 2023.

Shrikanth Narayanan

Honors & Awards

Awarded: *2023 International Speech Communication Association (ISCA) Medal for Scientific Achievement*, the most prestigious award offered by the [ISCA](#) in the field of human speech communication research at the global level. March, 2023.

Funding

Awarded: *RI Core: Medium: Structured variability in vocal tract articulation dynamics in speech*. The National Science Foundation four-year grant (IIS-2311676), to be undertaken at DISC, with co-PIs Drs. Dani Byrd, Louis Goldstein and Krishna Nayak. May, 2023.

Events

Chair: *Various aspects in speech and speaker recognition*. The International Conference on Acoustics, Speech, & Signal Processing ([ICASSP](#)), June 9 2023.

Jeremy Mason at AACR SSP

Shri Narayanan Awarded ISCA Medal

Keynote Speaker: *Multi-modal affective and social behavior analysis and synthesis in extended reality*. Mar 2023. IEEE VR 2023 Workshop on Multi-modal Affective and Social Behavior Analysis and Synthesis in Extended Reality (MASSXR).

Invited Talk/Panel: *Improving mental health and supporting self-regulation with technology*, Washington DC; Feb 2023 Keynote, Language-Based AI Agent Interaction with Children. IWSDS'23, Los Angeles, CA.

In the News

Who we are shapes what we say and how we say it. A conversation with Amazon Research Award recipient Dr. Narayanan on human-AI conversation and decoding intent and emotions. Reported in [Amazon Science](#), July 5, 2023.

Krishna Nayak

Funding

Awarded: *Volumetric Real-Time MRI at 0.55 Tesla*. NIH/NHLBI Grant 1U01HL167613-01, January, 2023.

Pending: *Improved fetal screening using 0.55T MRI*. PIs John Wood & Krishna Nayak. National Institutes of Health (NIH-NICHD).

Submitted LOI: *2023 Fall Clinical Pilot and Feasibility Award*. PI Roberta Kato. Cystic Fibrosis Foundation.

In the News

Moving images could revolutionize orthopedic care and research. This technology could provide important insights to improve diagnoses and better understand wrist anatomy. Reported in: [UC Davis Health](#). October, 2023.

The future of low-field MRI for pediatric imaging. A breakthrough research finding by Dr. John Wood, Director of Cardiovascular MRI at Children's Hospital Los Angeles and Dr. Nayak reported the first real-time, diagnostic quality MRI images of fetal heart disease. The

project represents a multicenter collaboration between Children's Hospital Los Angeles, USC Viterbi School of Engineering and The Hospital for Sick Children in Toronto. Reported in: [News Wise](#). June, 2023.

Training the Next Generation

Outreach: Tours of the Michelson Center Dynamic Imaging Science Center (DISC) were provided to multiple groups ranging from high school to graduate students. February-March 2023.

Niema Pahlevan

Funding

Submitted: *Sympathetic dominance in chronic migraine and its burden*. Co-I Niema M Pahlevan. National Institutes of Health (NIH)-R01.

Submitted: *Material vs shear-induced thrombogenicity of mechanical heart valves*. Co-I Niema M Pahlevan. National Institutes of Health (NIH)-R01.

Jayakanth Ravichandran

Funding

Awarded: *Multilayer thin film coatings for far ultraviolet spectropolarimetry*. NASA Jet Propulsion Laboratory. 2023.

Awarded: *Crystal growth and processing for anisotropic and non-linear infrared materials*. Office of Naval Research - DURIP. 2023.

Awarded: *Investigation of deposition methods for microphotonic thermal control coatings*. USC Research and Innovation SBIR/STTR Planning Award program. July, 2023.

Awarded: *High emissivity materials using multilayer oxides*. Air Force Office of Scientific Research. 2023.

Awarded: *Chemical analysis from atomic to bulk length scales*. USC Research and Innovation Dean's Matching Fund. The award

will be used to support, together with the Viterbi School of Engineering and the Dornsife College, the purchase of a Scanning Electron Microscope (SEM)/Focused Ion Beam (FIB). (James Boedicker, co-PI). June, 2023.

Awarded: *Development of abundant, inexpensive catalysts for hydrogen production*. Ershaghi Center for Energy Transition Seed Grant. 2023.

In the News

The Magic Behind the Microscope. The same USC software that aided the discovery of gravity waves now automates a unique 3D microscope that first revealed COVID-19. Reported in [Information Sciences Institute](#), April 17, 2023.

Remo Rohs

Honors & Awards

Named AAAS Fellow: The prestigious [American Association for the Advancement of Science](#) honor recognizes excellence in research, technology, industry and government, teaching, and communicating and interpreting science to the public. The honor is among the most prized in academia.

In the News

AI Sheds New Light on the 'Code of Life. Michelson Center researchers employ artificial intelligence to unveil the intricate world of DNA structure and chemistry, enabling unprecedented insights into gene regulation and disease. Reported in [USC Dornsife News](#), May 22, 2023.

Maryam Shanechi

In the News

Finalist: *Blavatnik National Awards*. Dr. Shanechi was recognized for her pioneering brain-machine interfaces, at the intersection of engineering, computing, and neuroscience, that model, decode, and control complex neural activity patterns. Reported in [Viterbi News](#), July 26, 2023.

Celebrated: 50 years of the USC Signal and Image Processing Institute (SIPI) innovations, honoring distinguished alumni while looking ahead to the next half century. Reported in [USC Viterbi News](#). February 22, 2023.

Acknowledged for [advanced technological](#) research to understand brain signals without invasive penetration. Interview with Viterbi School of Engineering Dean Yannis Yortsos. Reported in [Healthworld.com](#). January, 2023.

From untangling global supply chains to restoring memory, Trojan engineers seek to solve mysteries for the good of humanity such as "*How do we treat mental disorders when those disorders present differently in each unique patient's brain?*" Reported in [USC Viterbi News](#), Spring 2023.

Jennifer Treweek

Events

Organizer: *MEG-EEG Neuromodulation, Neuroengineering. Society for Brain Mapping & Therapeutics Annual Conference, (SBMT)*. 20th Annual World Congress. February 16, 2023.

Cristina Zavaleta

Funding

Awarded: *A New Raman-based Strategy to Identify tumor margins and guide surgical resection*. NIH/NIBIB, R01EB033918-01 (Zavaleta), April, 2023.

Awarded: A new multimodal molecular imaging approach to guide intra-operative tumor resection and post-operative treatment planning. New Investigators to *Promote Workforce Diversity in Genomics, Bioinformatics, or Bioengineering and Biomedical Imaging Research R01* grant from the National Institute of Biomedical Imaging and Bioengineering (NIBIB). Dr. Zavaleta is a two-time former CURE recipient (K22 and R21) NIH Early Investigator Advancement

Remo Rohs Named AAAS Fellow

Maryam Shanechi Is Blavatnik Award

Program ([EIAP](#)) Scholar from National Cancer Institute.

Events

Speaker: *Young Women's Career Conference for the Girls Academic Leadership Academy (GALA) Speaker Series*, the only all-girls public STEM school in California grades 6-12. March 24, 2023.

Speaker: Associated Students of Biomedical Engineering ([ASBME](#)) event, regarding her academic journey. February 25, 2023.

Speaker: *Multiplexed spatial profiling of cancer enabled by Raman imaging*. [Photonics West](#), San Francisco, CA. January 31, 2023.

Panelist: *Visualizing and quantifying drug distribution in tissue*, [SPIE Photonics West](#) conference ([SPIE](#)), San Francisco, CA., January 28, 2023.

In the News

Featured in [SPIE Women in Optics](#). (November, 2023) The International Society for Optics and Photonics ([SPIE](#)).

SPIE Celebrates Its Golden Anniversary

Cristina Zavaleta Featured in SPIE



Manuscripts & Publications

It is through publication of journal articles and books that research is disseminated to the scientific community and the public at large, helping to advance new knowledge and facilitate its application. Listed below are highlights of Michelson faculty publications.

Andrea Armani

Dielectric optical waveguide fabricated on a transparent substrate. Yuan J, Aoni RA, Armani AM. *Opt Lett.* 2023 Nov 15;48(22):5927-5930. doi: 10.1364/OL.504728.

Detecting disruption of HER2 membrane protein organization in cell membranes with nanoscale precision. Moradi Y, Lee JSH, Armani AM. *ACS Sens.* 2023 Nov 13. doi: 10.1021/acssensors.3c01437.

Effects of functional and nutraceutical foods in the context of the mediterranean diet in patients diagnosed with breast cancer. Flore G, Deledda A, Lombardo M, Armani A, Velluzzi F. *Antioxidants (Basel).* 2023 Oct 11;12(10):1845. doi: 10.3390/antiox12101845.

Very-low-calorie ketogenic diet vs hypocaloric balanced diet in the prevention of high-frequency episodic migraine: the EMIKETO randomized, controlled trial. Caprio M, Moriconi E, Camajani E, Feraco A, Marzolla V, Vitiello L, Proietti S, Armani A, Gorini S, Mammi C, Egeo G, Aurilia C, Fiorentini G, Tomino C, Barbanti P. *J Transl Med.* 2023 Oct 4;21(1):692. doi: 10.1186/s12967-023-04561-1.

Very low-calorie ketogenic diet: A valuable and fashionable nutritional therapy. When could it become dangerous? Gorini S,

Armani A, Caprio M. *Diabetes Metab Res Rev.* 2023 July 19;39(8):e3698. doi: 10.1002/dmrr.3698.

Accidental discovery of a Tetraodontidae (Sphoeroides marmoratus) within a cuttlefish (Sepia officinalis) bought in a fish shop in Italy: risk assessment associated with the presence of Tetrodotoxin. Malloggi C, Tinacci L, Giusti A, Galli F, Dall'Ara S, Marconi P, Gasperetti L, Armani A. *Ital J Food Saf.* 2023 Jun 8;12(2):11117. doi: 10.4081/ijfs.2023.11117.

First toxicological analysis of the pufferfish Sphoeroides pachygaster collected in italian waters (Strait of Sicily): Role of citizens science in monitoring toxic marine species. Malloggi C, Rizzo B, Giusti A, Guardone L, Gasperetti L, Dall'Ara S, Armani A. *Animals (Basel).* 2023 Jun 4;13(11):1873. doi: 10.3390/ani13111873.

Sustainable strategies for increasing legume consumption: culinary and educational approaches. Amoah I, Ascione A, Muthanna FMS, Feraco A, Camajani E, Gorini S, Armani A, Caprio M, Lombardo M. *Foods.* 2023 Jun 4;12(11):2265. doi: 10.3390/foods12112265.

Neutral effect of skeletal muscle mineralocorticoid receptor on glucose metabolism in mice. Feraco A, Gorini S, Mammi C, Lombardo M, Armani A, Caprio M.

Int J Mol Sci. 2023 Apr 18;24(8):7412. doi: 10.3390/ijms24087412.

Health effects of red wine consumption: a narrative review of an issue that still deserves debate. Lombardo M, Feraco A, Camajani E, Caprio M, Armani A. *Nutrients*. 2023 Apr 16;15(8):1921. doi: 10.3390/nu15081921.

An authentication survey on retail seafood products sold on the Bulgarian market underlines the need for upgrading the traceability system. Tinacci L, Stratev D, Strateva M, Zhelyazkov G, Kyuchukova R, Armani A. *Foods*. 2023 Mar 2;12(5):1070. doi: 10.3390/foods12051070.

James Boedicker

Utilizing a divalent metal ion transporter to control biogenic nanoparticle synthesis. Manasi Subhash Gangan, Kyle L Naughton, James Q Boedicker. August 16, 2023. *Journal of Industrial Microbiology and Biotechnology*. <https://doi.org/10.1093/jimb/kuad020>.

Stochastic effects in bacterial communication mediated by extracellular vesicles. Weaver BP, Haselwandter CA, Boedicker JQ. *Phys Rev E*. 2023 Feb 14;107(2-1):024409. doi: 10.1103/PhysRevE.107.024409. PMID: 36932546.

Dani Byrd

Viable signal periodicities in speech rhythm. J. Campbell, D. Byrd, L. Goldstein. August 7, 2023. *International Congress of Phonetic Sciences*. <https://guarant.cz/icphs2023/346.pdf>.

Does the articulatory modulation function encode stress? Jessica Campbell, Dani Byrd, Louis Goldstein. March 1, 2023. *The Journal of the Acoustical Society of America*. <https://doi.org/10.1121/10.0019198>.

Vadim Cherezov

Functional GPCR expression in eukaryotic LEXSY system. Luginina A, Maslov I, Khorn P, Volkov O, Khnykin A, Kuzmichev P, Shevtsov M, Belousov A, Kapranov I, Dashevskii D, Kornilov D, Bestsennaia E, Hofkens J, Hendrix J, Gensch T, Cherezov V, Ivanovich V, Mishin A, Borshchevskiy V. *J Mol Biol*. 2023 Dec 1;435(23):168310. doi: 10.1016/j.jmb.2023.168310.

Structural diversity of leukotriene G-protein coupled receptors. Aleksandra Luginina, Anastasiia Gusach, Elizaveta Lyapina, Polina Khorn, Nadezda Safronova, Mikhail Shevtsov, Daria Dmitrieva, Dmitrii Tasevskis, Tatiana Kotova, Ekaterina Smirnova, Valentin Borshchevskiy, Vadim Cherezov, Alexey Mishin. September 11, 2023. *J Biol Chem* <https://DOI:10.1016/j.jbc.2023.105247>.

MicroED structure of the human vasopressin 1B receptor. Shiriaeva A, Martynowycz MW, Nicolas WJ, Cherezov V, Gonen T. *bioRxiv*. 2023 Jul 6:2023.07.05.547888. doi: 10.1101/2023.07.05.547888.

Structural insights into angiotensin receptor signaling modulation by balanced and biased agonists. Bryan L Roth, Vsevolod Katritch, Vadim Cherezov, Haitao Zhan. *The EMBO Journal* (April 11, 2023). <https://www.embopress.org/doi/abs/10.15252/embj.2022112940>.

Sub-millisecond conformational dynamics of the A2A adenosine receptor revealed by single-molecule FRET. Maslov I., Volkov O., Khorn P., Orekhov P., Gusach A., Kuzmichev P., Gerasimov A., Luginina A., Coucke Q., Bogorodskiy A., Gordeliy V., Wanninger S., Barth A., Mishin A., Hofkens J., Cherezov V., Gensch T., Hendrix J., Borshchevskiy V. *Commun Biol* 6, 362 (April 3, 2023). <https://doi.org/10.1038/s42003-023-04727-z>.

The activation mechanism and antibody binding mode for orphan GPR20. Lin X., Jiang S., Wu Y., Wei X., Han G.W., Wu L., Liu J., Chen B., Zhang Z., Zhao S., Cherezov V., Xu F. *Cell Discov* 9, 23 (Feb 28, 2023). <https://doi.org/10.1038/s41421-023-00520-8>.

Eun Ji Chung

Nanoparticles-based technologies for cholera detection and therapy - SLAS Technology. November 2, 2023. <https://doi.org/10.1016/j.slast.2023.10.006>.

Long-term, in vivo therapeutic effects of a single dose of miR-145 micelles for atherosclerosis. D. Chin, N. Patel, Chin D., Patel N., Lee W., Sonali K., Cook J., Chung E.J. *Bioactive Materials, Bioact Mater.* 2023 Sep; 27: 327-336. doi: 10.1016/j.bioactmat.2023.04.001.

Synergistic treatment of genetic kidney disease with DNA methylation inhibitors. Chris Patrick. June 9, 2023. *AIP.org*. <https://doi.org/10.1063/10.0019798>.

Targeting the ADPKD methylome using nanoparticle-mediated combination therapy. Trinh, A., Huang, Y., Shao, H., Ram, A., Morival, J., Wang, J., Chung, E.J., Downing, T. June 9, 2023. *APL Bioeng*. <https://pubmed.ncbi.nlm.nih.gov/37305656/>.

Spotlight on genetic kidney diseases: a call for drug delivery and nanomedicine solutions. Trac N., Ashraf A., Giblin J., Prakash S., Mitragotri S., Chung E.J. *ACS Nano*. March 29, 2023. <https://pubs.acs.org/doi/10.1021/acsnano.2c12140>.

Extracellular vesicles as regulators of the extracellular matrix. Patel N., Ashraf A., Chung E.J. *Bioengineering*, 10(2): 136. March 29, 2023. <https://pubs.acs.org/doi/10.1021/acsnano.2c12140>.

In vitro delivery of mTOR inhibitors by kidney-targeted micelles for autosomal dominant polycystic kidney disease. Cox A., Tung

M., Li H., Hallows K.R., Chung E.J. *SLAS Technol.* 2023 Feb 19; February 19, 2023? S2472-6303(23)00011-0. doi: 10.1016/j.slast.2023.02.001.

Moh El-Naggar

Bacterial extracellular electron transfer components are spin selective. Niman CM, Sukenik N, Dang T, Nwachukwu J, Thirumurthy MA, Jones AK, Naaman R, Santra K, Das TK, Paltiel Y, Baczewski LT, El-Naggar MY. *J Chem Phys.* 2023 Oct 14;159(14):145101. doi: 10.1063/5.0154211.

*Bioprocess development for extraction and purification of cellulases from *Aspergillus niger* 3ASZ using statistical experimental design techniques.* Sorour AA, Olama ZA, El-Naggar MY, Ali SM. *Int J Biol Macromol.* 2023 Jul 1;242(Pt 1):124759. doi: 10.1016/j.ijbiomac.2023.124759.

*Soluble iron enhances extracellular electron uptake by *Shewanella oneidensis* MR-1.* Abuyen K, El-Naggar MY. *ChemElectroChem.* 2023 Feb 13;10(4):e202200965. doi: 10.1002/celec.202200965.

Stacey Finley

Synthetic living materials in cancer biology. Peyton, S.R., Chow, L.W., Finley, S.D. et al. October 2, 2023. *Nat Rev Bioeng* 1, 972-988. October 2023. <https://doi.org/10.1038/s44222-023-00105-w>.

Agent-based modeling of tumor-immune interactions reveals determinants of final tumor states. Manal Ahmidouch, Neel Tangella, Stacey D. Finley. *Biorxiv.org*. September 7, 2023. <https://doi.org/10.1101/2023.09.06.556617>.

Ensemble-based genome-scale modeling predicts metabolic differences between macrophage subtypes in colorectal cancer. P Gelbach, P.E. and Finley, S.D. *Cell.com*.

August 9, 2023. <https://doi.org/10.1016/j.isci.2023.107569>.

In revision: *Flux sampling in genome-scale metabolic modeling of microbial communities*. Gelbach, P.E.† and Finley, S.D. BMC Bioinformatics, bioRxiv preprint. April 20, 2023. <https://doi.org/10.1101/2023.04.18.537368>.

A data-driven Boolean model explains memory subsets and evolution in CD8+ T cell exhaustion. Geena V Ildefonso, Stacey D Finley. NPJ Syst Biol App. July 31, 2023. <https://doi.org/10.1038/s41540-023-00297-2>.

Submitted: *Information-theoretic analysis of a model of CAR-4-1BB-mediated NF κ B activation*. Tserunyan, V.† and Finley, S.D. (2023). Bulletin of Mathematical Biology. June 10, 2023. <https://doi.org/10.1007/s11538-023-01232-6>.

A systems and computational biology perspective on advancing CAR therapy. Tserunyan, V.† and Finley, S.D. September 2023. Seminars in Cancer Biology. May 2023 <https://doi.org/10.1016/j.semcancer.2023.05.009>.

Calibrating agent-based models to tumor images using representation learning. Cess, C.G.† and Finley, S.D. PLOS Computational Biology. April, 21, 2023. <https://doi.org/10.1371/journal.pcbi.1011070>.

Systematic Bayesian posterior analysis guided by Kullback-Leibler divergence facilitates hypothesis formation. Huber, H.A.†, Georgia, S.K., and Finley, S.D. Journal of Theoretical Biology. February 2023. <https://doi.org/10.1016/j.jtbi.2022.111341>.

Proof-of-concept to incorporate insights from multi-omics analyses of polymyxin B in combination with chloramphenicol against Klebsiella pneumoniae. Hanafin P.O., Abdul Rahim N., Sharma R., Cess C.G., Finley S.D., Bergen P.J., Velkov T., Li J., and Rao G.G.

(2023) CPT: Pharmacometrics & Systems Pharmacology. January 23, 2023 12(3): 387-400. <https://doi.org/10.1002/psp4.12923>.

Valery Fokin

Generation and aerobic oxidation of azavinyl captodative radicals. Aggarwal S, Richards WJ, Fokin VV. J Am Chem Soc. 2023 Sep 21. doi: 10.1021/jacs.3c06068.

Arenes participate in 1,3-dipolar cycloaddition within situ-generated diazoalkenes. Shubhangi Aggarwal, Alexander Vu, Dmitry B Eremin, Rudra Persaud, Valery V Fokin. Natural Chemistry. May 2023. DOI: 10.1038/s41557-023-01188-z.

Peter Foster

Dissipation and energy propagation across scales in an active cytoskeletal material. Foster P.J., Bae J., Lemma B., Zheng J., Ireland W., Chandrakar P., Boros R., Dogic Z., Needleman D.J., Vlassak J.J., PNAS, 2023; 120 (14); e2207662120. February 2023 doi:10.1073/pnas.2207662120.

Microscopic interactions control a structural transition in active mixtures of microtubules and molecular motors. Najma B., Baskaran A., Foster P.J., Duclos G. BioRxiv, January 2023. doi:10.1101/2023.01.04.522797.

Scott Fraser

Episodic live imaging of cone photoreceptor maturation in GNAT2-EGFP retinal organoids. Bai J, Koos DS, Stepanian K, Fouladian Z, Shayler DWH, Aparicio JG, Fraser SE, Moats RA, Cobrinik D. Dis Model Mech. 2023 Nov 21. doi: 10.1242/dmm.050193.

Hand2 represses non-cardiac cell fates through chromatin remodeling at cis-regulatory elements. Komatsu V, Cooper B, Yim P, Chan K, Gong W, Wheatley

L, Rohs R, Fraser SE, Trinh LA. bioRxiv. 2023 Sep 24:2023.09.23.559156. doi: 10.1101/2023.09.23.559156.

VoDEx: a Python library for time annotation and management of volumetric functional imaging data. Nadtochiy A, Luu P, Fraser SE, Truong TV. *Bioinformatics*. 2023 Sep 2;39(9):btad568. doi: 10.1093/bioinformatics/btad568.

Application of fluorescence lifetime imaging microscopy to monitor glucose metabolism in pancreatic islets in vivo. Wang Z, Archang M, Gurlo T, Wong E, Fraser SE, Butler PC. *Biomed Opt Express*. 2023 Jul 19;14(8):4170-4178. doi: 10.1364/BOE.493722. eCollection 2023 Aug 1.

Development of highly fluorogenic styrene probes for visualizing RNA in live cells. Moon Jung Kim, Yida Li, Jason A. Junge, Nathan K. Kim, Scott E. Fraser, and Chao Zhang. *ACS.org*, May 18, 2023. <https://pubs.acs.org/doi/full/10.1021/acscchembio.3c00141>.

A single-shot hyperspectral phasor camera for fast, multi-color fluorescence microscopy. Wang P, Kitano M, Keomanee-Dizon K, Truong TV, Fraser SE, Cutrale F. *Cell Rep Methods*. 2023 Mar 31;3(4):100441. doi: 10.1016/j.crmeth.2023.100441. eCollection 2023 Apr 24.

Episodic live imaging of cone photoreceptor maturation in GNAT2-EGFP retinal organoids. Bai J., Koos D.S., Stepanian K., Fouladian Z., Shayler D.W.H., Aparicio J.G., Fraser S.E., Moats R.A., Cobrinik D. *BioRxiv*, March 01, 2023. <https://doi.org/10.1101/2023.02.28.530518>.

baz1b loss-of-function in zebrafish produces phenotypic alterations consistent with the domestication syndrome. Torres-Pérez JV, Anagianni S, Mech AM, Havelange W, García-González J, Fraser SE, Vallortigara G, Brennan CH. *iScience*. 2023 Jan 20. <https://doi.org/10.1016/j.isci.2022.105704>.

HyU: Hybrid Unmixing for longitudinal in vivo imaging of low signal-to-noise fluorescence. Chiang H.J., Koo D.E.S., Kitano M., Burkitt S., Unruh J.R., Zavaleta C., Trinh L.A., Fraser S.E., Cutrale F. *Nature Methods*, January 19, 2023?. <https://doi.org/10.1038/s41592-022-01751-5>.

Cilia function as calcium-mediated mechanosensors that instruct left-right asymmetry. Djenoune L, Mahamdeh M, Truong TV, Nguyen CT, Fraser SE, Brueckner M, Howard J, Yuan S. *Science*. 2023 Jan 6;379(6627):71-78. doi: 10.1126/science.abq7317. Epub 2023 Jan 5.

Cornelius Gati

Molecular basis of anaphylatoxin binding, activation, and signaling bias at complement receptors. Yadav MK, Maharana J, Yadav R, Saha S, Sarma P, Soni C, Singh V, Saha S, Ganguly M, Li XX, Mohapatra S, Mishra S, Khant HA, Chami M, Woodruff TM, Banerjee R, Shukla AK, Gati C. *Cell*. 2023 Oct 26;186(22):4956-4973.e21. doi: 10.1016/j.cell.2023.09.020.

SLC6A1 variant pathogenicity, molecular function, and phenotype: a genetic and clinical analysis. Stefanski A, Pérez-Palma, E, Brünger T, Montanucci L, Gati C, et al. August 30, 2023. *Oxford Academic*. <https://doi.org/10.1093/brain/awad292>.

Decoding the mechanisms of allosterity. Khan S, Gati C. *eLifesciences.org*, May 18, 2023. DOI: 10.7554/eLife.88749.

Justin Haldar

New theory and faster computations for subspace-based sensitivity map estimation in multichannel MRI. R. A. Lobos, C.C. Chan, J. P. Haldar. July 21, 2023. *IEEE Transactions on Medical Imaging*. <https://doi.org/10.1109/TMI.2023.3297851>.

BrainSuite BIDS App: Containerized Workflows for MRI Analysis. Kim Y, Joshi AA, Choi S, Joshi SH, Bhushan C, Varadarajan D, Haldar JP, Leahy RM, Shattuck DW. bioRxiv. 2023 Mar 15:2023.03.14.532686. doi: 10.1101/2023.03.14.532686.

Single breath-hold CINE imaging with combined simultaneous multislice and region-optimized virtual coils. Kim D, Coll-Font J, Lobos RA, Stäb D, Pang J, Foster A, Garrett T, Bi X, Speier P, Haldar JP, Nguyen C. Magn Reson Med. March 2, 2023. doi: 10.1002/mrm.29620.

High-fidelity, high-spatial-resolution diffusion magnetic resonance imaging of ex vivo whole human brain at ultra-high gradient strength with structured low-rank echo-planar imaging ghost correction. Ramos-Llordén G, Lobos RA, Kim TH, Tian Q, Witzel T, Lee HH, Scholz A, Keil B, Yendiki A, Bilgiç B, Haldar JP, Huang SY. NMR Biomed. 2023 Feb;36(2):e4831. doi: 10.1002/nbm.4831.

James Hicks

Aqueous humor liquid biopsy as a companion diagnostic for retinoblastoma: implications for diagnosis, prognosis and therapeutic options. Five years of Progress. Berry JL, Pike S, Shah R, Reid MW, Peng CC, Wang Y, Yellapantula V, Biegel J, Kuhn P, Hicks J, Xu L. Am J Ophthalmol. 2023 Nov 29:S0002-9394(23)00489-0. doi: 10.1016/j.ajo.2023.11.020.

Cell state and cell type: deconvoluting circulating tumor cell populations in liquid biopsies by multi-omics. Welter L, Zheng S, Setayesh SM, Morikado M, Agrawal A, Nevarez R, Naghdloo A, Pore M, Higa N, Kolatkar A, Thiele JA, Sharma P, Moore HCF, Richer JK, Elias A, Pienta KJ, Zurita AJ, Gross ME, Shishido SN, Hicks J, Velasco CR, Kuhn P. Cancers (Basel). 2023 Aug 3;15(15):3949. doi: 10.3390/cancers15153949.

Plasticity of circulating tumor cells in small cell lung cancer. Jiyoun Seo. Mihir Kumar, Jeremy Mason, Fiona Blackhall, Nicholas Matsumoto, Caroline Dive, James Hicks, Peter Kuhn, Stephanie N Shishido. July 21, 2023. Scientific Reports. DOI: 10.1038/s41598-023-38881-5.

Simultaneous copy number alteration and single-nucleotide variation analysis in matched aqueous humor and tumor samples in children with retinoblastoma. Schmidt MJ, Prabakar RK, Pike S, Yellapantula V, Peng CC, Kuhn P, Hicks J, Xu L, Berry JL. Int J Mol Sci. 2023 May 11;24(10):8606. doi: 10.3390/ijms24108606.

Contrived materials and a data set for the evaluation of liquid biopsy tests: a blood profiling atlas in cancer (BLOODPAC) community study. Hernandez KM, Bramlett KS, Agius P, Baden J, Cao R, Clement O, Corner AS, Craft J, Dean DA 2nd, Dry JR, Grigaityte K, Grossman RL, Hicks J, Higa N, Holzer TR, Jensen J, Johann DJ, Katz S, Kolatkar A, Keynton JL, Lee JSH, Maar D, Martini JF, Meyer CG, Roberts PC, Ryder M, Salvatore L, Schageman JJ, Somiari S, Stetson D, Stern M, Xu L, Leiman LC. J Mol Diagn. 2023 Mar;25(3):143-155. doi: 10.1016/j.jmoldx.2022.12.003.

Vsevolod Katritch

Development of an automated, high-throughput assay to detect angiotensin AT2-Receptor Agonistic compounds by nitric oxide measurements in vitro. Souza-Silva IM, Peluso AA, Mortensen C, Nazarova AL, Stage TB, Sumners C, Katritch V, Steckelings UM. Peptides. 2023 Dec 22:171137. doi: 10.1016/j.peptides.2023.171137.

Pharmacological and physicochemical properties optimization for dual-target Dopamine D3 (D3R) and μ -Opioid (MOR) receptor ligands as potentially safer analgesics. Bonifazi A, Saab E, Sanchez J, Nazarova AL, Zaidi SA, Jahan K, Katritch

V, Canals M, Lane JR, Newman AH. *J Med Chem.* July 19, 2023. doi: 10.1021/acs.jmedchem.3c00417.

Structural insights into angiotensin receptor signaling modulation by balanced and biased agonists. Zhang D, Liu Y, Zaidi SA, Xu L, Zhan Y, Chen A, Guo J, Huang XP, Roth BL, Katritch V, Cherezov V, Zhang H. *EMBO J.* 2023 Jun 1;42(11):e112940. doi: 10.15252/embj.2022112940.

Ligand and G-protein selectivity in the μ -opioid receptor. Han J, Zhang J, Nazarova AL, Bernhard SM, Krumm BE, Zhao L, Lam JH, Rangari VA, Majumdar S, Nichols DE, Katritch V, Yuan P, Fay JF, Che T. *Nature.* 2023 May;617(7960):417-425. doi: 10.1038/s41586-023-06030-7.

Computational approaches streamlining drug discovery. Sadybekov AV, Katritch V. *Nature.* 2023 Apr;616(7958):673-685. doi: 10.1038/s41586-023-05905-z.

Eosinophils protect pressure overload- and β -adrenoreceptor agonist-induced cardiac hypertrophy. Yang C, Li J, Deng Z, Luo S, Liu J, Fang W, Liu F, Liu T, Zhang X, Zhang Y, Meng Z, Zhang S, Luo J, Liu C, Yang D, Liu L, Sukhova GK, Sadybekov A, Katritch V, Libby P, Wang J, Guo J, Shi GP. *Cardiovasc Res.* 2023 Mar 17;119(1):195-212. doi: 10.1093/cvr/cvac060.

Molecular mechanism of biased signaling at the kappa opioid receptor. El Daibani A, Paggi JM, Kim K, Laloudakis YD, Popov P, Bernhard SM, Krumm BE, Olsen RHJ, Diberto J, Carroll FI, Katritch V, Wünsch B, Dror RO, Che T. *Nat Commun.* 2023 Mar 11;14(1):1338. doi: 10.1038/s41467-023-37041-7.

Structural details of a Class B GPCR - arrestin complex revealed by genetically encoded crosslinkers in living cells. Aydin Y., Böttke T., Lam J.H., Ernicke S., Fortmann A., Tretbar M., Zarzycka B., Gurevich V., Katritch V., Coin I. March 1, 2023. *Nature Commun.* 14(1):1151.

<https://doi.org/10.1038/s41467-023-36797-2>.

Steve Kay

The negative effects of travel on student athletes through sleep and circadian disruption. Heller HC, Herzog E, Brager A, Poe G, Allada R, Scheer F, Carskadon M, de la Iglesia HO, Jang R, Montero A, Wright K, Mouraine P, Walker MP, Goel N, Hogenesch J, Van Gelder RN, Kriegsfeld L, Mah C, Colwell C, Zeitzer J, Grandner M, Jackson CL, Roxanne Prichard J, Kay SA, Paul K. *J Biol Rhythms.* 2023 Nov 18:7487304231207330. doi: 10.1177/07487304231207330.

Watching the clock in glioblastoma. Chan P, Rich JN, Kay SA. *Neuro Oncol.* 2023 Nov 2;25(11):1932-1946. doi: 10.1093/neuonc/noad107.

E-box binding transcription factors in cancer. Yuanzhong Pan, Pauline J. van der Watt and Steve Kay. August 3, 2023. *Frontiers in Oncology.* <https://doi.org/10.3389/fonc.2023.1223208>.

Epidermal GIGANTEA adjusts the response to shade at dusk by directly impinging on Phytochrome Interacting Factor 7 function. Martínez-Vasallo C, Cole B, Gallego-Bartolomé J, Chory J, Kay SA, Nohales MA. *bioRxiv.* 2023 Mar 23. doi: 10.1101/2023.03.21.533699.

Circadian regulator BMAL1:CLOCK promotes cell proliferation in hepatocellular carcinoma by controlling apoptosis and cell cycle. Qu M., Zhang G., Qu H., Vu A., Wu R., Tsukamoto H., Jia Z., Huang W., Lenz H. J., Rich J. N., and Kay S. A. (2023). *Proceedings of the National Academy of Sciences of the United States of America.* January 3, 2023. <https://doi.org/10.1073/pnas.2214829120>.

Carl Kesselman

Correction: Reproducible big data science: A case study in continuous FAIRness. Madduri R, Chard K, D'Arcy M, Jung SC, Rodriguez A, Sulakhe D, Deutsch E, Funk C, Heavner B, Richards M, Shannon P, Glusman G, Price N, Kesselman C, Foster I. PLoS One. 2023 Nov 21;18(11):e0294883. doi: 10.1371/journal.pone.0294883.

Mercedeh Khajavikhan

Nature of optical thermodynamic pressure exerted in highly multimoded nonlinear systems. Ren H, Pyrialakos GG, Wu FO, Jung PS, Efremidis NK, Khajavikhan M, Christodoulides DN. Phys Rev Lett. 2023 Nov 10;131(19):193802. doi: 10.1103/PhysRevLett.131.193802.

Thermalization of the Ablowitz-Ladik lattice in the presence of non-integrable perturbations. Selim MA, Pyrialakos GG, Wu FO, Musslimani Z, Makris KG, Khajavikhan M, Christodoulides D. Opt Lett. 2023 Apr 15;48(8):2206-2209. doi: 10.1364/OL.489165.

Coherence properties of light in highly multimoded nonlinear parabolic fibers under optical equilibrium conditions. Selim MA, Wu FO, Pyrialakos GG, Khajavikhan M, Christodoulides D. Opt Lett. 2023 Mar 1;48(5):1208-1211. doi: 10.1364/OL.483282.

Yasser Khan

The 2023 wearable photoplethysmography roadmap. Charlton PH, Allen J, Bailón R, Baker S, Behar JA, Chen F, Clifford GD, Clifton DA, Davies HJ, Ding C, Ding X, Dunn J, Elgendi M, Ferdoushi M, Franklin D, Gil E, Hassan MF, Hernesniemi J, Hu X, Ji N, Khan Y, Kontaxis S, Korhonen I, Kyriacou PA, Laguna P, Lázaro J, Lee C, Levy J, Li Y, Liu C, Liu J, Lu L, Mandic DP, Marozas V, Mejía-Mejía E, Mukkamala R, Nitzan M, Pereira T, Poon CCY, Ramella-Roman JC, Saarinen H,

Shandhi MMH, Shin H, Stansby G, Tamura T, Vehkaoja A, Wang WK, Zhang YT, Zhao N, Zheng D, Zhu T. Physiol Meas. 2023 Nov 29;44(11):111001. doi: 10.1088/1361-6579/acead2.

Peter Kuhn

Comprehensive single-cell immune profiling defines the patient multiple myeloma microenvironment following oncolytic virus therapy in a Phase Ib trial. Nawrocki ST, Olea J, Villa Celi C, Dadrastoussi H, Wu K, Tsao-Wei D, Colombo A, Coffey M, Fernandez Hernandez E, Chen X, Nuovo GJ, Carew JS, Mohrbacher AF, Fields P, Kuhn P, Siddiqi I, Merchant A, Kelly KR. Clin Cancer Res. 2023 Dec 15;29(24):5087-5103. doi: 10.1158/1078-0432.CCR-23-0229.

Aqueous humor liquid biopsy as a companion diagnostic for retinoblastoma: implications for diagnosis, prognosis and therapeutic options. Five years of Progress. Berry JL, Pike S, Shah R, Reid MW, Peng CC, Wang Y, Yellapantula V, Biegel J, Kuhn P, Hicks J, Xu L. Am J Ophthalmol. 2023 Nov 29:S0002-9394(23)00489-0. doi: 10.1016/j.ajo.2023.11.020.

Targeted single-cell proteomic analysis identifies new liquid biopsy biomarkers associated with multiple myeloma. Sonia M. Setayesh, Libere J. Ndacayisaba, Kate E. Rappard, Valerie Hennes, Luz Yurany Moreno Rueda, Guilin Tang, Pei Lin, Robert Z. Orłowski, David E. Symer, Elisabet E. Manasanch, Stephanie N. Shishido and Peter Kuhn. September 18, 2023. Nature.com. <https://doi.org/10.1038/s41698-023-00446-0>.

Cell state and cell type: deconvoluting circulating tumor cell populations in liquid biopsies by multi-omics. Serena Zheng, Sonia Maryam Setayesh, Michael Morikado, Arushi Agrawal, Rafael Nevarez, Amin Naghdloo, Milind Pore, Nikki Higa, Anand Kolatkar, Jana-Aletta Thiele, Priyanka Sharma, Halle C.

F. Moore, Jennifer K. Richer, Anthony Elias, Kenneth J. Pienta, Amado J. Zurita, Mitchell E. Gross, Stephanie N. Shishido, James Hicks, Carmen Ruiz Velasco and Peter Kuhn. August 3, 2023. MDPI.org. <https://doi.org/10.3390/cancers15153949>.

Plasticity of circulating tumor cells in small cell lung cancer. Seo J, Kumar M, Mason J, Blackhall F, Matsumoto N, Dive C, Hicks J, Kuhn P, Shishido SN. Sci Rep. 2023 Jul 21;13(1):11775. doi: 10.1038/s41598-023-38881-5.

Single cell clonotypic and transcriptional evolution of multiple myeloma precursor disease. Dang M, Wang R, Lee HC, Patel KK, Becnel MR, Han G, Thomas SK, Hao D, Chu Y, Weber DM, Lin P, Lutter-Berka Z, Berrios Nolasco DA, Huang M, Bansal H, Song X, Zhang J, Futreal A, Moreno Rueda LY, Symer DE, Green MR, Rojas Hernandez CM, Kroll M, Afshar-Khargan V, Ndacayisaba LJ, Kuhn P, Neelapu SS, Orłowski RZ, Wang L, Manasanch EE. Cancer Cell. 2023 Jun 12;41(6):1032-1047.e4. doi: 10.1016/j.ccell.2023.05.007.

Simultaneous copy number alteration and single-nucleotide variation analysis in matched aqueous humor and tumor samples in children with retinoblastoma. Michael J Schmidt, Rishvanth K Prabakar, Sarah Pike, Venkata Yellapantula, Chen-Ching Peng, Peter Kuhn, James Hicks, Liya Xu, Jesse L Berry. Int J Mol Sci. 2023 May 11;24(10):8606. doi: 10.3390/ijms24108606.

Investigation of liquid biopsy analytes in peripheral blood of individuals after SARS-CoV-2 infection. Qi E., Courcoubetis G., Liljegren E., Herrera E., Nguyen N., Nadri M., Ghandehari S., Kazemian E., Reckamp K., Merin N., Merchant A., Mason J., Figueiredo J., Shishido S., Kuhn P. eBioMedicine. March, 2023, Vol 90, 104519. <https://doi.org/10.1016/j.ebiom.2023.104519>.

Gianluca Lazzi

Author Correction: An extraocular electrical stimulation approach to slow down the progression of retinal degeneration in an animal model. Gonzalez Calle A, Paknahad J, Pollalis D, Kosta P, Thomas B, Tew BY, Salhia B, Louie S, Lazzi G, Humayun M. Sci Rep. 2023 Oct 23;13(1):18120. doi: 10.1038/s41598-023-45262-5.

An extraocular electrical stimulation approach to slow down the progression of retinal degeneration in an animal model. Gonzalez Calle A, Paknahad J, Pollalis D, Kosta P, Thomas B, Tew BY, Salhia B, Louie S, Lazzi G, Humayun M. Sci Rep. 2023 Sep 23;13(1):15924. doi: 10.1038/s41598-023-40547-1.

Electrical stimulation induced current distribution in peripheral nerves varies significantly with the extent of nerve damage: a computational study utilizing convolutional neural network and realistic nerve models. Du J, Morales A, Kosta P, Bouteiller JC, Martinez-Navarrete G, Warren DJ, Fernandez E, Lazzi G. Int J Neural Syst. 2023 Apr;33(4):2350022. doi: 10.1142/S0129065723500223.

Computational optimization of delivery parameters to guide the development of targeted nasal spray. Du J, Shao X, Bouteiller JC, Lu A, Asante I, Louie S, Humayun MS, Lazzi G. Sci Rep. 2023 Mar 12;13(1):4099. doi: 10.1038/s41598-023-30252-4.

Jeremy Mason

Plasticity of circulating tumor cells in small cell lung cancer. Seo J, Kumar M, Mason J, Blackhall F, Matsumoto N, Dive C, Hicks J, Kuhn P, Shishido SN. Sci Rep. 2023 Jul 21;13(1):11775. doi: 10.1038/s41598-023-38881-5.

Abstract 5579: Single cell characterization of circulating plasma cells and BCMA levels in patients with multiple myeloma. Sonia Maryam Setayesh, Stephanie Shishido, Libere Ndacayisaba, Amin Naghdloo, Jeremy Mason, Dean Tessone, Carli Kaleta, Robert Z. Orlowski, Elisabet E. Manasanch, James Hicks, Peter Kuhn. *Cancer Res.* April 4, 2023. doi.org/10.1158/1538-7445.AM2023-5579.

Investigation of liquid biopsy analytes in peripheral blood of individuals after SARS-CoV-2 infection. Qi E, Courcoubetis G, Liljegren E, Herrera E, Nguyen N, Nadri M, Ghandehari S, Kazemian E, Reckamp KL, Merin NM, Merchant A, Mason J, Figueiredo JC, Shishido SN, Kuhn P. *EBioMedicine.* March 12, 2023. doi: 10.1016/j.ebiom.2023.104519.

Charles McKenna

*Evidence of bisphosphonate-conjugated sitafloxacin eradication of established methicillin-resistant *S. aureus* infection with osseointegration in murine models of implant-associated osteomyelitis.* Ren Y, Weeks J, Xue T, Rainbolt J, de Mesy Bentley KL, Shu Y, Liu Y, Masters E, Cherian P, McKenna CE, Neighbors J, Ebetino FH, Schwarz EM, Sun S, Xie C. *Bone Res.* 2023 Oct 18;11(1):51. doi: 10.1038/s41413-023-00287-4.

Uridine bisphosphonates differentiate phosphoglycosyl transferase superfamilies. Seebald LM, Haratipour P, Jacobs MR, Bernstein HM, Kashemirov BA, McKenna CE, Imperiali B. *bioRxiv.* 2023 Sep 19:2023.09.19.558431. doi: 10.1101/2023.09.19.558431.

Synthesis and anti-cancer potential of potent peripheral MAOA inhibitors designed to limit blood:brain penetration. Jacobs MR, Olivero JE, Ok Choi H, Liao CP, Kashemirov BA, Katz JE, Gross ME, McKenna CE. *Bioorg Med Chem.* 2023 Sep 7;92:117425. doi:

10.1016/j.bmc.2023.117425. Epub 2023 Jul 26. PMID: 37544256.

Biologically-coupled bisphosphonate chaperones effectively deliver molecules to the site of soft tissue-bone healing. Kremen TJ, Jr., Shi BY, Wu SY, Sundberg O, Sriram V, Kim W, Sheyn D, Lyons KM, Wang W, McKenna CE, Nishimura I. *J Orthop Res.* April 23, 2023. doi: 10.1002/jor.25579.

Microwave-accelerated McKenna synthesis of phosphonic acids: An investigation. Dana Mustafa, Justin M. Overhulse, Boris A. Kashemirov, Charles E. McKenna. *MDPI.* April 4, 2023. DOI:10.3390/molecules28083497.

*Real-time impedance-based monitoring of the growth and inhibition of osteomyelitis biofilm pathogen *Staphylococcus aureus* treated with novel bisphosphonate-fluoroquinolone antimicrobial conjugates.* Sedghizadeh PP, Cherian P, Roshandel S, Tjokro N, Chen C, Junka AF, Hu E, Neighbors J, Pawlak J, Russell RGG, McKenna CE, Ebetino FH, Sun S, Sodagar E. *Int J Mol Sci.* 2023 Jan 19;24(3):1985. doi: 10.3390/ijms24031985.

Ellis Meng

The influence of intrinsic water and ion permeation of the dielectric properties of Parylene C films. Pawlik J.T., Barrera N.D., Meng E., Booth J., Long C., Orloff N., Yoon E., Stelson A. *IEEE Journal of Electromagnetics, RF and Microwaves in Medicine and Biology.* December 2023. doi: 10.1109/JERM.2023.3285049.

Polymer implantable electrode foundry: a shared resource for manufacturing polymer-based microelectrodes for neural interfaces. Scholten K, Xu H, Lu Z, Jiang W, Ortigoza-Diaz J, Petrossians A, Orler S, Gallonio R, Liu X, Song D, Meng E. *bioRxiv.* 2023 Nov 6:2023.11.05.565048. doi: 10.1101/2023.11.05.565048.

Characterization of thin film Parylene C device curvature and the formation of helices via thermoforming. Thielen B, Meng E. *J Micromech Microeng.* 2023 Sep 1;33(9):095007. doi: 10.1088/1361-6439/acdc33.

Making a case for endovascular approaches for neural recording and stimulation. Thielen B., Xu H., Fujii T., Rangwala S., Jiang W., Kammen A., Liu C., Selvan P., Song D., Mack W., Meng E. *Journal of Neural Engineering*, January 24, 2023. doi: 10.1088/1741-2552/acb086.

Shrikanth Narayanan

Relationship satisfaction, feelings of closeness and annoyance, and linkage in electrodermal activity. Timmons AC, Han SC, Chaspari T, Kim Y, Narayanan S, Duong JB, Simo Fiallo N, Margolin G. *Emotion.* 2023 Oct;23(7):1815-1828. doi: 10.1037/emo0001201.

SocialBit: protocol for a prospective observational study to validate a wearable social sensor for stroke survivors with diverse neurological abilities. White K, Tate S, Zafonte R, Narayanan S, Mehl MR, Shin M, Dhand A. *BMJ Open.* 2023 Aug 28;13(8):e076297. doi: 10.1136/bmjopen-2023-076297.

Multimodal neuroimaging data from a 5-week heart rate variability biofeedback randomized clinical trial. Yoo HJ, Nashiro K, Min J, Cho C, Mercer N, Bachman SL, Nasseri P, Dutt S, Porat S, Choi P, Zhang Y, Grigoryan V, Feng T, Thayer JF, Lehrer P, Chang C, Stanley JA, Head E, Rouanet J, Marmarelis VZ, Narayanan S, Wisnowski J, Nation DA, Mather M. *Sci Data.* 2023 Jul 29;10(1):503. doi: 10.1038/s41597-023-02396-5.

A machine learning approach to improve implementation monitoring of family-based preventive interventions in primary care. Berkel C, Knox DC, Flemotomos N, Martinez VR, Atkins DC, Narayanan SS, Rodriguez LA,

Gallo CG, Smith JD. *Implement Res Pract.* 2023 Jul 25;4:26334895231187906. doi: 10.1177/26334895231187906.

Wearable and mobile technologies for the evaluation and treatment of obsessive-compulsive disorder: scoping review. Frank AC, Li R, Peterson BS, Narayanan SS. *JMIR Ment Health.* 2023 Jul 18;10:e45572. doi: 10.2196/45572.

A machine-learning algorithm for the automated perceptual evaluation of dysphonia severity. van der Woerd B, Chen Z, Flemotomos N, Oljaca M, Sund LT, Narayanan S, Johns MM. *J Voice.* 2023 Jul 8:S0892-1997(23)00179-0. doi: 10.1016/j.jvoice.2023.06.006.

Creating musical features using multi-faceted, multi-task encoders based on transformers. Greer T, Shi X, Ma B, Narayanan S. *Sci Rep.* 2023 Jul 3;13(1):10713. doi: 10.1038/s41598-023-36714-z.

The Silent Treatment? Changes in patient emotional expression after silence. Soma CS, Wampold B, Flemotomos N, Peri R, Narayanan S, Atkins DC, Imel ZE. *Couns Psychother Res.* 2023 Jun;23(2):378-388. doi: 10.1002/capr.12537.

Modeling inter-individual differences in ambulatory-based multimodal signals via metric learning: a case study of personalized well-being estimation of healthcare workers. Paromita P, Mundnich K, Nadarajan A, Booth BM, Narayanan SS, Chaspari T. *Front Digit Health.* 2023 Jun 9;5:1195795. doi: 10.3389/fdgth.2023.1195795.

You never know what you are going to get: large-scale assessment of therapists' supportive counseling skill use. Zhang X, Tanana M, Weitzman L, Narayanan S, Atkins D, Imel Z. *Psychotherapy (Chic).* 2023 Jun 1;60(2):149-158. doi: 10.1037/pst0000460.

A review of speech-centric trustworthy machine learning: privacy, safety, and fairness. Tiantian Feng, Rajat Hebbar, Nicholas Mehlman, Xuan Shi, Aditya Kommineni, Shrikanth Narayanan. April 16, 2023, Vol. 12: No. 3, e17. <http://dx.doi.org/10.1561/116.00000084>.

Mel frequency spectral domain defenses against adversarial attacks on speech recognition systems. Mehlman N, Sreeram A, Peri R, Narayanan S. JASA Express Lett. 2023 Mar;3(3):035208. doi: 10.1121/10.0017680.

Krishna Nayak

Submillimeter lung MRI at 0.55T using balanced steady-state free precession with half-radial dual-echo readout (bSTAR). G Bauman, NG Lee, Y Tian, O Bieri, KS Nayak. Magnetic Resonance in Medicine. <https://doi.org/10.1002/mrm.29757>.

Fetal Cardiac Magnetic Resonance Imaging Solving An Unmet Need In Prenatal Diagnosis of Congenital Heart Disease. Jon Detterich, Brendan Grubbs, Jay Pruetz, John Wood, Ye Tian, Krishna Nayak. American Journal of Obstetrics & Gynecology MFM. <https://www.ajogmfm.org/>.

New clinical opportunities of low-field MRI: heart, lung, body, and musculoskeletal. Y Tian, KS Nayak. Magnetic Resonance Materials in Physics, Biology and Medicine. <https://doi.org/10.1007/s10334-023-01123-w>.

Real-Time Water/Fat Imaging at 0.55T with Spiral Out-In-Out-In Sampling. Y Tian, KS Nayak. Magnetic Resonance in Medicine. <https://doi.org/10.1002/mrm.29885>.

Feasibility of detecting actionable Lung Nodules using 0.55 Tesla MRI. Y Tian, KS Nayak. Magnetic Resonance in Medicine. <https://doi.org/10.1002/mrm.29885>.

Should manual dexterity be investigated as a marker of early Alzheimer's disease? rs-fMRI Evidence. Joshi AA, Shattuck DW, Leahy RM, and Chaudhari RM. OHBM 2023 Conference. <https://www.humanbrainmapping.org/i4a/pages/index.cfm?pageid=3277>.

DeepSVR: Slice to volume registration and reconstruction using Deep Learning. O Zamzam, AA Joshi, JC Wood, KS Nayak, RM Leahy. OHBM 2023 Conference. <https://www.humanbrainmapping.org/i4a/pages/index.cfm?pageid=3277>.

T1 and T2 measurement variability across commercial and prototype 0.55T systems. K Keenan, B Tasdelen, AE Campbell-Washburn, H Sharma, A Javed, R Ramasawmy, MN Martin, N Seiberlich, KS Nayak. ISMRM 2023 Conference. <https://submissions.miramart.com/ISMRM2023/ViewSubmissionTeaser.aspx>.

Modeling and selection of T1 and T2 tissue mimics for 0.0065T, 0.064T, 0.55T MRI using agarose with manganese, gadolinium, copper, or nickel. K Jordanova, Y Tian, S Shen, MN Martin, ME Poorman, RP Teixeira, KS Nayak, MS Rosen, KE Keenan. ISMRM 2023 Conference. <https://submissions.miramart.com/ISMRM2023/ViewSubmissionTeaser.aspx>.

Evaluation of a Wearable bluetooth sensor at 0.55T. F Munoz, KS Nayak, Y Khan. ISMRM 2023 Conference. <https://submissions.miramart.com/ISMRM2023/ViewSubmissionTeaser.aspx>.

Simultaneous multi-slice real-time cardiac MRI at 0.55T. E Yagiz, P Garg, KS Nayak, Y Tian. ISMRM 2023 Conference. <https://submissions.miramart.com/ISMRM2023/ViewSubmissionTeaser.aspx>.

Rapid 3D lung imaging with bSSFP stack of spiral out-in (SoSoi) sampling at 0.55T. Y Tian, NG Lee, Z Zhao, KS Nayak. ISMRM 2023 Conference. <https://submissions.miramart.com/ISMRM2023/ViewSubmissionTeaser.aspx>.

com/ISMRM2023/ViewSubmissionTeaser.aspx.

Submillimeter morphologic lung MRI at 0.55T using balanced steady-state free precession with half-radial dual-echo readout (bSTAR). G Baumann, NG Lee, Y Tian, O Bieri, KS Nayak. ISMRM 2023 Conference. <https://submissions.miramart.com/ISMRM2023/ViewSubmissionTeaser.aspx>.

Reproducibility of the bSTAR sequence and open-source implementation. NG Lee, G Bauman, O Bieri, KS Nayak. . ISMRM 2023 Conference. <https://ismrm2023-unofficial.netlify.app/>.

Fetal cardiac 3D CINE MRI at low field - whole heart slice-to-volume reconstruction from real-time spiral SSFP at 0.55T. Fetal cardiac 3D CINE MRI at low field - whole heart slice-to-volume reconstruction from real-time spiral SSFP at 0.55T. JFP van Amerom, Y Tian, DS Goolaub, JC Wood, J Detterich, KS Nayak, CK MacGowan. ISMRM 2023 Conference. <https://submissions.miramart.com/ISMRM2023/ViewSubmissionTeaser.aspx>.

Multi-resolution comparison of fetal CINE MRI at 0.55T. JFP van Amerom, Y Tian, DS Goolaub, JC Wood, J Detterich, KS Nayak, CK MacGowan. ISMRM 2023 Conference. <https://submissions.miramart.com/ISMRM2023/ViewSubmissionTeaser.aspx>.

Real-time fetal cardiac MRI at 0.55T enables assessment of ventricular function and heart and great vessel anatomy. Y Tian, J Detterich, JD Pruetz, AA Joshi, JC Wood, KS Nayak. ISMRM 2023 Conference. <https://submissions.miramart.com/ISMRM2023/ViewSubmissionTeaser.aspx>.

Open-source tools for multi-center multi-platform 0.55T relaxometry studies. B Tasdelen, R Ramasawmy, H Sharma, KE Keenan, A Campbell-Washburn, N Sieberlich, KS Nayak. ISMRM 2023 Conference. <https://ismrm2023-unofficial.netlify.app/>.

Rapid 3D lung imaging with bSSFP stack-of-spiral out-in (SoSoi) sampling at 0.55T. Y Tian, J Detterich, JD Pruetz, AA Joshi, JC Wood, KS Nayak. ISMRM 2023 Conference. <https://submissions.miramart.com/ISMRM2023/ViewSubmissionTeaser.aspx>.

Simultaneous multi-slice (SMS) real-time cardiac MRI at 0.55T. E Yagiz, P Garg, KS Nayak, Y Tian. ISMRM 2023 Conference. <https://submissions.miramart.com/ISMRM2023/ViewSubmissionTeaser.aspx>.

Real-time fetal cardiac MRI at 0.55T enables assessment of ventricular function and heart and great vessel anatomy. Y Tian, JA Detterich, J Wood, AA. Joshi, JD Pruetz, KS Nayak. . ISMRM 2023 Conference. <https://submissions.miramart.com/ISMRM2023/ViewSubmissionTeaser.aspx>.

Low-Field 0.55T MRI evaluation of the fetus. Ponrartana S, Nguyen HN, Cui SX, Nayak, KS et al. Pediatric Radiology. <https://doi.org/10.1007/s00247-023-05604-x>.

Niema Pahlevan

A new left ventricle vortex formation time for clinical assessment of diastolic filling efficiency based on direct mechanical ventricular-vascular coupling: evaluation in heart-failure & healthy cohort. Coskun Bilgi, Ben A Lin & Niema M Pahlevan. November 6, 2023. https://www.ahajournals.org/doi/10.1161/circ.148.suppl_1.16610.

A fourier-based methodology without numerical diffusion for conducting dye simulations and particle residence time calculations. Amlani F, Wei H*, and Pahlevan NM. November 15, 2023. Journal of Computational Physics. <https://doi.org/10.1016/j.jcp.2023.112472>.

A machine learning approach for computation of cardiovascular intrinsic frequencies. Alavi R*, Wang Q, Gorji H, and Pahlevan NM. October 26, 2023. PLoS

ONE. <https://doi.org/10.1371/journal.pone.0285228>.

Mechanistic insights on age-related changes in heart-aorta-brain hemodynamic coupling using a pulse wave model of the entire circulatory system. Aghilinejad A*, Amlani F, Mazandarani SP, King KS, and Pahlevan NM. October 18, 2023. American Journal of Physiology-Heart and Circulatory Physiology. <https://doi.org/10.1152/ajpheart.00314.2023>.

Evaluation of left ventricular pulsatile workload in heart failure with preserved ejection fraction using a single pressure waveform from Framingham Heart Study. Niroumandi S*, Wolfson AM, Vaidya AS, and Pahlevan NM. October 11, 2023. Hypertension. https://doi.org/10.1161/hyp.80.suppl_1.P367.

Fluid-based microbial processes modeling in Trichodesmium colony formation. Wei H*, Hutchins DA, Ronney PD, and Pahlevan NM. October 4, 2023. Physics of Fluids. <https://doi.org/10.1063/5.0165872>.

Instantaneous detection of acute myocardial infarction and ischemia from a single carotid pressure waveform in rats. Alavi R*, Dai W, Matthews RV, Kloner RA, and Pahlevan NM. October 3, 2023. European Heart Journal Open. 3(5): oead099. <https://doi.org/10.1093/ehjopen/oead099>.

Assessment of aortic characteristic impedance and arterial compliance from non-invasive carotid pressure waveform in the Framingham heart study. Soha Niroumandi, Rashid Alavi, Aaron Michael Wolfson, Ajay Shrikrishna Vaidya, Niema Mohammed Pahlevan. October 1, 2023. American Journal Cardiology. <https://doi.org/10.1016/j.amjcard.2023.07.076>.

On the longitudinal wave pumping in the fluid-filled compliant tubes. Aghilinejad A*, Rogers B*, Geng H*, and Pahlevan NM.

September 6, 2023. Physics of Fluids. <https://doi.org/10.1063/5.0165150>.

Framework development for patient-specific compliant aortic dissection phantom model fabrication: magnetic resonance imaging validation and deep-learning segmentation. Aghilinejad A*, Wei H*, Bilgi C*, Paredes A*, DiBartolomeo A, Magee G, and Pahlevan NM. June 13, 2023. Journal of Biomechanical Engineering. <https://doi.org/10.1115/1.4062539>.

Noninvasive and instantaneous detection of myocardial ischemia from a single carotid waveform using a physics-based machine learning methodology. Alavi R, Dai W, Kloner RA, Pahlevan NM. March 7, 2023. Journal of the American College of Cardiology. [https://doi.org/10.1016/S0735-1097\(23\)04456-X](https://doi.org/10.1016/S0735-1097(23)04456-X).

Screening left ventricular systolic dysfunction in children using intrinsic frequencies of carotid pressure waveforms measured by a novel smartphone-based device. Cheng AL, Liu J, Bravo S, Miller JC, and Pahlevan NM. March 1, 2023. Physiological Measurement. <https://doi.org/10.1088/1361-6579/acba7b>.

Thermal and postural effects on fluid mixing and irrigation patterns for intraventricular hemorrhage treatment. Bilgi C*, Amlani F, Wei H*, Rizzi N, and Pahlevan NM. January 21, 2023. Annals of Biomedical Engineering. <https://doi.org/10.1007/s10439-022-03130-9>.

Non-invasive pressure-only aortic wave intensity evaluation using hybrid fourier decomposition-machine learning approach. Aghilinejad A*, Wei H*, and Pahlevan NM. January 13, 2023. IEEE Transactions on Biomedical Engineering. <https://doi.org/10.1109/TBME.2023.3236918>.

Direct OD-3D coupling of a lattice Boltzmann methodology for fluid-structure aortic flow simulations. Wei H*, Amlani F, and Pahlevan NM. January 11, 2023. International

Journal for Numerical Methods in Biomedical Engineering. <https://doi.org/10.1002/cnm.3683>.

Jayakanth Ravichandran

Charge-density-wave resistive switching and voltage oscillations in ternary chalcogenide BaTiS₃. H. Chen, N. Wang, H. Liu, H. Wang, J. Ravichandran. September 22, 2023. Advanced Electronic Materials. <https://doi.org/10.1002/aelm.202300461>.

Charge-density-wave order and electronic phase transitions in a dilute d-band semiconductor. H. Chen, B. Zhao, J. Mutch, G. Y. Jung, G. Ren, S. Shabani, E. Seewald, S. Niu, J. Wu, N. Wang, M. Surendran, S. Singh, J. Luo, S. Ohtomo, G. Goh, B. C. Chakoumakos, S. J. Teat, B. Melot, H. Wang, A. N. Pasupathy, R. Mishra, J. -H. Chu, J. Ravichandran. August 4, 2023. Advanced Materials. <https://doi.org/10.1002/adma.202303283>.

Colossal optical anisotropy from atomic-scale modulations. H. Mei, G. Ren, B. Zhao, J. Salman, G. Y. Jung, H. Chen, S. Singh, A. S. Thind, J. Cavin, J. A. Hachtel, M. Chi, S. Niu, G. Joe, C. Wan, N. Settineri, S. J. Teat, B. C. Chakoumakos, J. Ravichandran, R. Mishra, M. A. Kats. August 2, 2023. Advanced Materials. <https://doi.org/10.1002/adma.202303588>.

Direct observation of strain-induced ferrochiral transition in Quasi-1D BaTiS₃. Ren G, Jung GY, Wang C, Chen H, Zhao B, Vasudevan RK, Lupini AR, Chi M, Hachtel JA, Xiao D, Ravichandran J, Mishra R. *Microsc Microanal*. 2023 Jul 22;29(Supplement_1):1624-1625. doi: 10.1093/micmic/ozad067.834.

Ruddlesden-Popper chalcogenides push the limit of mechanical stiffness and glass-like thermal conductivity in crystals. M. S. Bin Hoque, E. R. Hogle, B. Zhao, D.-L. Bao, H. Zhou, S. Thakur, E. Osei-Agyemang, K. Hattar, E. A. Scott, M. Surendran, J. A.

Tomko, J. T. Gaskins, K. Aryana, S. Makarem, G. Balasubramanian, A. Giri, T. Feng, J. A. Hachtel, J. Ravichandran, S. T. Pantelides, and P. E. Hopkins. (Submitted).

A hybrid pulsed laser deposition approach to grow thin films of chalcogenides. M. Surendran, S. Singh, H. Chen, C. Wu, A. Avishai, Y-T. Shao, and J. Ravichandran. (Submitted).

Giant modulation of refractive index from correlated atomic-scale disorder. B. Zhao, G. Ren, H. Mei, V. C. Wu, S. Singh, G. -Y. Jung, H. Chen, R. Giovine, S. Niu, A. S. Thind, J. Salman, N. S. Settineri, B. C. Chakoumakos, M. E. Manley, R. P. Hermann, A. R. Lupini, M. Chi, J. A. Hachtel, A. Simonov, S. J. Teat, R. J. Clement, M. A. Kats, J. Ravichandran, and R. Mishra. (Submitted).

Photoconductive effects in single crystals of BaZrS₃. B. Zhao, H. Chen, R. Ashan, F. Hou, E. R. Hogle, S. Singh, M. Shanmugasundaram, H. Zhao, H. Htoon, A. Hrayev, P. E. Hopkins, J. Seidel, R. Kapadia, and J. Ravichandran. (Submitted).

Remo Rohs

Probing the role of the protonation state of a minor groove-linker histidine in Exd-Hox-DNA binding. Jiang Y, Chiu TP, Mitra R, Rohs R. *Biophys J*. 2023 Dec 21:S0006-3495(23)04151-6. doi: 10.1016/j.bpj.2023.12.013.

Deep DNASHape: Predicting DNA shape considering extended flanking regions using a deep learning method. Jinsen Li, Tsu-Pei Chiu, Remo Rohs. *Biorxiv*. org. October 24, 2023. <https://doi.org/10.1101/2023.10.22.563383>.

CRISPR-Cas9 activities with truncated 16-nucleotide RNA guides are tuned by target duplex stability beyond the RNA/DNA hybrid. Li Y, Cooper BH, Liu Y, Wu D, Zhang X, Rohs R, Qin PZ. *Biochemistry*. 2023 Sep

5;62(17):2541-2548. doi: 10.1021/acs.biochem.3c00250.

DNA binding specificity of all four Saccharomyces cerevisiae forkhead transcription factors. Brendon H Cooper, Ana Carolina Dantas Machado, Yan Gan, Oscar M Aparicio, Remo Rohs. Nucleic Acids Research, May 13, 2023, <https://doi.org/10.1093/nar/gkad372>.

Physicochemical models of protein-DNA binding with standard and modified base pairs. Chiu TP, Rao S, Rohs R. Proc Natl Acad Sci U S A. 2023 Jan 24;120(4):e2205796120. doi: 10.1073/pnas.2205796120. Epub 2023 Jan 19.

Maryam Shanechi

Unsupervised learning of stationary and switching dynamical system models from Poisson observations. Song CY, Shanechi MM. J Neural Eng. 2023 Dec 12;20(6):066029. doi: 10.1088/1741-2552/ad038d.

Dynamical flexible inference of nonlinear latent factors and structures in neural population activity. Abbaspourzad H, Erturk E, Pesaran B, Shanechi MM. Nat Biomed Eng. 2023 Dec 11. doi: 10.1038/s41551-023-01106-1.

Multimodal subspace identification for modeling discrete-continuous spiking and field potential population activity. Ahmadipour P, Sani OG, Pesaran B, Shanechi MM. J Neural Eng. 2023 Nov 28. doi: 10.1088/1741-2552/ad1053.

Post-stimulus encoding of decision confidence in EEG: toward a brain-computer interface for decision making. Sadras N, Sani OG, Ahmadipour P, Shanechi MM. J Neural Eng. 2023 Sep 19;20(5). doi: 10.1088/1741-2552/acec14.

First-in-human prediction of chronic pain state using intracranial neural biomarkers. Shirvalkar P, Prosky J, Chin G, Ahmadipour

P, Sani OG, Desai M, Schmitgen A, Dawes H, Shanechi MM, Starr PA, Chang EF. Nat Neurosci. 2023 Jun;26(6):1090-1099. doi: 10.1038/s41593-023-01338-z.

Future directions in psychiatric neurosurgery. Proceedings of the 2022 American Society for Stereotactic and Functional Neurosurgery meeting on surgical neuromodulation for psychiatric disorders. Hitti FL, Widge AS, Riva-Posse P, Malone DA Jr, Okun MS, Shanechi MM, Foote KD, Lisanby SH, Ankudowich E, Chivukula S, Chang EF, Gunduz A, Hamani C, Feinsinger A, Kubu CS, Chiong W, Chandler JA, Carbutaru R, Cheeran B, Raike RS, Davis RA, Halpern CH, Vanegas-Arroyave N, Markovic D, Bick SK, McIntyre CC, Richardson RM, Dougherty DD, Kopell BH, Sweet JA, Goodman WK, Sheth SA, Pouratian N. Brain Stimul. 2023 May-Jun;16(3):867-878. doi: 10.1016/j.brs.2023.05.011.

Ye Tian

Submillimeter lung MRI at 0.55 T using balanced steady-state free precession with half-radial dual-echo readout (bSTAR). Bauman G, Lee NG, Tian Y, Bieri O, Nayak KS. Magn Reson Med. 2023 Nov;90(5):1949-1957. doi: 10.1002/mrm.29757.

New clinical opportunities of low-field MRI: heart, lung, body, and musculoskeletal. Tian Y, Nayak KS. MAGMA. 2023 Oct 30. doi: 10.1007/s10334-023-01123-w.

Neuroimaging-AI endophenotypes of brain diseases in the general population: towards a dimensional system of vulnerability. Wen J, Skampardon I, Tian YE, Yang Z, Cui Y, Erus G, Hwang G, Varol E, Boquet-Pujadas A, Chand GB, Nasrallah I, Satterthwaite T, Shou H, Shen L, Toga AW, Zalesky A, Davatzikos C. medRxiv. 2023 Aug 24:2023.08.16.23294179. doi: 10.1101/2023.08.16.23294179.

The genetic architecture of biological age in nine human organ systems. Wen J, Tian YE, Skampardoni I, Yang Z, Mamourian E, Anagnostakis F, Zhao B, Toga AW, Zalesky A, Davatzikos C. medRxiv. 2023 Jun 17;2023.06.08.23291168. doi: 10.1101/2023.06.08.23291168.

Low-field 0.55 T MRI evaluation of the fetus. Ponrartana S, Nguyen HN, Cui SX, Tian Y, Kumar P, Wood JC, Nayak KS. *Pediatr Radiol.* 2023 Jun;53(7):1469-1475. doi: 10.1007/s00247-023-05604-x.

Quantitative myocardial perfusion with a hybrid 2D simultaneous multi-slice sequence. Huang Q, Tian Y, Mendes J, Ranjan R, Adluru G, DiBella E. *Magn Reson Imaging.* 2023 May;98:7-16. doi: 10.1016/j.mri.2022.12.010.

Real-time water/fat imaging at 0.55T with spiral out-in-out-in sampling. Tian Y, Nayak KS. *Magn Reson Med.* 2024 Feb;91(2):649-659. doi: 10.1002/mrm.29885.

Contrast-optimal simultaneous multi-slice bSSFP cine cardiac imaging at 0.55 T. Tian Y, Cui SX, Lim Y, Lee NG, Zhao Z, Nayak KS. *Magn Reson Med.* 2023 Feb;89(2):746-755. doi: 10.1002/mrm.29472.

T1 mapping of myocardium in rats using self-gated golden-angle acquisition. Vitouš J, Jiřík R, Stračina T, Hendrych M, Nádeníček J, Macíček O, Tian Y, Krátká L, Dražanová E, Nováková M, Babula P, Panovský R, DiBella E, Starčuk Z. *Magn Reson Med.* 2024 Jan;91(1):368-380. doi: 10.1002/mrm.29846.

Kate White

Quantitative structural mapping of insulin vesicle maturation in beta cells. Deshmukh A, Loconte V, White KL. *Microsc Microanal.* 2023 Jul 22;29(29 Suppl 1):1166. doi: 10.1093/micmic/ozad067.597.

Soft x-ray tomography for mapping and quantifying intracellular organelle interactions. Loconte V, Singla J, Li A, Chen JH, Ekman A, McDermott G, Sali A, Gros ML, White KL, Larabell CA. *Microsc Microanal.* 2023 Jul 22;29(Supplement_1):1181. doi: 10.1093/micmic/ozad067.607.

Loss of ZNF148 enhances insulin secretion in human pancreatic β cells. de Klerk E, Xiao Y, Emfinger CH, Keller MP, Berrios DI, Loconte V, Ekman AA, White KL, Cardone RL, Kibbey RG, Attie AD, Hebrok M. *JCI Insight.* 2023 Jun 8;8(11):e157572. doi: 10.1172/jci.insight.157572.

Cristina Zavaleta

Multiplexing potential of NIR resonant and non-resonant Raman reporters for bio-imaging applications. Eremina OE, Schaefer S, Czaja AT, Awad S, Lim MA, Zavaleta C. *Analyst.* 2023 Nov 20;148(23):5915-5925. doi: 10.1039/d3an01298k.

Current and developing lymphatic imaging approaches for elucidation of functional mechanisms and disease progression. *Molecular Imaging and Biology.* May 17, 2023. <https://doi.org/10.1007/s11307-023-01827-4>.

Nanomaterial-based contrast agents. Hsu J., Tang Z., Eremina O., Sofias Marios A.S., Lammers T., Lovell F. J., Zavaleta C., Cai W., Cormode, D.P. *Nat Rev Methods.* April 13, 2023. <https://doi.org/10.1038/s43586-023-00211-4>.

Proceedings Paper: Topographic Raman imaging approach for surgical margin assessment and quantification of an expanded SERS nanoparticle library for highly multiplexed imaging assays. *Proc. SPIE PC12361, Molecular-Guided Surgery: Molecules, Devices, and Applications IX, PC1236106.* March 17, 2023. doi:10.1117/12.2649201.

HyU: Hybrid Unmixing for longitudinal in vivo imaging of low signal-to-noise fluorescence.

Chiang H.J., Koo D.E.S., Kitano M., et al. *Nat Methods* 20, 248-258. January 19, 2023.

<https://doi.org/10.1038/s41592-022-01751-5>.

Comparative study of non-resonant and resonant Raman reporters for multiplexing applications. To SERRS or not to SERRS?

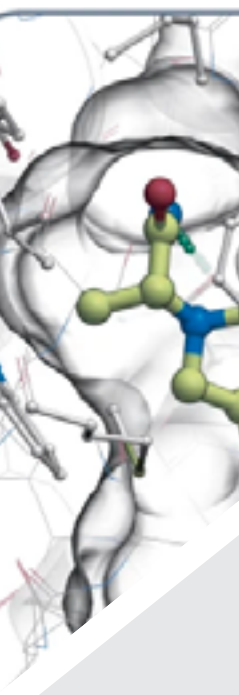
Eremina O.E., Schaefer S., Czaj A.T., Awa S., Li M.A., Zavaleta C. *Anal. Chem.*, 2023, submitted.



Featured Article

Computational approaches streamlining drug discovery

Anastasiia V. Sadybekov and Vsevolod Katritch, [Nature](#) — April 26, 2023



Despite amazing progress in basic life sciences and biotechnology, drug discovery and development (DDD) remain slow and expensive, taking on average approximately 15 years and approximately US\$2 billion to make a small-molecule drug. Although it is accepted that clinical studies are the priciest part of the development of each drug, most time-saving and cost-saving opportunities reside in the earlier discovery and preclinical stages. Preclinical efforts themselves account for more than 43% of expenses in pharma, in addition to major public funding, driven by the high attrition rate at every step from target selection to hit identification and lead optimization to the selection of clinical candidates. Moreover, the high failure rate in clinical trials (currently 90%) is largely explained by issues rooted in early discovery such as inadequate target validation or suboptimal ligand properties. Finding fast and accessible ways to discover more diverse pools of higher-quality chemical probes, hits and leads with optimal absorption, distribution, metabolism, excretion and toxicology (ADMET) and pharmacokinetics (PK) profiles at the early stages of DDD would improve outcomes in preclinical and clinical studies and facilitate more effective, accessible and safer drugs.

The concept of computer-aided drug discovery was developed in the 1970s and popularized by Fortune magazine in 1981, and has since been through several cycles of hype and disillusionment. There have been success stories along the way and, in general, computer-assisted approaches have become an integral, yet modest, part of the drug discovery process. In the past few years, however, several scientific and technological breakthroughs resulted in a tectonic shift towards embracing computational approaches as a key driving force for drug discovery in both academia and industry. Pharmaceutical and biotech companies are expanding their computational drug discovery efforts or hiring their first computational chemists. Numerous new and established drug discovery companies have raised billions in the past few years with business models that heavily rely on a combination of advanced physics-based molecular modelling with deep learning (DL) and artificial intelligence (AI). Although it is too early yet to expect approved drugs from the most recent computationally driven discovery efforts, they are producing a growing number of clinical candidates, with some campaigns specifically claiming target-to-lead times as low as 1-2 months, or target-to-clinic time under 1 year. Are these the signs of a major shift in the role that computational

approaches have in drug discovery or just another round of the hype cycle?

Let us look at the key factors defining the recent changes (Fig. 1). First, the structural revolution—from automation in crystallography to microcrystallography and most recently cryo-electron microscopy technology—has made it possible to reveal 3D structures for the majority of clinically relevant targets, often in a state or molecular complex relevant to its biological function. Especially impressive has been the recent structural turnaround for G protein-coupled receptors (GPCRs) and other membrane proteins that mediate the action of more than 50% of drugs, providing 3D templates for ligand screening and lead optimization. The second factor is a rapid and marked expansion of drug-like chemical space, easily accessible for hit and lead discovery. Just a few years ago, this space was limited to several million on-shelf compounds from vendors and in-house screening libraries in pharma. Now, screening can be done with ultra-large virtual libraries and chemical spaces of drug-like compounds, which can be readily made on-demand, rapidly growing beyond billions of compounds, and even larger generative spaces with theoretically predicted synthesizability (Box 1). The third factor involves emerging computational approaches that strive to take full advantage of the abundance of 3D structures and ligand data, supported by the broad availability of cloud and graphics processing unit (GPU) computing resources to support these methods at scale. This includes structure-based virtual screening of ultra-large libraries, using accelerated and modular screening approaches, as well as recent growth of data-driven machine learning (ML) and DL methods for predicting ADMET and PK properties and activities.

Although the impacts of the recent structural revolution and computing hardware in drug discovery are comprehensively reviewed elsewhere, here we focus on the ongoing

expansion of accessible drug-like chemical spaces as well as current developments in computational methods for ligand discovery and optimization. We detail how emerging computational tools applied in gigaspace can facilitate the cost-effective discovery of hundreds or even thousands of highly diverse, potent, target-selective and drug-like ligands for a desired target, and put them in the context of experimental approaches (Table 1). Although the full impact of new computational technologies is only starting to affect clinical development, we suggest that their synergistic combination with experimental testing and validation in the drug discovery ecosystem can markedly improve its efficiency in producing better therapeutics.

Full article can be found in the addendum.



Highlighted Publications

Detecting Disruption of HER2 Membrane Protein Organization in Cell Membranes with Nanoscale Precision

Yasaman Moradi, Jerry S. H. Lee, and Andrea M. Armani, [ACS Sensors](#) — November 13, 2023

The spatiotemporal organization of proteins within the cell membrane can affect numerous biological functions, including cell signaling, communication, and transportation.

Deviations from normal spatial arrangements have been observed in various diseases, and a better understanding of this process is a key stepping stone to advancing development of clinical interventions. However, given the nanometer length scales involved, detecting these subtle changes has primarily relied on complex super-resolution and single-molecule imaging methods. In this work, we demonstrate an alternative fluorescent imaging strategy for detecting protein organization based on a material that exhibits a unique photophysical behavior known as aggregation-induced emission (AIE). Organic AIE molecules have an increase in emission signal when they are in close proximity, and the molecular motion is restricted.

This property simultaneously addresses the

high background noise and low detection signal that limit conventional widefield fluorescent imaging. To demonstrate the potential of this approach, the fluorescent molecule sensor is conjugated to a human epidermal growth factor receptor 2 (HER2)-specific antibody and used to investigate the spatiotemporal behavior of HER2 clustering in the membrane of HER2-overexpressing breast cancer cells. Notably, the disruption of HER2 clusters in response to an FDA-approved monoclonal antibody therapeutic (Trastuzumab) is successfully detected using a simple widefield fluorescent microscope. While the sensor demonstrated here is optimized for sensing HER2 clustering, it is an easily adaptable platform. Moreover, given the compatibility with widefield imaging, the system has the potential to be used with high-throughput imaging techniques, accelerating investigations into membrane protein spatiotemporal organization.

Agent-based modeling of tumor-immune interactions reveals determinants of final tumor states

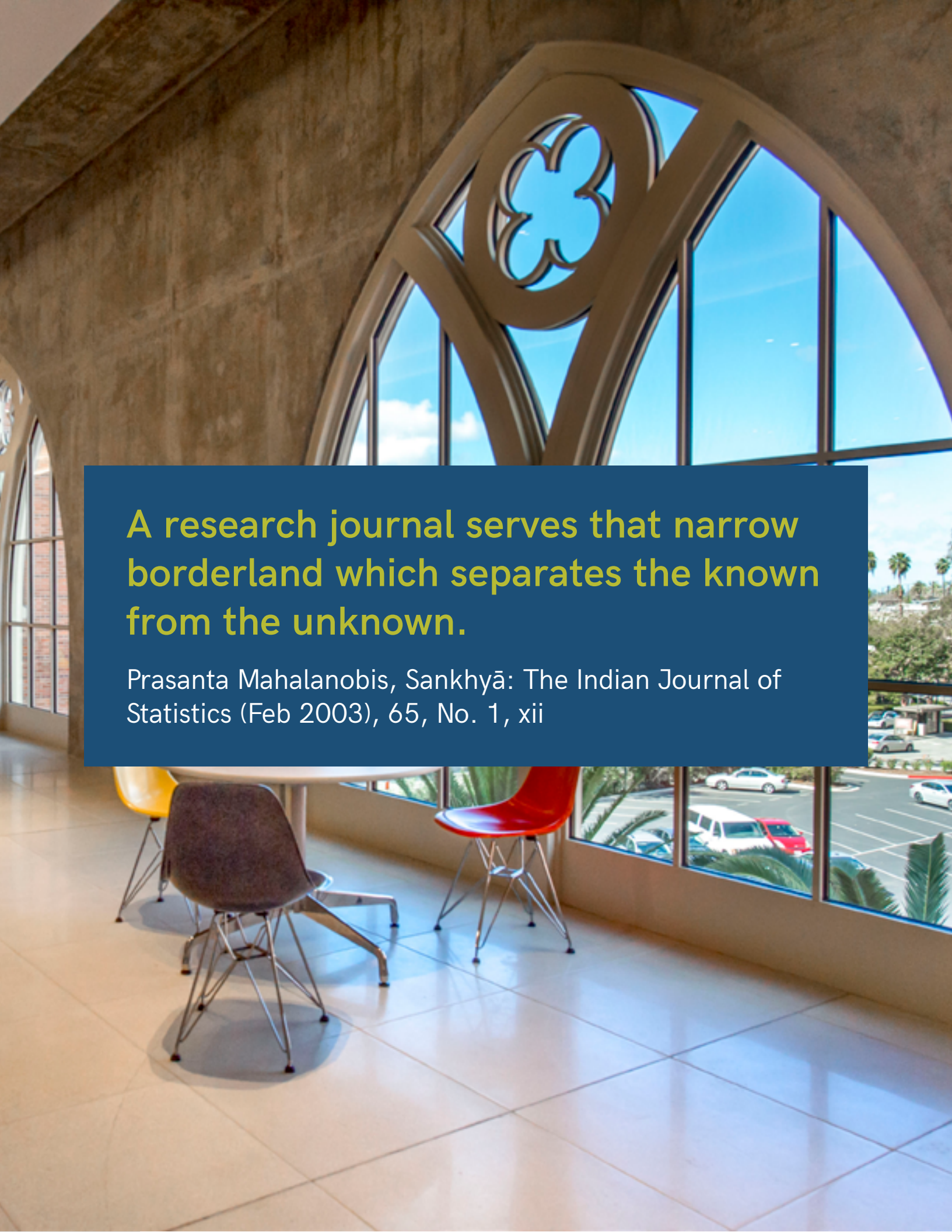
Manal Ahmidoucha, Neel Tangellab and Stacey D. Finley, [Molecular Imaging and Biology](#) — January 19, 2023

Interactions between tumor and immune cells in the tumor microenvironment (TME) influence tumor growth and the tumor's response to treatment. Excitingly, this complex landscape of tumor-immune interactions can be studied using

computational modeling. Mathematical oncology can provide quantitative insights into the TME, serving as a framework for understanding tumor dynamics. Here, we use an agent-based model to simulate the interactions among cancer cells, macrophages

(naïve, M1, and M2), and T cells (active CD8+ and inactive) in a 2D representation of the TME. Key diffusible factors, IL-4 and IFN- γ , are also incorporated. We apply the model to predict how cell-specific properties influence tumor progression. The model predictions and analyses revealed the relationships between different cell populations and highlighted the importance of macrophages and T cells in shaping the TME. Thus, we quantify how components of the TME influence the final tumor state and the effects of macrophage-based therapies. The findings emphasize the significant role of computational models in

unraveling the intricate dynamics of tumor-immune interactions and their potential for guiding the development of tailored immunotherapeutic strategies. This study provides a foundation for future investigations aiming to refine and expand the model, validate predictions experimentally, and pave the way for improved cancer treatments.

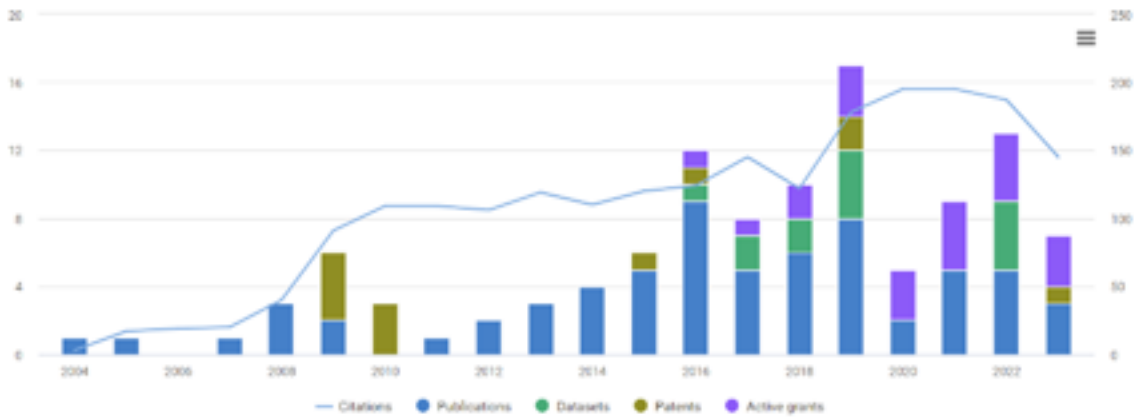


**A research journal serves that narrow
borderland which separates the known
from the unknown.**

Prasanta Mahalanobis, *Sankhyā: The Indian Journal of
Statistics* (Feb 2003), 65, No. 1, xii

James Boedicker

Publications 66 Citations 2,156	Datasets 13	Grants 6 Funding amount USD 8.8 M	Patents 12 Clinical Trials 0
---	-----------------------	---	---



Publications: Collaborations

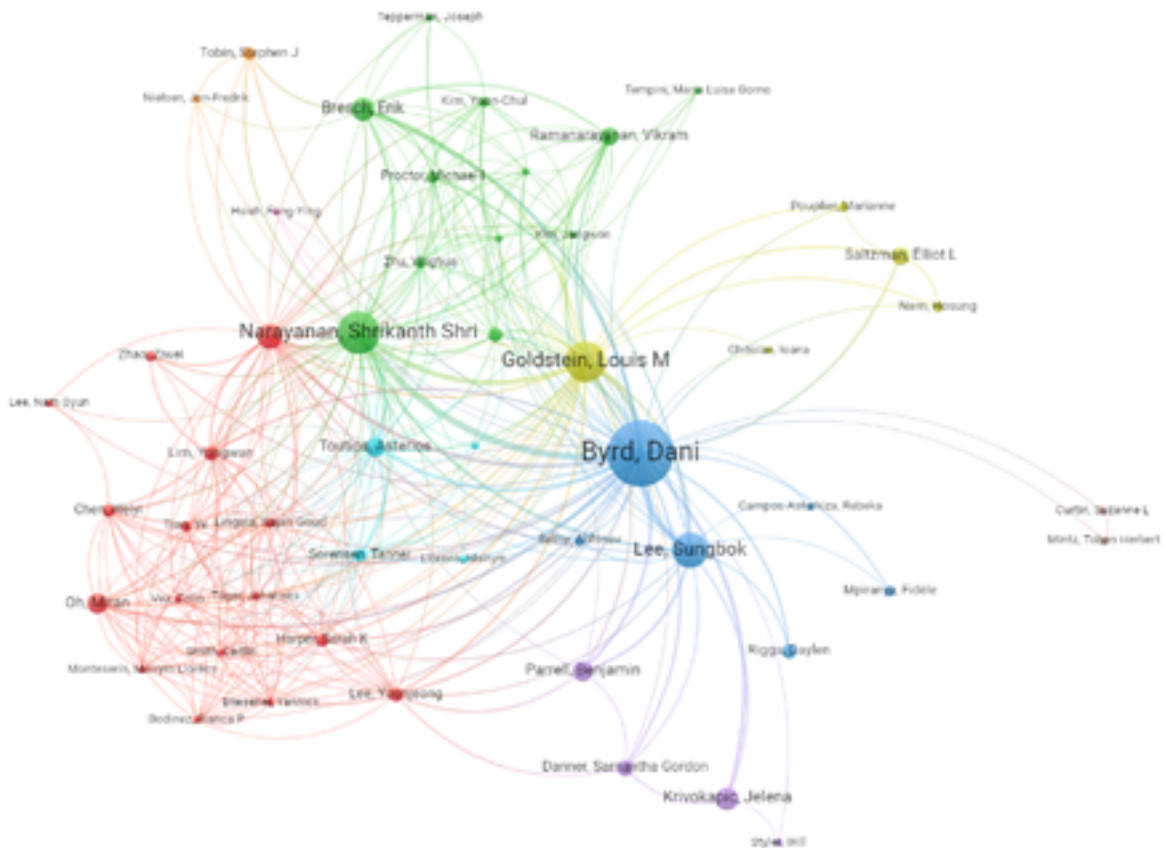


Dani Byrd

Publications 120 Citations 3,089	Datasets 27	Grants 6 Funding amount USD 10.7 M	Patents 0 <hr/> Clinical Trials 0
---	-----------------------	---	--

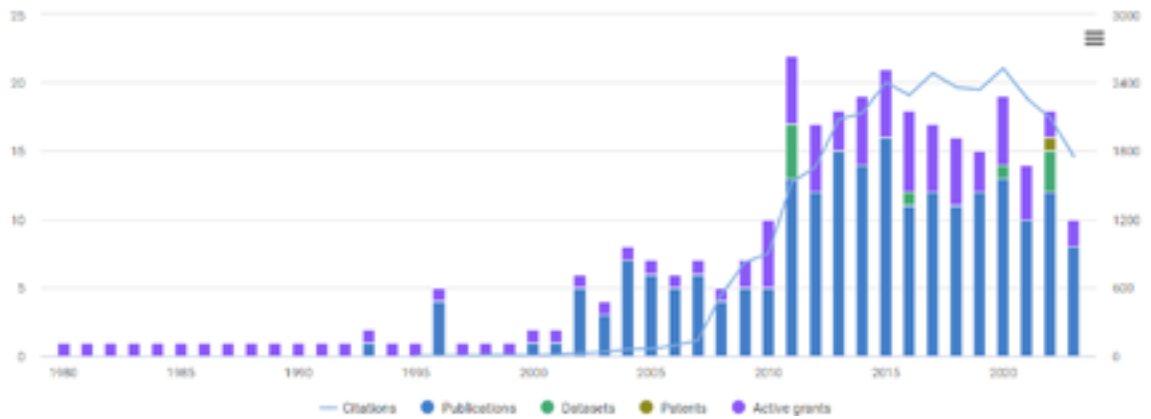


Publications: Collaborations

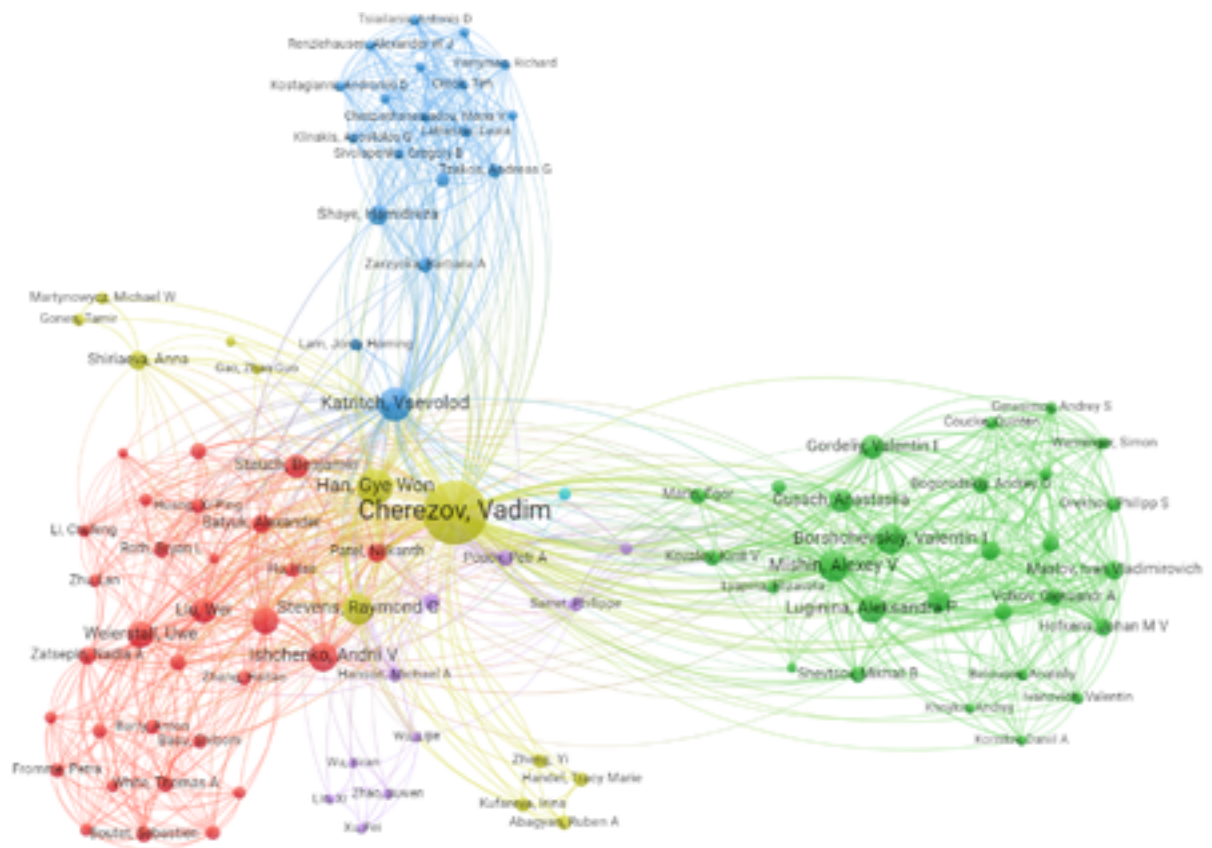


Vadim Cherezov

Publications 212 Citations 30,576	Datasets 9	Grants 14 Funding amount USD 72.3 M	Patents 1
			Clinical Trials 0

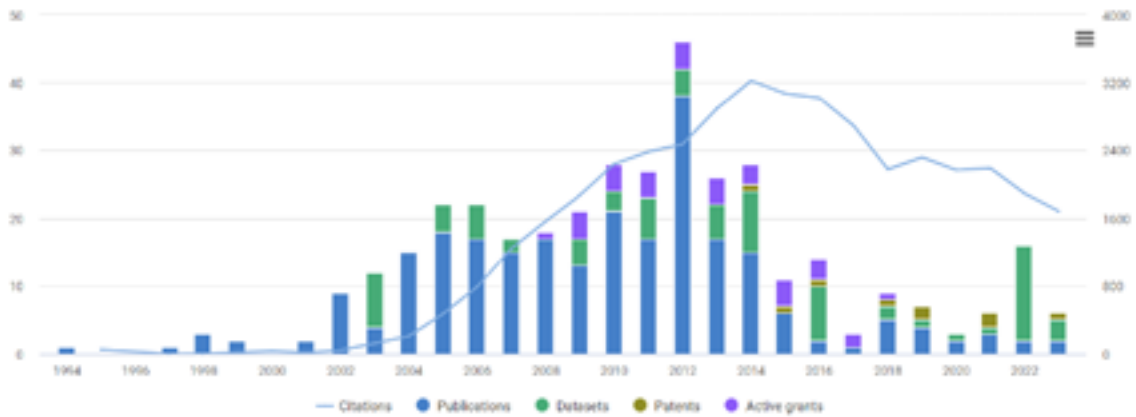


Publications: Collaborations

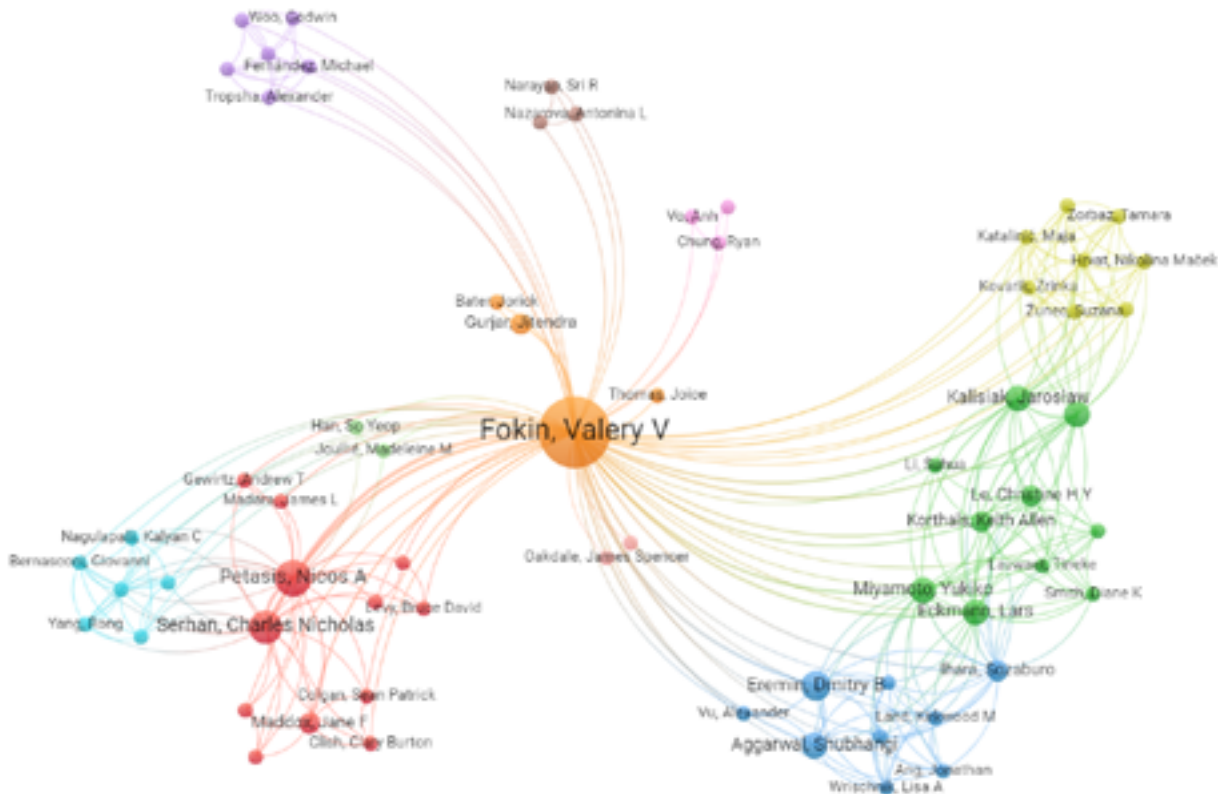


Valery Fokin

Publications 252 Citations 40,848	Datasets 81	Grants 7 Funding amount USD 33.6 M	Patents 9 <hr/> Clinical Trials 0
---	-----------------------	--	--

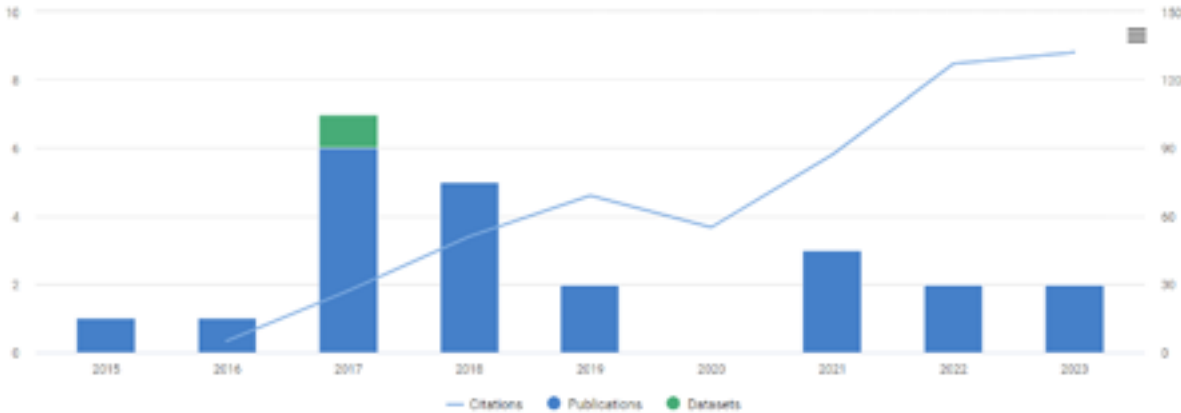


Publications: Collaborations



Peter Foster

Publications 22	Datasets 1	Grants 0	Patents 0
Citations 554		Funding amount 0	Clinical Trials 0

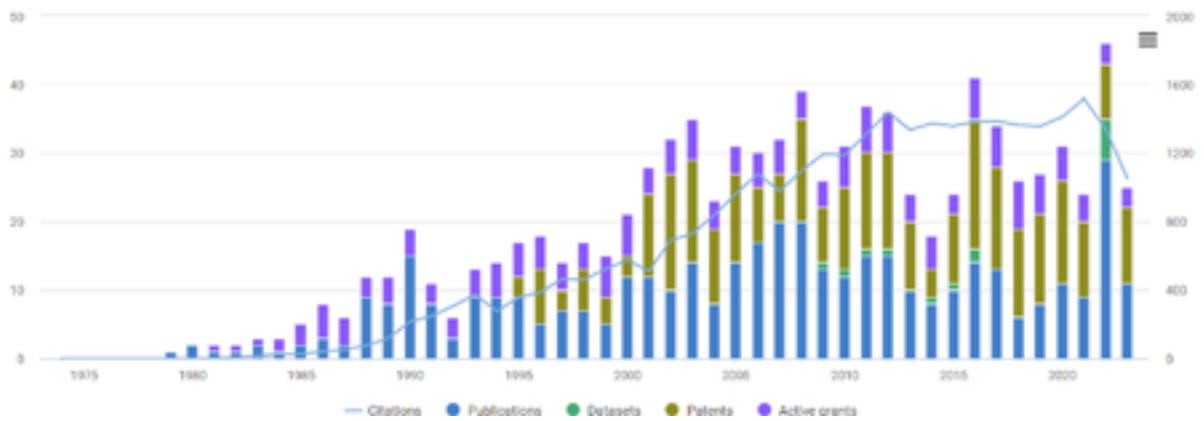


Publications: Collaborations

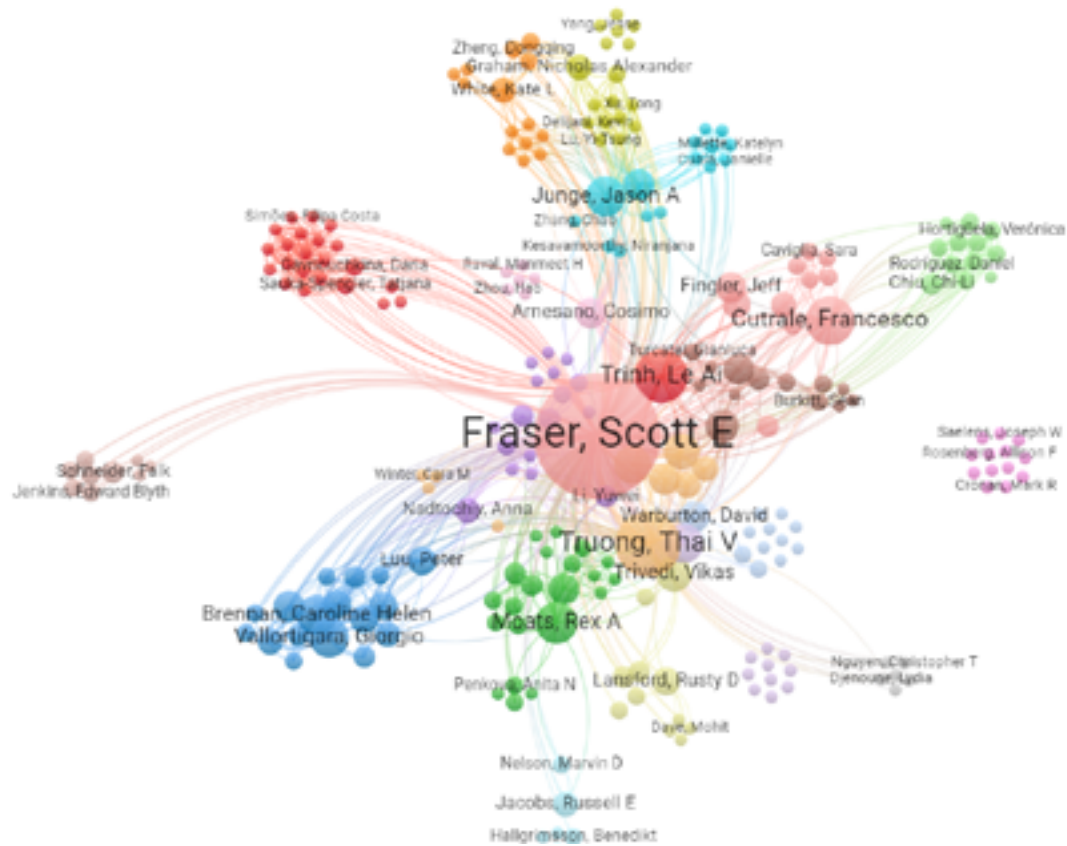


Scott Fraser

Publications 420 Citations 31,397	Datasets 14	Grants 36 Funding amount USD 105.4 M	Patents 302 <hr/> Clinical Trials 0
---	-----------------------	--	---



Publications: Collaborations

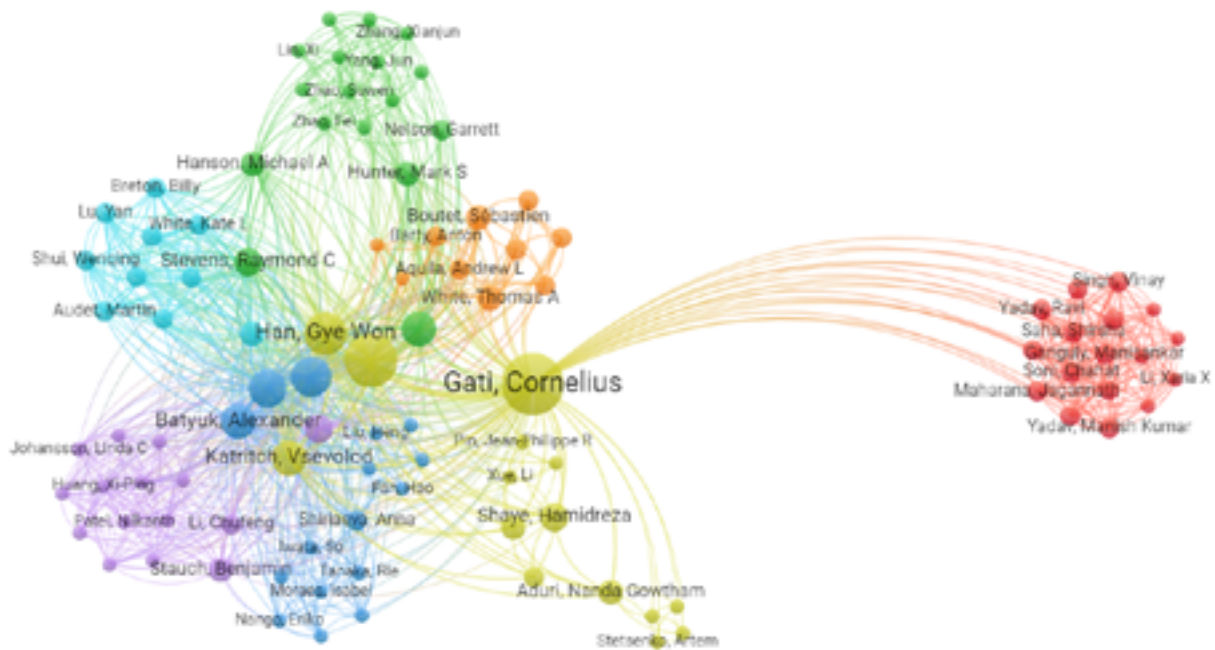


Cornelius Gati

Publications 77 Citations 5,427	Datasets 1	Grants 1 Funding amount 0	Patents 1 <hr/> Clinical Trials 0
--	-----------------------------	--	---



Publications: Collaborations

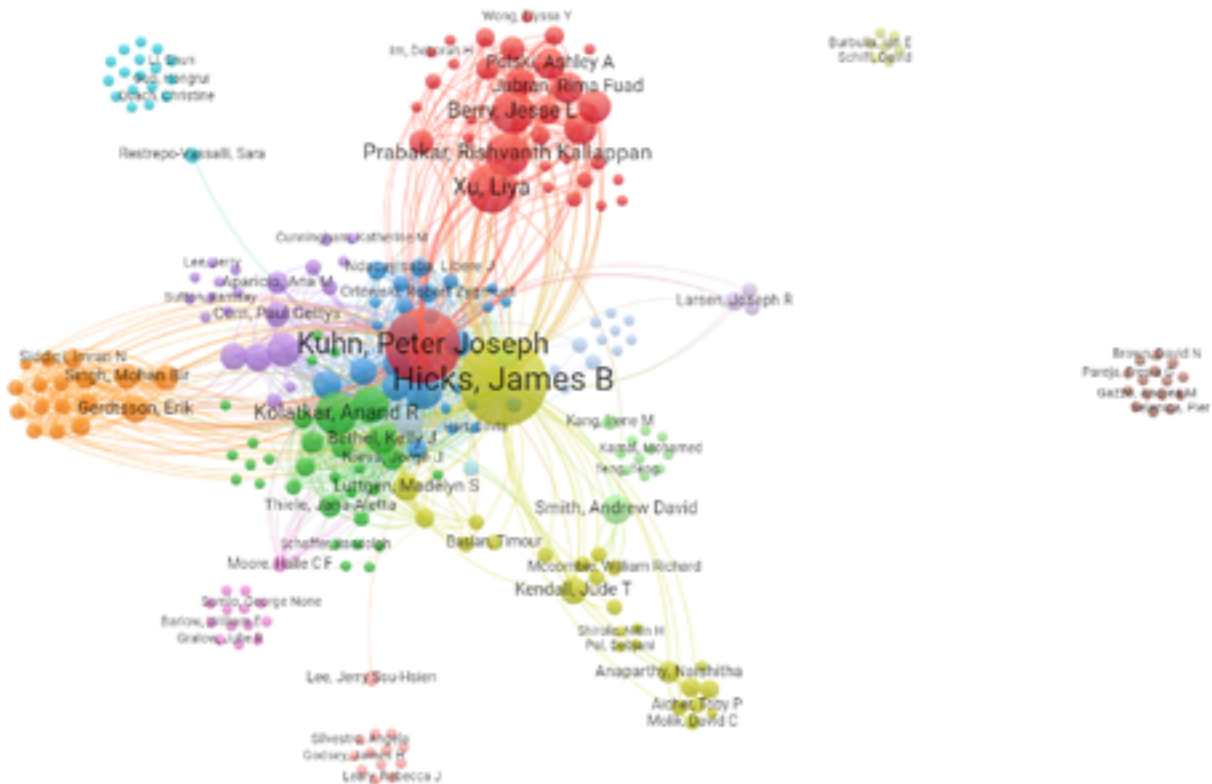


James Hicks

Publications 227 Citations 25,696	Datasets 17	Grants 14 Funding amount USD 4.6 M	Patents 4 <hr/> Clinical Trials 0
--	------------------------------	---	---

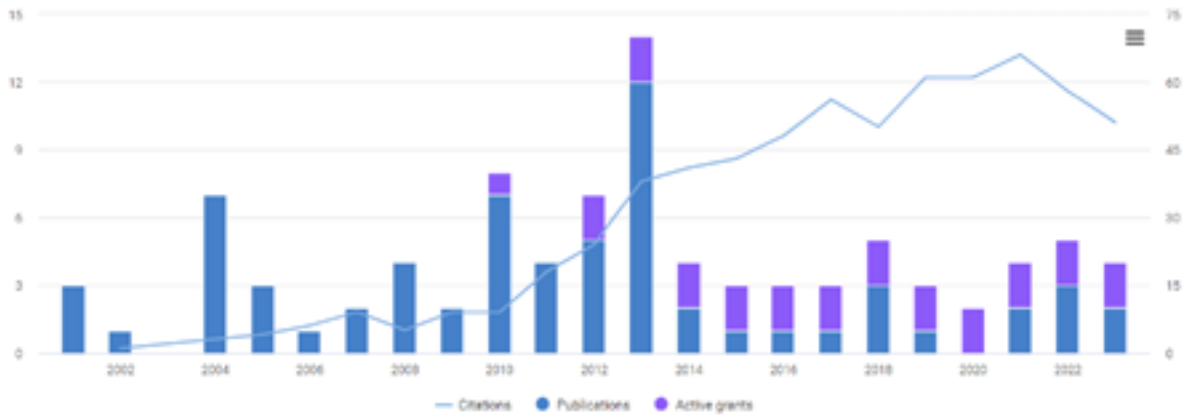


Publications: Collaborations



Khalil Iskarous

Publications 67 Citations 658	Datasets 0	Grants 6 Funding amount USD 4.1 M	Patents 0 <hr/> Clinical Trials 0
---	-----------------------------	---	---

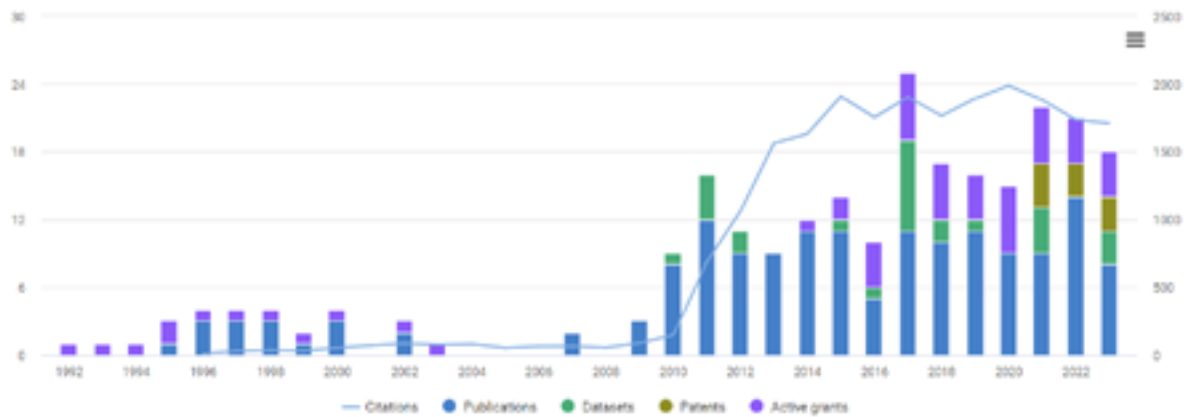


Publications: Collaborations

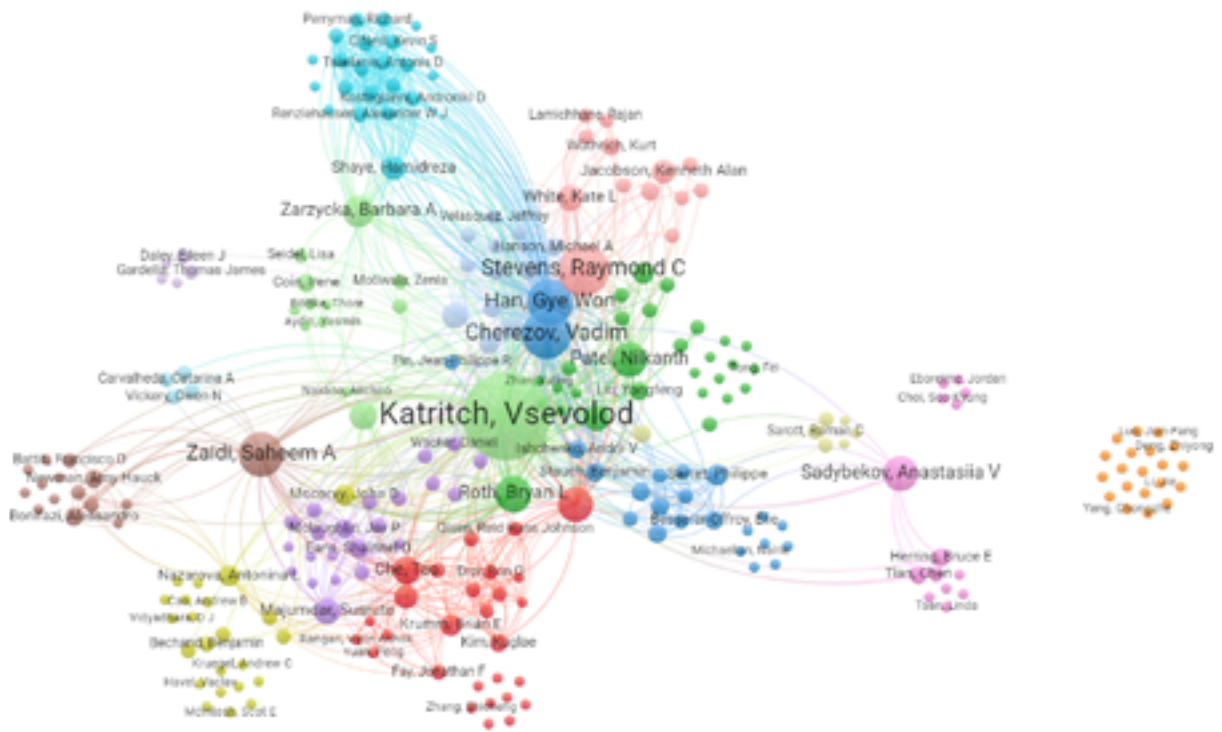


Vsevolod Katritch

Publications 158 Citations 22,377	Datasets 27	Grants 13 Funding amount USD 21.0 M	Patents 10 <hr/> Clinical Trials 0
--	------------------------------	--	--

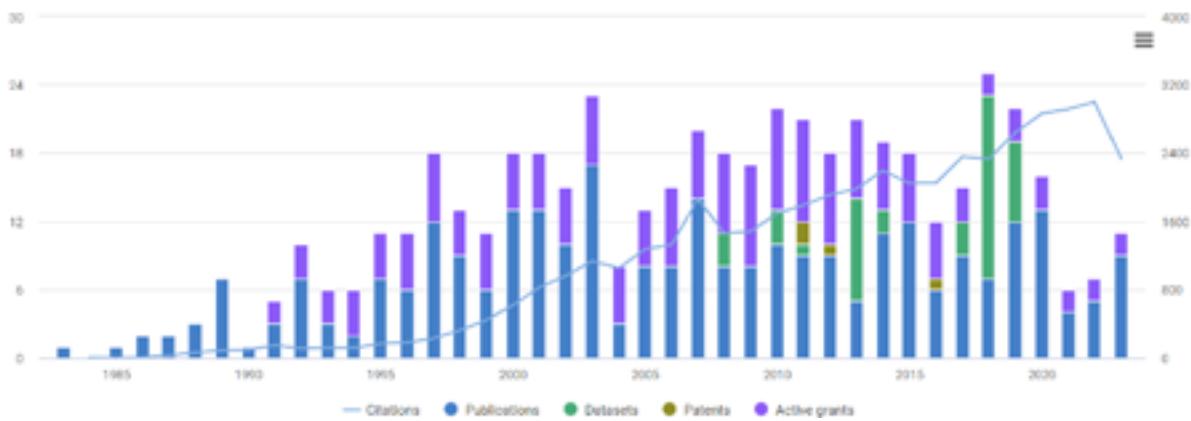


Publications: Collaborations

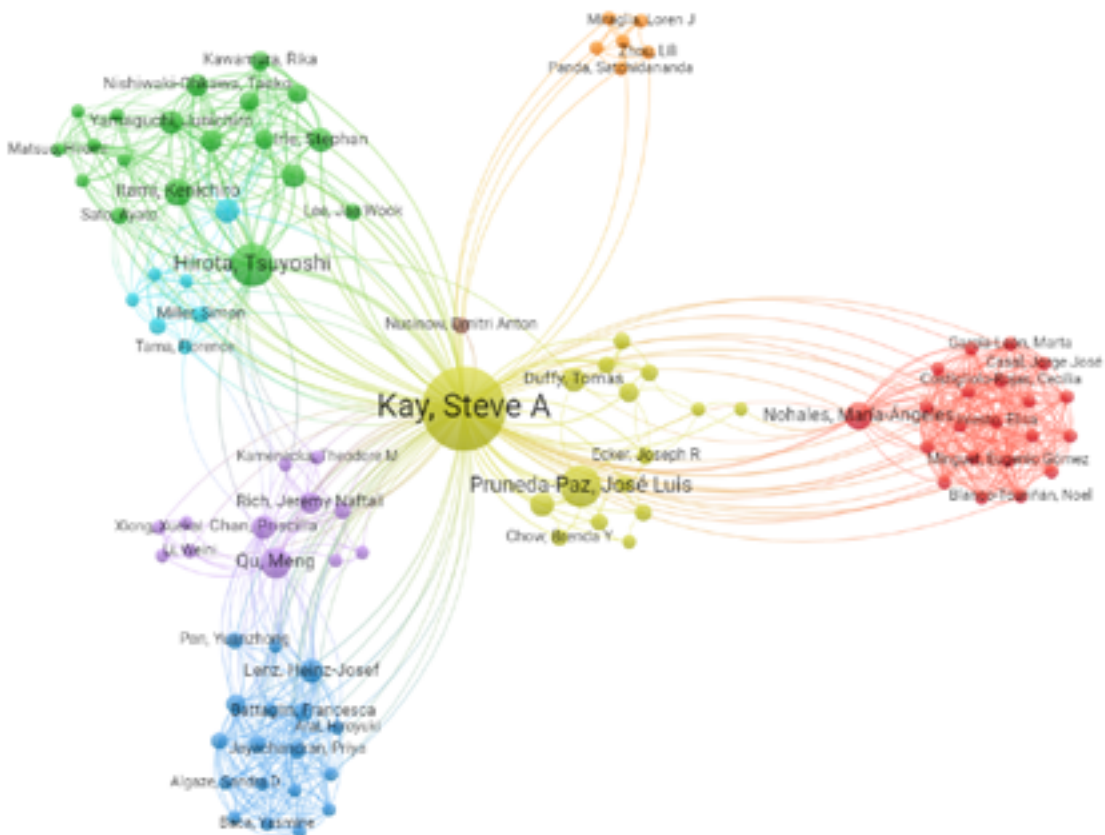


Steve Kay

Publications 295 Citations 46,216	Datasets 44	Grants 26 Funding amount USD 36.1 M	Patents 4 <hr/> Clinical Trials 0
--	-----------------------	---	--

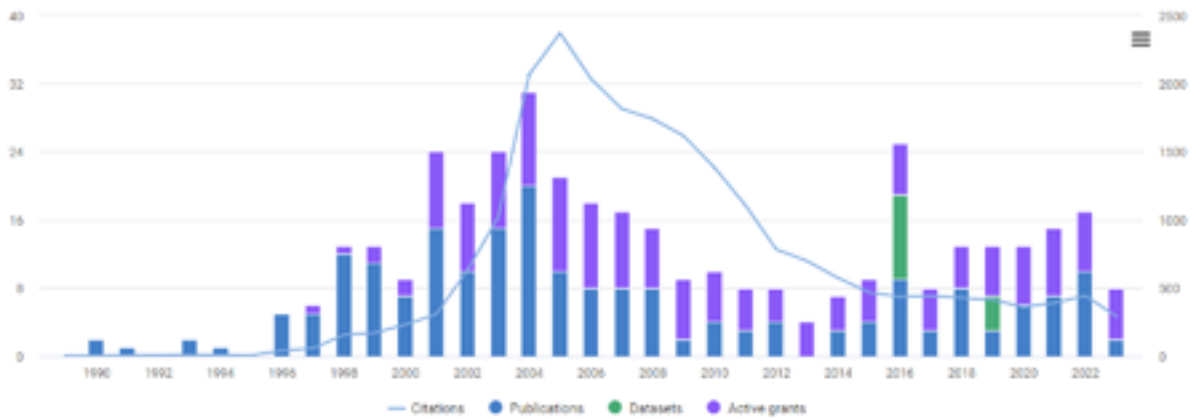


Publications: Collaborations

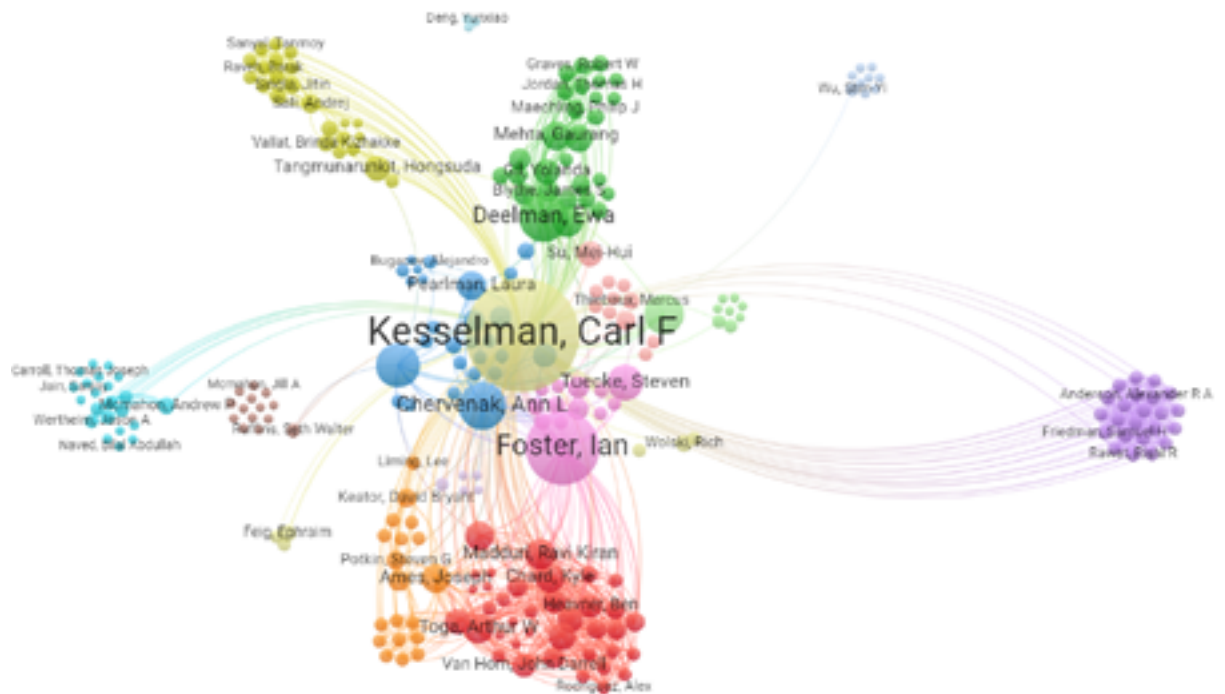


Carl Kesselman

Publications 208 Citations 22,501	Datasets 14	Grants 35 Funding amount USD 147.8 M	Patents 0
			Clinical Trials 0



Publications: Collaborations



Yasser Khan

Publications 37 Citations 3,956	Datasets 1	Grants 0 Funding amount 0	Patents 10 <hr/> Clinical Trials 0
--	-----------------------------	---	--

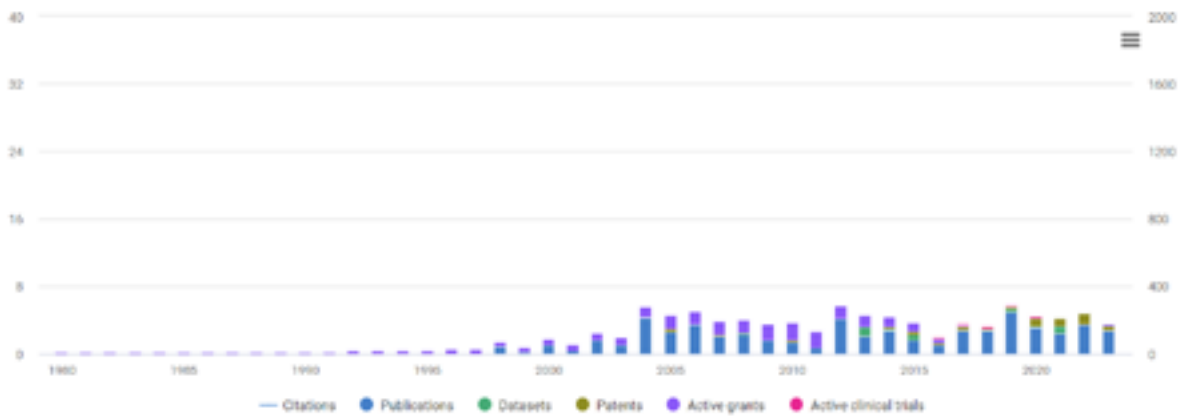


Publications: Collaborations

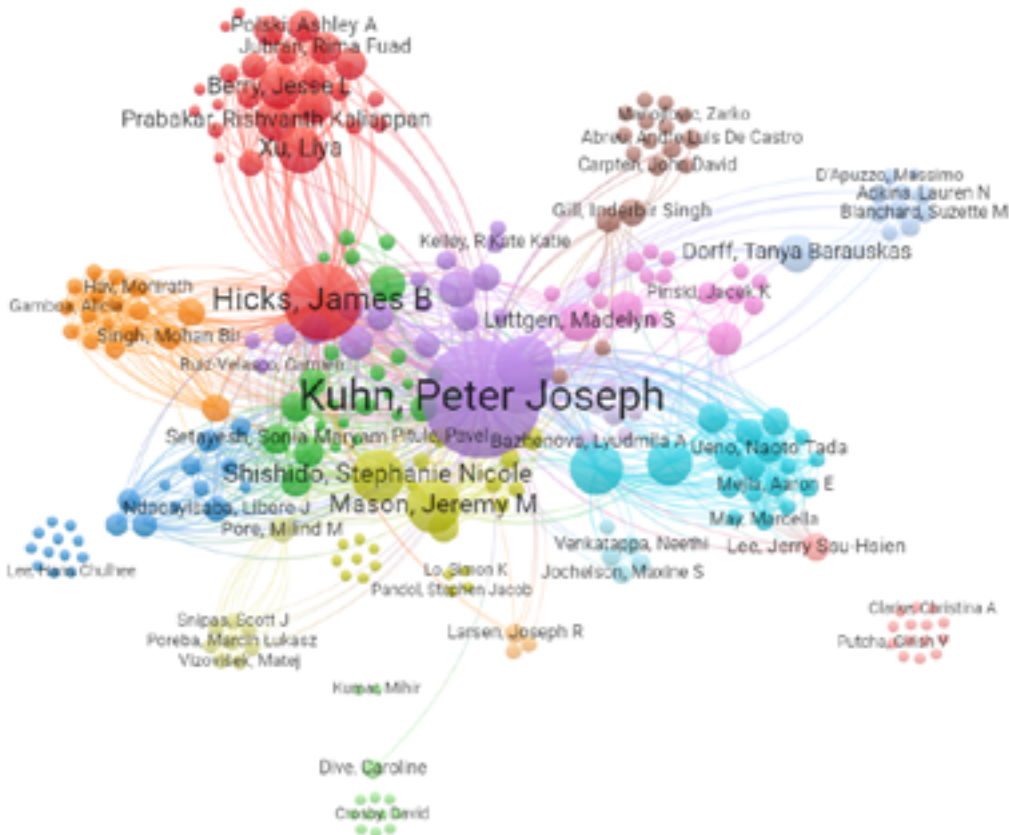


Peter Kuhn

Publications 331 Citations 19,129	Datasets 20	Grants 16 Funding amount USD 322.1 M	Patents 33 <hr/> Clinical Trials 1
---	-----------------------	--	--

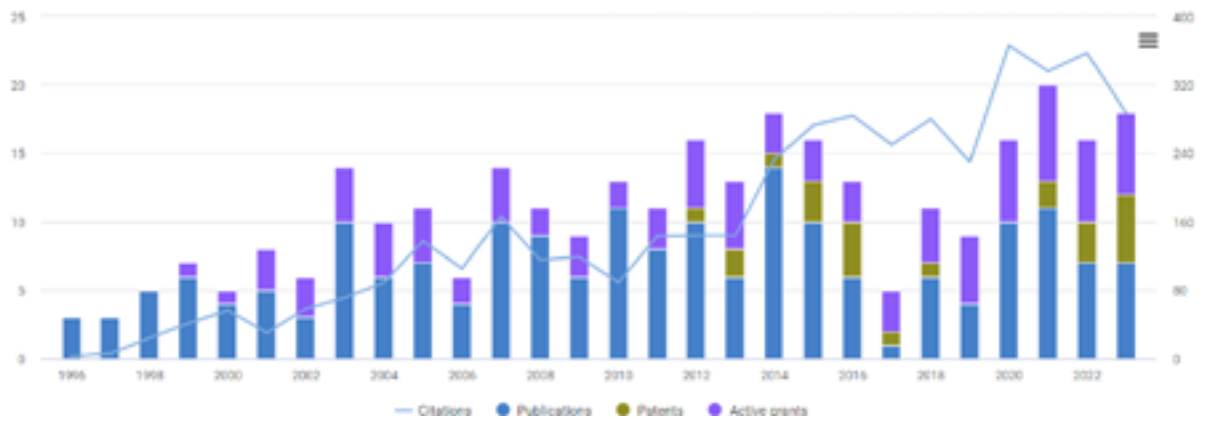


Publications: Collaborations

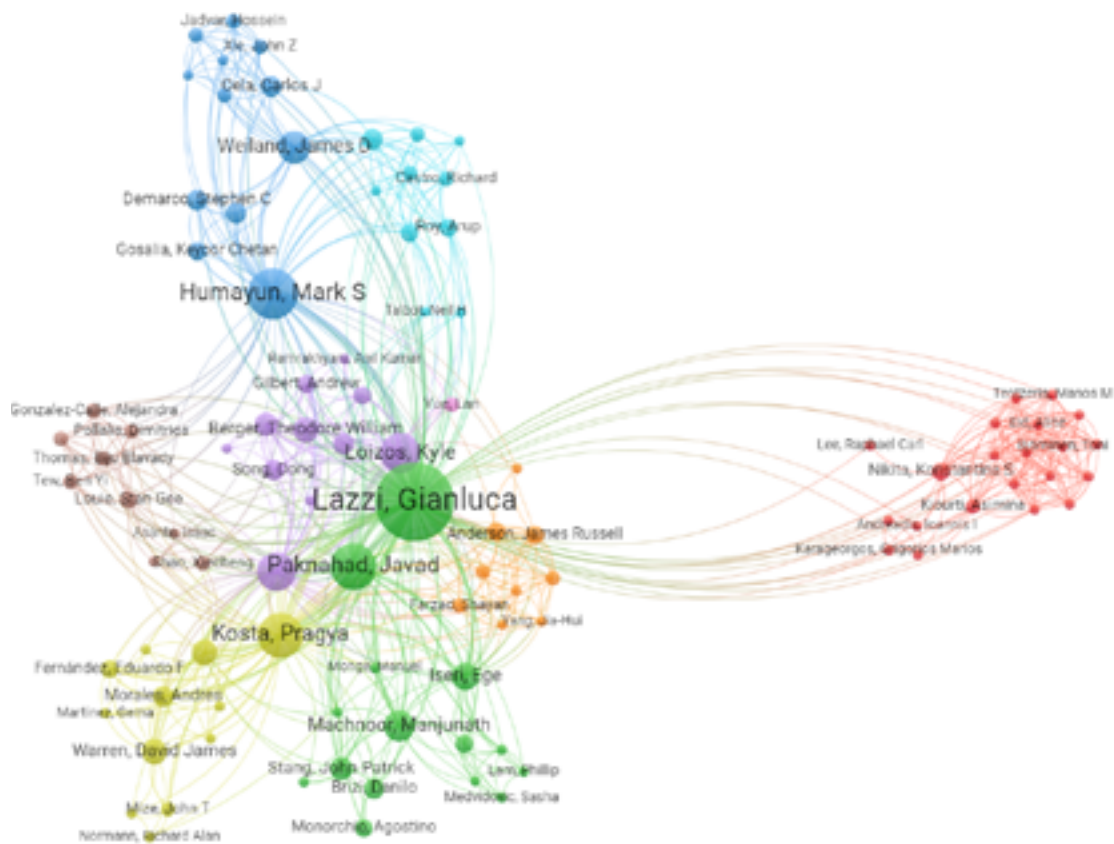


Gianluca Lazzi

Publications 192 Citations 4,438	Datasets 0	Grants 20 Funding amount USD 18.4 M	Patents 23 <hr/> Clinical Trials 0
--	-----------------------------	--	--

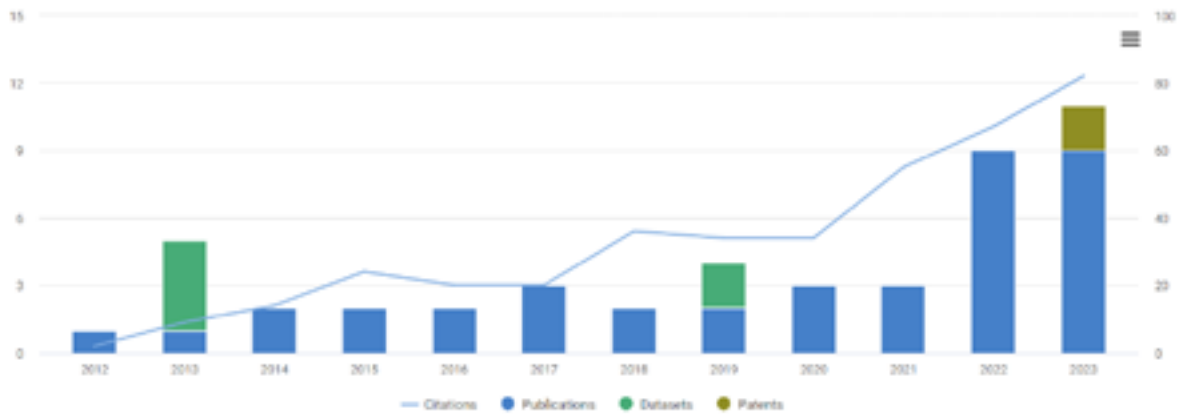


Publications: Collaborations

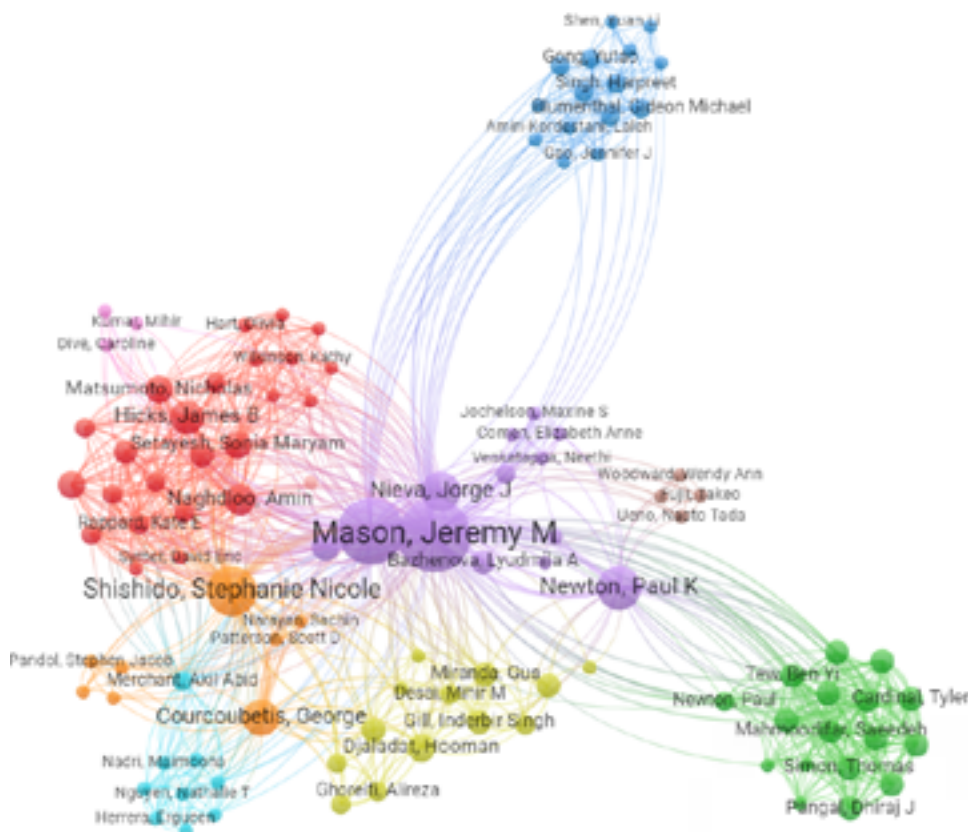


Jeremy Mason

Publications 39 Citations 397	Datasets 6	Grants 0 Funding amount 0	Patents 2 <hr/> Clinical Trials 0
--	-----------------------------	--	--

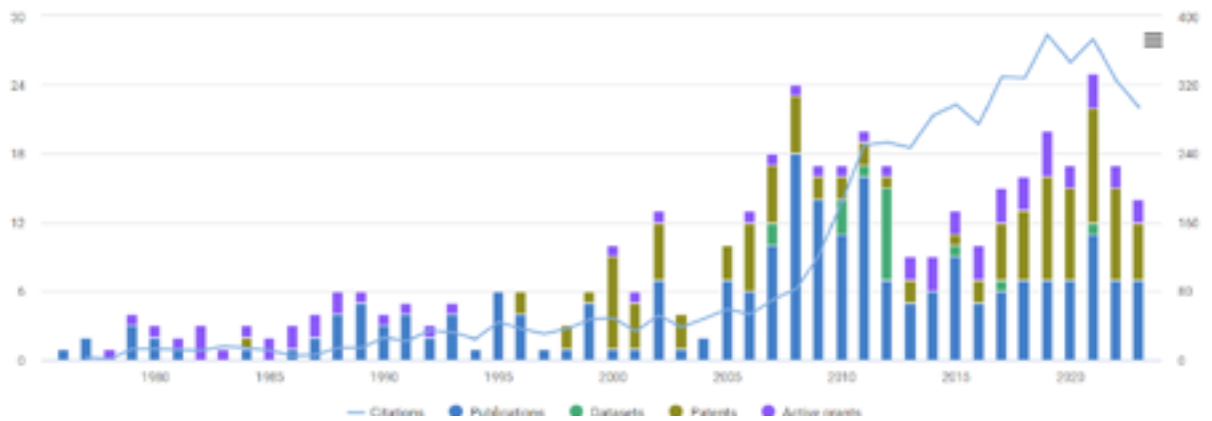


Publications: Collaborations

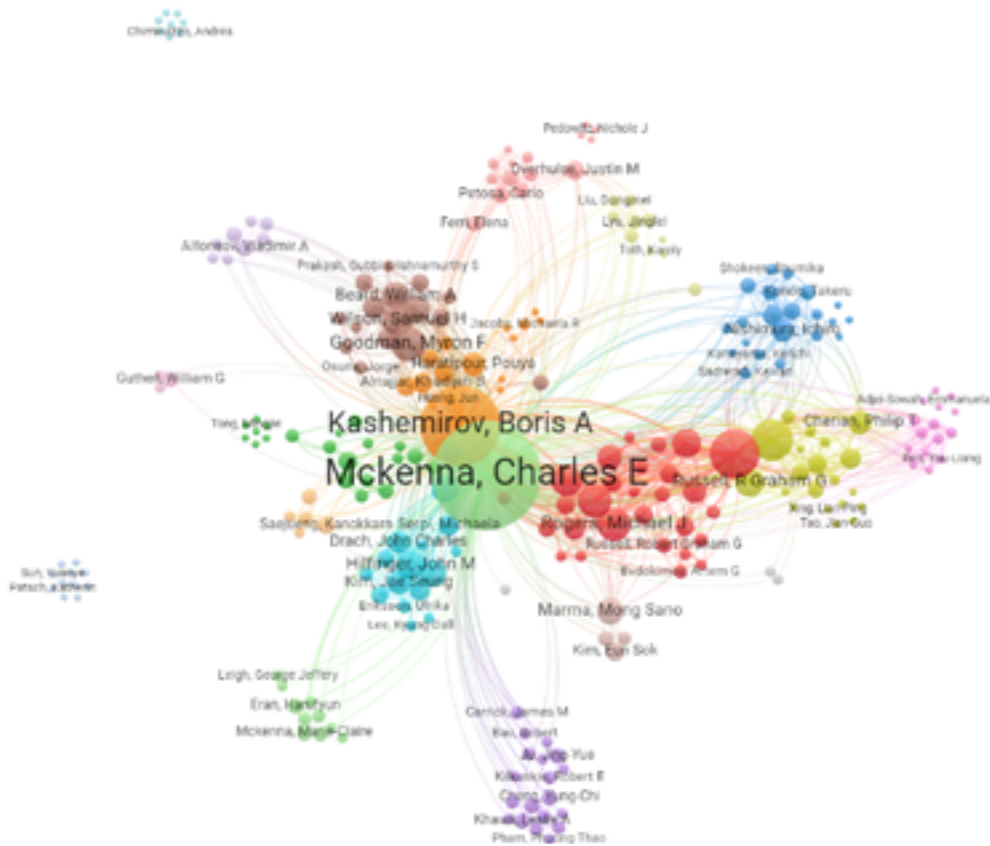


Charles E. McKenna

Publications 231 Citations 5,230	Datasets 17	Grants 14 Funding amount USD 16.6 M	Patents 108 <hr/> Clinical Trials 0
---	------------------------------	--	---

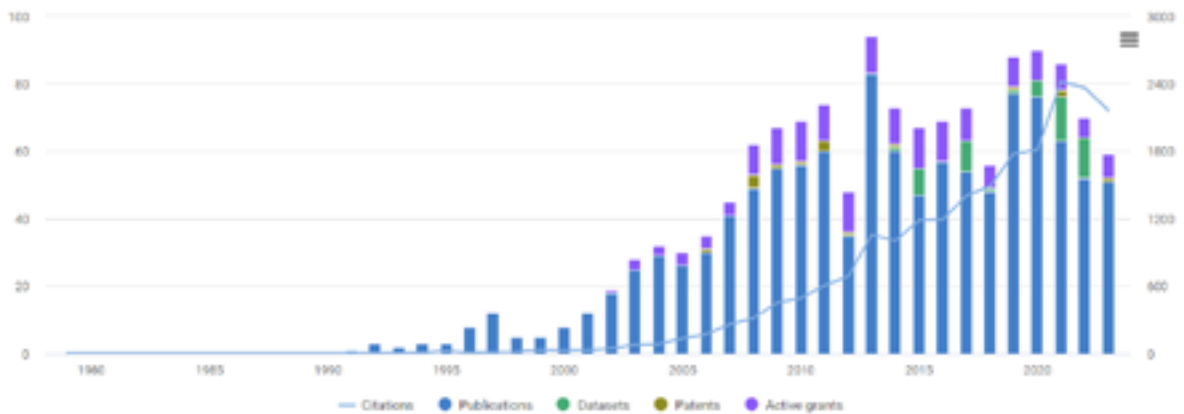


Publications: Collaborations

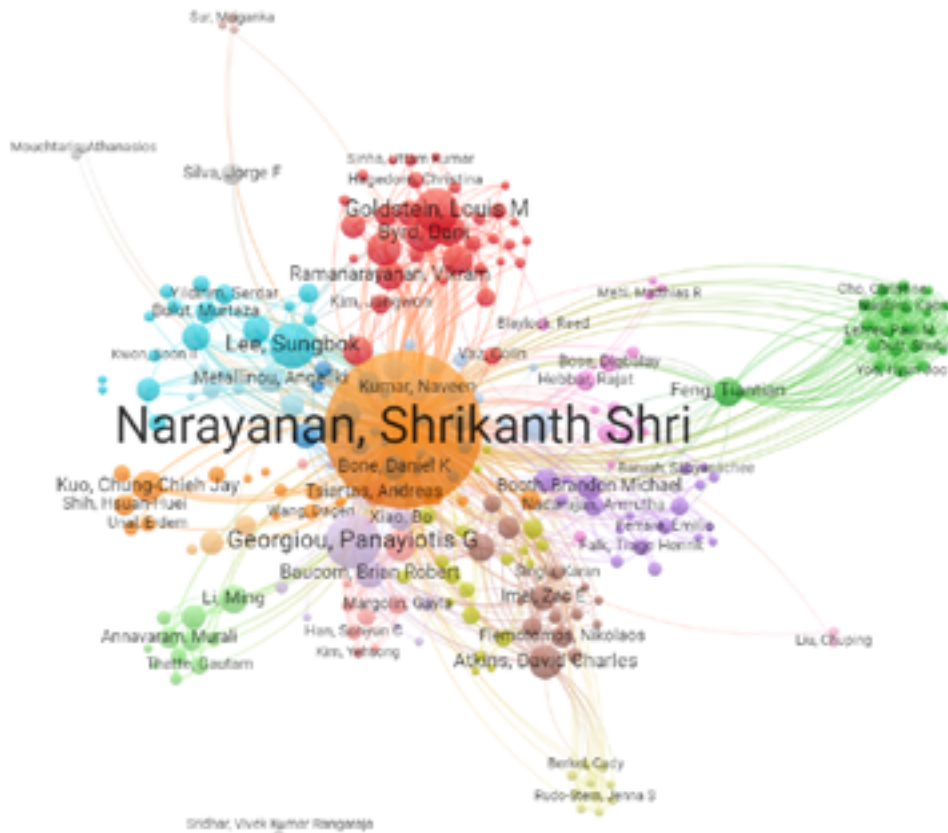


Shrikanth Narayanan

Publications 1,156 Citations 21,357	Datasets 50	Grants 30 Funding amount USD 33.0 M	Patents 16 <hr/> Clinical Trials 0
--	------------------------------	--	--

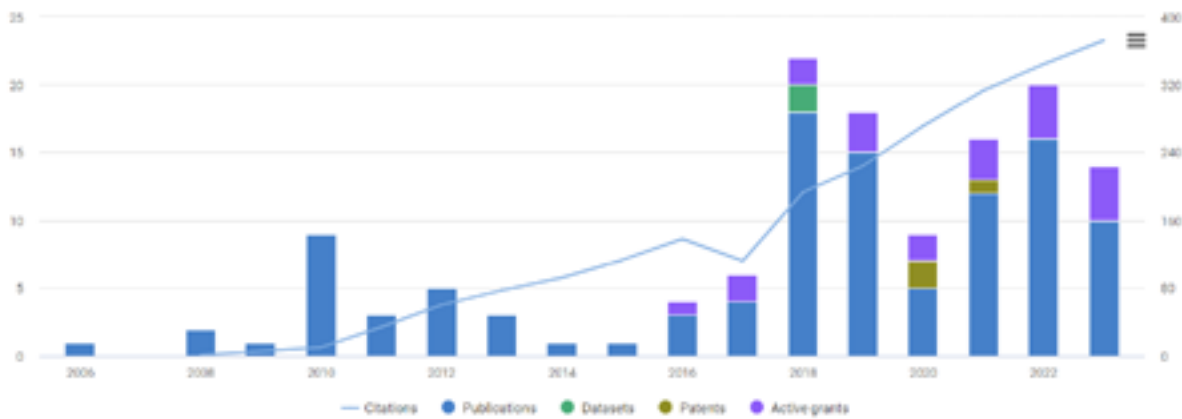


Publications: Collaborations

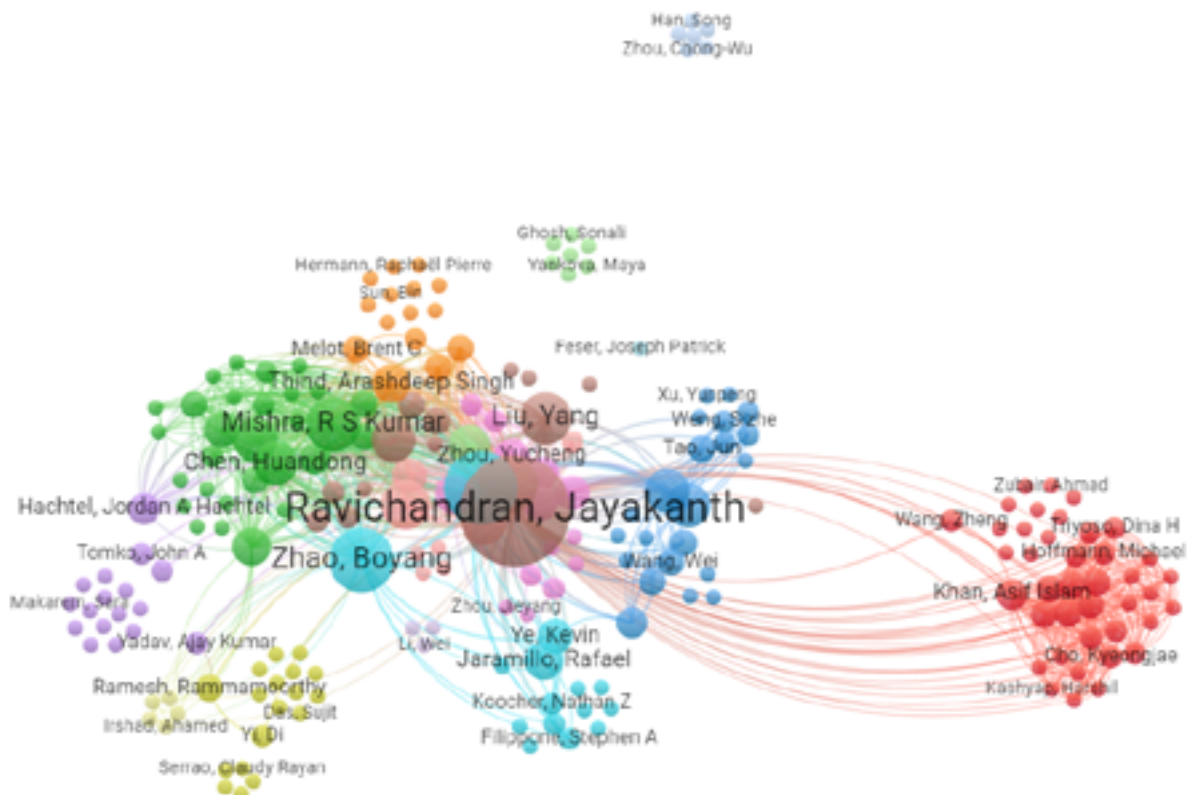


Jayakanth Ravichandran

Publications 109 Citations 2,358	Datasets 2	Grants 7 Funding amount USD 5.8 M	Patents 3 <hr/> Clinical Trials 0
---	-----------------------------	--	---

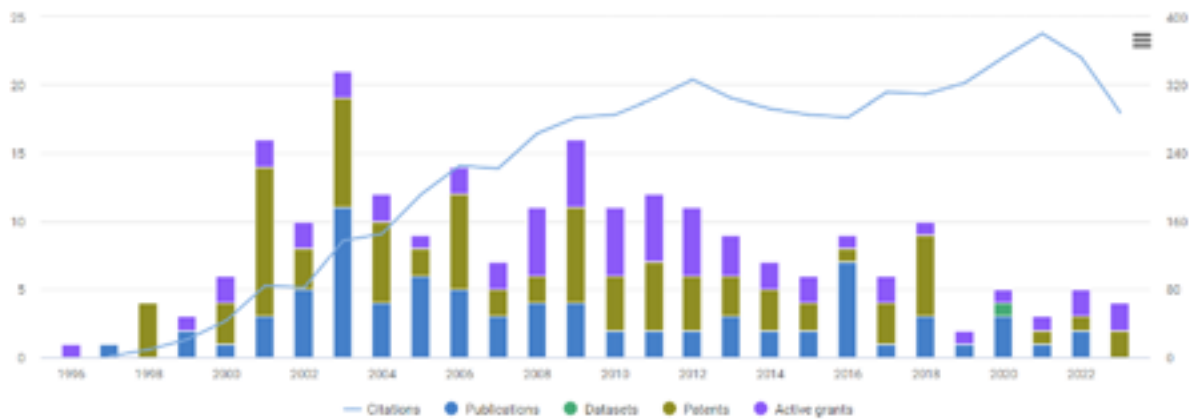


Publications: Collaborations

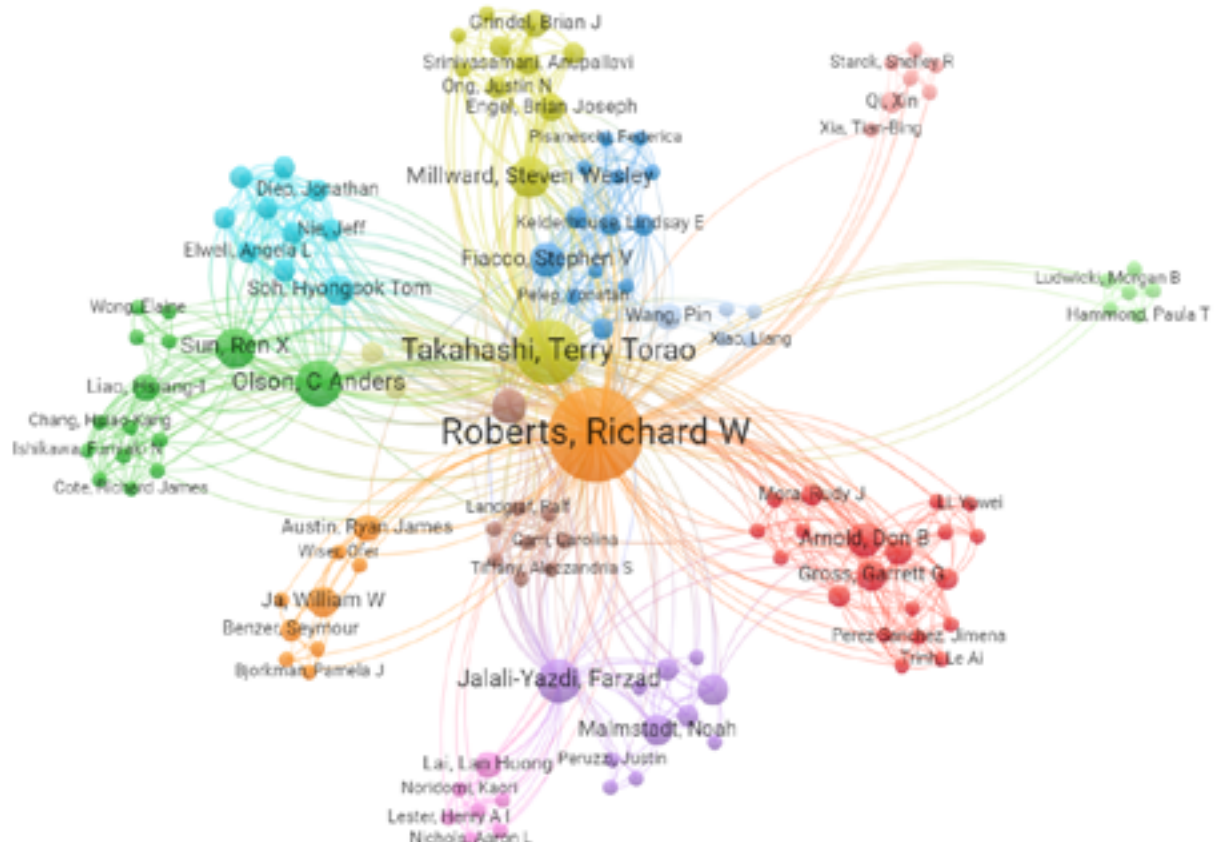


Richard Roberts

Publications 80 Citations 6,099	Datasets 2	Grants 11 Funding amount USD 12.2 M	Patents 90 <hr/> Clinical Trials 0
---	-----------------------------	--	--

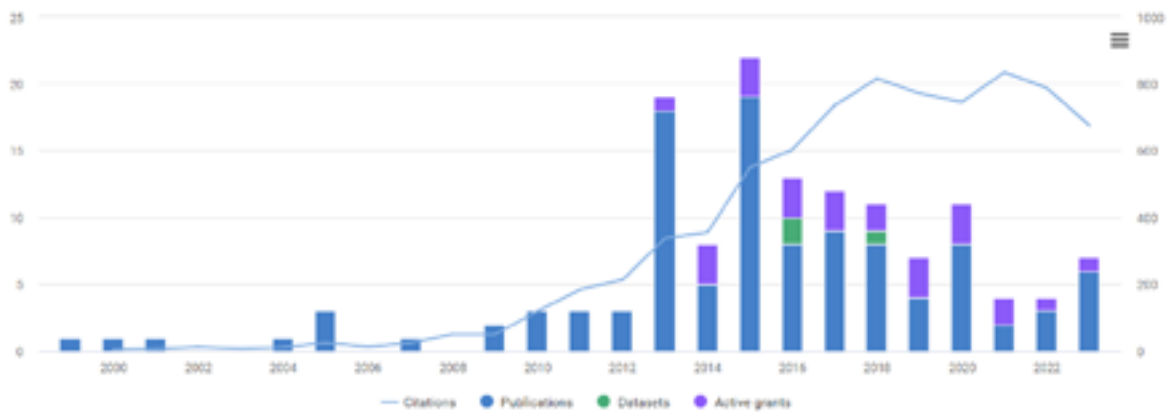


Publications: Collaborations

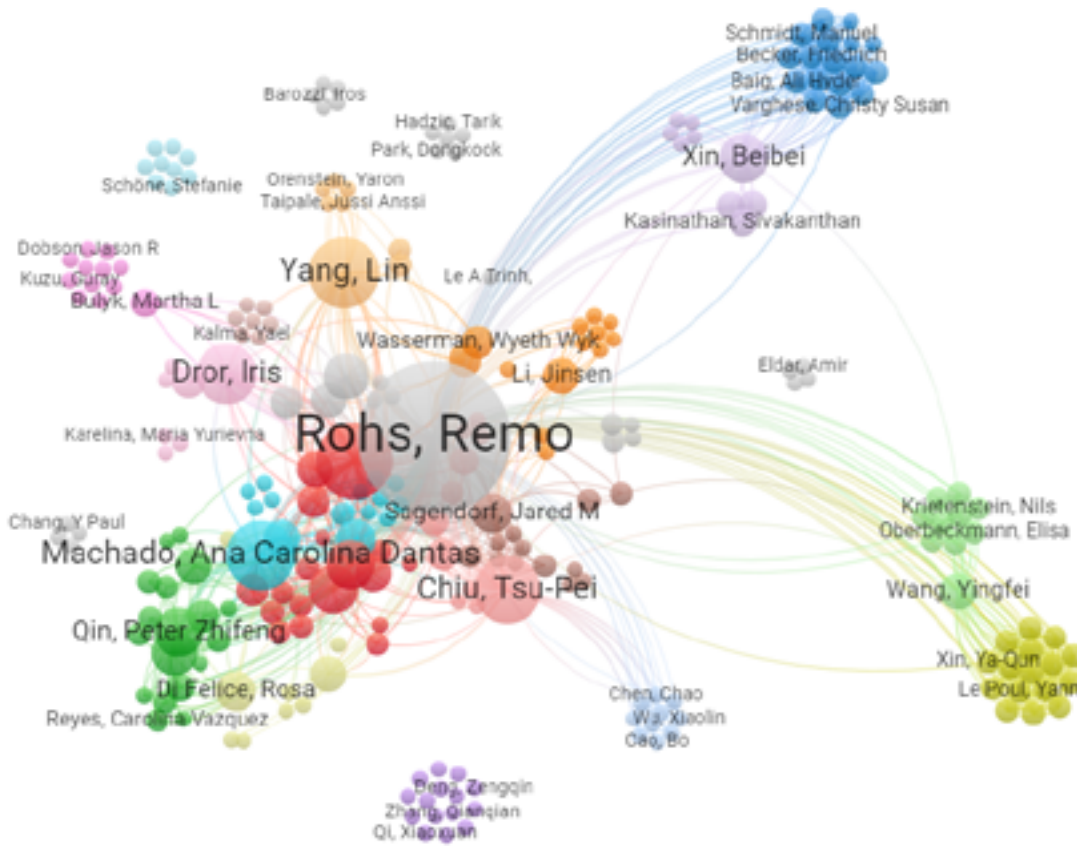


Remo Rohs

Publications 109 Citations 7,928	Datasets 3	Grants 5 Funding amount USD 6.9M	Patents 0
			Clinical Trials 0

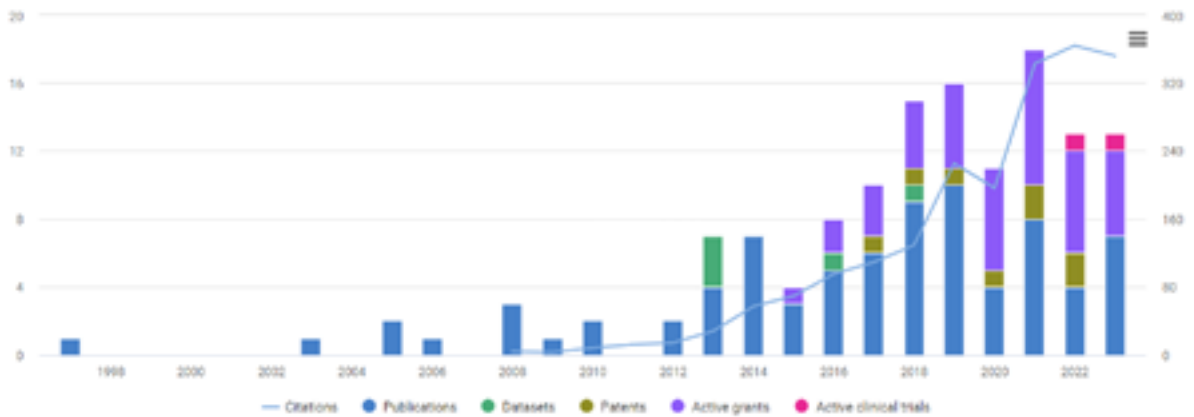


Publications: Collaborations

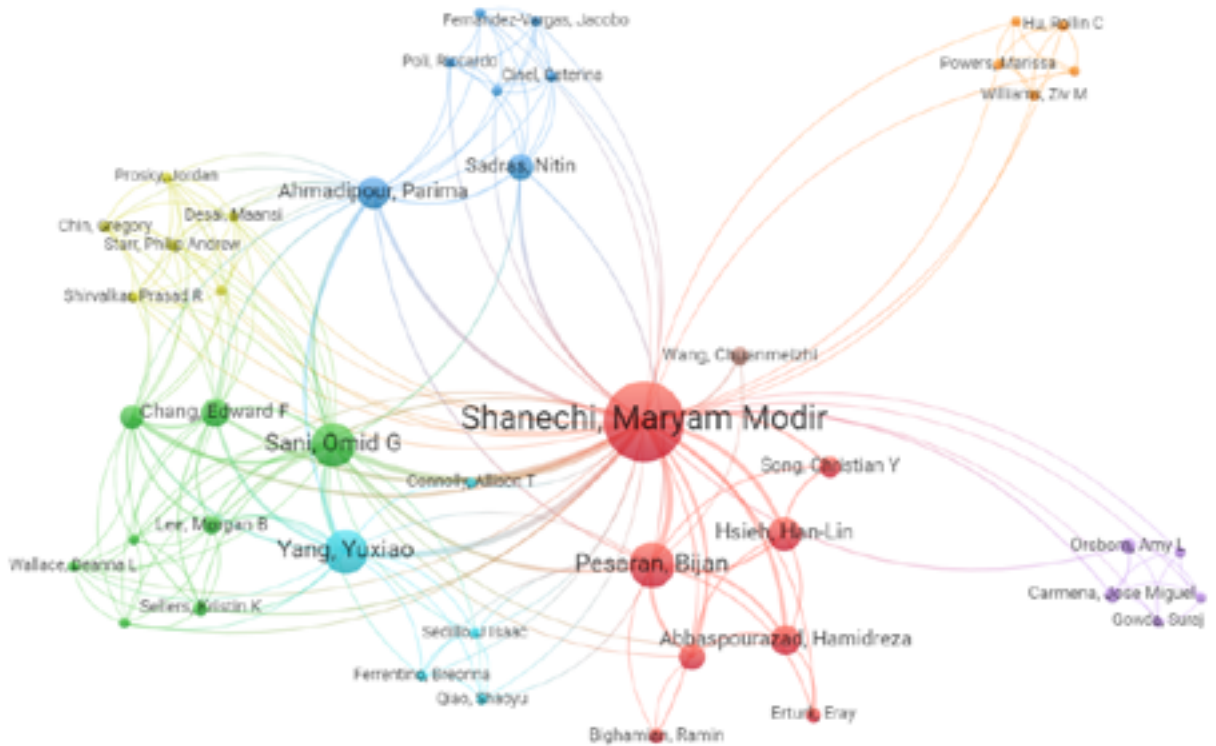


Maryam Shanechi

Publications 80 Citations 2,068	Datasets 5	Grants 8 Funding amount USD 16.0 M	Patents 8 <hr/> Clinical Trials 1
--	-----------------------------	---	---

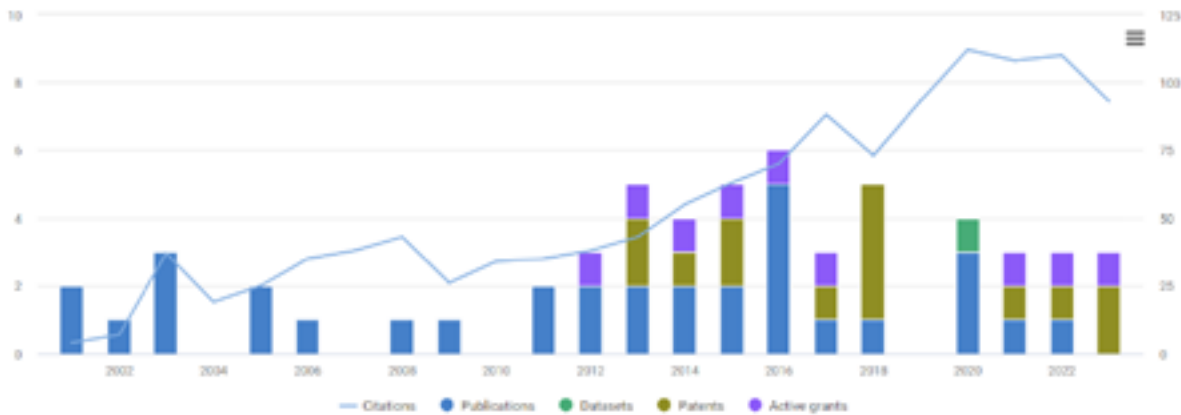


Publications: Collaborations

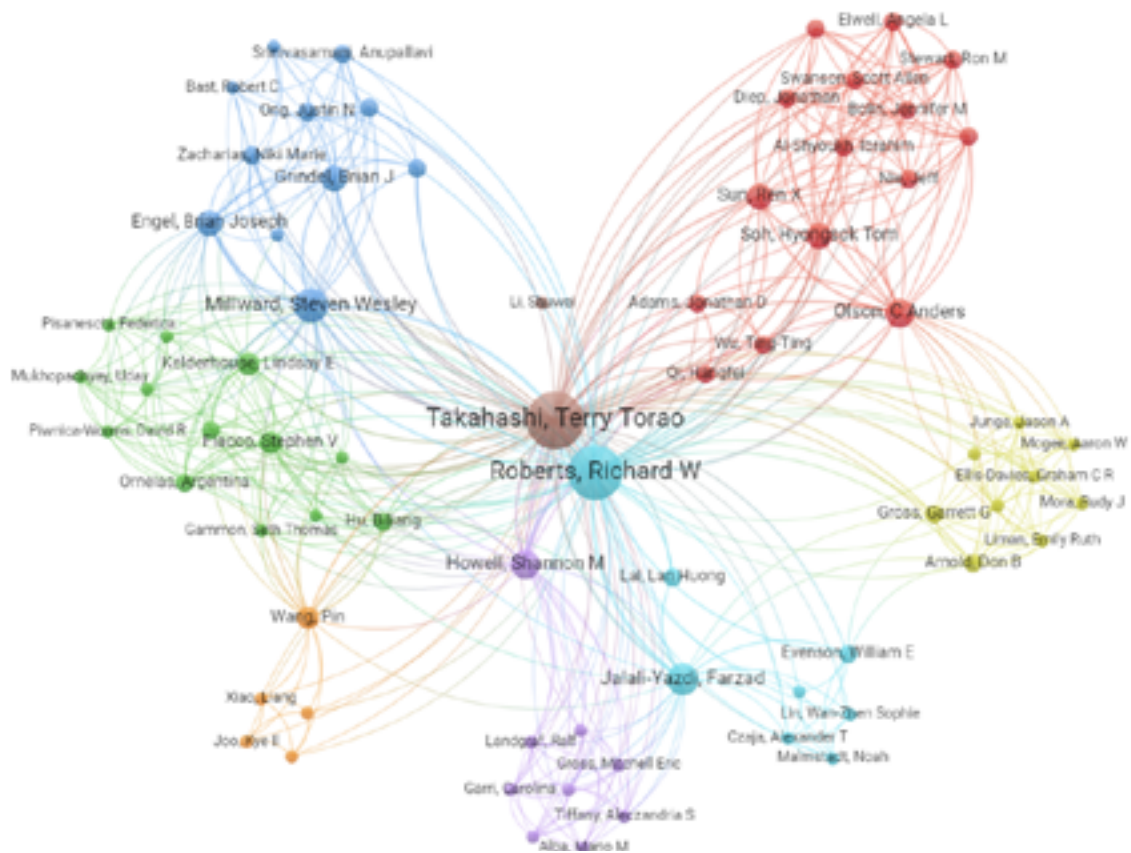


Terry Takahashi

Publications 33 Citations 1,250	Datasets 1	Grants 2 Funding amount USD 2.2 M	Patents 14
			Clinical Trials 0

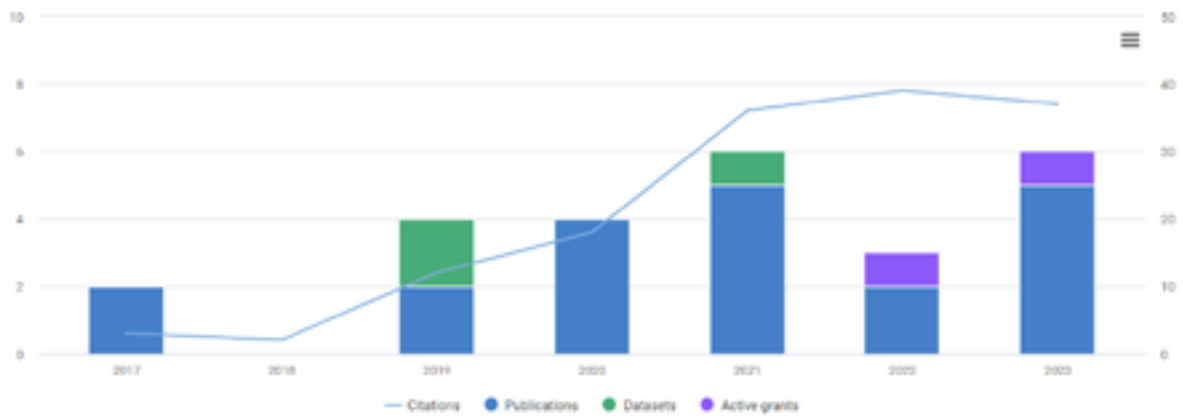


Publications: Collaborations

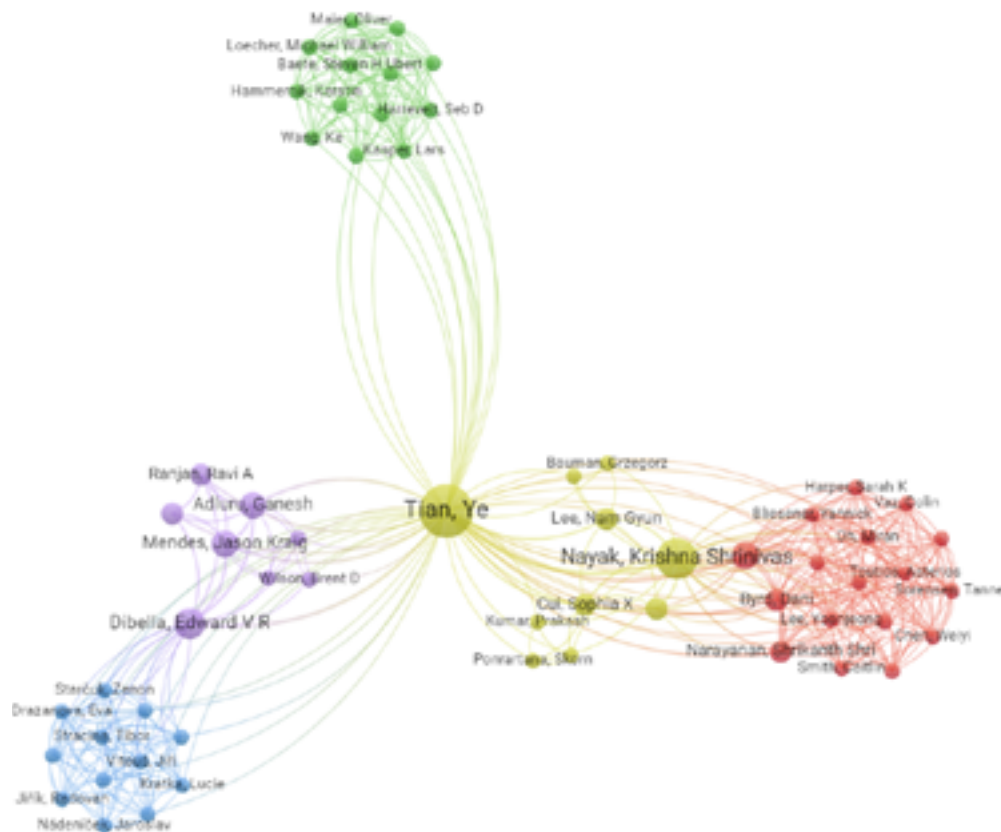


Ye Tian

Publications 20 Citations 147	Datasets 3	Grants 1 Funding amount USD 141 K	Patents 0 <hr/> Clinical Trials 0
--	-----------------------------	--	---

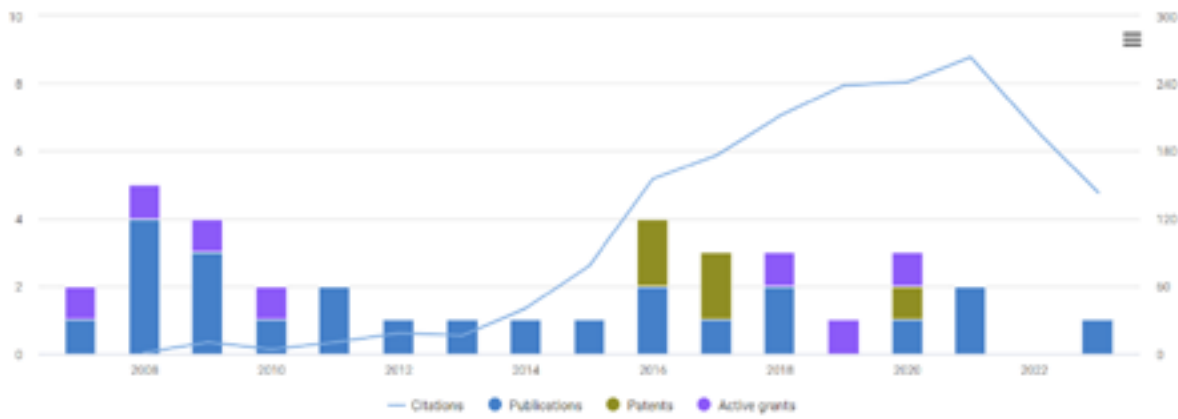


Publications: Collaborations

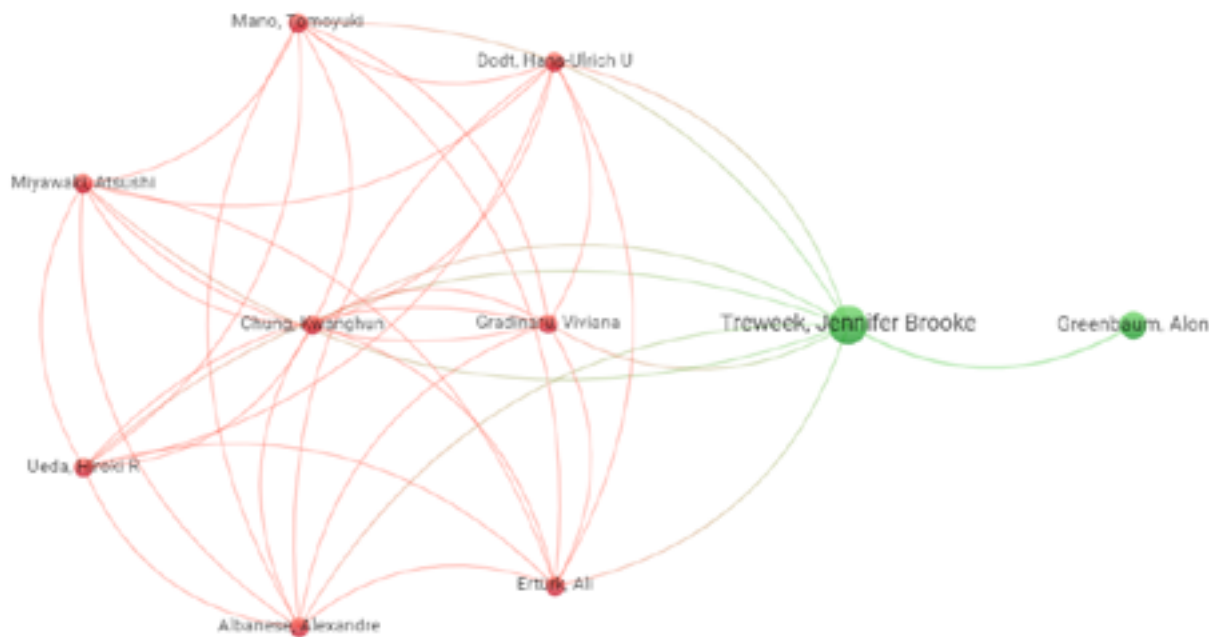


Jennifer Treweek

Publications 24 Citations 1,804	Datasets 0	Grants 2 Funding amount USD 142 K	Patents 5 <hr/> Clinical Trials 0
--	----------------------	--	--

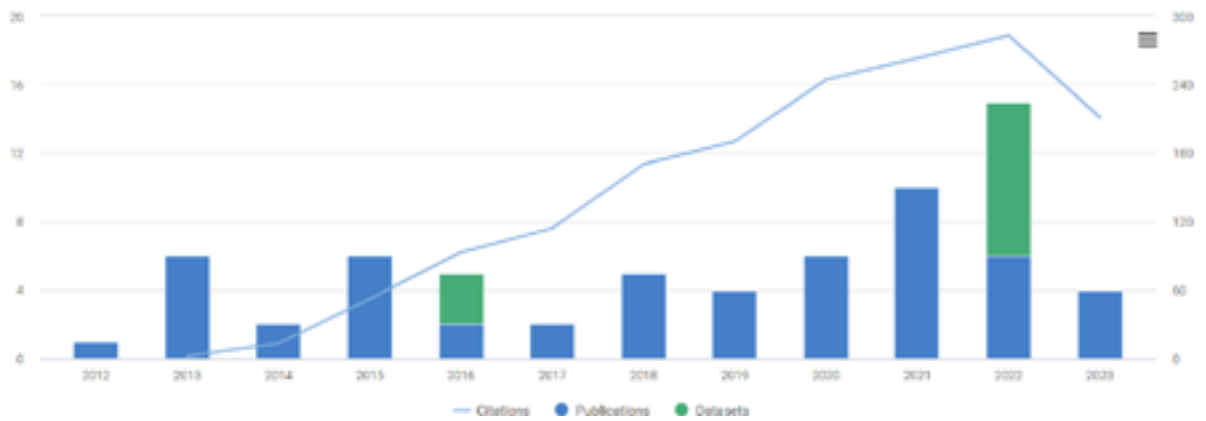


Publications: Collaborations

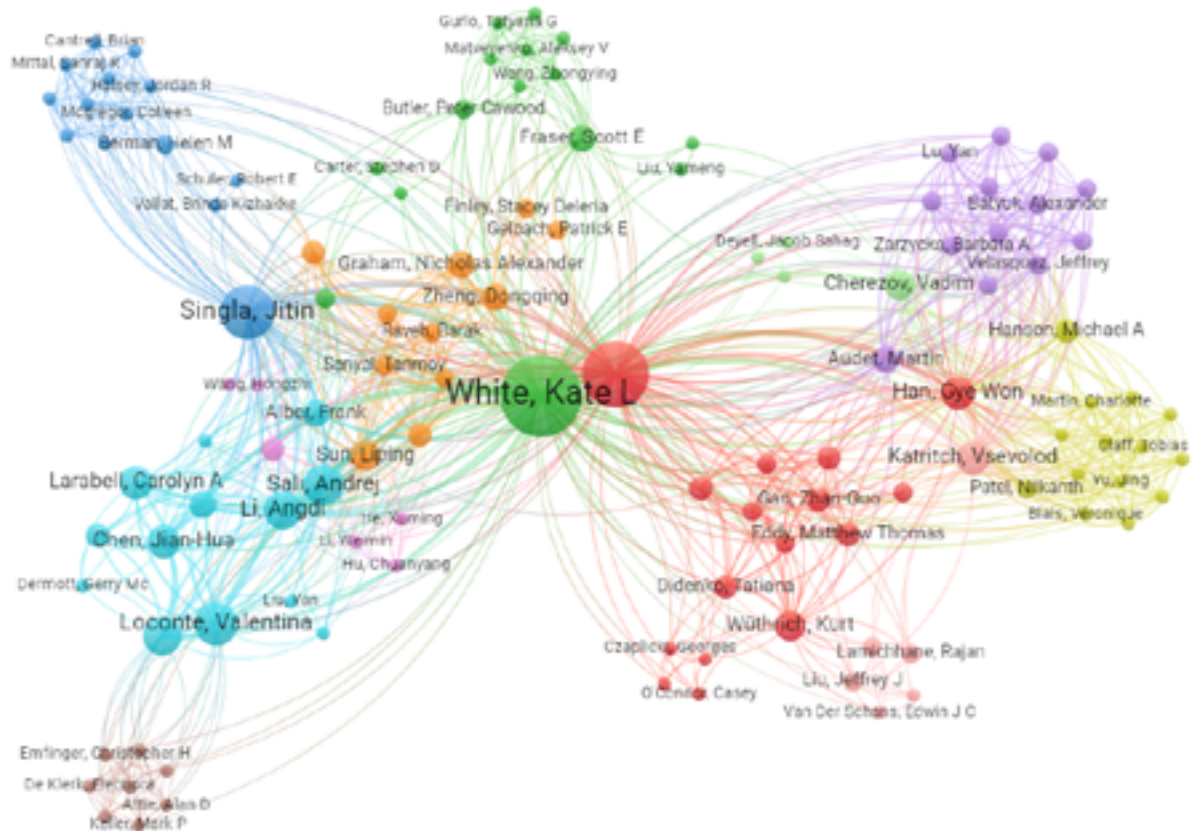


Kate White

Publications 54 Citations 1,636	Datasets 12	Grants 0 Funding amount 0	Patents 0 <hr/> Clinical Trials 0
--	------------------------------	--	---

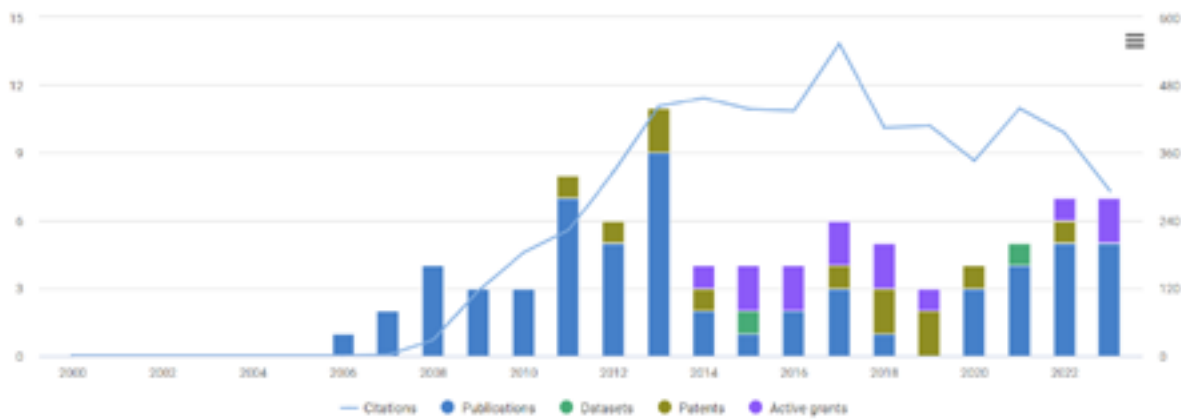


Publications: Collaborations

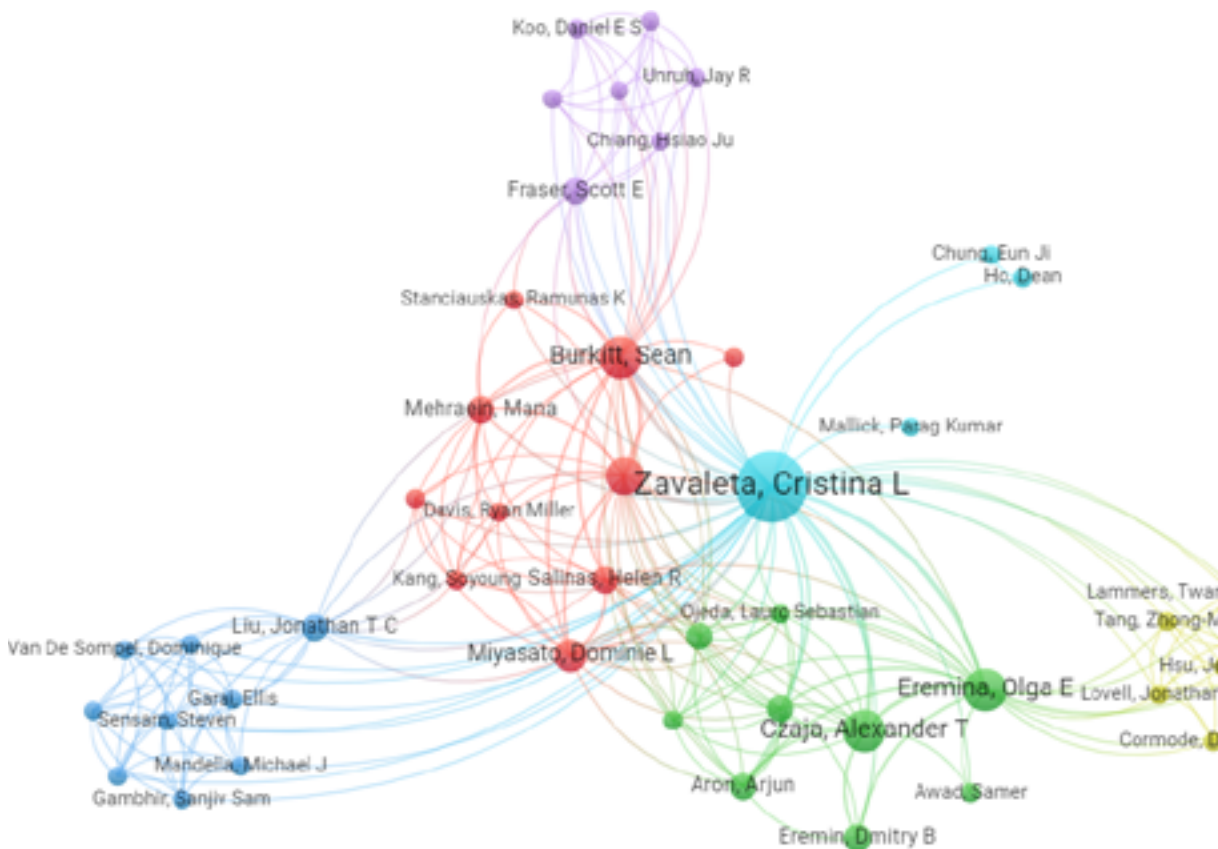


Cristina Zavaleta

Publications 60 Citations 5,491	Datasets 2	Grants 4 Funding amount USD 1.9 M	Patents 12
			Clinical Trials 0



Publications: Collaborations



Addendum: Journal Articles

Review

Computational approaches streamlining drug discovery

<https://doi.org/10.1038/s41586-023-05905-z>

Anastasiia V. Sadybekov^{1,2} & Vsevolod Katritch^{1,2,3}✉

Received: 21 April 2022

Accepted: 1 March 2023

Published online: 26 April 2023

 Check for updates

Computer-aided drug discovery has been around for decades, although the past few years have seen a tectonic shift towards embracing computational technologies in both academia and pharma. This shift is largely defined by the flood of data on ligand properties and binding to therapeutic targets and their 3D structures, abundant computing capacities and the advent of on-demand virtual libraries of drug-like small molecules in their billions. Taking full advantage of these resources requires fast computational methods for effective ligand screening. This includes structure-based virtual screening of gigascale chemical spaces, further facilitated by fast iterative screening approaches. Highly synergistic are developments in deep learning predictions of ligand properties and target activities in lieu of receptor structure. Here we review recent advances in ligand discovery technologies, their potential for reshaping the whole process of drug discovery and development, as well as the challenges they encounter. We also discuss how the rapid identification of highly diverse, potent, target-selective and drug-like ligands to protein targets can democratize the drug discovery process, presenting new opportunities for the cost-effective development of safer and more effective small-molecule treatments.

Despite amazing progress in basic life sciences and biotechnology, drug discovery and development (DDD) remain slow and expensive, taking on average approximately 15 years and approximately US\$2 billion to make a small-molecule drug¹. Although it is accepted that clinical studies are the priciest part of the development of each drug, most time-saving and cost-saving opportunities reside in the earlier discovery and preclinical stages. Preclinical efforts themselves account for more than 43% of expenses in pharma, in addition to major public funding¹, driven by the high attrition rate at every step from target selection to hit identification and lead optimization to the selection of clinical candidates. Moreover, the high failure rate in clinical trials (currently 90%)² is largely explained by issues rooted in early discovery such as inadequate target validation or suboptimal ligand properties. Finding fast and accessible ways to discover more diverse pools of higher-quality chemical probes, hits and leads with optimal absorption, distribution, metabolism, excretion and toxicology (ADMET) and pharmacokinetics (PK) profiles at the early stages of DDD would improve outcomes in preclinical and clinical studies and facilitate more effective, accessible and safer drugs.

The concept of computer-aided drug discovery³ was developed in the 1970s and popularized by *Fortune* magazine in 1981, and has since been through several cycles of hype and disillusionment⁴. There have been success stories along the way⁵ and, in general, computer-assisted approaches have become an integral, yet modest, part of the drug discovery process^{6,7}. In the past few years, however, several scientific and technological breakthroughs resulted in a tectonic shift towards embracing computational approaches as a key driving force for drug

discovery in both academia and industry. Pharmaceutical and biotech companies are expanding their computational drug discovery efforts or hiring their first computational chemists. Numerous new and established drug discovery companies have raised billions in the past few years with business models that heavily rely on a combination of advanced physics-based molecular modelling with deep learning (DL) and artificial intelligence (AI)⁸. Although it is too early yet to expect approved drugs from the most recent computationally driven discovery efforts, they are producing a growing number of clinical candidates, with some campaigns specifically claiming target-to-lead times as low as 1–2 months^{9,10}, or target-to-clinic time under 1 year¹¹. Are these the signs of a major shift in the role that computational approaches have in drug discovery or just another round of the hype cycle?

Let us look at the key factors defining the recent changes (Fig. 1). First, the structural revolution—from automation in crystallography¹² to microcrystallography^{13,14} and most recently cryo-electron microscopy technology^{15,16}—has made it possible to reveal 3D structures for the majority of clinically relevant targets, often in a state or molecular complex relevant to its biological function. Especially impressive has been the recent structural turnaround for G protein-coupled receptors (GPCRs)¹⁷ and other membrane proteins that mediate the action of more than 50% of drugs¹⁸, providing 3D templates for ligand screening and lead optimization. The second factor is a rapid and marked expansion of drug-like chemical space, easily accessible for hit and lead discovery. Just a few years ago, this space was limited to several million on-shelf compounds from vendors and in-house screening libraries in pharma. Now, screening can be done with ultra-large virtual libraries

¹Department of Quantitative and Computational Biology, University of Southern California, Los Angeles, CA, USA. ²Center for New Technologies in Drug Discovery and Development, Bridge Institute, Michelson Center for Convergent Biosciences, University of Southern California, Los Angeles, CA, USA. ³Department of Chemistry, University of Southern California, Los Angeles, CA, USA. ✉e-mail: katritch@usc.edu

Review

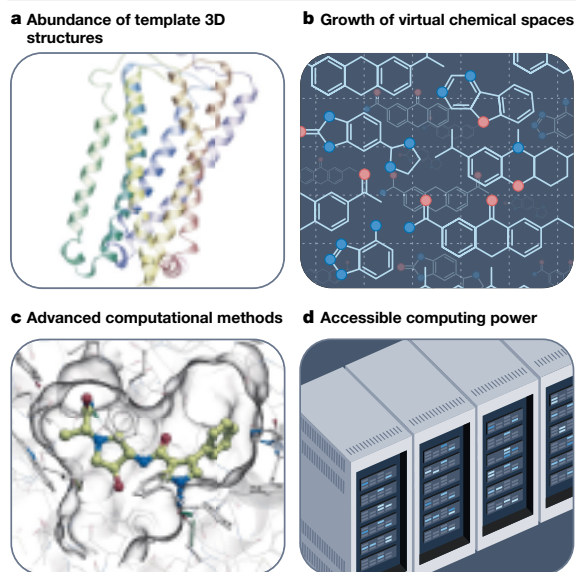


Fig. 1 Key factors driving VLS technology breakthroughs for generation of high-quality hits and leads. **a**, More than 200,000 protein structures in the PDB, plus private collections, have more than 90% of protein families covered with high-resolution X-ray and more recently cryo-electron microscopy structures, often in distinct functional states, with remaining gaps also filled by homology or AlphaFold2 models. **b**, The chemical space available for screening and fast synthesis has grown from about 10^7 on-shelf compounds in 2015 to more than 3×10^{10} on-demand compounds in 2022, and can be rapidly expanded beyond 10^{15} diverse and novel compounds. **c**, Computational methods for VLS include advances in fast flexible docking, modular fragment-based algorithms, DL models and hybrid approaches. **d**, Computational tools are supported by rapid growth of affordable cloud computing, GPU acceleration and specialized chips.

and chemical spaces of drug-like compounds, which can be readily made on-demand, rapidly growing beyond billions of compounds¹⁹, and even larger generative spaces with theoretically predicted synthesizability (Box 1). The third factor involves emerging computational approaches that strive to take full advantage of the abundance of 3D structures and ligand data, supported by the broad availability of cloud and graphics processing unit (GPU) computing resources to support these methods at scale. This includes structure-based virtual screening of ultra-large libraries^{20–22}, using accelerated^{23–25} and modular²⁶ screening approaches, as well as recent growth of data-driven machine learning (ML) and DL methods for predicting ADMET and PK properties and activities²⁷.

Although the impacts of the recent structural revolution¹⁷ and computing hardware in drug discovery²⁸ are comprehensively reviewed elsewhere, here we focus on the ongoing expansion of accessible drug-like chemical spaces as well as current developments in computational methods for ligand discovery and optimization. We detail how emerging computational tools applied in gigaspace can facilitate the cost-effective discovery of hundreds or even thousands of highly diverse, potent, target-selective and drug-like ligands for a desired target, and put them in the context of experimental approaches (Table 1). Although the full impact of new computational technologies is only starting to affect clinical development, we suggest that their synergistic combination with experimental testing and validation in the drug discovery ecosystem can markedly improve its efficiency in producing better therapeutics.

Expansion of accessible chemical space

Why bigger is better

The limited size and diversity of screening libraries have long been a bottleneck for detection of novel potent ligands and for the whole process of drug discovery. An average ‘affordable’ high-throughput screening (HTS) campaign²⁹ uses screening libraries of about 50,000–500,000 compounds and is expected to yield only a few true hits after secondary validation. Those hits, if any, are usually rather weak, non-selective, have suboptimal ADMET and PK properties and unknown binding mode, so their discovery entails years of painstaking trial-and-error optimization efforts to produce a lead molecule with satisfying potency and all the other requirements for preclinical development. Scaling of HTS to a few million compounds can be afforded only in big pharma, and it still does not make that much difference in terms of the quality of resulting hits. Likewise, virtual libraries that use in silico screening were traditionally limited to a collection of compounds available in stock from vendors, usually comprising fewer than 10 million unique compounds, therefore the scale advantage over HTS was marginal.

Although chasing the full coverage of the enormous drug-like chemical space (estimated at more than 10^{63} compounds)³⁰ is a futile endeavour, expanding the screening of on-demand libraries by several orders of magnitude to billions and more of previously unexplored drug-like compounds, either physical or virtual, is expected to change the drug discovery model in several ways. First, it can proportionally increase the number of potential hits in the initial screening³¹ (Fig. 2). This abundance of ligands in the library also increases the chances of identification of more potent or selective ligands, as well as ligands with better physicochemical properties. This has been demonstrated in ultra-large virtual screening campaigns for several targets, revealing highly potent ligands with affinities often in the mid-nanomolar to sub-nanomolar range^{20–23,26}. Second, the accessibility of hit analogues in the same on-demand spaces streamlines a generation of meaningful structure–activity relationship (SAR)-by-catalogue and further optimization steps, reducing the amount of elaborate custom synthesis. Last, although the library scale is important, properly constructed gigascale libraries can expand chemical diversity (even with a few chemical reactions³²), chemical novelty and patentability of the hits, as almost all on-demand compounds have never been synthesized before.

Physical libraries

Several approaches have been developed recently to push the library size limits in HTS, including combinatorial chemistry and large-scale pooling of the compounds for parallel assays. For example, affinity-selection mass spectrometry techniques can be applied to identify binders directly in pools of thousands of compounds³³ without the need for labelling. DNA-encoded libraries (DELs) and cost-effective approaches to generate and screen them have also been developed³⁴, making it possible to work with as many as approximately 10^{10} compounds in a single test tube³⁵. These methods have their own limitations; as DELs are created by tagging ligands with unique DNA sequences through a linker, DNA conjugation limits the chemistries possible for the combinatorial assembly of the library. Screening of DELs may also yield a large number of false negatives by blocking important moieties for binding and, more importantly, false positives by nonspecific binding of DNA labels, so expensive off-DNA resynthesis of hit compounds is needed for their validation. To avoid this resynthesis, it has been suggested to use ML modes trained on DEL results for each target to predict drug-like ligands from on-demand chemical spaces, as described in ref. 36.

Virtual on-demand libraries

In silico screening of virtual libraries by fast computational approaches has long been touted as a cost-effective way to overcome the limitations of physical libraries. Only recently, however, have synthetic chemistry

Box 1

Types of chemical libraries and spaces for drug discovery

Pharma companies amass collections of compounds for screening in-house, whereas in-stock collections from vendors (see the figure, part **a**) allow fast (less than 1 week) delivery, contain unique and advanced chemical scaffolds, are easily searchable and are HTS compatible. However, the high cost of handling physical libraries, their slow linear growth, limited size and novelty constrain their applications.

More recently, virtual on-demand chemical databases (fully enumerated) and spaces (not enumerated) allow fast parallel synthesis from available building blocks, using validated or optimized protocols, with synthetic success of more than 80% and delivery in 2–3 weeks (see the figure, part **b**). The virtual chemical spaces assure high chemical novelty and allow fast polynomial growth with the addition of new synthons and reaction scaffolds, including 4+ component reactions. Examples include Enamine REAL, Galaxy by WuXi, CHEMriya by Otava and private databases and spaces at pharmaceutical companies.

Generative spaces, unlike on-demand spaces, comprise theoretically possible molecules and collectively could comprise all chemical space (see the figure, part **c**). Such spaces are limited only by theoretical plausibility, estimated as 10^{23} – 10^{60} of drug-like compounds. Although allowing comprehensive space coverage, the reaction path and success rate of generated compounds are unknown, and thus require computational prediction of their practical synthesizability. Examples of generative spaces and their subsets include GDB-13, GDB-17, GDB-18 and GDBChEMBL.

a In-stock collections (10^6 – 10^7)

Molecules on vendors' shelves

More than 100 chemical vendors

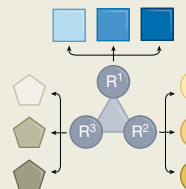
Custom synthesis

In-stock molecules

**b On-demand databases and spaces (10^{10} – 10^{15})**

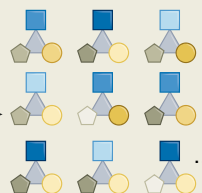
Virtual but readily synthesizable

More than 120,000 building blocks



More than 180 reactions (2 and 3 component)

On-demand molecules

**c Generative spaces (10^{23} – 10^{60})**

Theoretically possible organic molecules

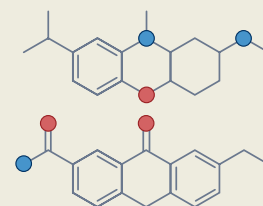
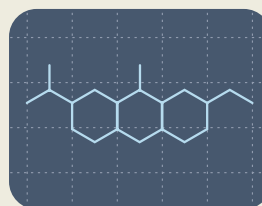
Graphs for n atoms

Hydrocarbon structures (saturated)

Skeletons (includes unsaturated)

Expanded skeletons (heteroatom substitution)

Chemically meaningful molecules



and cheminformatics approaches been developed to break out of these limits and construct virtual on-demand libraries that explore much larger chemical space, as reviewed in refs. 37,38. In 2017, the readily accessible (REAL) database by Enamine^{19,39} became the first commercially available on-demand library based on the robust reaction principle⁴⁰, whereas the US National Institutes of Health developed synthetically accessible virtual inventory (SAVI)⁴¹, which also uses Enamine building blocks. The REAL database uses carefully selected and optimized parallel synthesis protocols and a curated collection of in-stock building blocks, making it possible to guarantee the fast (less than 4 weeks), reliable (80% success rate) and affordable synthesis of a set of compounds²¹. Driven by new reactions and diverse building blocks, the fully enumerated REAL database has grown from approximately 170 million compounds in 2017 to more than 5.5 billion compounds in 2022 and comprises the bulk of the popular ZINC20 virtual screening database⁴². The practical utility of the REAL database has been recently demonstrated in several major prospective screening campaigns^{20,21,23,24}, some of them taking further hit optimization steps in the same chemical space, yielding selective nanomolar and even sub-nanomolar ligands without any custom synthesis^{20,21}. Similar ultra-large virtual libraries (that is, GalaXi (<http://www.wuxiapptec.com>)

and CHEMriya (<http://chemriya.com>)) are available commercially, although their synthetic success rates are yet to be published.

Virtual chemical spaces

The modular nature of on-demand virtual libraries supports further growth by the addition of reactions and building blocks. However, building, maintaining and searching fully enumerated chemical libraries comprising more than a few billion compounds become slow and impractical. Such gigascale virtual libraries are therefore usually maintained as non-enumerated chemical spaces, defined by a specific set of building blocks and reactions (or transforms), as comprehensively reviewed in ref. 38. Within pharma, one of the first published examples includes PGVL by Pfizer^{37,43}, the most recent version of which uses a set of 1,244 reactions and in-house reagents to account for 10^{14} compounds. Other biopharma companies have their own virtual chemical spaces^{38,44}, although their details are often not in the public domain. Among commercially available chemical spaces, GalaXi Space by WuXi (approximately 8 billion compounds), CHEMriya by Otava (11.8 billion compounds) and Enamine REAL Space (36 billion compounds)⁴⁵ are among the largest and most established. In addition to their enormous sizes, these virtual spaces are highly novel and diverse, and have

Review

Table 1 | Comparison of experimentally driven HTS, fragment-based ligand discovery, gigascale DEL screening and gigascale VLS

	HTS	Fragment-based ligand discovery	Gigascale DEL screening	Gigascale VLS
Initial library size	10 ⁵ –10 ⁷	10 ² –10 ⁵	10 ¹⁰	10 ¹⁰ –10 ¹⁵
Hit rate (%)	0.01–0.5	1–5	0.01–0.5	10–40*
Expected initial hit affinity	Weak (1–10 μM)	Very weak (100–1,000 μM) small fragments	Medium (0.1–10 μM)	Medium-high (0.01–10 μM)
Further steps to lead identifications	SAR by custom synthesis, QSAR-driven optimization	Merging or growing of fragments, structure-based and QSAR optimization	Label-free hit resynthesis, QSAR-driven optimization with custom synthesis	Extensive SAR-by-catalogue, structure-based and QSAR optimization
Expected number of custom syntheses to lead	500–1,000	500–1,000	200–500	0–50 (mostly on demand or easy parallel synthesis)
Composition of matter patentability	Hits are not novel, need modifications or scaffold hopping to achieve IP novelty	Fragment hits are not novel, require rational design to achieve IP novelty	Depends on the DNA-encoded library	Most hits are not previously synthesized and have IP novelty
Limitations	Modest library size, unknown binding mode, expensive equipment	Expensive NMR, X-ray and BIACORE equipment, many optimization steps	Many false positives, off-DNA resynthesis of hits needed	Computational resources (but reduced more than 1,000 times by modular VLS)

IP, intellectual property. *Fraction of predicted candidate hits that were confirmed experimentally.

minimal overlap (less than 10%) between each other⁴⁶. Currently, the largest commercial space, Enamine REAL Space, is an extension to the REAL database that maintains the same synthetic speed, rate and cost guarantees, covering more than 170 reactions and more than 137,000 building blocks (Box 1). Most of these reactions are two-component or three-component, but more four-component or even five-component reactions are being explored, enabling higher-order combinatorics. This space can be easily expanded to 10¹⁵ compounds based on available reactions and extended building block sets, for example, 680 million of make on demand (MADE) building blocks⁴⁷, although synthesis of such compounds involves more steps and is more expensive. To represent and navigate combinatorial chemical spaces without their full enumeration, specialized cheminformatics tools have been developed, from fragment-based chemical similarity searches⁴⁸ to more elaborate 3D molecular similarity search methods based on atomic property fields such as rapid isostere discovery engine (RIDE)³⁸.

An alternative approach proposed to building chemical spaces generates hypothetically synthesizable compounds following simple rules of synthetic feasibility and chemical stability. Thus, the generated databases (GDB) predict compounds that can be made of a specific number of atoms; for example, GDB-17 contained 166.4 billion molecules of up to 17 atoms of C, N, O, S and halogens⁴⁹, whereas GDB-18 made up of 18 atoms would reach an estimated 10¹³ compounds³⁸. Other generative approaches based on narrower definitions of chemical spaces are now used in de novo ligand design with DL-based generative chemistry (for example, ref. 50), as discussed below.

Although the synthetic success rate for some of the commercial on-demand chemical spaces (for example, Enamine REAL Space) have been thoroughly validated^{20–24,26,42}, synthetic accessibilities and success rates of other chemical spaces remain unpublished³⁸. These are important metrics for the practical sustainability of on-demand synthesis because reduced success rates or unreasonable time and cost would diminish its advantage over custom synthesis.

Computational approaches to drug design

Challenges of gigascale screening

Chemical spaces of gigascale and terrascale, provided that they maintain high drug likeness and diversity, are expected to harbour millions of potential hits and thousands of potential lead series for any target. Moreover, their highly tractable robust synthesis simplifies any downstream medicinal chemistry efforts towards final drug candidates.

Dealing with such virtual libraries, however, calls for new computational approaches that meet special requirements for both speed and accuracy. They have to be fast enough to handle gigascale libraries. If docking of a compound takes 10 s per CPU core, it would take more than 3,000 years to screen 10¹⁰ compounds on a single CPU core, or cost approximately US \$1 million on a computing cloud at the cheapest CPU rates. At the same time, gigascale screening must be extremely accurate, safeguarding against false-positive hits that effectively cheat the scoring function by exploiting its holes and approximations³¹. Even a one-in-a-million rate of false positives in a 10¹⁰ compound library would comprise 10,000 false hits, which may flood out any hit candidate selection. The artefact rate and nature may depend on the target and screening algorithms and should be carefully addressed in screening and post-processing. Although there is no one simple solution for such artefacts, some practical and reasonably cost-effective remedies include: (1) selection based on the consensus of two different scoring functions, (2) selection of highly diverse hits (many artefacts cluster to similar compounds), (3) hedging the bets from several ranges of scores³¹ and (4) manually curating the final list of compounds for any unusual interactions. Ultimately, it is highly desirable to fix as many remaining ‘holes in the scoring functions’ as possible, and reoptimize them for high selectivity in the range of scores where the top true hits of gigaspace are found. Missing some hits in screening (false negatives) would be well tolerated because of the huge number of potential hits in the 10¹⁰ space (for example, losing 50% of a million potential hits is perfectly fine), so some trade-off in score sensitivity is acceptable.

The major types of computational approaches to screening a protein target for potential ligands are summarized in Table 2. Below, we discuss some emerging technologies and how they can best fit into the overall DDD pipeline to take full advantage of growing on-demand chemical spaces.

Receptor structure-based screening

In silico screening by docking molecules of the virtual library into a receptor structure and predicting its ‘binding score’ is a well-established approach to hit and lead discovery and had a key role in recent drug discovery success stories^{11,17,51}. The docking procedure itself can use molecular mechanics, often in internal coordinate representation, for rapid conformational sampling of fully flexible ligands^{52,53}, using empirical 3D shape-matching approaches^{54,55}, or combining them in a hybrid docking funnel^{56,57}. Special attention is devoted to ligand scoring functions, which are designed to reliably remove non-binders to minimize

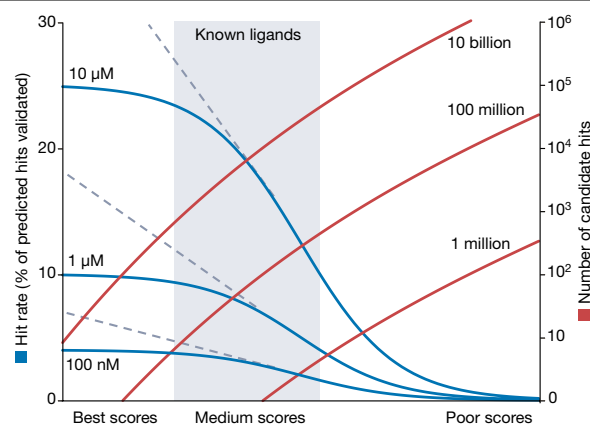


Fig. 2 | Benefits of a bigger chemical space. The red curves in log scale illustrate the distribution of screening hits with binding scores better than X for libraries of 10 billion, 100 million and 1 million compounds, as estimated from previous VLS and V-SYNTHES screening campaigns. The blue curves illustrate the approximate dependence of the experimental hit rate on the predicted docking score for 10- μ M, 1- μ M and 100-nM thresholds²⁰. This analysis (semi-quantitative, as it varies from target to target) suggests that screening of more than 100 million compounds lifts the limitations of smaller libraries, extending the tail of the hit distribution towards better binding scores with high hit rates, and allowing for identification of proportionally more experimental hits with higher affinity. Note also two important factors justifying further growth of screening libraries to 10 billion and more: (1) the candidate hits for synthesis and experimental testing are usually picked as a result of target-dependent post-processing of several thousands of top-scoring compounds, which selects for novelty, diversity, drug likeness and often interactions with specific receptor residues. Thus, the more good-scoring compounds that are identified, the better overall selection can be made. (2) Saturation of the hit rate curves at best scores is not a universal rule but a result of the limited accuracy of fast scoring functions used in screening. Using more accurate docking or scoring approaches (flexible docking, quantum mechanical and free energy perturbation) in the post-processing step can extend a meaningful correlation of binding score with affinity further left (grey dashed curves), potentially bringing even more high-affinity hits for gigascale chemical spaces.

false-positive predictions, which is especially relevant with the growth of library size. Blind assessments of the performance of structure-based algorithms have been routinely performed as a D3R Grand Challenge community effort^{58,59}, showing continuous improvements in ligand pose and binding energy predictions for the best algorithms.

Results of the many successful structure-based prospective screening campaigns have been published over the years covering all major classes of targets, most recently GPCRs, as reviewed in refs. 17,51,60, whereas countless more have been used in industry. The focused candidate ligand sets, predicted by such screening, often show useful (10–40%) hit rates in experimental testing⁶⁰, yielding novel hits for many targets with potencies in the 0.1–10- μ M range (for those that are published, at least). Further steps in optimization of the initial hits obtained from standard screening libraries of less than 10 million compounds, however, usually require expensive custom synthesis of analogues, which has been afforded only in a few published cases^{20,61}.

Identification of hits directly in much larger chemical spaces such as REAL Space not only can bring more and better hits³¹ but also supports their optimization, as any resulting hit has thousands of analogues and derivatives in the same on-demand space. This advantage was especially helpful for such challenging targets as SARS-CoV-2 main protease (M^{pro}), for which hundreds of standard virtual ligand screening (VLS) attempts came up empty-handed⁶² (see discussion on M^{pro} challenges in ‘Hybrid

in vitro–in silico approaches’ below). Although the initial hit rates were low even in the ultra-large screens, VirtualFlow²⁴ of the REAL database with 1.4 billion compounds still identified hits in the 10–100- μ M range, which were optimized via on-demand synthesis⁶³ to yield quality leads with the best compound Z222979552 (half maximal inhibitory concentration (IC_{50}) = 1.0 μ M). Another ultra-large screen of 235 million compounds, based on a newer M^{pro} structure with a non-covalent inhibitor (Protein Data Bank (PDB) ID: 6W63), also produced viable hits, fast optimization of which resulted in the discovery of nanomolar M^{pro} inhibitors in just 4 months by a combination of on-demand and simple custom chemistry⁶⁴. The best compound in this work had good in vitro ADMET properties, with an affinity of 38 nM and a cell-based antiviral potency of 77 nM, which are comparable to clinically used PF-07321332 (nirmatrelvir)⁶⁵.

With increasing library sizes, the computational time and cost of docking itself become the main bottleneck in screening, even with massively parallel cloud computing⁶⁰. Iterative approaches have been recently suggested to tackle libraries of this size; for example, VirtualFlow used stepwise filtering of the whole library with docking algorithms of increasing accuracy to screen approximately 1.4 billion Enamine REAL compounds^{23,24}. Although improving speed several-fold, the method still requires a fully enumerated library and its computational cost grows linearly with the number of compounds, limiting its applicability in rapidly expanding chemical spaces.

Modular synthon-based approaches

The idea of designing molecules from a limited set of fragments to optimally fill the receptor binding pocket has been entertained from the early years of drug discovery, implemented, for example, in the LUDI algorithm⁶⁶. However, custom synthesis of the designed compounds remained the major bottleneck of such approaches. The recently developed virtual synthon hierarchical enumeration screening (V-SYNTHES)²⁶ technology applies fragment-based design to on-demand chemical spaces, thus avoiding the challenges of custom synthesis (Fig. 3). Starting with the catalogue of REAL Space reactions and building blocks (synthons), V-SYNTHES first prepares a minimal library of representative chemical fragments by fully enumerating synthons at one of the attachment points, capping the other position (or positions) with a methyl or phenyl group. Docking-based screening then allows selection of the top-scoring fragments (for example, the top 0.1%) that are predicted to bind well into the target pocket. This is repeated for a second position (and then third and fourth positions, if available), and the resulting focused libraries are screened at each iteration against the target pocket. At the final step, the top approximately 50,000 full compounds from REAL Space are docked with more elaborate and accurate docking parameters or methods, and the top-ranking candidates are filtered for novelty, diversity and variety of desired drug-like properties. In post-processing, the best 50–500 compounds are selected for synthesis and testing. Our assessment suggests that combining synthons with the scaffolds and capping them with dummy minimal groups in the V-SYNTHES algorithm is a critical requirement for optimal fragment predictions because reactive groups of building blocks and scaffolds often create strong, yet false, interactions that are not present in the full molecule. Another important part of the algorithm is the evaluation of the fragment-binding pose in the target, which prioritizes those hits with minimal caps pointed into a region of the pocket where the fragment has space to grow.

Initially applied to discover new chemotypes for cannabinoid receptor CB_2 antagonists, V-SYNTHES has shown a hit rate of 23% for submicromolar ligands, which exceeded the hit rate of standard VLS by fivefold, while taking about 100 times less computational resources²⁶. A similar hit rate was found for the ROCK1 kinase screening in the same study, with one hit in the low nanomolar range²⁶. V-SYNTHES is being applied to other therapeutically relevant targets with well-defined pocket structures.

Review

Table 2 | Major types of virtual screening algorithms

Type	Approach	Scalability	Applications	Requirements	Examples
Protein structure based	Fast empirical docking	10^8 – 10^9	Separate ligands from non-binders	High-resolution structures	DOCK ⁵⁴ , GOLD ¹⁴⁹ , AutoDock ⁵⁵
	Molecular mechanics based	10^6 – 10^8	Separate ligands from non-binders	High-resolution structures	ICM docking ⁵² , ROSETTALigand ⁵³ , Glide ^{56,57}
	Flexible receptor docking	10^3 – 10^5	Separate ligands from non-binders	Medium-resolution structures	IFD-MD ¹⁵⁰
	Modular VLS	10^{10} – 10^{15}	Separate ligands from non-binders	High-resolution structures	V-SYNTHES ²⁶ , Chemical Space Docking ¹⁵¹
	Free energy calculations	10^2 – 10^3	Affinity ranking	High-resolution structures	FEP+ ¹¹² , AB-FEP ^{113,114}
	QM/MM	10^1 – 10^3	Ion binding, transition state	High-resolution structures	Reviewed in ref. 152
Ligand based	2D/3D QSAR	Up to 10^8	Screening and optimization	Ligand activity large datasets	AutoQSAR ¹⁵³ , APF ¹⁵⁴
	3D pharmacophore and APF screening	Up to 10^{10}	Screening	Ligand activity data	Reviewed in ref. 155, RIDE ⁹⁸
	ML/DL-QSAR	Up to 10^{10}	Screening and affinity predictions	Ligand activity large datasets	Q.E.D. ⁷⁸ , LSTM-NN ¹⁵⁶
	Chemical space search	Up to 10^{26}	Selection of analogues	Starting ligand (or ligands)	InfiniSee ⁴⁵
	QSPR-DL	Up to 10^{10}	Predict solubility, lipophilicity, bioavailability, brain permeability, among others	Large datasets on ligand properties	AstraZeneca PK prediction ⁷³ , prediction of oral bioavailability ⁷²⁻⁷⁴
Hybrid	3D interaction fingerprints	Up to 10^{10}	Improved docking and ligand selection	Data on ligand activity and protein–ligand 3D complexes	SIFT ¹⁵⁷
	3D/graph DL	10^6 – 10^9	Affinity prediction	Data on ligand activity and protein–ligand 3D complexes	Graph-CNN ^{82,83} , 3D-CNN ^{84,85}
	Dock/DL iterations	10^8 – 10^{10}	Separate ligands from non-binders	High-resolution structures	MolPal ²⁵ , active learning ¹¹⁰ , deep docking ¹¹¹
	Dock to AI 3D protein models	10^6 – 10^8	Separate ligands from non-binders	Protein target sequence	AlphaFold ^{99,100} , RosettaFold ¹⁰¹
	DL-based 3D score function	10^6 – 10^8	Separate ligands from non-binders	High-resolution structures	RT-CNN ⁹⁸

Examples are for illustration only; we apologize for including only a few of the many important programs and tools that are available, due to space limitations. APF, atomic property field; FEP, free energy perturbation; AB-FEP, absolute protein–ligand binding FEP; LSTM-NN, long short-term memory networks–neural networks; SIFT, structural interaction fingerprint; CNN, convolutional neural networks; QM/MM, hybrid quantum mechanics/molecular mechanics; RT-CNN, radial topological CNN; IFD-MD, induced-fit docking molecular dynamics.

A similar approach, chemical space docking, has been implemented by BioSolveIT, so far for two-component reactions⁶⁷. This method is even faster, as it docks individual building block fragments and then enumerates them with scaffolds and other synthons. However, there are trade-offs for the extra speed: docking of smaller fragments without scaffolds is less reliable, and their reactive groups often have dissimilar properties from the reaction product. This may introduce strong receptor interactions that are irrelevant to the final compound and can misguide the fragment selection. This is especially true for cycloaddition reactions and three-component scaffolds, which need further validation in chemical space docking.

Apart from supporting the abundance, chemical diversity and potential quality of hits, structure-based modular approaches are especially effective in identifying hits with robust chemical novelty, as they (1) do not rely on information for existing ligands and (2) identify ligands that have never been synthesized before. This is an important factor in assuring the patentability of the chemical matter for hit compounds and the lead series arising from gigascale screening. Moreover, thousands of easily synthesizable analogues assure extensive SAR-by-catalogue for the best hits, which, for example, enabled approximately 100-fold potency and selectivity improvement for the CB₂ V-SYNTHES hits²⁶. Availability of the multilayer on-demand chemical space extensions (for example, supported by MADE building blocks⁴⁷) can also greatly streamline the next steps in lead optimization through ‘virtual MedChem’, thus reducing extensive custom synthesis.

Data-driven approaches and DL

In the era of AI-based face recognition, ChatGPT and AlphaFold⁶⁸, there is enormous interest in applications of data-driven DL approaches across drug discovery, from target identification to lead optimization to translational medicine (as reviewed in refs. 69–71).

Data-driven approaches have a long history in drug discovery, in which ML algorithms such as support vector machine, random forest and neural networks have been used extensively to predict ligand properties and on-targets activities, albeit with mixed results. Accurate quantitative structure–property relationship (QSPR) models can predict physicochemical (for example, solubility and lipophilicity) and pharmacokinetic (for example, bioavailability and blood–brain barrier penetration) properties, in which large and broad experimental datasets for model training are available and continue to grow^{72–74}. ML is also implemented in many quantitative SAR (QSAR) algorithms⁷⁵, in which the training set and the resulting models are focused on a given target and a chemical scaffold, helping to guide lead affinity and potency optimization. Methods based on extensive ligand–target binding datasets, chemical similarity clustering and network-based approaches have also been suggested for drug repurposing^{76,77}.

The advent of DL takes data-driven models to the next level, allowing analysis of much larger and diverse datasets while deriving more complicated non-linear relationships, with vast literature describing specific DL methodologies and applications to drug discovery^{27,70}. By its ‘learning from examples’ nature, AI requires comprehensive ligand

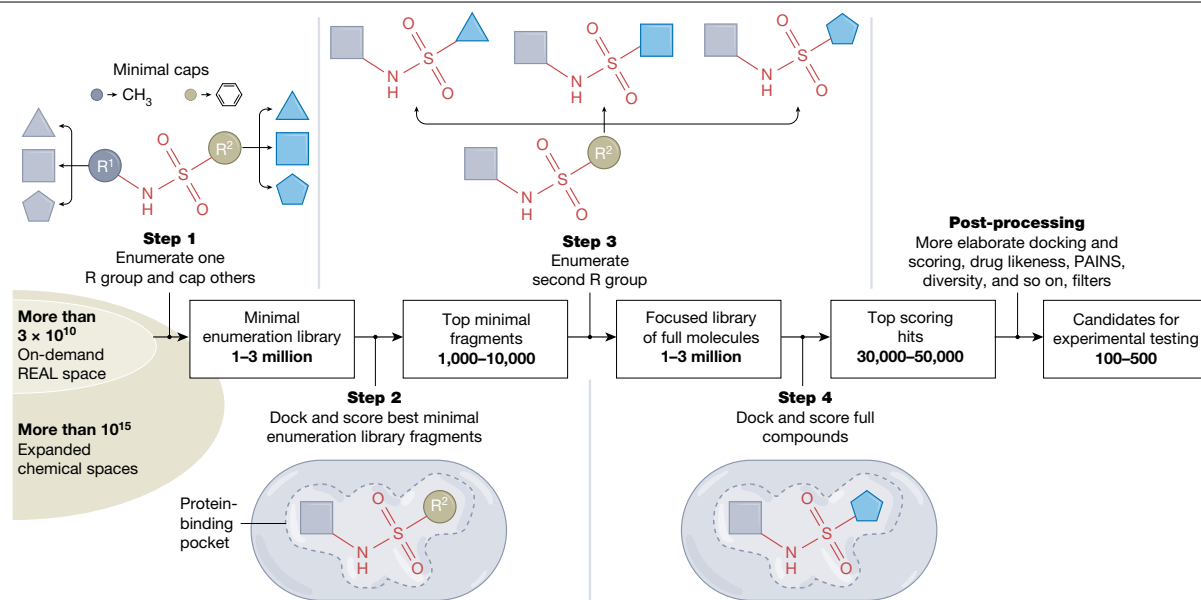


Fig. 3 | Synthon-based hierarchical screening. An overview of the V-SYNTHES algorithm allowing effective screening of more than 31 billion compounds in REAL Space or even larger chemical spaces, while performing enumeration and docking of only small fractions of molecules. The algorithm, illustrated here using a two-component reaction based on a sulfonamide scaffold with R_1 and R_2

synthons, can be applied to hundreds of optimized two-component, three-component or more-component reactions by iteratively repeating steps 3 and 4 until fully enumerated molecules optimally fitting the target pocket are obtained. PAINS, pan assay interference compounds.

datasets for training the predictive models. For QSPR, large public and private databases have been accumulated, with various properties such as solubility, lipophilicity or in vitro proxies for oral bioavailability and brain permeability experimentally measured for many thousands of diverse compounds, allowing prediction of these properties in a broad range of new compounds.

The quality of QSAR models, however, differs for different target classes depending on data availability, with the most advances achieved for the kinase superfamily and aminergic GPCRs. An unbiased benchmark of the best ML QSAR models was given by a recent IDG-DREAM Drug-Kinase Binding Prediction Challenge with the participation of more than 200 experts⁷⁸. The top predictive models in this blind assessment included kernel learning, gradient boosting and DL-based algorithms. The top-performing model (from team Q.E.D) used a kernel regression, protein sequence similarity and affinity values of more than 60,000 compound–kinase pairs between 13,608 compounds and 527 kinases from ChEMBL⁷⁹ and Drug Target Commons⁸⁰ databases as the training data. The best DL model used as many as 900,000 experimental ligand-binding data points for training, but still trailed the much simpler kernel model in performance. The best models achieved a Spearman rank coefficient of 0.53 with a root-mean-square error of 0.95 for the predicted versus experimental pK_d values in the challenge set. Such accuracy was found to be on par with the accuracy and recall of single-point experimental assays for kinase inhibition, and may be useful in screenings for the initial hits for less explored kinases and guiding lead optimization. Note, however, that the kinase family is unique as it is the largest class of more than 500 targets, all possessing similar orthosteric binding pockets and sharing high cross-selectivity. The distant second family with systematic cross-reactivity comprises about 50 aminergic GPCRs, whereas other GPCR families and other cross-reactive protein families are much smaller. The performance and generalizability of ML and DL methods for these and other targets remain to be tested.

The development of broadly generalizable or even universal models is the key aspiration of AI-driven drug discovery. One of the directions

here is to extract general models of binding affinities (binding score functions) from data on both known ligand activities and corresponding protein–ligand 3D structures, for example, collected in the PDBbind database⁸¹ or obtained from docking. Such models explore various approaches to represent the data and network architectures, including spatial graph-convolutional models^{82,83}, 3D deep convolutional neural networks^{84,85} or their combinations⁸⁶. A recent study, however, found that regardless of neural network architecture, an explicit description of non-covalent intermolecular interactions in the PDBbind complexes does not provide any statistical advantage compared with simpler approximations of only ligand or only receptor that omit the interactions⁸⁷. Therefore, the good performances of DL models based on PDBbind rely on memorizing similar ligands and receptors, rather than on capturing general information about their binding. One possible explanation for this phenomenon is that the PDBbind database does not have an adequate presentation of ‘negative space’, that is, ligands with suboptimal interaction patterns to enforce the training.

This mishap exemplifies the need for a better understanding of behaviour of DL models and their dependence on the training data, which is widely recognized in the AI community. It has been shown that DL models, especially based on limited datasets lacking negative data, are prone to overtraining and spurious performance, sometimes leading to whole classes of models deemed ‘useless’⁸⁸ or severely biased by subjective factors defining the training dataset⁸⁹. Statistical tools are being developed to define the applicability range and carefully validate the performance of the models. One of the proposed concepts is the predictability, computability and stability framework for ‘veridical data science’⁹⁰. Adequate selection of quality data has been specifically identified by leaders of the AI community as the major requirement for closing the ‘production gap’, or the inability of ML models to succeed when they are deployed in the real world, thus calling for a data-centric approach to AI^{91,92}. There have also been attempts to develop tools to make AI ‘explainable’, that is, able to formulate some general trends in the data, specifically in the drug discovery applications⁹³.

Review

Despite these challenges and limitations, AI is already starting to make a substantial effect on drug discovery, with the first AI-based drug candidates making it into the preclinical and clinical studies. For kinases, the AI-driven compounds were reported as potent and effective *in vivo* inhibitors of the receptor tyrosine kinase DDR1, which is involved in fibrosis⁹. Phase I clinical trials have been announced for ISM001-055 (also known as INS018_055) for the treatment of idiopathic pulmonary fibrosis¹⁰, although the identity of the compound and its target has not been disclosed. For GPCRs, AI-driven compounds targeting 5-HT_{1A}, dual 5-HT_{1A}–5-HT_{2A} and A_{2A} receptors have recently entered clinical trials, providing further support for the AI-driven drug discovery concept. These first success stories are coming from kinase and GPCR families with already well-studied pharmacology, and the compounds show close chemical similarity to known high-affinity scaffolds⁹⁴. It is important for the next generation of DL drug candidates to improve in novelty and applicability range.

Hybrid computational approaches

As discussed above, physics-based and data-driven approaches have distinct advantages and limitations in predicting ligand potency. Structure-based docking predictions are naturally generalizable to any target with 3D structures and can be more accurate, especially in eliminating false positives as the main challenge of screening. Conversely, data-driven methods may work in lieu of structures and can be faster, especially with GPU acceleration, although they struggle to generalize beyond data-rich classes of targets. Therefore, there are numerous ongoing efforts to combine physics-based and data-driven approaches in some synergistic ways in general⁹⁵, and in drug discovery specifically⁹⁶.

In virtual screening approaches, a synergetic use of physics-based docking with data-based scoring functions may be highly beneficial. Moreover, if the physics-based and data-based scoring functions are relatively independent and both generate enrichment in the selected focused libraries, their combination can reduce the false-positive rates and improve the quality of the hits. This synergy is reflected in the latest 3DR Grand Challenge 4 results for ligand IC₅₀ predictions⁹⁹, in which the top methods that used a combination of both physics-based and ML scoring outperformed those that did not use ML. Going forward, thorough benchmarking of physics-based, ML and hybrid approaches will be a key focus of a new Critical Assessment of Computational Hit-finding Experiments (CACHE), which will assess five specific scenarios relevant to practical hit and lead discovery and optimization⁹⁷.

At a deeper level, the results of accurate physics-based docking (in addition to experimental data, for example, from PDBbind⁸¹) can be used to train generalized graph or 3D DL models predicting ligand–receptor affinity. This would help to markedly expand the training dataset and balance positive and negative (suboptimal binding) examples, which is important to avoid the overtraining issues described in ref. 87. Such DL-based 3D scoring functions for predicting molecular binding affinity from a docked protein–ligand complex are being developed and benchmarked, most recently RTCNN⁹⁸, although their practical utility remains to be demonstrated.

To expand the range of structure-based docking applicability to those targets lacking high-resolution structures, it is also tempting to use AI-derived AlphaFold2 (refs. 99,100) or RosettaFold¹⁰¹ 3D models, which already show utility in many applications, including protein–protein and protein–peptide docking¹⁰². Traditional homology models based on close protein similarity, especially when refined with known ligands¹⁰³, have been used in small-molecule docking and virtual screening¹⁰⁴, therefore AlphaFold2 is expected to further expand the scope of structural modelling and its accuracy. In a recent report, AlphaFold2 models, augmented by other AI approaches, helped to identify a cyclin-dependent kinase 20 (CDK20) small-molecule inhibitor, although at a modest affinity of 8.9 μM (ref. 105). More general benchmarking of the performance of AlphaFold2 models in virtual screening,

however, gives mixed results. In a benchmark focused on targets with existing crystal structures, most AlphaFold2 models had to be cleaned from loops blocking the binding pocket and/or augmented with known ion or other cofactors to achieve reasonable enrichment of hits¹⁰⁶. For the more practical cases of targets lacking experimental structures, especially for target classes with less obvious structural homologies in the ligand-binding pocket, the performance of AlphaFold2 models in small-molecule docking showed disappointing results in recent assessments for GPCR and antibacterial targets^{107,108}. The recently developed AphaFill approach¹⁰⁹ for ‘transplanting’ small-molecule cofactors and ligands from PDB structures to homologous AlphaFold2 models can potentially help to validate and optimize these models, although further assessment of their utility for docking and virtual screening is ongoing.

To speed up virtual screening of ultra-large chemical libraries, several groups have suggested hybrid iterative approaches, in which results of structure-based docking of a sparse library subset are used to train ML models, which are then used to filter the whole library to further reduce its size. These methods, including MolPal²⁵, Active Learning¹¹⁰ and DeepDocking¹¹¹, report as much as 14–100 reduction in the computational cost for libraries of 1.4 billion compounds, although it is not clear how they would scale to rapidly growing chemical spaces.

We should emphasize here that scoring functions in fast-docking algorithms and ML models are primarily designed and trained to effectively separate potential target binders from non-binders, although they are not very accurate in predictions of binding affinities or potencies. For more accurate potency predictions, the smaller focused library of candidate binders selected by the initial AI or docking-based screening can be further analysed and ranked using more elaborate physics-based tools, including free energy perturbation methods for relative¹¹² and absolute^{113–115} free energy of ligand binding. Although these methods are much slower, utilization of GPU accelerated calculations²⁸ holds the potential for their broader application in post-processing in virtual screening campaigns to further enrich the hit rates for high-affinity candidates (Fig. 2), as well as in lead optimization stages.

Future challenges

Further growth of readily accessible chemical spaces

The advent of fast and practical methods for screening gigascale chemical spaces for drug discovery stimulates further growth of these on-demand spaces, supporting better diversity and the overall quality of identified hits and leads. Specifically developed for V-SYNTHES screening, the xREAL extension of Enamine REAL Space now comprises 173 billion compounds¹¹⁶, and can be further expanded to 10¹⁵ compounds and beyond by tapping into an even larger building block set (for example, to 680 million of MADE building blocks⁴⁷), by including four-component or five-component scaffolds, and by using new click-like chemistries as they are discovered. Real-world testing of MADE-enhanced REAL Space, and other commercial and proprietary chemical spaces will allow a broader assessment of their synthesizability and overall utility^{38,117,118}. In parallel, specialized ultra-large libraries can be built for important scaffolds underrepresented in general purpose on-demand spaces, for example, screening of a virtual library of 75 million easily synthesizable tetrahydropyridines recently yielded potent agonists for the 5-HT_{2A} receptor¹¹⁹.

Further growth of the on-demand chemical space size and diversity is also supported by recent development of new robust reactions for the click-like assembly of building blocks. As well as ‘classical’ azide-alkyne cycloaddition click chemistry¹²⁰, recognized by the 2022 Nobel Prize in chemistry¹²¹, and optimized click-like reactions including SuFEx¹²², more recent developments such as Ni-electrocatalysed doubly decarboxylative cross-coupling¹²³ show promise. Other carbon–carbon forming reactions use methyliminodiacetic acid boronates for Csp²–Csp² couplings¹²⁴, and most recently tetramethyl *N*-methyliminodiacetic

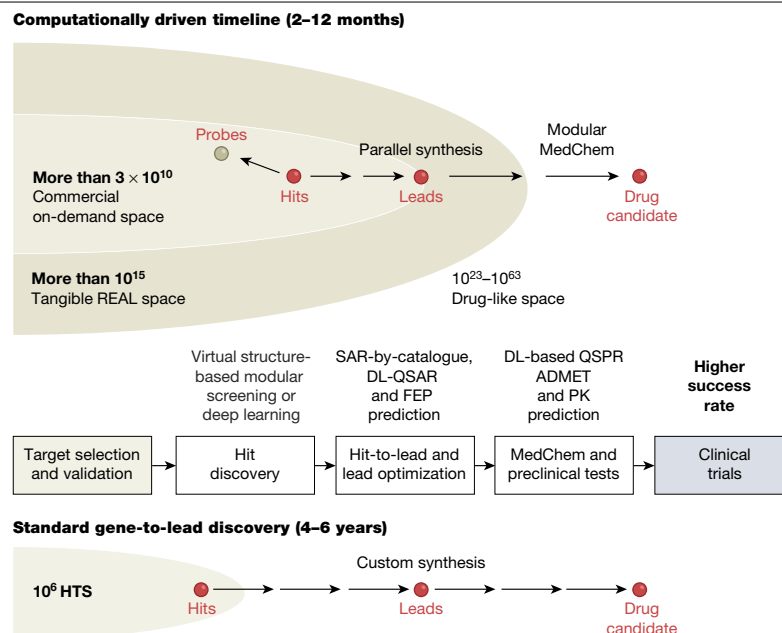


Fig. 4 | Computationally driven drug discovery. Schematic comparison of the standard HTS plus custom synthesis-driven discovery pipeline versus the computationally driven pipeline. The latter is based on easily accessible

on-demand or generative virtual chemical spaces, as well as structure-based and AI-based computational tools that streamline each step of the drug discovery process.

acid boronates¹²⁵ for stereospecific Csp^3 -C bond formation. Each of these reactions applied iteratively can generate new on-demand chemical spaces of billions of diverse compounds operating with a limited number of building blocks. Similar to the routinely used automatic assembly of amino acids in peptide synthesis, fully automated processes could be carried out with robots capable of producing a library of drug-like compounds on demand using combinations of a few thousand diverse building blocks¹²⁶⁻¹²⁸. Such machines are already working, although scaling-up production of thousands of specialized building blocks remains the bottleneck.

The development of more robust generative chemical spaces can also be supported by new computational approaches in synthetic chemistry, for example, predictions of new iterative reaction sequences¹²⁹ or synthetic routes and feasibility from DL-based retrosynthetic analysis¹³⁰. In generative models, synthesizability predictions can be coupled with predictions of potency and other properties towards higher levels of automated chemical design¹³¹. Thus, generative adversarial networks combined with reinforcement learning (GAN-RL) were recently used to predict synthetic feasibility, novelty and biological activity of compounds, enabling the iterative cycle of *in silico* optimization, synthesis and testing of the ligands *in vitro*^{50,132}. When applied within a set of well-established reactions and pharmacologically explored classes of targets, these approaches already yield useful hits and leads, leading to clinical candidates^{50,132}. However, the wider potential of automated chemical design concepts and robotic synthesis in drug discovery remains to be seen.

Hybrid *in vitro*-*in silico* approaches

Although blind benchmarking and recent prospective screening success stories for the growing number of targets support utility of modern computational tools, there are whole classes of challenging targets, in which existing *in silico* screening approaches are not expected to fare very well by themselves. Some of the hardest cases are targets with cryptic or shallow pockets that have to open or undergo a substantial

induced fit to engage ligand, as often found when targeting allosteric sites, for example, in kinases or GPCRs, or protein-protein interactions in signalling pathways.

Although bioinformatics and molecular dynamics approaches can help to detect and analyse allosteric and cryptic pockets¹³³, computational tools alone are often insufficient to support ligand discovery for such challenging sites. The cryptic and shallow pockets, however, have been rather successfully handled by fragment-based drug discovery approaches, which start with experimental screening for the binding of small fragments. The initial hits are found by very sensitive methods, such as BIACORE, NMR, X-ray^{134,135} and potentially cryo-electron microscopy¹³⁶, to reliably detect weak binding, usually in the 10–100- μ M range. The initial screening of the target can be also performed with fragments decorated by a chemical warhead enabling proximity-driven covalent attachment of a low-affinity ligand¹³⁷. In either case, elaboration of initial fragment hits to full high-affinity ligands is the key bottleneck of fragment-based drug discovery, which requires a major effort involving 'growing' the fragment or linking two or more fragments together. This is usually an iterative process involving custom ligand design and synthesis that can take many years^{134,138}. At the same time, structure-based virtual screening can help to computationally elaborate the fragments to match the experimentally identified conformation of the target binding pocket. Most cost-effectively, this approach can be applied when fragment hits are identified from the on-demand space building blocks or their close analogues for easy elaboration in the same on-demand space¹³⁹.

The recent examples of hybrid fragment-based computational design approaches targeting SARS-CoV-2 inhibitors highlight the challenges presented by such targets and allow head-to-head comparisons to ultra-large VLS. One of the studies was aimed at the SARS-CoV-2 NSP3 conserved macrodomain enzyme (Mac1), which is a target critical for the pathogenesis and lethality of the virus. Building on crystallographic detection of the low-affinity (180 μ M) fragments weakly binding Mac1 (ref. 139), merging of the fragments identified a 1- μ M

Review

hit, quickly optimized by catalogue synthesis to a 0.4- μM lead¹⁴⁰. In the same study, an ultra-scale screening of 400 million REAL database identified more than 100 new diverse chemotypes of drug-like ligands, with follow-up SAR-by-catalogue optimization yielding a 1.7- μM lead¹⁴⁰. For the SARS-CoV-2 main protease M^{pro}, the COVID Moonshot initiative published results of crystallographic screening of 1,500 small fragments with 71 hits bound in different subpockets of the shallow active site, albeit none of them showing in vitro inhibition of protease even at 100 μM (ref. 141). Numerous groups crowdsourcing the follow-up computational design and screening of merged and growing fragments helped to discover several SAR series, including a non-covalent M^{pro} inhibitor with an enzymatic IC₅₀ of 21 μM . Further optimization by both structure-based and AI-driven computational approaches, which used more than 10 million MADE Enamine building blocks, led to the discovery of preclinical candidates with cell-based IC₅₀ in the approximately 100-nM range, approaching the potency of nirmatrelvir⁶⁵. The enormous scale, urgency and complexity of this Moonshot effort with more than 2,400 compounds synthesized on demand and measured in more than 10,000 assays are unprecedented and this highlights the challenges of de novo design of non-covalent inhibitors of M^{pro}.

Beyond the Moonshot initiative, a flood of virtual screening efforts yielded mostly disappointing results⁶², for example, the antimalaria drug ebelselen, which was proposed in an early virtual screen¹⁴², failed in clinical trials. Most of these studies, however, screened small-ligand sets focused on repurposing existing drugs, lacked experimental support and used the first structure of M^{pro} solved in a covalent ligand complex (PDB ID: 6LU7) that was suboptimal for docking non-covalent molecules¹⁴².

In comparison, several studies screening ultra-large libraries were able to identify de novo non-covalent M^{pro} inhibitors in the 10–100- μM range^{24,62,63,143}, while experimentally testing only a few hundred synthesized on-demand compounds. One of these studies further elaborated on these weak VLS hits by testing their Enamine on-demand analogues, revealing a lead with IC₅₀ = 1 μM in cell-based assays, and validating its non-covalent binding crystallographically⁶³. Another study based on a later, more suitable non-covalent co-crystal structure of M^{pro} (PDB ID: 6W63) used an ultra-large docking and optimization strategy to discover even more potent 38-nM lead compounds⁶⁴. Note that, although the results of the initial ultra-large screenings for M^{pro} were modest, they were on par with the much more elaborate and expensive efforts of the Moonshot hybrid approach, with simple on-demand optimization leading to similar-quality preclinical candidates. These examples suggest that even for challenging shallow pockets, structure-based virtual screening can often provide a viable alternative when performed at gigascale and supported by accurate structures, sufficient testing and optimization effort.

Outlook towards computer-driven drug discovery

With all the challenges and caveats, the emerging capability of in silico tools to effectively tap into the enormous abundance and diversity of drug-like on-demand chemical spaces at the key target-to-hit-to-lead-to-clinic stages make it tempting to call for the transformation of the DDD ecosystem from computer-aided to computer-driven¹⁴⁴ (Fig. 4). At the early hit identification stage, the ultra-scale virtual screening approaches, both structure-based and AI-based, are becoming mainstream in providing fast and cost-effective entry points into drug discovery campaigns. At the hit-to-lead stage, the more elaborate potency prediction tools such as free energy perturbation and AI-based QSAR often guide rational optimization of ligand potency. Beyond the on-target potency and selectivity, various data-driven computational tools are routinely used in multiparameter optimization of the lead series that includes ADMET and PK properties. Of note, chemical spaces of more than 10¹⁰ diverse compounds are likely to contain millions of initial hits for each target²⁰ (Box 1), thousands of potent and selective leads and, with some limited medicinal chemistry in the same highly tractable chemical space, drug candidates ready for preclinical studies.

To harness this potential, the computational tools need to become more robust and better integrated into the overall discovery pipeline to ensure their impact in translating initial hits into preclinical and clinical development.

One should not forget here that any computational models, however useful or accurate, may never ensure that all of the predictions are correct. In practice, the best virtual screening campaigns result in 10–40% of candidate hits confirmed in experimental validation, whereas the best affinity predictions used in optimization rarely have accuracy better than 1 kcal mol⁻¹ root-mean-square error. Similar limitations apply to current computational models predicting ADMET and PK properties. Therefore, computational predictions always need experimental validation in robust in vitro and in vivo assays at each step of the pipeline. At the same time, experimental testing of predictions also provides data that can feed back into improving the quality of the models by expanding their training datasets, especially for the ligand property predictions. Thus, the DL-based QSPR models will greatly benefit from further accumulating data in cell-permeability assays such as CACO-2 and MDCK, as well as new advanced technologies such as organs-on-a-chip or functional organoids to provide better estimates of ADMET and PK properties without cumbersome in vivo experiments. The ability to train ADMET and PK models with in vitro assay data representing the most relevant species for drug development (typically mouse, rat and human) would also help to address species variability as a major challenge for successful translational studies. All of this creates a virtuous cycle for improving computational models to the point at which they can drive compound selection for most DDD end points. When combined with more accurate in vitro testing, this may reduce and eventually eliminate animal test requirements (as recently indicated by FDA)¹⁴⁵.

Building hybrid in silico–in vitro pipelines with easy access to the enormous on-demand chemical space at all stages of the gene-to-lead process can help to generate abundant pools of diverse lead compounds with optimal potency, selectivity and ADMET and PK properties, resulting in less compromise in multiparameter optimization for clinical candidates. Running such data-rich computationally driven pipelines requires overarching data management tools for drug discovery, many of them being implemented in pharma and academic DDD centres^{146,147}. Building computationally driven pipelines will also help to reveal weak or missing links, in which new approaches and additional data may be needed to generate improved models, thus helping to fill the remaining computational gaps in the DDD pipeline. Provided this systematic integration continues, computer-driven ligand discovery has a great potential to reduce the entry barriers for generating molecules for numerous lines of inquiry, whether it is in vivo probes for new and understudied targets¹⁴⁸, polypharmacology and pluridimensional signalling, or drug candidates for rare diseases and personalized medicine.

1. Austin, D. & Hayford, T. Research and development in the pharmaceutical industry. *CBO* <https://www.cbo.gov/publication/57126> (2021).
2. Sun, D., Gao, W., Hu, H. & Zhou, S. Why 90% of clinical drug development fails and how to improve it? *Acta Pharm. Sin.* **12**, 3049–3062 (2022).
3. Bajorath, J. Computer-aided drug discovery. *F1000Res.* **4**, F1000 Faculty Rev-1630 (2015).
4. Van Drie, J. H. Computer-aided drug design: the next 20 years. *J. Comput. Aided Mol. Des.* **21**, 591–601 (2007).
5. Talele, T. T., Khedkar, S. A. & Rigby, A. C. Successful applications of computer aided drug discovery: moving drugs from concept to the clinic. *Curr. Top. Med. Chem.* **10**, 127–141 (2010).
6. Macalino, S. J. Y., Gosu, V., Hong, S. & Choi, S. Role of computer-aided drug design in modern drug discovery. *Arch. Pharmacol. Res.* **38**, 1686–1701 (2015).
7. Sabe, V. T. et al. Current trends in computer aided drug design and a highlight of drugs discovered via computational techniques: a review. *Eur. J. Med. Chem.* **224**, 113705 (2021).
8. Jayatunga, M. K., Xie, W., Ruder, L., Schulze, U. & Meier, C. AI in small-molecule drug discovery: a coming wave. *Nat. Rev. Drug Discov.* **21**, 175–176 (2022).
9. Zhavoronkov, A. et al. Deep learning enables rapid identification of potent DDR1 kinase inhibitors. *Nat. Biotechnol.* **37**, 1038–1040 (2019).

This study claims the discovery of a lead candidate in just 21 days, using generative AI, synthesis, and in vitro and in vivo testing of the compounds.

10. US National Library of Medicine. *ClinicalTrials.gov* <https://clinicaltrials.gov/ct2/show/NCT05154240#contactlocation> (2022).
11. Schrödinger. Schrödinger announces FDA clearance of investigational new drug application for SGR-1505, a MALT1 inhibitor. *Schrödinger* <https://ir.schrodinger.com/node/8621/pdf> (2022).
This press release states that combined physics-based and ML methods enabled a computational screen of 8.2 billion compounds and the selection of a clinical candidate after 10 months and only 78 molecules synthesized.
12. Jones, N. Crystallography: atomic secrets. *Nature* **505**, 602–603 (2014).
13. Liu, W. et al. Serial femtosecond crystallography of G protein-coupled receptors. *Science* **342**, 1521–1524 (2013).
14. Nannenga, B. L. & Gonen, T. The cryo-EM method microcrystal electron diffraction (MicroED). *Nat. Methods* **16**, 369–379 (2019).
15. Fernandez-Leiro, R. & Scheres, S. H. Unravelling biological macromolecules with cryo-electron microscopy. *Nature* **537**, 339–346 (2016).
16. Renaud, J.-P. et al. Cryo-EM in drug discovery: achievements, limitations and prospects. *Nat. Rev. Drug Discov.* **17**, 471–492 (2018).
17. Congreve, M., de Graaf, C., Swain, N. A. & Tate, C. G. Impact of GPCR structures on drug discovery. *Cell* **181**, 81–91 (2020).
18. Santos, R. et al. A comprehensive map of molecular drug targets. *Nat. Rev. Drug Discov.* **16**, 19–34 (2017).
19. Grygorenko, O. O. et al. Generating multibillion chemical space of readily accessible screening compounds. *iScience* **23**, 101681 (2020).
20. Lyu, J. et al. Ultra-large library docking for discovering new chemotypes. *Nature* **566**, 224–229 (2019).
This is ultra-large docking study also carefully assessed the advantages and potential pitfalls of expanding chemical space.
21. Stein, R. M. et al. Virtual discovery of melatonin receptor ligands to modulate circadian rhythms. *Nature* **579**, 609–614 (2020).
This study shows ultra-large docking that resulted in subnanomolar hits for a GPCR.
22. Alon, A. et al. Structures of the sigma2 receptor enable docking for bioactive ligand discovery. *Nature* **600**, 759–764 (2021).
23. Gorgulla, C. et al. An open-source drug discovery platform enables ultra-large virtual screens. *Nature* **580**, 663–668 (2020).
This study shows an iterative library filtering as a first approach to accelerate ultra-large virtual screening.
24. Gorgulla, C. et al. A multi-pronged approach targeting SARS-CoV-2 proteins using ultra-large virtual screening. *iScience* **24**, 102021 (2021).
25. Graff, D. E., Shakhnovich, E. I. & Coley, C. W. Accelerating high-throughput virtual screening through molecular pool-based active learning. *Chem. Sci.* **12**, 7866–7881 (2021).
This study introduces acceleration of ultra-large screening by iteratively combining DL and docking.
26. Sadybekov, A. A. et al. Synthon-based ligand discovery in virtual libraries of over 11 billion compounds. *Nature* **601**, 452–459 (2022).
This study introduces the modular concept for screening gigascale spaces, V-SYNTHES, and validates its performance on GPCR and kinase targets.
27. Yang, X., Wang, Y., Byrne, R., Schneider, G. & Yang, S. Concepts of artificial intelligence for computer-assisted drug discovery. *Chem. Rev.* **119**, 10520–10594 (2019).
28. Pandey, M. et al. The transformational role of GPU computing and deep learning in drug discovery. *Nat. Mach. Intell.* **4**, 211–221 (2022).
29. Blay, V., Tolani, B., Ho, S. P. & Arkin, M. R. High-throughput screening: today's biochemical and cell-based approaches. *Drug Discov. Today* **25**, 1807–1821 (2020).
30. Bohacek, R. S., McMartin, C. & Guida, W. C. The art and practice of structure-based drug design: a molecular modeling perspective. *Med. Res. Rev.* **16**, 3–50 (1996).
31. Lyu, J., Irwin, J. J. & Shoichet, B. K. Modeling the expansion of virtual screening libraries. *Nat. Chem. Biol.* <https://doi.org/10.1038/s41589-022-01234-w> (2023).
32. Tomberg, A. & Boström, J. Can easy chemistry produce complex, diverse, and novel molecules? *Drug Discov. Today* **25**, 2174–2181 (2020).
33. Muchiri, R. N. & van Breemen, R. B. Affinity selection–mass spectrometry for the discovery of pharmacologically active compounds from combinatorial libraries and natural products. *J. Mass Spectrom.* **56**, e4647 (2021).
34. Fitzgerald, P. R. & Paegel, B. M. DNA-encoded chemistry: drug discovery from a few good reactions. *Chem. Rev.* **121**, 7155–7177 (2021).
35. Neri, D. & Lerner, R. A. DNA-encoded chemical libraries: a selection system based on encoding organic compounds with amplifiable information. *Annu. Rev. Biochem.* **87**, 479–502 (2018).
36. McCloskey, K. et al. Machine learning on DNA-encoded libraries: a new paradigm for hit finding. *J. Med. Chem.* **63**, 8857–8866 (2020).
37. Walters, W. P. Virtual chemical libraries. *J. Med. Chem.* **62**, 1116–1124 (2019).
38. Warr, W. A., Nicklaus, M. C., Nicolau, C. A. & Rarey, M. Exploration of ultralarge compound collections for drug discovery. *J. Chem. Inf. Model.* **62**, 2021–2034 (2022).
This is a comprehensive review of the history and recent developments of the on-demand and generative chemical spaces.
39. Enamine. REAL Database. *Enamine* <https://enamine.net/compound-collections/real-compounds/real-database> (2020).
40. Hartenfeller, M. et al. A collection of robust organic synthesis reactions for in silico molecule design. *J. Chem. Inf. Model.* **51**, 3093–3098 (2011).
41. Patel, H. et al. SAVI, in silico generation of billions of easily synthesizable compounds through expert-system type rules. *Sci. Data* **7**, 384 (2020).
42. Irwin, J. J. et al. ZINC20: A free ultralarge-scale chemical database for ligand discovery. *J. Chem. Inf. Model.* **60**, 6065–6073 (2020).
43. Hu, Q. et al. Pfizer Global Virtual Library (PGVL): a chemistry design tool powered by experimentally validated parallel synthesis information. *ACS Comb. Sci.* **14**, 579–589 (2012).
44. Nicolau, C. A., Watson, I. A., Hu, H. & Wang, J. The Proximal Lilly Collection: mapping, exploring and exploiting feasible chemical space. *J. Chem. Inf. Model.* **56**, 1253–1266 (2016).
45. Enamine. REAL Space. *Enamine* <https://enamine.net/library-synthesis/real-compounds/real-space-navigator> (2022).
46. Bellmann, L., Penner, P., Gastreich, M. & Rarey, M. Comparison of combinatorial fragment spaces and its application to ultralarge make-on-demand compound catalogs. *J. Chem. Inf. Model.* **62**, 553–566 (2022).
47. Enamine. Make on-demand building blocks (MADE). *Enamine* <https://enamine.net/building-blocks/made-building-blocks> (2022).
48. Hoffmann, T. & Gastreich, M. The next level in chemical space navigation: going far beyond enumerable compound libraries. *Drug Discov. Today* **24**, 1148–1156 (2019).
49. Ruddigkeit, L., van Deursen, R., Blum, L. C. & Reymond, J.-L. Enumeration of 166 billion organic small molecules in the chemical universe database GDB-17. *J. Chem. Inf. Model.* **52**, 2864–2875 (2012).
50. Vanhaelen, Q., Lin, Y.-C. & Zhavoronkov, A. The advent of generative chemistry. *ACS Med. Chem. Lett.* **11**, 1496–1505 (2020).
51. Ballante, F., Kooistra, A. J., Kampen, S., de Graaf, C. & Carlsson, J. Structure-based virtual screening for ligands of G protein-coupled receptors: what can molecular docking do for you? *Pharmacol. Rev.* **73**, 527–565 (2021).
52. Neves, M. A., Totrov, M. & Abagyan, R. Docking and scoring with ICM: the benchmarking results and strategies for improvement. *J. Comput. Aided Mol. Des.* **26**, 675–686 (2012).
53. Meiler, J. & Baker, D. ROSETTALIGAND: protein-small molecule docking with full side-chain flexibility. *Proteins* **65**, 538–548 (2006).
54. Lorber, D. M. & Shoichet, B. K. Flexible ligand docking using conformational ensembles. *Protein Sci.* **7**, 938–950 (1998).
55. Trott, O. & Olson, A. J. AutoDock Vina: improving the speed and accuracy of docking with a new scoring function, efficient optimization, and multithreading. *J. Comput. Chem.* **31**, 455–461 (2010).
56. Halgren, T. A. et al. Glide: a new approach for rapid, accurate docking and scoring. 2. Enrichment factors in database screening. *J. Med. Chem.* **47**, 1750–1759 (2004).
57. Friesner, R. A. et al. Glide: a new approach for rapid, accurate docking and scoring. 1. Method and assessment of docking accuracy. *J. Med. Chem.* **47**, 1739–1749 (2004).
58. Gaieb, Z. et al. D3R grand challenge 3: blind prediction of protein-ligand poses and affinity rankings. *J. Comput. Aided Mol. Des.* **33**, 1–18 (2019).
59. Parks, C. D. et al. D3R grand challenge 4: blind prediction of protein-ligand poses, affinity rankings, and relative binding free energies. *J. Comput. Aided Mol. Des.* **34**, 99–119 (2020).
60. Bender, B. J. et al. A practical guide to large-scale docking. *Nat. Protoc.* **16**, 4799–4832 (2021).
61. Manglik, A. et al. Structure-based discovery of opioid analgesics with reduced side effects. *Nature* **537**, 185–190 (2016).
62. Cerón-Carrasco, J. P. When virtual screening yields inactive drugs: dealing with false theoretical friends. *ChemMedChem* **17**, e202200278 (2022).
63. Rossetti, G. G. et al. Non-covalent SARS-CoV-2 M^{pro} inhibitors developed from in silico screen hits. *Sci. Rep.* **12**, 2505 (2022).
64. Lutten, A. et al. Ultralarge virtual screening identifies SARS-CoV-2 main protease inhibitors with broad-spectrum activity against coronaviruses. *J. Am. Chem. Soc.* **144**, 2905–2920 (2022).
This study compares fragment-based and ultra-large screening-based discovery of lead candidates for the challenging target.
65. Owen, D. R. et al. An oral SARS-CoV-2 M^{pro} inhibitor clinical candidate for the treatment of COVID-19. *Science* **374**, 1586–1593 (2021).
66. Böhm, H.-J. The computer program LUDI: a new method for the de novo design of enzyme inhibitors. *J. Comput. Aided Mol. Des.* **6**, 61–78 (1992).
67. Beroza, P. et al. Chemical space docking enables large-scale structure-based virtual screening to discover ROCK1 kinase inhibitors. *Nat. Commun.* **13**, 6447 (2022).
68. Jumper, J. et al. Applying and improving AlphaFold at CASP14. *Proteins* **89**, 1711–1721 (2021).
69. Vamathevan, J. et al. Applications of machine learning in drug discovery and development. *Nat. Rev. Drug Discov.* **18**, 463–477 (2019).
70. Schneider, P. et al. Rethinking drug design in the artificial intelligence era. *Nat. Rev. Drug Discov.* **19**, 353–364 (2020).
This article provides a comprehensive introduction to DL approaches in drug discovery.
71. Elbadawi, M., Gaisford, S. & Basit, A. W. Advanced machine-learning techniques in drug discovery. *Drug Discov. Today* **26**, 769–777 (2021).
72. Bender, A. & Cortés-Ciriano, I. Artificial intelligence in drug discovery: what is realistic, what are illusions? Part 1: ways to make an impact, and why we are not there yet. *Drug Discov. Today* **26**, 511–524 (2021).
73. Davies, M. et al. Improving the accuracy of predicted human pharmacokinetics: lessons learned from the AstraZeneca drug pipeline over two decades. *Trends Pharmacol. Sci.* **41**, 390–408 (2020).
74. Schneckenner, S. et al. Prediction of oral bioavailability in rats: transferring insights from in vitro correlations to (deep) machine learning models using in silico model outputs and chemical structure parameters. *J. Chem. Inf. Model.* **59**, 4893–4905 (2019).
75. Cherkasov, A. et al. QSAR modeling: where have you been? Where are you going to? *J. Med. Chem.* **57**, 4977–5010 (2014).
76. Keiser, M. J. et al. Predicting new molecular targets for known drugs. *Nature* **462**, 175–181 (2009).
77. Guney, E., Menche, J., Vidal, M. & Barabási, A.-L. Network-based in silico drug efficacy screening. *Nat. Commun.* **7**, 10331 (2016).
78. Cichońska, A. et al. Crowdsourced mapping of unexplored target space of kinase inhibitors. *Nat. Commun.* **12**, 3307 (2021).
79. Gaulton, A. et al. ChEMBL: a large-scale bioactivity database for drug discovery. *Nucleic Acids Res.* **40**, D1100–D1107 (2012).

Review

80. Tang, J. et al. Drug Target Commons: a community effort to build a consensus knowledge base for drug–target interactions. *Cell Chem. Biol.* **25**, 224–229.e222 (2018).
81. Liu, Z. et al. PDB-wide collection of binding data: current status of the PDBbind database. *Bioinformatics* **31**, 405–412 (2015).
82. Gaudelet, T. et al. Utilizing graph machine learning within drug discovery and development. *Brief. Bioinform.* **22**, bbab159 (2021).
83. Son, J. & Kim, D. Development of a graph convolutional neural network model for efficient prediction of protein–ligand binding affinities. *PLoS ONE* **16**, e0249404 (2021).
84. Stepniewska-Dziubinska, M. M., Zielenkiewicz, P. & Siedlecki, P. Improving detection of protein–ligand binding sites with 3D segmentation. *Sci. Rep.* **10**, 5035 (2020).
85. Jiménez, J., Škaličič, M., Martínez-Rosell, G. & De Fabritiis, G. KDEEP: protein–ligand absolute binding affinity prediction via 3D-convolutional neural networks. *J. Chem. Inf. Model.* **58**, 287–296 (2018).
86. Jones, D. et al. Improved protein–ligand binding affinity prediction with structure-based deep fusion inference. *J. Chem. Inf. Model.* **61**, 1583–1592 (2021).
87. Volkov, M. et al. On the frustration to predict binding affinities from protein–ligand structures with deep neural networks. *J. Med. Chem.* **65**, 7946–7958 (2022).
88. Roberts, M. et al. Common pitfalls and recommendations for using machine learning to detect and prognosticate for COVID-19 using chest radiographs and CT scans. *Nat. Mach. Intell.* **3**, 199–217 (2021).
89. Bekker, W. et al. Machine learning may sometimes simply capture literature popularity trends: a case study of heterocyclic Suzuki–Miyaura coupling. *J. Am. Chem. Soc.* **144**, 4819–4827 (2022).
90. Yu, B. & Kumbier, K. Veridical data science. *Proc. Natl Acad. Sci. USA* **117**, 3920–3929 (2020).
- This perspective article lays a foundation for veridical AI.**
91. Ng, A., Laird, D. & He, L. Data-centric AI competition. *DeepLearning AI* <https://https-deeplearning-ai.github.io/data-centric-comp/> (2021).
92. Miranda, L. J. Towards data-centric machine learning: a short review. *LJ Miranda* <https://miranda921.github.io/notebook/2021/07/30/data-centric-ml/> (2021).
93. Jiménez-Luna, J., Grisoni, F. & Schneider, G. Drug discovery with explainable artificial intelligence. *Nat. Mach. Intell.* **2**, 573–584 (2020).
94. Willis, T. AI drug discovery: assessing the first AI-designed drug candidates to go into human clinical trials. *CAS* <https://www.cas.org/resources/cas-insights/drug-discovery/ai-designed-drug-candidates> (2022).
95. Meng, C., Seo, S., Cao, D., Griesemer, S. & Liu, Y. When physics meets machine learning: a survey of physics-informed machine learning. Preprint at <https://doi.org/10.48550/arXiv.2203.16797> (2022).
96. Thomas, M., Bender, A. & de Graaf, C. Integrating structure-based approaches in generative molecular design. *Curr. Opin. Struct. Biol.* **79**, 102559 (2023).
97. Ackloo, S. et al. CACHE (Critical Assessment of Computational Hit-finding Experiments): a public–private partnership benchmarking initiative to enable the development of computational methods for hit-finding. *Nat. Rev. Chem.* **6**, 287–295 (2022).
- This is an important community initiative for comprehensive performance assessment of computational drug discovery methods.**
98. MolSoft. Rapid isostere discovery engine (RIDE). *MolSoft* <http://molsoft.com/RIDE.html> (2022).
99. Jumper, J. et al. Highly accurate protein structure prediction with AlphaFold. *Nature* **596**, 583–589 (2021).
100. Tunyasuvunakool, K. et al. Highly accurate protein structure prediction for the human proteome. *Nature* **596**, 590–596 (2021).
101. Baek, M. et al. Accurate prediction of protein structures and interactions using a three-track neural network. *Science* **373**, 871–876 (2021).
102. Akdel, M. A structural biology community assessment of AlphaFold2 applications. *Nat. Struct. Mol. Biol.* **29**, 1056–1067 (2022).
103. Katritch, V., Rueda, M. & Abagyan, R. Ligand-guided receptor optimization. *Methods Mol. Biol.* **857**, 189–205 (2012).
104. Carlsson, J. et al. Ligand discovery from a dopamine D₃ receptor homology model and crystal structure. *Nat. Chem. Biol.* **7**, 769–778 (2011).
105. Ren, F. et al. AlphaFold accelerates artificial intelligence powered drug discovery: efficient discovery of a novel cyclin-dependent kinase 20 (CDK20) small molecule inhibitor. *Chem. Sci.* **14**, 1443–1452 (2023).
106. Zhang, Y. et al. Benchmarking refined and unrefined AlphaFold2 structures for hit discovery. *J. Chem. Inf. Model.* **63**, 1656–1667 (2023).
107. He, X.-h. et al. AlphaFold2 versus experimental structures: evaluation on G protein-coupled receptors. *Acta Pharmacol. Sin.* **44**, 1–7 (2022).
108. Wong, F. et al. Benchmarking AlphaFold-enabled molecular docking predictions for antibiotic discovery. *Mol. Syst. Biol.* **18**, e11081 (2022).
109. Hekkelman, M. L., de Vries, I., Joosten, R. P. & Perrakis, A. AlphaFill: enriching AlphaFold models with ligands and cofactors. *Nat. Methods* **20**, 205–213 (2023).
110. Yang, Y. et al. Efficient exploration of chemical space with docking and deep learning. *J. Chem. Theory Comput.* **17**, 7106–7119 (2021).
111. Gentile, F. et al. Artificial intelligence-enabled virtual screening of ultra-large chemical libraries with deep docking. *Nat. Protoc.* **17**, 672–697 (2022).
112. Schindler, C. E. M. et al. Large-scale assessment of binding free energy calculations in active drug discovery projects. *J. Chem. Inf. Model.* **60**, 5457–5474 (2020).
113. Chen, W., Cui, D., Abel, R., Friesner, R. A. & Wang, L. Accurate calculation of absolute protein–ligand binding free energies. Preprint at <https://doi.org/10.26434/chemrxiv-2022-2t0dq-v2> (2022).
114. Khalak, Y. et al. Alchemical absolute protein–ligand binding free energies for drug design. *Chem. Sci.* **12**, 13958–13971 (2021).
115. Courmia, Z. et al. Rigorous free energy simulations in virtual screening. *J. Chem. Inf. Model.* **60**, 4153–4169 (2020).
116. xREAL Chemical Space, *ChemSpace*, <https://chem-space.com/services#v-synthes> (2023).
117. Rarey, M., Nicklaus, M. C. & Warr, W. Special issue on reaction informatics and chemical space. *J. Chem. Inf. Model.* **62**, 2009–2010 (2022).
118. Zabolotna, Y. et al. A close-up look at the chemical space of commercially available building blocks for medicinal chemistry. *J. Chem. Inf. Model.* **62**, 2171–2185 (2022).
119. Kaplan, A. L. et al. Bespoke library docking for 5-HT_{2A} receptor agonists with antidepressant activity. *Nature* **610**, 582–591 (2022).
120. Krasinski, A., Fokin, V. V. & Sharpless, K. B. Direct synthesis of 1,5-disubstituted-4-magneso-1,2,3-triazoles, revisited. *Org. Lett.* **6**, 1237–1240 (2004).
121. The Nobel Prize in Chemistry. *nobelprize.org*, <https://www.nobelprize.org/prizes/chemistry/2022/summary/> (2022).
122. Dong, J., Sharpless, K. B., Kwisnek, L., Oakdale, J. S. & Fokin, V. V. SuFEx-based synthesis of polysulfates. *Angew. Chem. Int. Ed. Engl.* **53**, 9466–9470 (2014).
123. Zhang, B. et al. Ni-electrocatalytic Csp³–Csp³ doubly decarboxylative coupling. *Nature* **606**, 313–318 (2022).
124. Gillis, E. P. & Burke, M. D. Iterative cross-coupling with MIDA boronates: towards a general platform for small molecule synthesis. *Aldrichimica Acta* **42**, 17–27 (2009).
125. Blair, D. J. et al. Automated iterative Csp³–C bond formation. *Nature* **604**, 92–97 (2022).
- This study provides a chemical approach for automation of the C–C bond formation in small-molecule synthesis.**
126. Li, J. et al. Synthesis of many different types of organic small molecules using one automated process. *Science* **347**, 1221–1226 (2015).
127. Trobe, M. & Burke, M. D. The molecular industrial revolution: automated synthesis of small molecules. *Angew. Chem. Int. Ed.* **57**, 4192–4214 (2018).
128. Bublauskas, A. et al. Digitizing chemical synthesis in 3D printed reactionware. *Angew. Chem. Int. Ed.* **61**, e202116108 (2022).
129. Molga, K. et al. A computer algorithm to discover iterative sequences of organic reactions. *Nat. Synth.* **1**, 49–58 (2022).
130. Segler, M. H. S., Preuss, M. & Waller, M. P. Planning chemical syntheses with deep neural networks and symbolic AI. *Nature* **555**, 604–610 (2018).
131. Goldman, B., Kearnes, S., Kramer, T., Riley, P. & Walters, W. P. Defining levels of automated chemical design. *J. Med. Chem.* **65**, 7073–7087 (2022).
132. Grisoni, F. et al. Combining generative artificial intelligence and on-chip synthesis for de novo drug design. *Sci. Adv.* **7**, eabg3338 (2021).
133. Wagner, J. R. et al. Emerging computational methods for the rational discovery of allosteric drugs. *Chem. Rev.* **116**, 6370–6390 (2016).
134. Davis, B. J. & Hubbard, R. E. in *Structural Biology in Drug Discovery* (ed. Renaud, J.-P.) 79–98 (2020).
135. de Souza Neto, L. R. et al. In silico strategies to support fragment-to-lead optimization in drug discovery. *Front. Chem.* **8**, 93 (2020).
136. Saur, M. et al. Fragment-based drug discovery using cryo-EM. *Drug Discov. Today* **25**, 485–490 (2020).
137. Kuljanin, M. et al. Reimagining high-throughput profiling of reactive cysteines for cell-based screening of large electrophile libraries. *Nat. Biotechnol.* **39**, 630–641 (2021).
138. Muegge, I., Martin, Y. C., Hajduk, P. J. & Fesik, S. W. Evaluation of PMF scoring in docking weak ligands to the FK506 binding protein. *J. Med. Chem.* **42**, 2498–2503 (1999).
139. Schuller, M. et al. Fragment binding to the Nsp3 macrodomain of SARS-CoV-2 identified through crystallographic screening and computational docking. *Sci. Adv.* **7**, eabf8711 (2021).
140. Gahbauer, S. et al. Iterative computational design and crystallographic screening identifies potent inhibitors targeting the Nsp3 macrodomain of SARS-CoV-2. *Proc. Natl Acad. Sci. USA* **120**, e2212931120 (2023).
- This article demonstrates the application of both hybrid fragment screening-and-merging design and ultra-large library screening to a challenging viral target.**
141. Achdout, H. et al. Open science discovery of oral non-covalent SARS-CoV-2 main protease inhibitor therapeutics. Preprint at <https://doi.org/10.1101/2020.10.29.339317> (2022).
142. Jin, Z. et al. Structure of M^{pro} from SARS-CoV-2 and discovery of its inhibitors. *Nature* **582**, 289–293 (2020).
143. Ton, A. T., Gentile, F., Hsing, M., Ban, F. & Cherkasov, A. Rapid identification of potential inhibitors of SARS-CoV-2 main protease by deep docking of 1.3 billion compounds. *Mol. Inform.* **39**, e2000028 (2020).
144. Frye, L., Bhat, S., Akinsanya, K. & Abel, R. From computer-aided drug discovery to computer-driven drug discovery. *Drug Discov. Today Technol.* **39**, 111–117 (2021).
145. Wadman, M. FDA no longer needs to require animal tests before human drug trials. *Science*, <https://doi.org/10.1126/science.adg6264> (2023).
146. Stiefel, N. et al. FOCUS—development of a global communication and modeling platform for applied and computational medicinal chemists. *J. Chem. Inf. Model.* **55**, 896–908 (2015).
147. Schrodinger. LiveDesign. *Schrodinger* https://www.schrodinger.com/sites/default/files/general_ld_rgb_080119_forweb.pdf, (accessed 5 April 2023).
148. Müller, S. et al. Target 2035—update on the quest for a probe for every protein. *RSC Med. Chem.* **13**, 13–21 (2022).
149. Verdonk, M. L., Cole, J. C., Hartshorn, M. J., Murray, C. W. & Taylor, R. D. Improved protein–ligand docking using GOLD. *Proteins* **52**, 609–623 (2003).
150. Miller, E. B. et al. Reliable and accurate solution to the induced fit docking problem for protein–ligand binding. *J. Chem. Theory Comput.* **17**, 2630–2639 (2021).
151. Chemical space docking. *BioSolveIT* <https://www.biosolveit.de/application-academy/chemical-space-docking/> (2022).
152. Cavasotto, C. N. in *Quantum Mechanics in Drug Discovery* (ed. Heifetz, A.) 257–268 (Springer, 2020).
153. Dixon, S. L. et al. AutoQ SAR: an automated machine learning tool for best-practice quantitative structure–activity relationship modeling. *Future Med. Chem.* **8**, 1825–1839 (2016).
154. Totrov, M. Atomic property fields: generalized 3D pharmacophoric potential for automated ligand superposition, pharmacophore elucidation and 3D QSAR. *Chem. Biol. Drug Des.* **71**, 15–27 (2008).
155. Schaller, D. et al. Next generation 3D pharmacophore modeling. *WIREs Comput. Mol. Sci.* **10**, e1468 (2020).

156. Chakravarti, S. K. & Alla, S. R. M. Descriptor free QSAR modeling using deep learning with long short-term memory neural networks. *Front. Artif. Intell.* **2**, 17 (2019).
157. Deng, Z., Chuaqui, C. & Singh, J. Structural interaction fingerprint (SIF): a novel method for analyzing three-dimensional protein-ligand binding interactions. *J. Med. Chem.* **47**, 337–344 (2004).

Acknowledgements We thank A. Brooun, A. A. Sadybekov, S. Majumdar, M. M. Babu, Y. Moroz and V. Cherezov for helpful discussions.

Author contributions All authors contributed to the writing of the manuscript.

Competing interests The University of Southern California are in the process of applying for a patent application (no. 63159888) covering the V-SYNTHES method that lists V.K. as a co-inventor.

Additional information

Correspondence and requests for materials should be addressed to Vsevolod Katritch.

Peer review information *Nature* thanks Alexander Tropsha and the other, anonymous, reviewer(s) for their contribution to the peer review of this work.

Reprints and permissions information is available at <http://www.nature.com/reprints>.

Publisher's note Springer Nature remains neutral with regard to jurisdictional claims in published maps and institutional affiliations.

Springer Nature or its licensor (e.g. a society or other partner) holds exclusive rights to this article under a publishing agreement with the author(s) or other rightsholder(s); author self-archiving of the accepted manuscript version of this article is solely governed by the terms of such publishing agreement and applicable law.

© Springer Nature Limited 2023

Detecting Disruption of HER2 Membrane Protein Organization in Cell Membranes with Nanoscale Precision

Yasaman Moradi, Jerry S. H. Lee, and Andrea M. Armani*

Cite This: <https://doi.org/10.1021/acssensors.3c01437>

[Read Online](#)

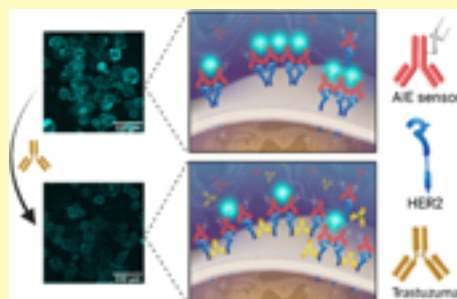
ACCESS |

[Metrics & More](#)

[Article Recommendations](#)

[Supporting Information](#)

ABSTRACT: The spatiotemporal organization of proteins within the cell membrane can affect numerous biological functions, including cell signaling, communication, and transportation. Deviations from normal spatial arrangements have been observed in various diseases, and a better understanding of this process is a key stepping stone to advancing development of clinical interventions. However, given the nanometer length scales involved, detecting these subtle changes has primarily relied on complex super-resolution and single-molecule imaging methods. In this work, we demonstrate an alternative fluorescent imaging strategy for detecting protein organization based on a material that exhibits a unique photophysical behavior known as aggregation-induced emission (AIE). Organic AIE molecules have an increase in emission signal when they are in close proximity, and the molecular motion is restricted. This property simultaneously addresses the high background noise and low detection signal that limit conventional widefield fluorescent imaging. To demonstrate the potential of this approach, the fluorescent molecule sensor is conjugated to a human epidermal growth factor receptor 2 (HER2)-specific antibody and used to investigate the spatiotemporal behavior of HER2 clustering in the membrane of HER2-overexpressing breast cancer cells. Notably, the disruption of HER2 clusters in response to an FDA-approved monoclonal antibody therapeutic (Trastuzumab) is successfully detected using a simple widefield fluorescent microscope. While the sensor demonstrated here is optimized for sensing HER2 clustering, it is an easily adaptable platform. Moreover, given the compatibility with widefield imaging, the system has the potential to be used with high-throughput imaging techniques, accelerating investigations into membrane protein spatiotemporal organization.



KEYWORDS: aggregation-induced emission, fluorescent sensor, imaging, microscopy, transmembrane proteins

Transmembrane proteins play a critical role in governing fundamental cell processes, such as cell signaling and cell division. However, in many cases, it is not simply the presence or absence of a given protein but its spatiotemporal organization within the membrane that modulates biological processes.^{1,2} Therefore, the ability to decipher these dynamic interactions is key to unraveling how they mediate the cellular signal transductions, which play a role in a range of health conditions.

At a fundamental science level, several methods exist for measuring the spatial organization of membrane receptors, including electron microscopy,^{3,4} optical and fluorescence microscopy-based techniques,^{5–10} and proximity-based assays.^{11–13} Among these, electron microscopy provides the highest resolution. However, because it is not compatible with live cells, it can only provide static snapshots of dynamic processes that do not fully capture the behavior of receptors in the membrane. Alternatively, super-resolution imaging technologies can be used. However, these are not conducive to high-throughput sample analysis methods and rely on extremely specialized instrumentation.¹⁴ Given the complexity of these interactions, the ability to acquire large data sets and

perform a high-dimensional analysis is key to unraveling the underlying biological control mechanisms.

To overcome these challenges requires rethinking our approach to imaging. One strategy is to develop new types of fluorescent probes that can serve as proximity sensors and operate in a high-throughput system, and one promising material system is based on organic molecules that exhibit aggregation-induced emission (AIE) behavior.

Aggregation-induced emission (AIE) describes a photophysical property in which the fluorescent intensity of a fluorophore aggregate is higher than when the molecule is well dispersed in solution.¹⁵ This behavior is attributed to a restriction of the intramolecular rotations, which increases the emissivity of the molecule.^{16,17} In contrast, most commercially

Received: July 13, 2023

Revised: October 25, 2023

Accepted: October 30, 2023

available fluorescent compounds exhibit the opposite behavior due to strong π - π interactions, and their emission is reduced or completely quenched when they aggregate in the solid state or are in high-concentration solutions.^{17,18} To date, AIE molecules have been used for biomolecule sensing in solution,^{19–22} bioimaging,^{23–28} monitoring protein folding/unfolding processes in cells,²⁹ and sensing the interaction of proteins in solution.^{30–32} Therefore, a material exhibiting an AIE response has the potential of being utilized for studying the spatial arrangement of membrane receptors on the nanometer length scale using conventional fluorescent microscopy.

In this work, we develop a fluorophore based on tetraphenylethylene (TPE), an AIE molecule, for studying the clustering behavior of HER2 in HER2-overexpressing breast cancer cells and investigate the response of the HER2 cluster to a therapeutic. HER2 is involved in the regulation of several signaling pathways that lead to an increase in cell proliferation in several types of cancer.^{33,34} Because HER2 is known to localize in clusters on the membrane,^{3,35,36} one therapeutic strategy is the disruption of this organization.^{37,38} To study this dynamic nanoscale process, the TPE-based probe is conjugated to an antibody specific to the extracellular domain of HER2. As shown in Figure 1a, when the HER2 proteins are separated, the developed fluorophore sensor is not emissive. However, when the concentration of HER2 increases and clusters form, the molecule undergoes a fluorescent turn-on process due to the AIE behavior of the TPE (Figure 1b). Because only HER2 molecules in close proximity initiate the turn-on process, this approach overcomes many of the previous

limitations by providing a method to detect HER2 clustering and simultaneously reducing background noise. Furthermore, since AIE is a reversible process, the dynamic interactions of HER2 proteins in response to external stimuli, such as therapeutics, can be studied.

EXPERIMENTAL SECTION

The detailed information on the chemicals and reagents, instrumentation, synthesis, bioconjugation, and characterization results of the intermediates and final molecule as well as the validation of the cell lines are presented in the Supporting Information.

Synthesis and Characterization of the AIE Sensor. The synthetic details and NMR spectra confirming the synthesis of TPE-NHS are included in the SI. Post synthesis, the absorption and emission spectra of TPE-NHS were characterized in distilled water, DMSO, and DMEM cell media. Furthermore, the AIE response of TPE-NHS molecule was confirmed. Lastly, the potential for Trastuzumab to directly interact with TPE-NHS was studied. All details and results are listed in SI.

To develop the AIE sensor, the TPE-NHS molecule was conjugated to HER2-specific antibody through a micelle-mediated bioconjugation reaction that leveraged the intrinsic lysine residues of the HER2-specific antibody. The details of the bioconjugation reaction, purification of free TPE-NHS using a gel spin column, conjugation confirmation, and optical characterization methods are included in the SI.

Direct Immunofluorescent Imaging. SKBR3 cells (ATCC, HTB-30) and MCF7 cells (ATCC, HTB-22) were seeded at the density of 7,000 cells per well in a 96-well glass-bottom plate (Cellvis, P96-0-N) and incubated for 3 days before running the assay to reach the approximate confluency of 70%. After 3 days, the medium was removed, and the cells were fixed using 4% Paraformaldehyde (Alfa Aesar, J62478), washed 3 times (5 min each), and blocked using 2% BSA blocking buffer (Thermo Scientific 37525) for 1 h. The antibody dye conjugates (Fluorescein-HER2 Ab as the positive control and different TPE-HER2 Ab conjugates) were diluted to the concentration of 10 $\mu\text{g}/\text{mL}$ in 0.1% BSA solution, added to the fixed SKBR3 and MCF7 cells, and left at 4 $^{\circ}\text{C}$ overnight. The samples were washed with 1 \times PBS 2 times and imaged on a Zeiss Axio Observer connected to an X-cite Series 120Q light source using the excitation and emission filters of interest using a 20 \times objective. The TPE filter cube has an excitation of G365, BS of 395, and emission BP of 535/30. The Fluorescein filter cube has an excitation BP of 500/25, BS of 515, and emission BP of 535/30.

Colocalization Immunofluorescent Imaging. SKBR3 cells were seeded at the density of 7,000 cells per well in a 96-well glass-bottom plate (Cellvis, P96-0-N) and incubated for 3 days before running the assay to reach the approximate confluency of 70%. After 3 days, the media was removed, and the cells were fixed using 4% paraformaldehyde (Alfa Aesar, J62478), washed 3 times (5 min each), and blocked using 2% BSA blocking buffer (Thermo Scientific 37525) for 1 h. Then, a staining solution consisting of 20 $\mu\text{g}/\text{mL}$ TPE-HER2 Ab and 20 $\mu\text{g}/\text{mL}$ Texas Red-HER2 Ab (Invitrogen, T20175) in 0.1% BSA was added to the cells. After overnight staining at 4 $^{\circ}\text{C}$, fixed SKBR3 cells were washed and imaged in the bright-field channel, TPE channel (filter cube with the excitation of G365, BS of 395, and emission BP of 535/30), and Texas Red channel (filter cube with the excitation BP of 550/25, BS of 570, and emission BP of 605/70) on Zeiss Axio Observer widefield fluorescent microscope using a 20 \times objective.

Analysis of the Impact of Trastuzumab on HER2 Clusters. SKBR3 cells (ATCC, HTB-30) were seeded at the density of 7000 cells per well in a 96-well glass-bottom plate (Cellvis, P96-0-N) and incubated for 3 days. After reaching the ideal cell confluency on day 3, different concentrations of Trastuzumab (Selleckchem, A2007) in McCoy media (from 0 to 100 $\mu\text{g}/\text{mL}$) were prepared by serial dilution. The old cell media was replaced with the Trastuzumab media and incubated for 2, 8, and 24 h. Then, cells were fixed and washed by following the direct immunofluorescent protocol. TPE-

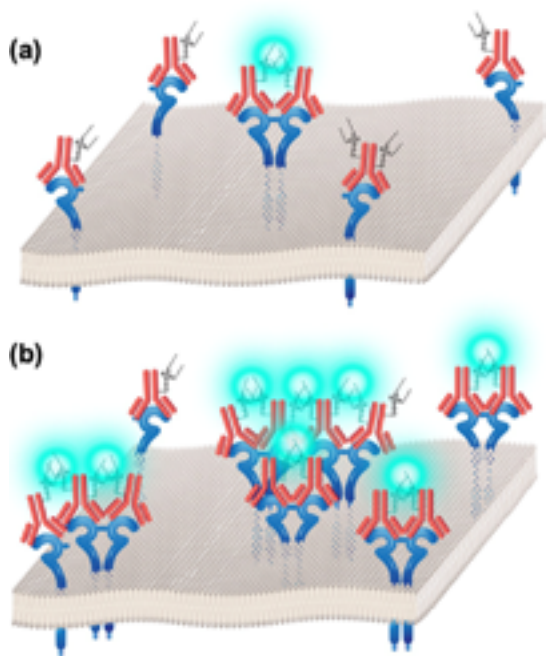


Figure 1. Schematic of AIE sensor for localized detection and visualization of HER2 clusters or HER2s that are localized in each other's proximity on (a) HER2-negative (low HER2 expression) and (b) HER2-positive (overexpressing) cell surfaces.

HER2 Ab and Fluorescein-HER2 Ab at concentrations of 10 $\mu\text{g}/\text{mL}$ in 0.1% BSA solution were added to the fixed cells and left at 4 $^{\circ}\text{C}$ overnight. The samples were washed with 1 \times PBS 2 times and imaged on a Zeiss Axio Observer using a 20 \times objective. The TPE filter cube with excitation of G365, BS of 395, and emission BP of 535/30 and the Fluorescein filter cube with excitation BP of 500/25, BS of 515, and emission BP of 535/30 were used. The imaging parameters were held constant for all of the wells, allowing this value to be used for comparison across conditions. Postimaging, the data was analyzed based on the description in the Image Analysis section.

Image Analysis. An in-house developed image analysis tool that is available on GitHub was used to track the fluctuations in the fluorescent signal post treatment. The image analysis tool uses an edge detection algorithm to define the region of interest (ROI), which is the cell area. Then, the defined mask was applied to the fluorescent image. Summation of the pixel values of the masked region and the total masked area (number of pixels) was extracted from each fluorescent image. Dividing the summation of the pixel values by the masked area, a value representing the average fluorescent intensity per fluorescent image was calculated. A detailed description of the image analysis platform is included in the SI.

RESULTS AND DISCUSSION

Design Rationale of the AIE Molecule. The primary design criteria for the fluorescent sensor are to maintain high biological specificity while achieving nanoscale spatial sensitivity. One common strategy to endow specificity to a fluorescent probe is to conjugate the molecule directly to the amine groups that are located on the Fc-region of the antibody.³⁹ In this work, the TPE-based molecule was functionalized with *N*-hydroxy succinimide (NHS) ester, which subsequently bound to a monoclonal antibody specific to HER2.^{39,40} In addition, a pair of hydrocarbon chains were added to increase the probability of intermolecular restriction as the HER2 proteins cluster.

The length of the TPE-NHS was modeled using density functional theory (QChem). This value sets the minimum and maximum interaction distances between a pair of TPE molecules that could give rise to the AIE response. Based on the results, detection of TPE-NHS is in the range of 2–6 nm (Figure 2). Additional details on the modeling are presented in the SI (Figure S1).

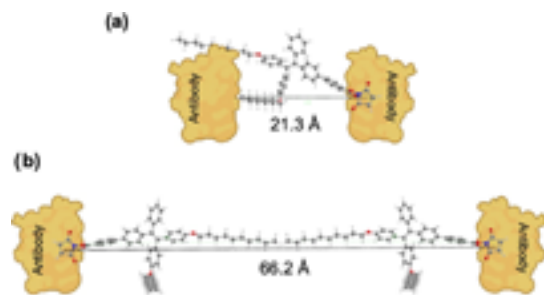


Figure 2. Distance of the NHS ester portion of TPE-NHS from the end of the hydrocarbon chains in the ground state can determine the detection range of the AIE sensor. The TPE-bound antibodies binding to HER2 protein can detect (a) a minimum distance of 21.3 Å upon interaction of the TPE-NHS molecule from the shorter side with the surface of a nearby HER2-bound antibody and (b) the maximum distance of 66.2 Å upon interaction of two molecules from their longest length.

Synthesis and Characterization of the AIE Molecule.

The synthesis process of TPE-NHS molecule is shown in Scheme 1a,^{41–43} and the different chemical groups of TPE-NHS are color-coded to highlight their role in the molecule's operation. The intermediate and final structures were confirmed with NMR (Figures S2–S9).

The spectral properties (absorption and emission) of TPE-NHS were characterized over a range of solvents with different polarities. According to the results in Figure S10, TPE-NHS demonstrates slight solvatochromic shifts in the absorbance and more significant shifts in the emission spectrum in DMSO, distilled water, and DMEM cell media. Previous work has shown that solvatochromism in organic molecules can be attributed to the stabilization of the electronic excited state of the molecule by the polar solvent, and this response is largely attributed to the hydrogen bonding abilities of the specific solvent.⁴⁴ However, other solvent properties can also play a role. The observed results align with prior studies of solvatochromism in AIE molecules.^{45–47}

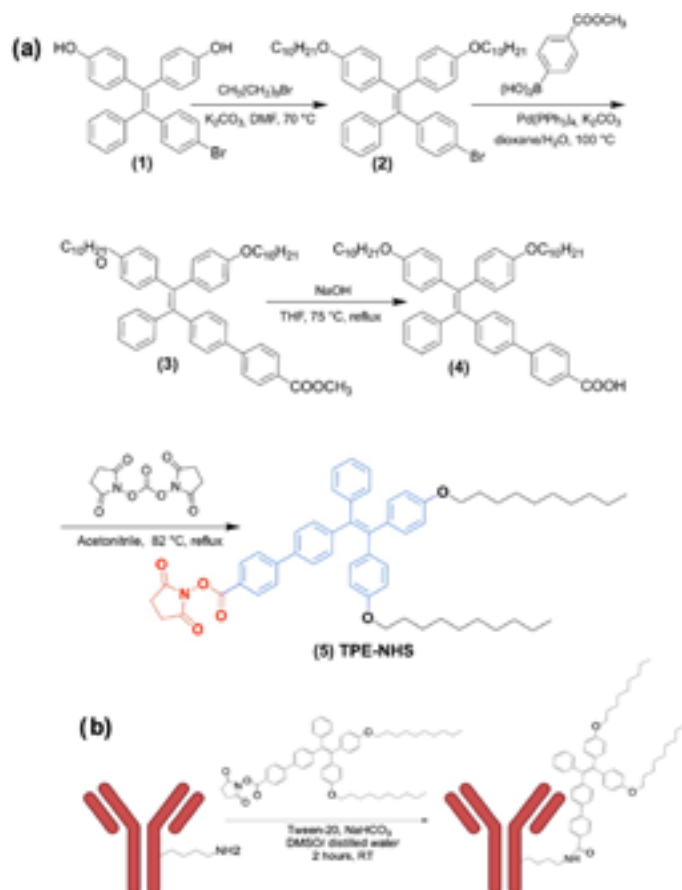
Solubility testing confirmed that the amphiphilic TPE-NHS is soluble in mildly polar dimethyl sulfoxide (DMSO), which has a relative polarity of 0.44.⁴⁸ The AIE response of TPE-NHS was confirmed by using two approaches. First, increasing the concentration of the molecule in the 99 (v/v) % solution of distilled water/DMSO results in the initiation of aggregation-induced fluorescence at concentrations above 10 μM (Figure S11a). Second, by increasing the relative volume ratio of distilled water/DMSO, the TPE-NHS begins aggregating, and the fluorescent emission in the system increases (Figure S11b).

The proposed application of this sensor is detecting the effect of Trastuzumab on HER2 clustering using the AIE response of TPE. Therefore, it is important to ensure that Trastuzumab does not directly interact with the fluorescent behavior of the TPE. A series of experiments were performed using the same range of Trastuzumab concentrations as in the cell line studies. No effect on the AIE response was observed (Figure S12). Additional details are in the SI.

AIE Sensor Development and Characterization. To endow specificity to the TPE-NHS dye, we conjugated it to an antibody specific to the extracellular domain of the HER2. This conjugation process relied on NHS ester bonding with the amines that are part of the lysine residue, forming an amide bond with the HER2 antibody. Due to the potential of antibodies to denature and lose biological specificity, the NHS ester-amine conjugation chemistry is performed in aqueous solutions (Scheme 1b, Figure S13). To reduce the formation of aggregates and increase the bioconjugation yield, a micelle-mediated conjugation process using Tween 20 was performed.⁴⁹ To optimize the Tween 20 concentration in the reaction solution, a series of TPE-NHS/HER2 antibody conjugation reactions using a range of Tween 20 concentrations were performed. Based on the results from the optimization study (Figure S14), 0.025 (v/v) % of Tween 20 was used in the antibody bioconjugation process.

To confirm the conjugation of TPE-NHS with the HER2 antibody, MALDI mass spectrometry was used. Results presented in Figure S15 show a simultaneous shift and broadening of the peak after the antibody conjugation process is performed. The software reported a 1.015 kDa shift in the m/z values of the HER2 antibody and TPE-HER2 Ab (TPE-NHS conjugated to HER2 Antibody) spectrum. Considering the fact that the expected molecular weight of each TPE-NHS post conjugation is 749 g/mol, this result demonstrates the

Scheme 1. (a) Schematic of Synthesis of TPE-NHS (compound 5); the Three Key Components of TPE-NHS Are Indicated in Red (NHS Ester), Blue (AIE Group), and Black (Alkane Chain) and (b) Schematic of the AIE Sensor Development by Conjugation of TPE-NHS to the Lysin Residue of the Antibody



conjugation of TPE to the HER2 antibody with an estimated average dye to antibody ratio of 1.35. Furthermore, a complementary SDS-PAGE assay further confirmed the formation of the TPE-HER2 Ab (Figure S16).

After conjugation, the optical absorption and emission wavelengths of the developed AIE sensor were characterized in $1\times$ PBS. The absorption maximum of the conjugated molecule is 354 nm, and the emission wavelength is centered at 518 nm (Figure S17), which indicates a clear Stokes shift of 164 nm. Importantly, these results confirm that the fluorescent behavior of the dye has not been significantly altered by the bioconjugation process.

Evaluation of the AIE Sensitivity, Cytotoxicity, and HER2 Target Specificity of the AIE Sensor (TPE-HER2 Ab). The aggregation-induced emission behavior of TPE-HER2 Ab was analyzed by measuring the emission over a range of sample concentrations in $1\times$ PBS (Figures 3a and S18). Results in Figure 3b show an increasing trend in the fluorescent emission intensity at concentrations above 0.04 mg/mL, which confirms that the expected AIE behavior of the AIE probe is maintained after antibody conjugation.

Before applying TPE-HER2 Ab in cell imaging applications, the cytotoxicity of the TPE-NHS probe was evaluated on two different breast cancer cell lines, SKBR3 and MCF7, using concentrations up to $50\ \mu\text{M}$. SKBR3 overexpresses HER2, and MCF7 is a HER2- low expressing cell line.⁵⁰ The HER2 expression levels of these cell lines were confirmed using indirect immunofluorescent staining and Western blotting (Figure S19). Based on the CellTiter-Glo (CTG) assay results, no significant impact on cell viability was observed over the entire range of TPE-NHS concentrations studied as compared to the positive and negative controls (Figure S20). This observation confirms the low cytotoxicity of the compound and its potential applicability in live cell imaging studies.

In order for the TPE-HER2 Ab to accurately monitor the HER2 clustering process, it must selectively bind to HER2. The specificity of the TPE-HER2 Ab is evaluated by performing a colocalization, competition fluorescent imaging measurement using the SKBR3 cell line. Texas Red was selected as the second fluorophore because the excitation (emission) wavelengths of Texas Red do not overlap with the excitation (emission) wavelengths of TPE, allowing for colocalization to be easily determined by merging the

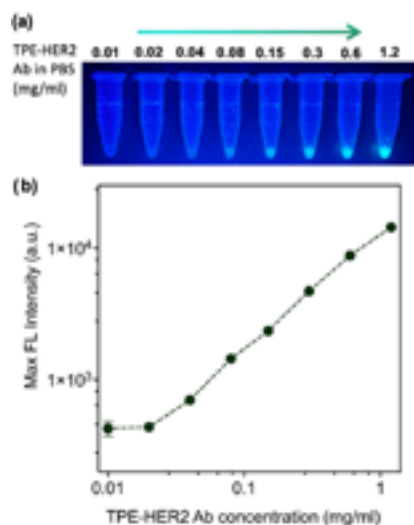


Figure 3. Fluorescent Behavior of TPE-HER2 Ab. (a) Optical images of different concentrations of TPE-HER2 Ab in 1× PBS excited by a 365 nm UV lamp. (b) Maximum FL intensity at each concentration of TPE-HER2 Ab in 1× PBS plotted against the concentration of TPE-HER2 Ab in each sample. In some cases, the error bars are not visible because they are smaller than the symbols.

fluorescent images (Figure S22). Both fluorophores were conjugated to the same type of HER2 antibody, removing the variability of the antibody binding site and affinity from the measurement. An identical series of colocalization imaging measurements is performed using Fluorescein in place of the TPE.

Bright-field and fluorescent images of the HER2-overexpressing SKBR3 cells labeled with Texas Red-HER2 Ab and TPE-HER2 Ab are shown in Figure 4a–c. The emission signal from each fluorophore is easily observable. One approach to quantify the signal quality is the signal-to-noise ratio (SNR). According to basic signal processing theory, an SNR above 1 is considered detectable. For the present images, the SNR of TPE and Texas Red are 10.23 ± 0.50 and 20.66 ± 2.22 , respectively. Therefore, both fluorophores provide robust detection signals. The details of the SNR calculation are included in the SI.

When the Texas Red and TPE fluorescent images are merged (Figure 4d), the colocalization of the TPE and the Texas Red is qualitatively evident. The same colocalization experiment using Fluorescein-HER2 Ab and Texas Red-HER2 Ab was also performed as a control measurement, and similar results were obtained (Figure S23).

To quantitatively analyze colocalization, the photon intensities in the Texas Red and the TPE channels are spatially correlated (Figure 4e). This analysis is also performed for the previously discussed Fluorescein control measurement (Figure 4f). Furthermore, the Pearson correlation coefficient (PCC) of the TPE/Texas Red-HER2 Ab and the Fluorescein/Texas Red-HER2 Ab were calculated.⁵¹ Across multiple images, the PCC values of the TPE/Texas Red and the Fluorescein/Texas Red channels were calculated to be 0.74 ± 0.06 and 0.65 ± 0.03 , respectively (Figure S24). Therefore, the TPE-HER2 Ab was able to specifically target HER2 on SKBR3

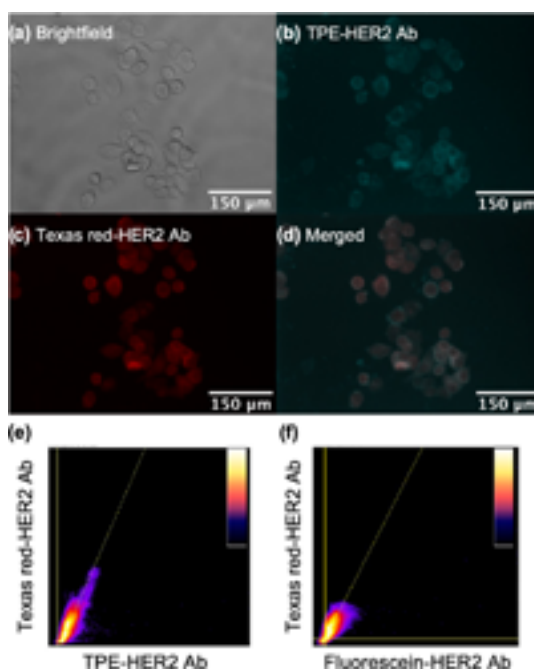


Figure 4. Colocalization competition analysis of TPE-HER2 Ab and Texas Red-HER2 Ab in SKBR3 (HER2-overexpressing) cells. Images of SKBR3 cells stained with 20 $\mu\text{g}/\text{mL}$ of TPE-HER2 Ab and 20 $\mu\text{g}/\text{mL}$ of Texas Red-HER2 Ab are shown in (a) bright-field channel, (b) TPE fluorescent channel, (c) Texas Red fluorescent channel, and (d) merged channel of TPE and Texas Red fluorescent channels. 2D intensity histogram of (e) TPE: Texas Red channels and (f) Fluorescein: Texas Red channels were used for photon intensity correlation analysis.

cells, setting the stage for HER2 cluster detection and analysis using this AIE-based imaging probe.

AIE Sensor (TPE-HER2 Ab) for Detection of HER2 Clustering in Cancer Cells. The TPE-HER2 Ab imaging agent was used to detect HER2-HER2 interactions and HER2 clustering in two different breast cancer cell lines (SKBR3 and MCF7).

One challenge with antibody-based assays is batch-to-batch variations in the antibody reactivity. To remove this variable and potential measurement confound, all measurements were performed with the same antibody lot.⁵² As shown in Figure 5a–c, the fluorescent emission signal from the TPE in the HER2-overexpressing SKBR3 cells was clearly identifiable with an SNR of 9.67 ± 1.48 . This signal is directly related to the AIE fluorescence mechanism of the TPE moiety. Namely, as the HER2 clusters form, the TPE molecular motion becomes restricted and the fluorescent intensity increases. In contrast, in the HER2-low expressing MCF7 cells, the fluorescent signal is barely detectable, with an SNR of 6.13 ± 0.76 . (Figure 5d–f). This difference is due to a lack of HER2 clustering as well as a low HER2 concentration, and it is in agreement with the cell line validation assays.

Taken together, these observations in the SKBR3 and MCF7 cell lines confirm the ability of the TPE-HER2 Ab imaging agent to selectively target HER2 in cells and to detect HER2 clusters in the cell membrane. These findings set the stage for

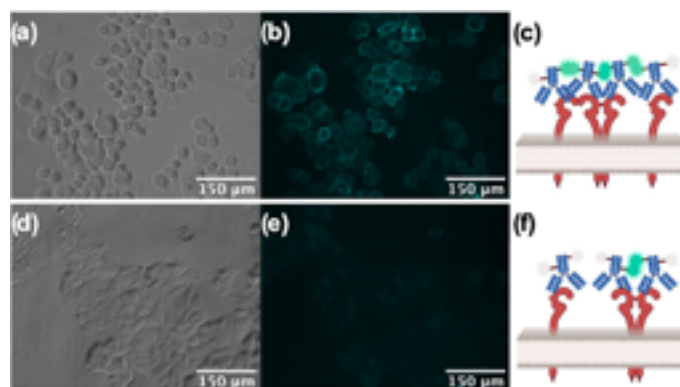


Figure 5. Bright-field and fluorescent images of (a, b) SKBR3 (HER2 overexpressing) and (d, e) MCF7 (HER2-low expressing) cells stained with 10 μg/mL of TPE-HER2 Ab along with the illustration of the TPE-mediated fluorescent turn-on process on the surface of (c) SKBR3 and (f) MCF7 cells.

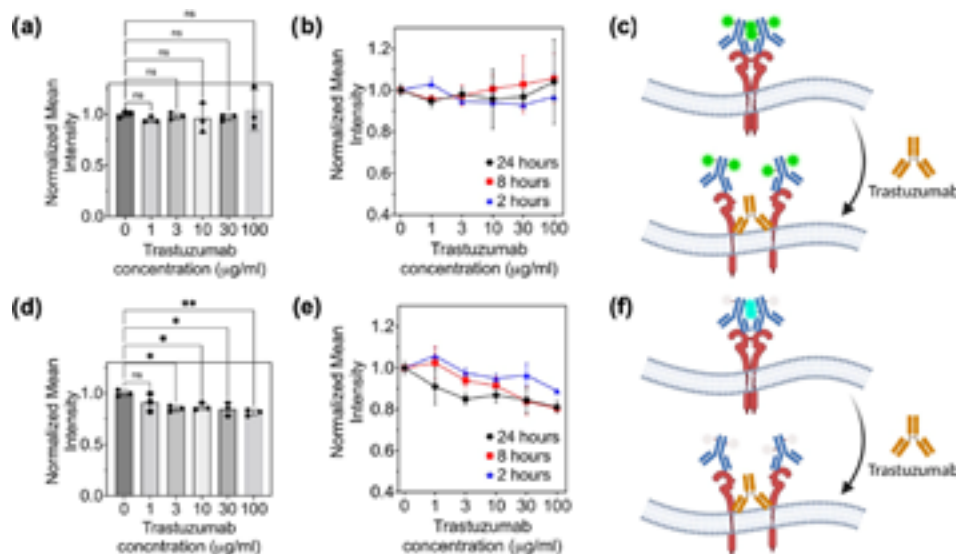


Figure 6. Normalized mean fluorescent intensity of SKBR3 cells stained with (a, b) 10 μg/mL Fluorescein-HER2 Ab and (d, e) 10 μg/mL TPE-HER2 Ab after treatment with a range of concentrations of Trastuzumab (0 μg/mL to 100 μg/mL) for (a, d) 24 h and (b, e) different time intervals of 2, 8, and 24 h all in one plot. The data is collected in triplicate, and on average, each data point consists of 30 SKBR3 cells. (* $p < 0.05$ and ** $p < 0.01$). Schematic of HER2-overexpressing SKBR3 cell membrane indicating the fluorescent response of (c) Fluorescein-HER2 Ab and (f) TPE-HER2 Ab stained HER2 proteins after Trastuzumab treatment.

monitoring the dynamic process of HER2 cluster formation and disruption.

AIE Sensor for Analyzing the Impact of Cancer Cell Therapeutic Treatment on HER2 Clusters.

Trastuzumab (Herceptin) is a humanized monoclonal antibody that has been approved by the Food and Drug Administration (FDA) for patients with HER2-positive invasive breast cancer.⁵³ This therapeutic is a HER2-specific antibody that binds the juxtamembrane portion of the HER2 extracellular domain.^{54,55} Several mechanisms of action have been proposed, including prevention of HER2-receptor dimerization.^{54,56,57} However, it is not clear if dimerization inhibition alone is sufficient to achieve the therapeutic results that are observed.^{54,58} Another hypothesis is that changing the biophysical pattern and

distribution of HER2 clusters on the cell membrane gives rise to the observed effect.^{55,59} The TPE-HER2 Ab imaging agent developed here is uniquely suited to provide insight into this scientific question.

SKBR3 cells were seeded in a 96-well plate in triplicate and were treated with Trastuzumab concentrations ranging from 0 to 100 μg/mL for 2, 8, and 24 h. The concentration and time ranges were based on prior Trastuzumab studies.^{59–61} Subsequently, the TPE-HER2 Ab imaging agent was added to the plates following the developed direct immunofluorescence staining protocol. In parallel, the Fluorescein-HER2 Ab was used as a control. Fluorescent imaging was performed using a widefield fluorescent microscope with a 20× objective, and the images were analyzed and quantified using an in-house

developed computational method. Details are included in the SI (Figure S25).

In the assay using Fluorescein-HER2 Ab, the average fluorescent intensity does not noticeably change in any of the Trastuzumab incubation times or concentrations used (Figures 6a–c and S26). Specifically, the SNR varies from 15.90 ± 0.90 to 15.74 ± 1.80 over the course of the 24 h imaging measurement, which is within the error of the SNR values. Therefore, even with a robust SNR value, there is no detectable change. Because Fluorescein-HER2 Ab is not sensitive to the proximity of the receptors, this result indicates that the HER2 expression is constant, and the absolute concentration of HER2 in the cell membrane is not changed. This result is expected. However, it does not provide insight into the mechanism of action of Trastuzumab and its impact on the HER2 clustering process.

In contrast, by monitoring the fluorescence intensity, TPE-HER2 Ab provides information about the HER2 clustering behavior. With 2 and 8 h of Trastuzumab treatment, a decrease in cluster formation is observed only at the highest concentrations (Figures 6e and S26). However, with 24 h of treatment, the clustering process is reduced with all concentrations above $1 \mu\text{g/mL}$ studied in this work (Figure 6d–e). In comparing the SNR values over the course of the 24 h imaging measurement, the SNR changes from 11.85 ± 0.55 to 10.73 ± 0.57 .

This response to Trastuzumab is in agreement with prior studies exploring the impact of Trastuzumab on HER2 clusters in HER2-overexpressing cells.⁵⁸ This result reveals that the decreasing fluorescent trend is due to the interaction between Trastuzumab and the HER2 clusters. These findings confirm the capability of our AIE sensor (TPE-HER2 Ab) for the detection and visualization of HER2 clustering dynamics upon exposure to an external stimulus like therapeutics.

CONCLUSIONS

In summary, we developed a targeted imaging agent based on the combination of an AIE fluorophore with a monoclonal antibody and used it to monitor the clustering process of HER2 in response to a HER2-targeting therapeutic (Trastuzumab). The TPE-HER2 Ab conjugate system is specific to the target and can visualize the HER2 clustering process in HER2-overexpressing cells.⁶² Furthermore, using the developed fluorescent probe, the impact of Trastuzumab on the proximity of HER2 in the SKBR3 cells can be readily visualized and determined. The results demonstrate an easily generalizable method for studying the distribution and nanoscale localization of membrane-bound proteins. Given the target specificity of TPE-HER2 Ab and biocompatibility of TPE-NHS, this AIE sensor has the potential of being optimized for studying the dynamics of HER2 clusterization in live cells. Furthermore, while the focus of this work is on using HER2 antibodies, by shifting to peptide or similar engineered targeting moieties, quantification of the signal could be possible. This additional capability could lead to applications in developing improved therapeutics or in understanding membrane dynamics.^{63,64}

ASSOCIATED CONTENT

Supporting Information

The Supporting Information is available free of charge at <https://pubs.acs.org/doi/10.1021/acssensors.3c01437>.

DFT modeling of TPE-NHS, detailed synthesis procedures and characterization, UV–vis absorption and fluorescence spectra of TPE-NHS, effect of Trastuzumab on TPE-NHS emission, bioconjugation optimization imaging, MALDI and SDS-PAGE bioconjugation characterization, UV–vis absorption and fluorescence spectra of TPE-HER2 Ab, cell culture procedures, cell line validation through immunofluorescent imaging and Western blot, cell viability assay, SNR calculation protocol description, control multi-channel fluorescent imaging, control colocalization assay, Pearson correlation coefficient data, detailed image analysis protocol description, and data for the AIE-based trastuzumab treatment assay (PDF)

AUTHOR INFORMATION

Corresponding Author

Andrea M. Armani – Mork Family Department of Chemical Engineering and Materials Science, University of Southern California, Los Angeles, California 90089, United States; Ellison Institute of Technology, Los Angeles, California 90064, United States; orcid.org/0000-0001-9890-5104; Email: armani@usc.edu

Authors

Yasaman Moradi – Mork Family Department of Chemical Engineering and Materials Science, University of Southern California, Los Angeles, California 90089, United States; Ellison Institute of Technology, Los Angeles, California 90064, United States; orcid.org/0009-0001-1616-7513

Jerry S. H. Lee – Mork Family Department of Chemical Engineering and Materials Science, University of Southern California, Los Angeles, California 90089, United States; Ellison Institute of Technology, Los Angeles, California 90064, United States; Keck School of Medicine, University of Southern California, Los Angeles, California 90089, United States; orcid.org/0000-0003-1515-0952

Complete contact information is available at: <https://pubs.acs.org/doi/10.1021/acssensors.3c01437>

Author Contributions

A.M.A. and Y.M. were responsible for experimental design and data analysis. Y.M. performed the experiments. A.M.A., J.S.H.L., and Y.M. wrote and revised the manuscript. A.M.A. and J.S.H.L. supervised the project. All coauthors have given approval to the final version of the manuscript.

Funding

This work was supported by the Office of Naval Research (N00014-22-1-2466, N00014-21-1-2044), Uniformed Services University of the Health Sciences (USUHS) award from the Defense Health Program to the Murtha Cancer Center Research Program administered by the Henry M. Jackson Foundation for the Advancement of Military Medicine (HU00011820032), and the Ellison Institute of Technology. Disclaimer: The contents of this publication are the sole responsibility of the authors and do not necessarily reflect the views, opinions, or policies of the USUHS, the Henry M. Jackson Foundation for Advancement of Military Medicine, Inc., the Department of Defense, the Department of the Army, Navy, or Air Force. Mention of trade names, commercial products, or organization does not imply endorsement by the U.S. Government.

Notes

The authors declare the following competing financial interest(s): J.S.H.L. serves as Chief Science and Innovation Officer for Ellison Institute, LLC (paid); board of trustee for Health and Environmental Institute, Inc. (unpaid, travel support); and scientific advisory board for AtlasXomics, Inc., and ATOM, Inc. (unpaid, travel support). A.M.A. serves as the Senior Director of Engineering and Physics for Ellison Institute, LLC (paid).

ACKNOWLEDGMENTS

The authors would like to thank Soheil Soltani for development of the image analysis MATLAB code, Yingmu Zhang for assisting with chemical design, Jonathan Katz for assisting with mass spectroscopy experimental design, the Multiomics Mass Spectrometry Core (MMSC) at USC School of Pharmacy for MALDI data acquisition, and Kian Kani and Carolina Garri for assisting with bioassay designs.

ABBREVIATIONS

AIE, aggregation-induced emission; TPE, tetraphenylethylene; HER2, human epidermal growth factor receptor 2; DMSO, dimethyl sulfoxide; DMEM, Dulbecco's modified Eagle's medium; BSA, bovine serum albumin; Ab, antibody; PBS, phosphate-buffered saline; BP, band-pass; NMR, nuclear magnetic resonance; MALDI, matrix-assisted laser desorption/ionization; SDS-PAGE, sodium dodecyl-sulfate polyacrylamide gel electrophoresis; CTG, CellTiter-Glo; SNR, signal-to-noise ratio; PCC, Pearson correlation coefficient; FDA, Food and Drug Administration

REFERENCES

- Bethani, I.; Skånland, S. S.; Dikic, I.; Acker-Palmer, A. Spatial Organization of Transmembrane Receptor Signalling. *EMBO J.* **2010**, *29* (16), 2677–2688.
- Buddingh, B. C.; Llopis-Lorente, A.; Abdelmohsen, L. K. E. A.; van Hest, J. C. M. Dynamic Spatial and Structural Organization in Artificial Cells Regulates Signal Processing by Protein Scaffolding. *Chem. Sci.* **2020**, *11* (47), 12829–12834.
- Peckys, D. B.; Korf, U.; De Jonge, N. Local Variations of HER2 Dimerization in Breast Cancer Cells Discovered by Correlative Fluorescence and Liquid Electron Microscopy. *Sci. Adv.* **2015**, *1* (6), No. e1500165.
- Parker, K.; Trampert, P.; Tinnemann, V.; Peckys, D.; Dahmen, T.; de Jonge, N. Linear Chains of HER2 Receptors Found in the Plasma Membrane Using Liquid-Phase Electron Microscopy. *Biophys. J.* **2018**, *115* (3), 503–513.
- Dorsch, S.; Klotz, K. N.; Engelhardt, S.; Lohse, M. J.; Bünnemann, M. Analysis of Receptor Oligomerization by FRAP Microscopy. *Nat. Methods* **2009**, *6* (3), 225–230.
- Nagy, P.; Jenei, A.; Kirsch, A. K.; Szöllosi, J.; Damjanovich, S.; Jovin, T. M. Activation-Dependent Clustering of the ErbB2 Receptor Tyrosine Kinase Detected by Scanning near-Field Optical Microscopy. *J. Cell Sci.* **1999**, *112* (11), 1733–1741.
- Petersen, N. O.; Brown, C.; Kaminski, A.; Rocheleau, J.; Srivastava, M.; Wiseman, P. Analysis of Membrane Protein Cluster Densities and Sizes in Situ by Image Correlation Spectroscopy. *Faraday Discuss.* **1999**, *111* (111), 289–305.
- Stoneman, M. R.; Raicu, V. Fluorescence-Based Detection of Proteins and Their Interactions in Live Cells. *J. Phys. Chem. B* **2023**, *127* (21), 4708–4721.
- Pan, Y.; Lu, S.; Lei, L.; Lamberto, I.; Wang, Y.; B Pasquale, E.; Wang, Y. Genetically Encoded FRET Biosensor for Visualizing EphA4 Activity in Different Compartments of the Plasma Membrane. *ACS Sens* **2019**, *4* (2), 294–300.
- Bousmah, Y.; Valenta, H.; Bertolin, G.; Singh, U.; Nicolas, V.; Pasquier, H.; Tramier, M.; Merola, F.; Erard, M. TdLanYFP, a Yellow, Bright, Photostable, and PH-Insensitive Fluorescent Protein for Live-Cell Imaging and Förster Resonance Energy Transfer-Based Sensing Strategies. *ACS Sens* **2021**, *6* (11), 3940–3947.
- Ang, Y. S.; Li, J. J.; Chua, P. J.; Ng, C. T.; Bay, B. H.; Yung, L. Y. L. Localized Visualization and Autonomous Detection of Cell Surface Receptor Clusters Using DNA Proximity Circuit. *Anal. Chem.* **2018**, *90* (10), 6193–6198.
- Söderberg, O.; Gullberg, M.; Jarvius, M.; Ridderstråle, K.; Leuchowius, K.-J.; Jarvius, J.; Wester, K.; Hydbring, P.; Bahram, F.; Larsson, L.-G.; Landegren, U. Direct Observation of Individual Endogenous Protein Complexes in Situ by Proximity Ligation. *Nat. Methods* **2006**, *3* (12), 995–1000.
- Weibrecht, I.; Leuchowius, K.-J.; Clausson, C.-M.; Conze, T.; Jarvius, M.; Howell, W. M.; Kamali-Moghaddam, M.; Söderberg, O. Proximity Ligation Assays: A Recent Addition to the Proteomics Toolbox. *Expert Rev. Proteomics* **2010**, *7* (3), 401–409.
- Dhiman, S.; Anian, T.; Gonzalez, B. S.; Tholen, M. M. E.; Wang, Y.; Albertazzi, L. Can Super-Resolution Microscopy Become a Standard Characterization Technique for Materials Chemistry? *Chem. Sci.* **2022**, *13* (8), 2152–2166.
- Luo, J.; Xie, Z.; Xie, Z.; Lam, J. W. Y.; Cheng, L.; Chen, H.; Hoi Sing Kwok, S. K.; Kwok, H. S.; Zhan, X.; Liu, Y.; Ben Zhong Tang, Z. T.; Tang, B. Z. Aggregation-Induced Emission of 1-Methyl-1,2,3,4,5-Pentaphenylsilole. *Chem. Commun.* **2001**, *18* (18), 1740–1741.
- Suzuki, S.; Sasaki, S.; Sairi, A. S.; Iwai, R.; Tang, B. Z.; Konishi, G. Principles of Aggregation-Induced Emission: Design of Deactivation Pathways for Advanced AIEgens and Applications. *Angew. Chem., Int. Ed.* **2020**, *59* (25), 9856–9867.
- Hong, Y.; Lam, J. W. Y.; Tang, B. Z. Aggregation-Induced Emission. *Chem. Soc. Rev.* **2011**, *40* (11), 5361–5388.
- Bünau, G. J. B. Birks: Photophysics of Aromatic Molecules. Wiley-Interscience, London 1970. 704 Seiten. Preis: 210s. *Ber. Bunsen-Ges. Phys. Chem.* **1970**, *74* (12), 1294–1295.
- Chen, S.; Du, K.; Wang, S.; Liang, C.; Shang, Y.; Xie, X.; Tang, G.; Li, J.; Wang, B.; Yu, X.; Chang, Y. A Non-Immunized and BSA-Template Aggregation-Induced Emission Sensor for Noninvasive Detection of Cystatin C in the Clinical Diagnosis of Diabetes Nephropathy. *ACS Sens.* **2023**, *8* (4), 1431–1439.
- Zhuang, Y.; Xu, Q.; Huang, F.; Gao, P.; Zhao, Z.; Lou, X.; Xia, F. Ratiometric Fluorescent Bioprobe for Highly Reproducible Detection of Telomerase in Bloody Urines of Bladder Cancer Patients. *ACS Sens.* **2016**, *1* (5), 572–578.
- Li, B.; Pan, W.; Liu, C.; Guo, J.; Shen, J.; Feng, J.; Luo, T.; Situ, B.; Zhang, Y.; An, T.; Xu, C.; Zheng, W.; Zheng, L. Homogenous Magneto-Fluorescent Nanosensor for Tumor-Derived Exosome Isolation and Analysis. *ACS Sens.* **2020**, *5* (7), 2052–2060.
- Zhou, T.; Wang, Q.; Liu, M.; Liu, Z.; Zhu, Z.; Zhao, X.; Zhu, W. An AIE-based Enzyme-activatable Fluorescence Indicator for Western Blot Assay: Quantitative Expression of Proteins with Reproducible Stable Signal and Wide Linear Range. *Aggregate* **2021**, *2* (2), No. e22.
- Ma, K.; Zhang, F.; Sayyadi, N.; Chen, W.; G Anwer, A.; Care, A.; Xu, B.; Tian, W.; M Goldys, E.; Liu, G. Turn-on^o Fluorescent Aptasensor Based on AIEgen Labeling for the Localization of IFN- γ in Live Cells. *ACS Sens.* **2018**, *3* (2), 320–326.
- Dai, Y.; He, F.; Ji, H.; Zhao, X.; Misal, S.; Qi, Z. Dual-Functional NIR AIEgens for High-Fidelity Imaging of Lysosomes in Cells and Photodynamic Therapy. *ACS Sens.* **2020**, *5* (1), 225–233.
- Jana, P.; Koppayithodi, S.; Murali, M.; Saha, M.; Kumar Maiti, K.; Bandyopadhyay, S. Detection of Sialic Acid and Imaging of Cell-Surface Glycan Using a Fluorescence–SERS Dual Probe. *ACS Sens.* **2023**, *8* (4), 1693–1699.
- Shi, H.; Liu, J.; Geng, J.; Zhong Tang, B.; Liu, B. Specific Detection of Integrin $\text{Av}\beta3$ by Light-Up Bioprobe with Aggregation-Induced Emission Characteristics. *J. Am. Chem. Soc.* **2012**, *134* (23), 9569–9572.

- (27) Zhang, Y.; Yan, Y.; Xia, S.; Wan, S.; E Steenwinkel, T.; Medford, J.; Durocher, E.; L Luck, R.; Werner, T.; Liu, H. Cell Membrane-Specific Fluorescent Probe Featuring Dual and Aggregation-Induced Emissions. *ACS Appl. Mater. Interfaces* **2020**, *12* (18), 20172–20179.
- (28) Liu, X.; Duan, Y.; Liu, B. Nanoparticles as Contrast Agents for Photoacoustic Brain Imaging. *Aggregate* **2021**, *2* (1), 4–19.
- (29) Sabouri, S.; Liu, M.; Zhang, S.; Yao, B.; Soleimanejad, H.; Baxter, A. A.; Armendariz-Vidales, G.; Subedi, P.; Duan, C.; Lou, X.; Hogan, C. F.; Heras, B.; Poon, I. K. H.; Hong, Y. Construction of a Highly Sensitive Thiol-Reactive AIEgen-Peptide Conjugate for Monitoring Protein Unfolding and Aggregation in Cells. *Adv. Healthcare Mater.* **2021**, *10* (24), No. e2101300.
- (30) Jia, L.; Wang, W.; Yan, Y.; Hu, R.; Sang, J.; Zhao, W.; Wang, Y.; Wei, W.; Cui, W.; Yang, G.; Lu, F.; Zheng, J.; Liu, F. General Aggregation-Induced Emission Probes for Amyloid Inhibitors with Dual Inhibition Capacity against Amyloid β -Protein and α -Synuclein. *ACS Appl. Mater. Interfaces* **2020**, *12* (28), 31182–31194.
- (31) Hu, R.; Yap, H. K.; Fung, Y. H.; Wang, Y.; Cheong, W. L.; So, L. Y.; Tsang, C. S.; Lee, L. Y. S.; Lo, W. K. C.; Yuan, J.; Sun, N.; Leung, Y. C.; Yang, G.; Wong, K. Y. Light up Protein-Protein Interaction through Bioorthogonal Incorporation of a Turn-on Fluorescent Probe into β -Lactamase. *Mol. Biosyst.* **2016**, *12* (12), 3544–3549.
- (32) Gao, M.; Tang, B. Z. Fluorescent Sensors Based on Aggregation-Induced Emission: Recent Advances and Perspectives. *ACS Sens.* **2017**, *2* (10), 1382–1399.
- (33) Brennan, P. J.; Kumogai, T.; Berezov, A.; Murali, R.; Greene, M. I. HER2/Neu: Mechanisms of Dimerization/Oligomerization. *Oncogene* **2000**, *19* (53), 6093–6101.
- (34) Wolff, A. C.; Elizabeth Hale Hammond, M.; Allison, K. H.; Harvey, B. E.; Mangu, P. B.; Bartlett, J. M. S.; Bilous, M.; Ellis, I. O.; Fitzgibbons, P.; Hanna, W.; Jenkins, R. B.; Press, M. F.; Spears, P. A.; Vance, G. H.; Viale, G.; McShane, L. M.; Dowsett, M. Human Epidermal Growth Factor Receptor 2 Testing in Breast Cancer: American Society of Clinical Oncology/ College of American Pathologists Clinical Practice Guideline Focused Update. *J. Clin. Oncol.* **2018**, *36* (20), 2105–2122.
- (35) Yang, S.; Raymond-Stintz, M. A.; Ying, W.; Zhang, J.; Lidke, D. S.; Steinberg, S. L.; Williams, L.; Oliver, J. M.; Wilson, B. S. Mapping ErbB Receptors on Breast Cancer Cell Membranes during Signal Transduction. *J. Cell Sci.* **2007**, *120* (16), 2763–2773.
- (36) Kaufmann, R.; Müller, P.; Hildenbrand, G.; Hausmann, M.; Cremer, C. Analysis of Her2/Neu Membrane Protein Clusters in Different Types of Breast Cancer Cells Using Localization Microscopy. *J. Microsc.* **2011**, *242* (1), 46–54.
- (37) Slamon, D. J.; Leyland-Jones, B.; Shak, S.; Fuchs, H.; Paton, V.; Bajamonde, A.; Fleming, T.; Eiermann, W.; Wolter, J.; Pegram, M.; Baselga, J.; Norton, L. Use of Chemotherapy plus a Monoclonal Antibody against HER2 for Metastatic Breast Cancer That Overexpresses HER2. *N. Engl. J. Med.* **2001**, *344* (11), 783–792.
- (38) Agus, D. B.; Gordon, M. S.; Taylor, C.; Natale, R. B.; Karlan, B.; Mendelson, D. S.; Press, M. F.; Allison, D. E.; Sliwkowski, M. X.; Lieberman, G.; Kelsey, S. M.; Fyfe, G. Phase I Clinical Study of Pertuzumab, a Novel HER Dimerization Inhibitor, in Patients With Advanced Cancer. *J. Clin. Oncol.* **2005**, *23* (11), 2534–2543.
- (39) Hermanson, G. T. *Bioconjugate Techniques*, 3rd ed.; Academic Press: London, 2013.
- (40) Shi, X.; Yu, C. Y. Y.; Su, H.; Kwok, R. T. K.; Jiang, M.; He, Z.; Lam, J. W. Y.; Tang, B. Z. A Red-Emissive Antibody-AIEgen Conjugate for Turn-on and Wash-Free Imaging of Specific Cancer Cells. *Chem. Sci.* **2017**, *8* (10), 7014–7024.
- (41) Zhang, Y.; He, J.; Saris, P. J. G.; Chae, H. U.; Das, S.; Kapadia, R.; Armani, A. M. Multifunctional Photoresponsive Organic Molecule for Electric Field Sensing and Modulation. *J. Mater. Chem. C* **2022**, *10* (4), 1204–1211.
- (42) Chen, J.; Jiang, H.; Zhou, H.; Hu, Z.; Niu, N.; Shahzad, S. A.; Yu, C. Specific Detection of Cancer Cells through Aggregation-Induced Emission of a Light-up Bioprobe. *Chem. Commun.* **2017**, *53* (15), 2398–2401.
- (43) Zhao, E.; Chen, Y.; Wang, H.; Chen, S.; Lam, J. W. Y.; Leung, C. W. T.; Hong, Y.; Tang, B. Z. Light-Enhanced Bacterial Killing and Wash-Free Imaging Based on AIE Fluorogen. *ACS Appl. Mater. Interfaces* **2015**, *7* (13), 7180–7188.
- (44) Landis, R. F.; Yazdani, M.; Creran, B.; Yu, X.; Nandwana, V.; Cooke, G.; Rotello, V. M. Solvatochromic Probes for Detecting Hydrogen-Bond-Donating Solvents. *Chem. Commun.* **2014**, *50* (35), 4579–4581.
- (45) Zhang, Y.; Li, D.; Li, Y.; Yu, J. Solvatochromic AIE Luminogens as Supersensitive Water Detectors in Organic Solvents and Highly Efficient Cyanide Chemosensors in Water. *Chem. Sci.* **2014**, *5* (7), 2710–2716.
- (46) Tang, A.; Chen, Z.; Deng, D.; Liu, G.; Tu, Y.; Pu, S. Aggregation-Induced Emission Enhancement (AIEE)-Active Tetraphenylethene (TPE)-Based Chemosensor for Hg with Solvatochromism and Cell Imaging Characteristics. *RSC Adv.* **2019**, *9* (21), 11865–11869.
- (47) Karaman, M.; Demir, N.; Bilgili, H.; Yakali, G.; Gokpek, Y.; Demic, S.; Kaya, N.; Can, M. Synthesis, Characterization, Aggregation-Induced Enhanced Emission and Solvatochromic Behavior of Dimethyl 4'-(Diphenylamino)Biphenyl-3,5-Dicarboxylate: Experimental and Theoretical Studies. *New J. Chem.* **2020**, *44* (27), 11498–1156.
- (48) Welton, T.; Reichardt, C. *Solvents and Solvent Effects in Organic Chemistry*; John Wiley & Sons, Hoboken, 2010.
- (49) Hu, X.; Lerch, T. F.; Xu, A. Efficient and Selective Bioconjugation Using Surfactants. *Bioconjugate Chem.* **2018**, *29* (11), 3667–3676.
- (50) Smith, S. E.; Mellor, P.; Ward, A. K.; Kendall, S.; McDonald, M.; Vizeacoumar, F. S.; Vizeacoumar, F. J.; Napper, S.; Anderson, D. H. Molecular Characterization of Breast Cancer Cell Lines through Multiple Omic Approaches. *Breast Cancer Res.* **2017**, *19* (1), 65.
- (51) Dunn, K. W.; Kamocka, M. M.; McDonald, J. H. A Practical Guide to Evaluating Colocalization in Biological Microscopy. *Am. J. Physiol.: Cell Physiol.* **2011**, *300* (4), 723–742.
- (52) Bradbury, A.; Plückthun, A. Reproducibility: Standardize Antibodies Used in Research. *Nature* **2015**, *518* (7537), 27–29.
- (53) Oh, D.-Y.; Bang, Y.-J. HER2-Targeted Therapies — a Role beyond Breast Cancer. *Nat. Rev. Clin. Oncol.* **2020**, *17* (1), 33–48.
- (54) Hudis, C. A. Trastuzumab — Mechanism of Action and Use in Clinical Practice. *N. Engl. J. Med.* **2007**, *357* (1), 39–51.
- (55) Leahy, D. J.; Cho, H.-S.; Mason, K.; Ramyar, K. X.; Stanley, A. M.; Gabelli, S. B.; Denney, D. W. Structure of the Extracellular Region of HER2 Alone and in Complex with the Herceptin Fab. *Nature* **2003**, *421* (6924), 756–760.
- (56) Ghosh, R.; Narasanna, A.; Wang, S. E.; Liu, S.; Chakrabarty, A.; Balko, J. M.; González-Angulo, A. M.; Mills, G. B.; Penuel, E.; Winslow, J.; Sperinde, J.; Dua, R.; Pidaparthy, S.; Mukherjee, A.; Leitzel, K.; Kostler, W. J.; Lipton, A.; Bates, M.; Arteaga, C. L. Trastuzumab Has Preferential Activity against Breast Cancers Driven by HER2 Homodimers. *Cancer Res.* **2011**, *71* (5), 1871–1882.
- (57) Molina, M. A.; Codony-Servat, J.; Albanell, J.; Rojo, F.; Arribas, J.; Baselga, J. Trastuzumab (Herceptin), a Humanized Anti-HER2 Receptor Monoclonal Antibody, Inhibits Basal and Activated HER2 Ectodomain Cleavage in Breast Cancer Cells. *Cancer Res.* **2001**, *61* (12), 4744–4749.
- (58) Valabrega, G.; Montemurro, F.; Aglietta, M. Trastuzumab: Mechanism of Action, Resistance and Future Perspectives in HER2-Overexpressing Breast Cancer. *Ann. Oncol.* **2007**, *18* (6), 977–984.
- (59) Chung, I.; Reichelt, M.; Shao, L.; Akita, R. W.; Koeppe, H.; Rangell, L.; Schaefer, G.; Mellman, I.; Sliwkowski, M. X. High Cell-Surface Density of HER2 Deforms Cell Membranes. *Nat. Commun.* **2016**, *7* (1), No. 12742.
- (60) Burguin, A.; Furrer, D.; Ouellette, G.; Jacob, S.; Diorio, C.; Durocher, F. Trastuzumab Effects Depend on HER2 Phosphorylation in HER2-Negative Breast Cancer Cell Lines. *PLoS One* **2020**, *15* (6), No. e0234991, DOI: 10.1371/journal.pone.0234991.

(61) Canonici, A.; Ivers, L.; Conlon, N. T.; Pedersen, K.; Gaynor, N.; Browne, B. C.; O'Brien, N. A.; Gullo, G.; Collins, D. M.; O'Donovan, N.; Crown, J. HER-Targeted Tyrosine Kinase Inhibitors Enhance Response to Trastuzumab and Pertuzumab in HER2-Positive Breast Cancer. *Invest. New Drugs* **2019**, *37* (3), 441–451.

(62) Moradi, J.; Lee, J. S. H.; Armani, A. M. Detection and visualization of HER2 clustering using an Aggregation Induced Emission based fluorescent probe molecule. 2023, arXiv:2305.03799. arXiv.org e-Print archive. <https://arxiv.org/abs/2305.03799>.

(63) Casaletto, J. B.; McClatchey, A. I. Spatial Regulation of Receptor Tyrosine Kinases in Development and Cancer. *Nat. Rev. Cancer* **2012**, *12* (6), 387–400.

(64) Leuchowius, K.-J.; Jarvius, M.; Wickström, M.; Rickardson, L.; Landegren, U.; Larsson, R.; Söderberg, O.; Fryknäs, M.; Jarvius, J. High Content Screening for Inhibitors of Protein Interactions and Post-Translational Modifications in Primary Cells by Proximity Ligation. *Mol. Cell. Proteomics* **2010**, *9* (1), 178–183.

Agent-based modeling of tumor-immune interactions reveals determinants of final tumor states

Manal Ahmidouch^a, Neel Tangella^b and Stacey D. Finley^{b,c,d}

^aSchool of Medicine, University of North Carolina at Chapel Hill, Chapel Hill, NC 27599, USA.

^bDepartment of Quantitative and Computational Biology, University of Southern California, Los Angeles, CA 90089, USA.

^cAlfred E. Mann Department of Biomedical Engineering, University of Southern California, Los Angeles, CA 90089, USA

^dMork Family Department of Chemical Engineering and Materials Science, University of Southern California, Los Angeles, CA 90089, USA.

Corresponding Author: Stacey D. Finley, email - sfinley@usc.edu

Abstract

Interactions between tumor and immune cells in the tumor microenvironment (TME) influence tumor growth and the tumor's response to treatment. Excitingly, this complex landscape of tumor-immune interactions can be studied using computational modeling. Mathematical oncology can provide quantitative insights into the TME, serving as a framework for understanding tumor dynamics. Here, we use an agent-based model to simulate the interactions among cancer cells, macrophages (naïve, M1, and M2), and T cells (active CD8+ and inactive) in a 2D representation of the TME. Key diffusible factors, IL-4 and IFN- γ , are also incorporated. We apply the model to predict how cell-specific properties influence tumor progression. The model predictions and analyses revealed the relationships between different cell populations and highlighted the importance of macrophages and T cells in shaping the TME. Thus, we quantify how components of the TME influence the final tumor state and the effects of macrophage-based therapies. The findings emphasize the significant role of computational models in unraveling the intricate dynamics of tumor-immune interactions and their potential for guiding the development of tailored immunotherapeutic strategies. This study provides a foundation for future investigations aiming to refine and expand the model, validate predictions experimentally, and pave the way for improved cancer treatments.

Introduction

As cancer immunotherapies demonstrate success in certain tumor settings and amass attention¹, creating models to simulate the effects of these treatment becomes increasingly crucial. In particular, mathematical models of tumor growth are able to account for the complex and adaptive interactions between tumor and immune cells². Immune cells have the innate ability to detect malignant tumor cells as “not self” and destroy them. Tumor cells, however, are able to suppress this immune function and alter immune cells such that they assist in tumor growth, rather than diminish it³. The altered immune cells also suppress the immune system⁴. Thus, significant effort has been focused on developing immunotherapies that overcome such tumor-promoting interactions⁵.

Macrophage-targeted therapies hold great promise due to the vital role macrophages play in tumor progression⁶. There are two broad classes of macrophages identified using *in vitro* studies, termed M1 and M2⁷. M1 macrophages are able to activate neighboring T cells. In contrast, M2 macrophages prevent neighboring CD8+ T cells from becoming activated by secreting inhibitory cytokines such as interleukin-4 (IL-4). Tumor cells also secrete IL-4, contributing to the anti-tumor effect of macrophages⁸. When the T cells become fully activated, they proliferate and kill the nearby cancer cells. They also secrete interferon- γ (IFN- γ), which attracts M1 macrophages to the tumor site and further promotes M1 activity⁹. In sum, M1 macrophages promote T cell activation to produce CD8+ T cells and M2 macrophages inhibit it, with the CD8+ T cells destroying the tumor cells via cytolytic activity¹⁰.

Many current immunotherapies target immunosuppressive mechanisms. However, since tumor-immune interactions are complex, the result of these immunotherapies can differ from what is expected when studied using experimental models¹¹. Additionally, given the intricacy of the tumor microenvironment (TME), *in vitro* and *in vivo* studies alone cannot resolve the potential effects of immunotherapy. Excitingly, the tumor and immune cell interactions can be better understood using computational models^{2,12}. Computational models allow us to simulate a plethora of immune cell interactions, in less time and with fewer resources than with a purely experimental approach. Importantly, the information used in these computational models is based on previous biological experiments, so the models can be used to make reliable and physiologically-relevant predictions of tumor behavior¹³. While many computational models

simulate individual interactions within the TME, it is ideal to create a detailed model to more fully represent the TME and the immune cell interactions involved. In particular, agent-based models (ABMs) combine individual interactions into a complex system of cellular behaviors, making them ideal for modeling the TME¹⁴. ABMs are commonly utilized to capture the spatial characteristics of a system. These models consist of individual agents representing cells that interact with their neighbors based on experiment-derived rules that reflect the cells' biological roles¹⁵. By following these rules, the agents behave in a way that captures the overall behavior of the system.

In this study, we employ an ABM to simulate the early growth of tumors in a 2D representation, resembling a tumor slice¹⁶. Our model incorporates three primary cell types: T cells, macrophages, and cancer cells. Additionally, we consider the production and diffusion of diffusible factors using partial differential equations. The parameter values used in the model are derived from previous modeling efforts or are based on experimental observations. By varying these parameters, we can simulate the dynamic tumor behavior, ultimately establishing whether a tumor progresses towards a pro-tumor state or an anti-tumor end state. By investigating the intricate dynamics of tumor-immune cell interactions through our ABM, we aim to shed light on the underlying mechanisms governing tumor behavior and response to immunotherapy. In particular, we uncover relationships between subsets of cells and how these relationships evolve over time to shape tumor growth. We quantify how specific cell types at discrete times influence the final tumor state. Overall, our work provides a more detailed understanding of how distinct cell types and their interactions contribute to tumor progression.

Methods

Model Overview

An ABM was employed to simulate the interactions among diverse cell populations within the TME. The model represents the early stages of tumor development and incorporates three primary cell types: cancer cells, macrophages, and T cells. The model also incorporates two diffusible factors, IL-4 and IFN- γ , which play crucial roles in influencing the immune state of the TME. The simulation takes place in a two-dimensional environment, comprised of a 100-by-100 grid representing a 1.5 mm² tissue slice. Thus, each site within the grid is 1.5 μ m². As this is approximately the diameter of cells, each site can be occupied by only one cell at a time. Detailed information about the ABM used in this study can be found in¹⁶ and accessed at the GitHub repository here: <https://github.com/FinleyLabUSC/Early-TME-ABM-PLOS-Comp-Bio>.

Cell Populations

The primary cell types included in the model are cancer cells, macrophages (naïve, M1, and M2), and T cells (active CD8+ and inactive). M1 macrophages are able to activate neighboring T cells, while M2 macrophages inhibit T cells from becoming active. Cancer cells are the main contributors to tumor growth, while macrophages and T cells interact with the cancer cells to influence tumor growth. It is important to note that this model aims to understand generalized tumor behavior rather than focusing on a specific tumor type. The simulations were first performed without the application of any treatment.

Macrophages initially enter the microenvironment as naïve M0 macrophages, and their polarization into the M1 or M2 state is determined by the presence of diffusible factors in the local environment at a given time. IL-4, secreted by the tumor cells and M2 macrophages, promotes a pro-tumor state. In comparison, IFN- γ , secreted by activated T cells, induces M1 differentiation, thereby fostering an anti-tumor environment. Macrophages sense the concentrations of IL-4 and IFN- γ in their local microenvironment and process these input signals

via an intracellular signaling model encoded as a trained neural network, resulting in differentiation. Macrophages can re-differentiate every 24 hours based on the local diffusible factors.

The recruitment of T cells into the TME is crucial for tumor eradication. In the model, T cells possess the ability to migrate towards the tumor and undergo full activation upon encountering a cancer cell. Once fully activated, T cells can proliferate and effectively eliminate neighboring cancer cells. Additionally, fully active T cells secrete IFN- γ , which influences the differentiation of naïve macrophages into the M1 macrophage state, enhancing the anti-tumor environment.

Simulation of Diffusible Factors

To simulate the production and diffusion of IL-4 and IFN- γ , the model incorporates partial differential equations that describe the spatiotemporal evolution of the diffusible factors. Parameters for these equations were derived from previous modeling efforts or experimental observations.

Parameter Alteration and Simulation Design

To investigate the impact of specific parameters on the TME, we conducted simulations over a 200-day period. Each simulation was repeated 100 times to account for the inherent stochasticity of ABMs, and the resulting data were averaged at each time point for analysis. The key parameters under investigation were the cancer cell cycle length, macrophage recruitment rate, and T cell recruitment rate. We explored cell cycle lengths of 20, 25, and 30 hours, T cell recruitment rates of 1, 5, and 10 cells/hour and macrophage recruitment rates of 1×10^{-9} and 1×10^{-8} cells/site/second.

Outcome Measures

The primary outcome measure assessed in this study was the number of cancer cells at each time point throughout the simulation. This served as a quantifiable indicator of tumor growth. By monitoring the changes in cancer cell population size over time, we gained insights into the dynamics of tumor growth. Additionally, the dynamic population sizes of different cell types within the TME were analyzed to gain a comprehensive understanding of their relationships. The behaviors of macrophages (naïve, M1, and M2) and T cells (inactive and active CD8) were studied to evaluate their influence on the TME and potential roles in tumor progression or suppression.

In addition to studying temporal dynamics, we also examined the end state for each cell type. The end state refers to the final population size of a given cell type at the conclusion of the simulation. By identifying and analyzing the end states, we gained valuable insights into the regulatory mechanisms within the TME. This analysis allowed us to characterize the final configurations of cell populations and understand the interplay between different cell types.

Data Analysis

Data visualization techniques were employed to depict the population size trends of cell types and to compare the impact of different parameter settings on tumor growth.

Partial Least Squares Analysis

A common technique used to perform regression on high-dimensional data is partial least-squares (PLS). Partial least squares regression (PLSR) aims to reduce the dimensionality of the data by constructing latent variables that represent the inputs. In our study, we employ a modified version of PLS called partial least squares discriminant analysis (PLS-DA). PLS-DA is a supervised learning approach that is particularly suitable for modeling relationships between

species' concentrations and their contributions to different simulation end states. PLS-DA as a method for understanding feature importance in high-dimensional datasets has seen increasing use in the field of metabolomics¹⁷. The inputs to the PLS-DA model (also called “predictors”) are the number of cellular and molecular species of each type at discrete time points. For the output, we define two categories representing favorable and unfavorable TME end states, allowing us to perform PLS-DA and examine the features of the TME that influence the model's outcome. Here, a favorable end state is when the number of active CD8+ T cells exceeds the number of cancer cells. In contrast, an unfavorable end state is when the number of cancer cells exceeds the number of active CD8+ T cells.

Model Selection

We vary the number of components used in PLS-DA to determine the model with the highest predictive power. To select the PLS-DA model with the highest predictive power and control against PLS-DA's tendency to overfit, we perform k -fold cross-validation. This technique involves splitting the input data into k groups, where one group serves as the test set and the remaining $k-1$ groups are used as the training set. We shuffle the data before each iteration of cross-validation to ensure equal representation. The PLS-DA model that achieves the highest accuracy on the test dataset is selected for subsequent model projection and analysis.

VIP Score

The variable importance of projection (VIP) score is a common metric accompanying PLS-DA models. It quantifies the relative importance of each input variable to the model¹⁸. The VIP score is calculated as the weighted sum of squared correlations between the model components and the original predictor variable. Typically, a VIP score of 1 or greater is considered indicative of above-average importance¹⁸, and we use this threshold here.

Loadings

Analyzing the loadings in a PLS-DA model is crucial for determining the direct linear contributions of input variables to the model projection. Strongly positive or negative loadings indicate that the input variable plays a more significant role in discriminating the model's outputs compared to inputs with loadings close to zero. In our study, given the definition of the two TME end states, inputs with positive loadings drive the system towards a favorable end state, while those with negative loadings drive it towards an unfavorable end state.

By employing PLS-DA, selecting the optimal model, and analyzing VIP scores and loadings, we identify the key inputs and their contributions in driving the TME towards favorable or unfavorable end states. This analysis provides insights into the underlying mechanisms and factors influencing the TME dynamics.

Results

Cell-specific properties strongly influence tumor growth.

The predicted dynamics observed in our simulations provide valuable insights into the relationships between different cell types within the TME. We first examined how tumor dynamics were affected by cell-specific properties, including immune cell recruitment and the length of the cancer cell cycle (**Figure 1**), as these are tumor-specific properties that will vary within the TME.

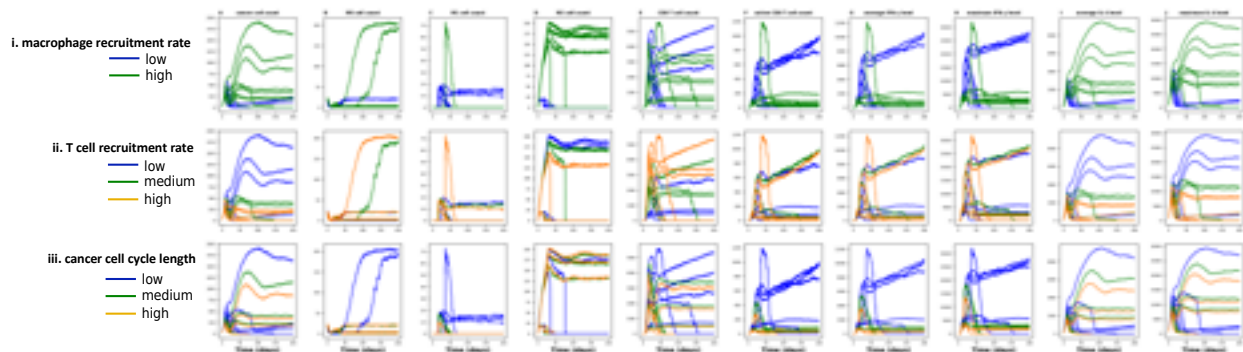


Fig 1. Effect of immune cell recruitment rates and cell cycle length on cell population sizes. A) cancer cell count. B) M0 cell count. C) M1 cell count. D) M2 cell count. E) CD8 T cell count. F) active CD8 T cell count. G) average IFN- γ level. H) maximum IFN- γ . I) average IL-4 level. J) maximum IL-4 level. Time courses for the 100 replicates of the model are plotted and averaged at each time point. Cell cycle lengths of 20, 25, and 30 hours, T cell recruitment rates of 1, 5, and 10 cells/hour and macrophage recruitment rates of 1×10^{-8} and 1×10^{-7} cells/site/second were explored.

Model predictions show that the balance between macrophage and T cell recruitment rates, as well as the length of the cancer cell growth cycle, influences the population sizes of different cell types and the levels of immune-related factors (**Figure 1**). Increasing the macrophage recruitment rate was found to promote a pro-tumor microenvironment, resulting in an increase in the cancer cell population (Figure 1A, row (i)). This was accompanied by an increase in the M2 macrophage population, indicating increased differentiation of naïve macrophages to the immunosuppressive state. Interestingly, the higher macrophage recruitment rate was associated with a smaller active CD8+ T cell population and lower IFN- γ levels (Figure 1F, row (i), G, row (i), and H, row (i)), suggesting a dampened anti-tumor immune response. Additionally, elevated macrophage recruitment rates led to higher IL-4 concentrations (Figure 1I, row (i) and J, row (i)), contributed by cancer cells and M2 macrophages.

Compared to increasing the macrophage recruitment rate, higher T cell recruitment contributed to an anti-tumor microenvironment, characterized by a lower number of cancer cells (Figure 1A, row (ii)). This was accompanied by fewer M2 macrophages and lower IL-4 levels (Figure 1D, row (ii), I, row (ii) and J, row (ii)). Interestingly, we did not observe a direct relationship between the size of the T cell population and the rate of T cell recruitment.

Finally, varying the length of the cancer cell growth cycle had a significant impact on the tumor microenvironment. In general, shorter cell cycle lengths created an anti-tumor microenvironment, marked by higher populations of naïve macrophages, M1 macrophages, and activated CD8+ T cells (Figure 1B, row (iii), C, row (iii), and F, row (iii)). This was accompanied by higher IFN- γ levels, indicating an enhanced anti-tumor immune response (Figure 1G and H). The secretion of IFN- γ by activated CD8+ T cells played a crucial role in promoting the differentiation of naïve macrophages into the M1 state. Notably, the length of the cell cycle did not significantly affect IL-4 levels.

The time courses of the population sizes indicate relationships between cell types.

In addition to investigating how TME-specific model parameters influence tumor dynamics, we explored the relationships between TME components. We observed a strong similarity between the dynamics of cancer cells and the concentrations of IL-4 in the TME (**Figure 2A, I, and J**). Both the average and maximum levels of IL-4 exhibited similar patterns to the number of cancer cells, indicating a close relationship between IL-4 and tumor activity. Notably, tumor cells

themselves secrete IL-4, directly influencing the concentration of IL-4 within the TME and contributing to the pro-tumor effects. The dynamics of active CD8+ T cells mirrored those of IFN- γ , including both average and maximum IFN- γ levels (**Figure 2F, G, and H**). This correspondence highlights the intricate interactions within the TME, where fully activated T cells secrete IFN- γ , promoting differentiation of naïve macrophages to the M1 state. In contrast, the dynamics of macrophages did not exhibit any distinct trends in relation to the other cell population counts or cytokine levels, suggesting complex and context-dependent behavior. Similarly, the total CD8+ T cell count did not display a clear trend, indicating their population size is also independent of other TME factors. These findings provide valuable insights into the dynamic interplay between different cell populations within the TME, highlighting the significant roles played by IL-4 and IFN- γ in influencing tumor behavior and the activity of immune cells.

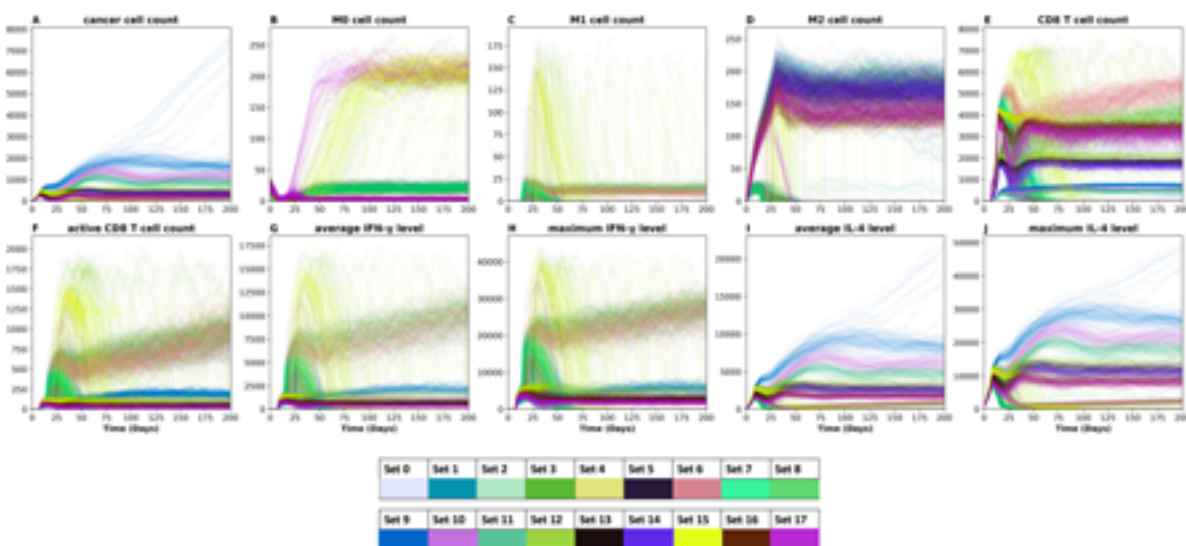


Fig 2. Predicted dynamics demonstrate relationships between different cell types. A) cancer cell count. B) M0 cell count. C) M1 cell count. D) M2 cell count. E) CD8 T cell count. F) active CD8 T cell count G) average IFN- γ level. H) maximum IFN- γ . I) average IL-4 level. J) maximum IL-4 level. All 100 simulations for each parameter set are shown, throughout the 200-day time course.

The dynamics of pairs of TME components reveal relationship between cancer cells and active CD8+ cells, underscoring their interconnected dynamics within the TME. **Figure 3** shows the dynamic relationships between cancer cells and every other cell type and diffusible factor in the model. We plot the time courses for the 100 replicates of the model, averaged at each time point, for the immune cell recruitment rates and cancer cell cycle lengths considered above (**Figure 1**). Thus, there are 18 curves represented in **Figure 3**. In the final state (darkest points), a noticeable divergence is observed in the relationship between cancer cells and other cell types, particularly active CD8+ T cells, suggesting distinct tumor states. Most prominently, two states emerge from our simulations (**Figure 3E**): a pro-tumor state characterized by a low count of active CD8+ T cells and a high count of cancer cells, and an anti-tumor state marked by a high count of active CD8+ cells and a low count of cancer cells. This dichotomy highlights the opposing effects of CD8+ T cells on tumor growth, indicating the pivotal role of T cells in shaping the tumor microenvironment. Since the activation of CD8+ T cells is dependent on IFN- γ , there is also a relationship between the cancer cell count and IFN- γ levels (**Figure 3F and G**). We again see two clear regimes: low IFN- γ and high cancer cell count; and high IFN- γ with few cancer cells. Thus, there is a tight link between cancer cells, CD8+ T cells, and IFN- γ .

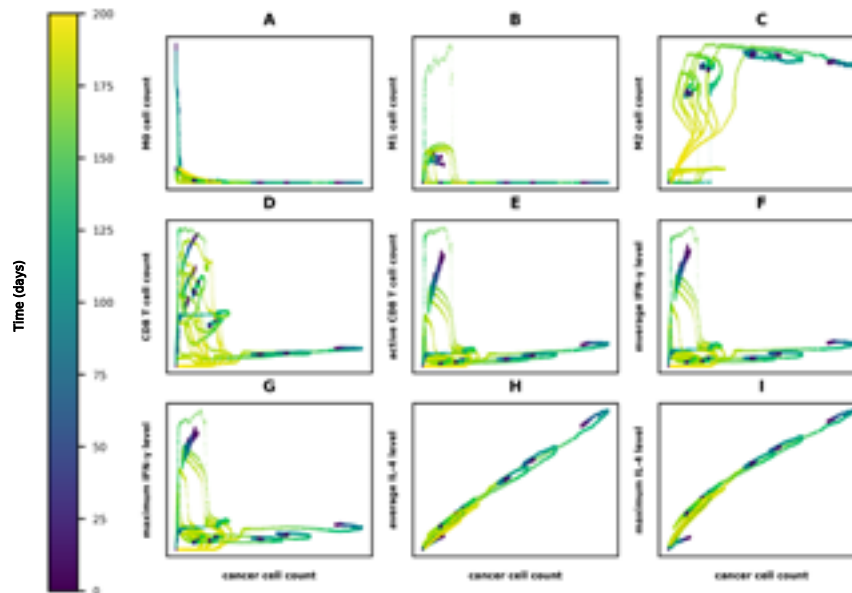


Fig 3. Dynamic relationships present between cancer cells and components of the TME. Cancer cell count versus A) M0 cell count, B) M1 cell count, C) M2 cell count, D) CD8 T cell count, E) active CD8 T cell count, I) average IFN- γ level, J) maximum IFN- γ level, H) IL-4 level, and I) maximum IL-4 level.

Furthermore, we find a significant relationship between M2 macrophages and the population of cancer cells (**Figure 3C**). Initially, as the M2 macrophage population increases, the size of the cancer cell population also increases. This makes sense, as cancer cells influence macrophages through the secretion of IL-4, which promotes the transition of naïve macrophages to M2 macrophages. M2 macrophages also secrete IL-4, creating a positive feedback loop that further reinforces their influence on the cancer cell population. Thus, we also see a direct relationship between the cancer cell trajectories and IL-4 levels (**Figure 3H,I**). The number of cancer cells increases proportionally as the IL-4 concentration increases. Interestingly, we observe a point in the simulation where the cancer cell population begins to decline, accompanied by a decrease in the M2 macrophage population. This downward trajectory suggests that other factors beyond the relationship between M2 macrophages and cancer cells come into play, potentially influencing the dynamics of the tumor microenvironment. These findings highlight that the mutual influence between M2 macrophages and cancer cells, mediated by IL-4, contributes to the dynamics of the tumor microenvironment.

The tumor end state can be characterized by the ratio of cancer cells to T cells.

The interaction between cancer cells and active CD8+ T cells emerges as a critical determinant of the final state within the tumor microenvironment. We investigated the relationship between the numbers of cancer cells and CD8+ T cells, where two distinct regimes can be discerned (**Figure 4A**). We defined a favorable anti-tumor state to be where the number of CD8+ T cells exceeds the number of cancer cells (yellow region in **Figure 4A**). Similarly, an unfavorable pro-tumor state occurs when the number of cancer cells is greater than the number of CD8+ T cells (purple region in **Figure 4A**). Thus, the threshold between these states is an equal number of cancer cells and CD8+ T cells (**Figure 4A**, dashed black line). We further focused on the final tumor state (**Figure 4B**) to study how particular cell populations and diffusible factors influence the tumor end-state. Here, we display the final number of active CD8+ T cell and cancer cell for

all 100 replicates of the 18 parameter combinations shown in **Figure 4A**. The yellow data points represent the anti-tumor state, indicating a robust immune response, with active CD8+ T cells effectively suppressing tumor growth. Conversely, the purple data points represent the pro-tumor state, suggesting a suppressed immune state and creating a favorable environment for tumor growth to prevail. The contrasting pro- and anti-tumor states highlight the significance of the interplay between cancer cells and active CD8+ T cells in shaping the overall dynamics and outcomes of the TME.

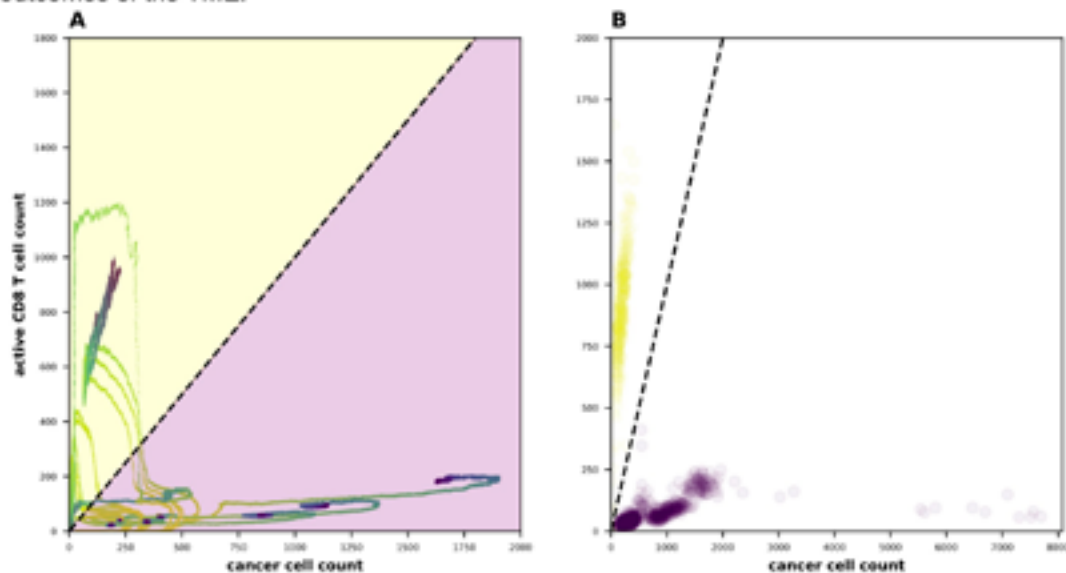


Fig 4. Ratio of cancer cell to active CD8 cells defines final state of the TME. The color scheme differentiates two distinct end-states based on the relationship between these cell populations. The yellow data points represent the anti-tumor state, characterized by a low cancer cell count and a high count of active CD8 cells. The purple data points represent the pro-tumor state, exhibiting a high cancer cell count and a low count of active CD8 cells.

Regression analysis quantifies components of the TME influence the tumor end state.

We performed regression analysis to determine how specific components of the TME (naïve, M1, and M2 macrophages, and average and maximum levels of IL-4 and IFN- γ) influence the predicted final tumor state (ratio of cancer cells to active CD8+ T cells). We performed cross-validation to quantify the predictive ability of the regression analysis. The training accuracy was greater than 0.85 for all test models (Supplementary Figure S1), indicating this analysis can be used to quantify the relationship between TME components and the predict tumor end state. We use the VIP score for each component to quantify how strongly a TME component influences the end state (**Figure 5A**), where a VIP score greater than one indicates a strong influence on the final tumor state. Furthermore, we consider the direction in which the TME component shifts the end state. Here, the loadings of each cell population were examined to assess their contributions to the tumor microenvironment at specific time points and their association with the tumor microenvironment state. The resulting **Figure 5B** displays these loadings, with yellow bars representing variables associated with an anti-tumor state and purple bars indicating variables associated with a pro-tumor state. Notably, variables with a VIP score above 1, indicated by bolded bars, were considered to have significant importance in the model.

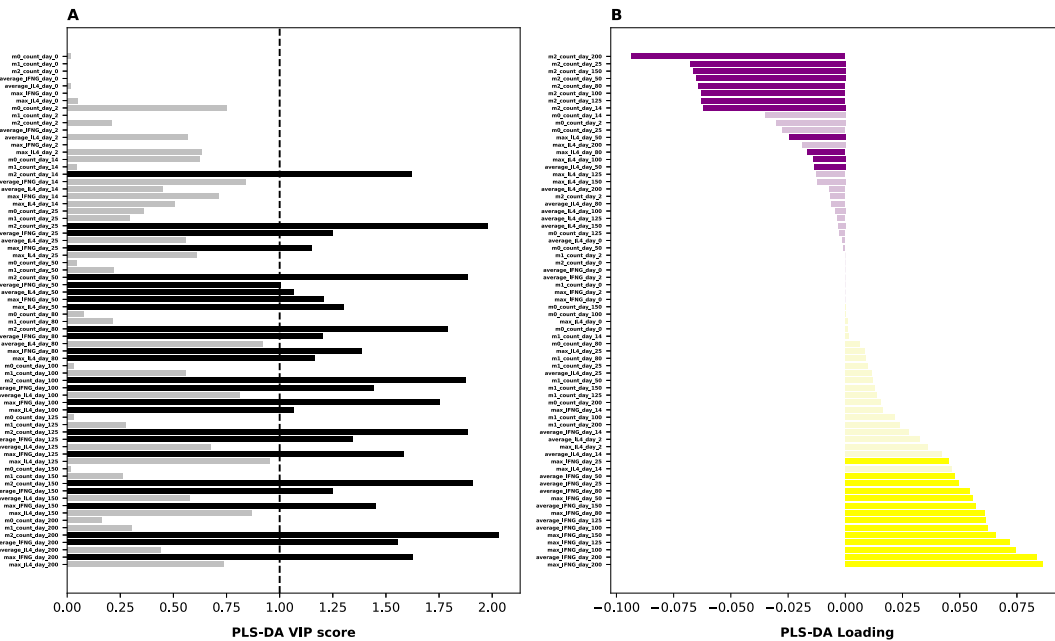


Fig 5. Regression analysis reveals influential factors associated with the final tumor state. A) VIP scores for model inputs from PLS-DA, with black indicating variables that have a VIP score above 1. B) PLS-DA loading values among the cell populations indicates significant influence on the tumor microenvironment. Pro-tumor state indicated by the purple bars and anti-tumor state indicated by the yellow bars. Darker bars indicate inputs with VIP score greater than 1.

Our analysis predicts that at particular time points, the M2 count, average IFN- γ , maximum IFN- γ , and both maximum and average levels of IL-4 influence the end state. We considered the impact of the TME components at 10 distinct time points: day 0, 2, 14, 25, 50, 80, 100, 125, 150, and 200. Prior to day 14, none of the TME components are shown to strongly contribute to the tumor end state. However, starting at day 14 and continuing throughout the 200-day simulation, the number of M2 macrophages is predicted to be a major contributor to the final tumor state (**Figure 5A**). As expected, the negative loading of the M2 count (**Figure 5B**) shows that higher numbers of M2 macrophages shift the tumor towards the unfavorable pro-tumor state. At day 25, the average and maximum IFN- γ levels emerge as significant contributors, promoting an anti-tumor state throughout the remaining time points. Moreover, after day 25, IL-4 appears as a significant contributor, particularly during specific time points. The average and maximum IL-4 levels at day 50 and the maximum IL-4 levels at day 80 are identified as key factors in influencing the number of cancer cells. However, it is important to acknowledge that the influence of IL-4 is not consistent throughout the entire time course. This suggests that IL-4 plays a significant role in certain stages of tumor progression, while its impact may be less pronounced during other times. We further confirm the importance of M2, IL-4, and IFN- γ by plotting their values for each tumor end state (Supplementary Figures S2-S5). Altogether, these findings highlight the influential role of M2 count and IL-4 levels at specific time points in promoting an anti-tumor state, while average and maximum IFN- γ levels promote a pro-tumor state within the TME.

Given the significant role of macrophages in shaping the final tumor state, we investigated the impact of macrophage-based immunotherapies on altering the tumor end state. We simulated

three treatments: inhibiting macrophage recruitment to the tumor, depleting macrophages in the tumor, and reeducating M2 macrophages to go to the M1 state. For each case, we ran 100 replicates and analyzed the tumor end state (**Figure 6**). We determined the fraction of end states that are unfavorable (“pro-tumor”: the number of cancer cells exceeds the number of CD8+ T cells) and the fraction of favorable end states (“anti-tumor”: there are more CD8+ T cells than cancer cells). In the absence of any treatment, most of the end states were classified as unfavorable (**Figure 7**), aligning with expectations. However, when evaluating the three different treatments, we found that the reeducation approach, aimed at converting macrophages into an immune-promoting phenotype, emerged as the most effective strategy in promoting an anti-tumor end state. This finding suggests that targeting and reprogramming macrophages holds promise as a therapeutic strategy to shift the tumor microenvironment towards an immune-responsive and anti-tumor state.

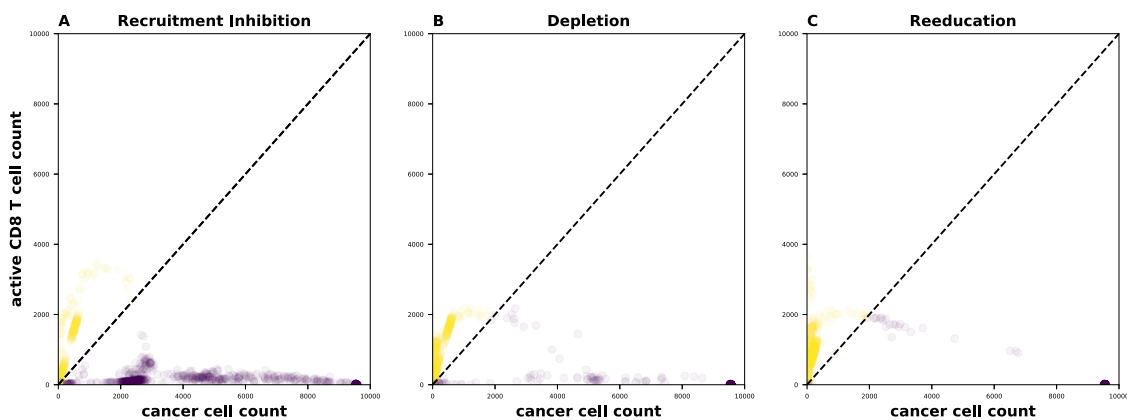


Fig 6. Impact of macrophage-based immunotherapies on tumor end state. A) Recruitment inhibition B) Depletion C) Reeducation. 100 replicates were run for each case and tumor end state was analyzed. Yellow indicates an anti-tumor end state. Purple indicates a pro-tumor end state.

Discussion

In this study, we utilized an ABM to simulate the interactions between tumor and immune cells within the TME. The model incorporated three primary cell types: cancer cells, macrophages (naïve, M1, and M2), and T cells (active CD8+ and inactive). We also considered the production and diffusion of two key diffusible factors, IL-4 and IFN- γ , which play crucial roles in influencing the immune state of the TME. By varying parameters such as cancer cell cycle length and the rates at which macrophages and T cells are recruited, we simulated the dynamic behavior of the tumor and investigated the effects of these cell-specific properties factors on tumor progression. Our analysis revealed the relationships between different cell populations and highlighted the importance of macrophages and T cells in shaping the TME.

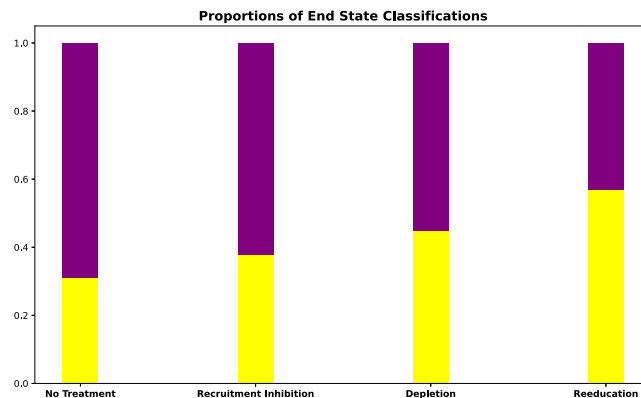


Fig. 7. Proportion of pro- and anti-tumor end states after macrophage-based immunotherapy treatments. Yellow indicates an anti-tumor state. Purple indicates the pro-tumor state. Macrophage-based treatment increases the predicted proportion of anti-tumor end state classifications.

It is important to address the concept of pro-tumor and anti-tumor end states within the TME and the factors that contribute to them. Our findings consider that a high number of active CD8+ T cells and low numbers of cancer cells are associated with an anti-tumor end state¹⁹. Conversely, a pro-tumor end state is characterized by a low presence of active CD8+ T cells and a high density of cancer cells, indicating a compromised immune response and a supportive environment for tumor growth¹⁹. Given these definitions, we explored how TME components contribute to these pro-tumor and anti-tumor end states. The presence of macrophages in the TME plays a crucial role, as macrophages can exhibit different phenotypes with opposing effects on tumor progression²⁰. M1 macrophages have immune-stimulatory properties and promote an anti-tumor response, while M2 macrophages have immune-suppressive properties and contribute to a pro-tumor environment²¹. Therefore, the balance between M1 and M2 macrophages is critical in shaping the TME and determining the end state. The production and diffusion of key diffusible factors, such as IL-4 and IFN- γ , influence the immune state of the TME as well. IL-4 is typically associated with an immune-suppressive environment, promoting a pro-tumor state, while IFN- γ is linked to an immune-stimulatory environment, favoring an anti-tumor response²². The levels and distribution of these factors within the TME can significantly impact the immune cell populations and their interactions, thereby influencing the end state. Our work quantifies the importance of these TME components, at specific times during tumor progression. By establishing the influence of the TME factors, we can use the model to inform strategies to target the influential TME components.

The study demonstrated that macrophage-based immunotherapies, specifically the reeducation approach targeting macrophage phenotype conversion, showed promise in promoting an anti-tumor end state within the TME. By reprogramming macrophages to an immune-promoting phenotype, the study suggests that it may be possible to shift the tumor microenvironment towards an immune-responsive, anti-tumor state. These findings provide valuable insights into the potential of targeting macrophages as a therapeutic strategy for cancer treatment²³.

This study addresses the complexity of tumor-immune cell interactions and the crucial role played by macrophages in tumor progression. By employing an ABM, the study provides a detailed understanding of the dynamics within the TME and sheds light on the underlying mechanisms that govern tumor behavior and response to immunotherapy. The use of

computational models, based on biological experiments, allows for reliable and physiologically-relevant predictions of tumor behavior, which may not be feasible with purely experimental approaches²⁴. The study emphasizes the significance of using computational modeling to gain a mechanistic and quantitative understanding of tumor-immune interactions. Furthermore, the study highlights the potential of macrophage-based immunotherapies as a promising avenue for cancer treatment²⁵. Overall, our findings contribute to ongoing efforts to develop more effective immunotherapies and personalized treatment strategies for cancer patients²⁶.

While the ABM used in this study provides valuable insights into the dynamics of the TME, it is important to acknowledge its limitations. The model represents an idealized 2D representation of the tumor slice, and the simulations were performed without considering the influence of other factors such as angiogenesis, genetic heterogeneity, or the presence of other immune cell types. Therefore, the model may not fully capture the complexity and heterogeneity of the actual tumor microenvironment. Future studies should aim to incorporate these additional factors to obtain a more comprehensive understanding of tumor-immune interactions. Moreover, the parameter values used in the model were derived from previous modeling efforts or based on experimental observations. While this approach provides a basis for reliable predictions, it is essential to acknowledge that the model's accuracy depends on the accuracy of these parameter values. Future studies may refine these parameters and validating the model predictions using experimental data.

Building upon the insights gained from this study, future research directions can focus on several aspects. Firstly, incorporating additional cell types and factors into the ABM, such as other immune cell populations, cytokines, and the tumor microenvironment's extracellular matrix, will provide a more comprehensive representation of the TME and enable a deeper understanding of the intricate interactions within it. Secondly, further exploration of macrophage-based immunotherapies is warranted. While the reeducation approach showed promise in promoting an anti-tumor end state, more in-depth investigations are needed to optimize the therapy and assess its efficacy in preclinical and clinical settings. Future studies should consider the development of targeted therapies that selectively modulate macrophage phenotypes to maximize the immune response against tumors while minimizing potential side effects. Finally, combining computational modeling combined with experimental approaches, such as *in vitro* and *in vivo* preclinical studies, can provide a more holistic perspective on tumor-immune interactions. Experimental validation of the model predictions, as well as the integration of patient-specific data, can enhance the accuracy and translational potential of computational models.

Conclusions

This study highlights the importance of computational modeling in understanding the complex dynamics of tumor-immune interactions within the tumor microenvironment. The findings underscore the potential of macrophage-targeted immunotherapies and provide insights into the underlying mechanisms that govern tumor behavior. While acknowledging the study's limitations, future research can build upon these findings to refine and expand the models, explore new therapeutic strategies, and ultimately contribute to the development of more effective and personalized cancer treatments.

Author Contributions

S.D.F. conceived of the study. M.A. carried out computational model simulations. M.A. and N.T. performed analyses. S.D.F. supervised the project and provided financial support. All authors discussed the results and contributed to the final manuscript.

Declaration of Interests

The authors declare no competing interests.

Acknowledgements

The authors thank Dr. Colin Cess for guidance in performing model simulations. This work was supported by the USC Summer Oncology Research Fellowship (M.A.), the USC Student Opportunities for Academic Research (N.T.), and the USC Center for Computational Modeling of Cancer.

Data Availability

No new data was generated as part of this study. The agent-based model used in this work has been previously published and is available publicly.

References

1. Zhang, Y. & Zhang, Z. The history and advances in cancer immunotherapy: understanding the characteristics of tumor-infiltrating immune cells and their therapeutic implications. *Cell. Mol. Immunol.* **17**, 807–821 (2020).
2. Mahlbacher, G. E., Reihmer, K. C. & Frieboes, H. B. Mathematical modeling of tumor-immune cell interactions. *J. Theor. Biol.* **469**, 47–60 (2019).
3. Mantovani, A., Marchesi, F., Malesci, A., Laghi, L. & Allavena, P. Tumour-associated macrophages as treatment targets in oncology. *Nat. Rev. Clin. Oncol.* **14**, 399–416 (2017).
4. Munn, D. H. & Bronte, V. Immune suppressive mechanisms in the tumor microenvironment. *Curr. Opin. Immunol.* **39**, 1–6 (2016).
5. Liu, Y., Li, C., Lu, Y., Liu, C. & Yang, W. Tumor microenvironment-mediated immune tolerance in development and treatment of gastric cancer. *Front. Immunol.* **13**, 1016817 (2022).
6. Nywening, T. M. *et al.* Phase 1b study targeting tumour associated macrophages with CCR2 inhibition plus FOLFIRINOX in locally advanced and borderline resectable pancreatic cancer. *Lancet Oncol.* **17**, 651–662 (2016).
7. Genin, M., Clement, F., Fattaccioli, A., Raes, M. & Michiels, C. M1 and M2 macrophages derived from THP-1 cells differentially modulate the response of cancer cells to etoposide. *BMC Cancer* **15**, 577 (2015).
8. Cheng, Y. *et al.* PKN2 in colon cancer cells inhibits M2 phenotype polarization of tumor-associated macrophages via regulating DUSP6-Erk1/2 pathway. *Mol. Cancer* **17**, 13 (2018).
9. Zagorulya, M. *et al.* Tissue-specific abundance of interferon-gamma drives regulatory T cells to restrain DC1-mediated priming of cytotoxic T cells against lung cancer. *Immunity* **56**, 386-405.e10 (2023).
10. Hanahan, D. & Coussens, L. M. Accessories to the Crime: Functions of Cells Recruited to the Tumor Microenvironment. *Cancer Cell* **21**, 309–322 (2012).
11. Vanneman, M. & Dranoff, G. Combining Immunotherapy and Targeted Therapies in Cancer Treatment. *Nat. Rev. Cancer* **12**, 237–251 (2012).
12. Gong, C. *et al.* A computational multiscale agent-based model for simulating spatio-temporal tumour immune response to PD1 and PDL1 inhibition. *J. R. Soc. Interface* (2017) doi:10.1098/rsif.2017.0320.
13. Chamseddine, I. M. & Rejniak, K. A. Hybrid modeling frameworks of tumor development and treatment. *Wiley Interdiscip. Rev. Syst. Biol. Med.* **12**, e1461 (2020).

14. Norton, K.-A., Gong, C., Jamalian, S. & Popel, A. S. Multiscale Agent-Based and Hybrid Modeling of the Tumor Immune Microenvironment. *Process. Basel Switz.* **7**, 37–37 (2019).
15. Vodovotz, Y. & An, G. Agent-based models of inflammation in translational systems biology: A decade later. *Wiley Interdiscip. Rev. Syst. Biol. Med.* **11**, e1460 (2019).
16. Cess, C. G. & Finley, S. D. Multi-scale modeling of macrophage-T cell interactions within the tumor microenvironment. *PLoS Comput. Biol.* **16**, e1008519 (2020).
17. Worley, B., Halouska, S. & Powers, R. Utilities for Quantifying Separation in PCA/PLS-DA Scores Plots. *Anal. Biochem.* **433**, 102–104 (2013).
18. Cho, H.-W. *et al.* Discovery of metabolite features for the modelling and analysis of high-resolution NMR spectra. *Int. J. Data Min. Bioinforma.* **2**, 176–192 (2008).
19. Lukhele, S. *et al.* The transcription factor IRF2 drives interferon-mediated CD8+ T cell exhaustion to restrict anti-tumor immunity. *Immunity* **55**, 2369-2385.e10 (2022).
20. Nowak, M. & Klink, M. The Role of Tumor-Associated Macrophages in the Progression and Chemoresistance of Ovarian Cancer. *Cells* **9**, 1299 (2020).
21. Mills, C. D. M1 and M2 Macrophages: Oracles of Health and Disease. *Crit. Rev. Immunol.* **32**, 463–488 (2012).
22. Anderson, N. M. & Simon, M. C. Tumor Microenvironment. *Curr. Biol. CB* **30**, R921–R925 (2020).
23. Anderson, N. R., Minutolo, N. G., Gill, S. & Klichinsky, M. Macrophage-Based Approaches for Cancer Immunotherapy. *Cancer Res.* **81**, 1201–1208 (2021).
24. Zangooui, M. H., Margolis, R. & Hoyt, K. Multiscale computational modeling of cancer growth using features derived from microCT images. *Sci. Rep.* **11**, 18524 (2021).
25. Cao, X. *et al.* Promoting antibody-dependent cellular phagocytosis for effective macrophage-based cancer immunotherapy. *Sci. Adv.* **8**, eabl9171 (2023).
26. Esfahani, K. *et al.* A review of cancer immunotherapy: from the past, to the present, to the future. *Curr. Oncol. Tor. Ont* **27**, S87–S97 (2020).

Notes

USC Michelson Center for Convergent Bioscience

We thank Araceli Roach for the layout, graphic arts and design, Amy Wood for assistance in information gathering, as well as creating the tables and charts for the At a Glance section and Michael Yarsky for proofreading.

Silvia da Costa, Ph.D.
Director, Research Initiatives and Infrastructure
Editor and Scientific Writer